Functional and structural brain changes after dopamine D2 receptors blockade

Selvaggi, Pierluigi

Awarding institution:
King's College London

To my dad

Functional and structural brain changes after dopamine D_2 receptors blockade

by

Pierluigi Selvaggi

A thesis submitted in fulfilment of the requirements for the degree of Doctor of Philosophy at King's College London

Department of Neuroimaging

Institute of Psychiatry, Psychology and Neuroscience

King's College London

Acknowledgements

This is perhaps the most challenging chapter of my thesis to write. During my PhD at the Institute of Psychiatry, Psychology & Neuroscience, King's College London and through collaborations with other research institutions, I had the privilege to meet a considerable number of bright and incredible people. To all of them, even if not specifically mentioned here, my very warm thank you.

My very first special thanks are to my first supervisor, Prof. Mitul Mehta, an inspiring scientist who has supported and empowered me through these years. He taught me the importance of rigour in scientific research from experimental design to statistics, to produce knowledge that is beneficial for patients. I am very grateful to him also for his patience and his support in difficult moments.

A big thank you also to Dr. Ottavia Dipasquale, my second supervisor, who in addition to the invaluable support she gave me in imaging analyses also inspired and motivated my investigations. This thesis would have been much different without her practical and emotional advice.

I must thank Dr. Mattia Veronese. Most of the research questions addressed in the present thesis were born in the office I shared with him at the Centre for Neuroimaging Sciences, King's College London, before being discussed with supervisors and collaborators. His contagious enthusiasm has been an additional engine throughout my PhD.

A big thank you to Prof. Oliver Howes and Dr. Tiago Reis Marques who gave me the incredible opportunity to collaborate with the Psychiatric Imaging Group, at the London Institute of Medical Sciences, Imperial College London to run one of the main projects of this PhD: the NECTAR study. Through this crucial collaboration, I had the chance to expand my investigations and address research questions arising from previous projects. A warm thank you to Dr. Martin Osugo, Dr. Uzma Zahid and all researchers and staff in the Psychiatric Imaging Group, at the London Institute of Medical Sciences, Imperial College London. My PhD would have not been possible without their work and support.

I also thank Prof. Federico Turkheimer, a visionary and rigorous scientist. From him, I learned how the combination of curiosity and critical thinking can lead to innovation in scientific research. A thank you also to Prof. Steven Williams who allowed me to join the Department of Neuroimaging, King's College London in 2015 as a visiting researcher from Italy. Throughout my visiting period and my PhD, I always felt at home at the Department of Neuroimaging. I thank all researchers and staff of the Department of Neuroimaging. I will never forget these years, among the brightest and most inspiring of my life.

A heartful thanks to my wife, Rossella Pisani who always believed in me, especially in difficult moments. She has been my keenest supporter and my strength during these years. A big kiss also to Irene, my little daughter, whom I love.

I would like to wholeheartedly thank my family. My sister, Agata Selvaggi, my mother, Irene Varvara and my father Francesco Selvaggi, have always supported me, celebrating my achievements, sometimes even more than I did. A special thank is to my father to whom this thesis is dedicated. I wish you were here. But do not worry the "book" will be at home, on the table, for you to read.

Abstract

Dopamine D_2 (D_2R) receptor blockade exerted by antipsychotics is the current standard for the treatment of psychosis. However, the effects on brain structure and function are still under debate. In addition, most studies examining brain changes have been conducted in patients where results are confounded by disease state and trait effects and placebo-controlled designs are difficult to perform for ethical concerns. As a result, disentangling between disease and treatment effects is challenging. Whilst previous studies in healthy volunteers have shown that acute single exposure to D_2R antagonism is associated with alterations in brain structure and function, it remains unclear whether these effects are detectable after prolonged D_2R blockade. Moreover, structural, and functional Magnetic Resonance Imaging (MRI) findings after antipsychotic administration in humans have rarely been directly linked with pharmacodynamics at D_2R. To address all these issues, the present thesis illustrates the results of three studies. The first study tested the association between the main effects of single-dose antipsychotic administration on cerebral perfusion and spatial distribution of D_2R across the entire brain, the second investigated changes in brain structure and function after sustained D_2R blockade in healthy volunteers and the third examined differences in brain perfusion between non-medicated patients at their first episode of psychosis (FEP) and healthy controls (HC).

Study 1. I analysed Cerebral Blood Flow (CBF) data as assessed with Arterial Spin Labelling (ASL) from a placebo-controlled study in healthy volunteers, who received a single dose of three different D_2R antagonists and tested the association of the main effects of the drugs on CBF against non-displaceable binding potential (BP_{ND}) [^{18}F]-Fallypride Positron Emission Tomography (PET) normative maps and brain *post-mortem* microarray mRNA expression data for the *DRD2* gene from the Allen Human Brain Atlas (AHBA). For all antipsychotics, CBF changes were directly proportional to brain D_2R densities and *DRD2* mRNA expression measures. In addition, the spatial relationship between ΔCBF and D_2R profiles varied between the different antipsychotics tested, possibly reflecting differential affinities.

Study 2. I analysed data from a double-blinded, randomized, crossover, placebo-controlled study in healthy volunteers who received either amisulpride 400mg or a placebo daily for seven days. T1 maps and brain volume estimation were derived from the MP2RAGE sequence. Pseudo-continuous ASL and resting-state multi-echo fMRI sequences were used

to assess CBF and functional connectivity respectively. Using the Spearman correlation, I tested the association between drug effects and extrapyramidal symptoms (EPS). In addition, to explore inter-individual variability in drug response, I implemented a pharmacokinetic/pharmacodynamic (PK/PD) framework from pre-clinical studies which modelled plasma drug concentration in a repeated dose regimen, receptor occupancy and brain changes after sustained D_2R blockade. No differences were found between amisulpride and placebo conditions in both T1 maps and brain volumes. Amisulpride increased CBF in the striatum and reduced functional connectivity between its sensorimotor subdivision and the primary motor cortex as compared with placebo. The PK/PD model revealed a monotonically increasing relationship between changes in CBF and receptor occupancy as predicted by preclinical models. Finally, a greater reduction in functional connectivity was associated with greater EPS.

Study 3. I examined CBF in FEP free from antipsychotic medication compared to HC. Both absolute and relative-to-global CBF was assessed. I also investigated the association between baseline CBF and treatment response in a partially nested follow-up study. The comparison revealed significantly lower absolute CBF in the frontal cortex and no differences in the basal ganglia. Whole brain voxel-wise analysis revealed widespread cortical reductions in absolute CBF in large cortical clusters that encompassed occipital, parietal, and frontal cortices. No differences were found in relative CBF in the selected region of interest and voxel-wise analysis. Relative frontal CBF was correlated with the percentage change in total Positive and Negative Syndrome Scale (PANSS) after antipsychotic treatment.

My PhD shows that both acute and sustained D_2R blockade induces increased CBF in the basal ganglia in healthy volunteers and that the magnitude of the effects reflects the spatial distribution of D_2R in the brain and inter-individual variability in D_2R occupancy. These findings from experiments inform the negative finding in the clinical study where no difference was found in striatal perfusion between non-medicated FEP and healthy controls, indicating that increased striatal perfusion in psychosis is likely a treatment effect. My PhD also extends previous evidence from single-dose studies to show that sustained blockade of D_2R over a week is not associated with changes in brain tissue structure and volume. Finally, the results of my PhD also indicate that D_2R blockade also has non-local effects by altering cortico-striatal functional connectivity which could potentially serve as a biomarker for EPS.

Publications

Publications arising from this PhD thesis

Published

Selvaggi P, Hawkins PCT, Dipasquale O, Rizzo G, Bertolino A, Dukart J, Sambataro F, Pergola G, Williams SCR, Turkheimer F, Zelaya F, Veronese M, Mehta MA. *Increased cerebral blood flow after a single dose of antipsychotics in healthy volunteers depends on dopamine D2 receptor density profiles*. Neuroimage. 2019 Mar; 188:774-784. DOI: 10.1016/j.neuroimage.2018.12.028. Epub 2018 Dec 13. PMID: 30553916.

Selvaggi P, Jauhar S, Kotoula V, Pepper F, Veronese M, Santangelo B, Zelaya F, Turkheimer FE, Mehta MA, Howes OD. *Reduced cortical cerebral blood flow in antipsychotic-free first-episode psychosis and relationship to treatment response*. Psychol Med. 2022 Aug 25:1-11. DOI: 10.1017/S0033291722002288. Epub ahead of print. PMID: 36004510.

Selvaggi P, Rizzo G, Mehta MA, Turkheimer FE, Veronese M. *Integration of human whole-brain transcriptome and neuroimaging data: Practical considerations of current available methods*. J Neurosci Methods. 2021 May 1;355:109128. DOI: 10.1016/j.jneumeth.2021.109128. Epub 2021 Mar 17. PMID: 33722642.

Accepted

Selvaggi P, Osugo M, Dipasquale O, Zahid U, Whitehurst T, Onwordi Ellis, Statton B, Wood T, Veronese M, Marques TR, Murray R, Mehta MA, Howes O. *Effects of sustained D_2 Receptors Blockade on Brain Structure and Function in Healthy Volunteers.* Accepted to the SOBP 2023 Conference as poster presentation.

Co-authored manuscripts published during this PhD thesis

Patania A, **Selvaggi P**, Veronese M, Dipasquale O, Expert P, Petri G. *Topological gene expression networks recapitulate brain anatomy and function*. Netw Neurosci. 2019 Jul 1;3(3):744-762. doi: 10.1162/netn_a_00094. PMID: 31410377; PMCID: PMC6663211.

Dipasquale O, **Selvaggi P**, Veronese M, Gabay AS, Turkheimer F, Mehta MA. Receptor-Enriched Analysis of functional connectivity by targets (REACT): *A novel, multimodal analytical approach informed by PET to study the pharmacodynamic response of the brain under MDMA*. Neuroimage. 2019 Jul 15;195:252-260. doi: 10.1016/j.neuroimage.2019.04.007. Epub 2019 Apr 4. PMID: 30953835; PMCID: PMC6547164.

Turkheimer FE, **Selvaggi P**, Mehta MA, Veronese M, Zelaya F, Dazzan P, Vernon AC. *Normalizing the Abnormal: Do Antipsychotic Drugs Push the Cortex Into an Unsustainable Metabolic Envelope?* Schizophr Bull. 2020 Apr 10;46(3):484-495. doi: 10.1093/schbul/sbz119. Erratum in: Schizophr Bull. 2020 Jan 17;:null. PMID: 31755955; PMCID: PMC7147598.

van der Meer D, Rokicki J, Kaufmann T, Córdova-Palomera A, Moberget T, Alnæs D, Bettella F, Frei O, Doan NT, Sønderby IE, Smeland OB, Agartz I, Bertolino A, Bralten J, Brandt CL, Buitelaar JK, Djurovic S, van Donkelaar M, Dørum ES, Espeseth T, Faraone SV, Fernández G, Fisher SE, Franke B, Haatveit B, Hartman CA, Hoekstra PJ, Håberg AK, Jönsson EG, Kolskår KK, Le Hellard S, Lund MJ, Lundervold AJ, Lundervold A, Melle I, Monereo Sánchez J, Norbom LC, Nordvik JE, Nyberg L, Oosterlaan J, Papalino M, Papassotiropoulos A, Pergola G, de Quervain DJF, Richard G, Sanders AM, **Selvaggi P**, Shumskaya E, Steen VM, Tønnesen S, Ulrichsen KM, Zwiers MP, Andreassen OA, Westlye LT; Alzheimer's Disease Neuroimaging Initiative; Pediatric Imaging, Neurocognition and Genetics Study. *Brain scans from 21,297 individuals reveal the genetic architecture of hippocampal subfield volumes*. Mol Psychiatry. 2020 Nov;25(11):3053-3065. DOI: 10.1038/s41380-018-0262-7. Epub 2018 Oct 2. PMID: 30279459; PMCID: PMC6445783.

Townsend L, Pillinger T, **Selvaggi P**, Veronese M, Turkheimer F, Howes O. *Brain glucose metabolism in schizophrenia: a systematic review and meta-analysis of ^{18}FDG-PET studies in schizophrenia*. Psychol Med. 2022 Jun 22:1-18. doi: 10.1017/S003329172200174X. Epub ahead of print. PMID: 35730361.

Patel Y et al. *Virtual Ontogeny of Cortical Growth Preceding Mental Illness*. Biol Psychiatry. 2022 Aug 15;92(4):299-313. doi: 10.1016/j.biopsych.2022.02.959. Epub 2022 Mar 4. PMID: 35489875.

Constantinides et al. (2022). Brain ageing in schizophrenia: evidence from 26 international cohorts via the ENIGMA Schizophrenia consortium. *Molecular psychiatry*, 10.1038/s41380-022-01897-w. Advance online publication. https://doi.org/10.1038/s41380-022-01897-w

Singh, N., MacNicol, E., DiPasquale, O., Randall, K., Lythgoe, D., Mazibuko, N., Simmons, C., **Selvaggi, P.**, Stephenson, S., Turkheimer, F. E., Cash, D., Zelaya, F., & Colasanti, A. (2023). The effects of acute Methylene Blue administration on cerebral blood flow and metabolism in humans and rats. *Journal of cerebral blood flow and metabolism: official journal of the International Society of Cerebral Blood Flow and Metabolism*, 271678X231157958. Advance online publication. https://doi.org/10.1177/0271678X231157958

Sampogna, G. et al. (2022). The Complex Interplay Between Physical Activity and Recovery Styles in Patients With Severe Mental Disorders in a Real-World Multicentric Study. *Frontiers in psychiatry*, *13*, 945650. https://doi.org/10.3389/fpsyt.2022.945650

Oliver D, Davies C, Zelaya F, **Selvaggi P**, De Micheli A, Catalan A, Baldwin H, Arribas M, Modinos G, Crossley NA, Allen P, Egerton A, Jauhar S, Howes OD, McGuire P and Fusar-Poli P (2023) Parsing neurobiological heterogeneity of the clinical high-risk state for psychosis: A pseudo-continuous arterial spin labelling study. *Front. Psychiatry* 14:1092213. doi: 10.3389/fpsyt.2023.1092213

Raio, A., Pergola, G., Rampino, A., Russo, M., D'Ambrosio, E., **Selvaggi, P.**, De Chiara, V., Altamura, M., Brudaglio, F., Saponaro, A., Semisa, D., Bertolino, A., Antonucci, L. A., Blasi, G., & Apulian Network on Risk for Psychosis (2023). Similarities and differences between multivariate patterns of cognitive and socio-cognitive deficits in schizophrenia, bipolar disorder and related risk. *Schizophrenia (Heidelberg, Germany)*, *9*(1), 11. https://doi.org/10.1038/s41537-023-00337-0

Table of Contents

Table of Figures

Table of Tables

Table of Equations

Abbreviations

Abbreviation	Meaning	First use
$5HT_2AR$	serotonin-2A receptor	page 27
$5HT_2BR$	serotonin-2B receptor	page 103
$5HT_2CR$	serotonin-2C receptor	page 28
$5HT_7R$	serotonin-7 receptor	page 103
AE	Adverse Event	page 84
AFNI	Analysis of Functional NeuroImages	page 77
AHBA	Allen Human Brain Atlas	page 24
ALFF	Amplitude of Low-Frequency Fluctuations	page 36
ANCOVA	Analysis of Covariance	page 78
ANOVA	Analysis of Variance	page 113
ANTs	Advanced Normalization Tools	page 76
ASL	Arterial Spin Labelling	page 33
BA	Brodmann Area	page 56
BET	Brain Extraction Tool	page 76
BF	Bayes Factor	page 115
BOLD	Blood Oxygen Level Dependent	page 40
BP_{ND}	non-displaceable Binding Potential	page 35
CBF	Cerebral Blood Flow	page 24
CBV	Cerebral Blood Volume	page 35
CHR-P	Clinical High Risk for Psychosis	page 33
CSF	Cerebrospinal Fluid	page 50
D_1R	Dopamine D1 receptors	page 35
D_2R	Dopamine D2 Receptors	page 23
DARTEL	Diffeomorphic Anatomical Registration Through Exponential Lie Algebra	page 51
DPAs	Dopamine Partial Aagonists	page 28
EPI	Echo-Planar Imaging	page 75
EPS	Extrapyramidal Symptoms	page 26
ESRS	Extrapyramidal Symptoms Rating Scale	page 72
FA	Fractional Anisotropy	page 30
FC	Functional Connectivity	page 23
FD	Framewise Displacement	page 77
FDR	False Discovery Rate	page 78
FEP	First Episode Psychosis	page 24
FGAs	First Generation Antipsychotics	page 25
fMRI	Functional Magnetic Resonance Imaging	page 23
FOV	Field of View	page 50
FSL	Functional Software Library	page 51
FU1	Follow-up 1	page 73

FU2	Follow-up 2	page 73
FWE	Family Wise Error	page 52
FWHM	Full width at half maximum	page 51
HAL	haloperidol 3mg treatment group	page 49
HC	Healthy Controls	page 23
highRIS	risperidone 2mg treatment group	page 49
ICA	Independent Component Analysis	page 36
ICC	Intraclass Coefficient	page 126
ICV	Intracranial volume	page 114
K_d	dissociation or affinity constant	page 39
lowRIS	risperidone 0.5mg treatment group	page 49
MATLAB	MATrix LABoratory	page 80
MENGA	Multimodal Environment for Neuroimaging and Genomic Analysis	page 55
MIAKAT	Molecular Imaging And Kinetic Analysis Toolbox	page 80
MNI	Montreal Neurological Institute	page 41
MPRAGE	Magnetization Prepared - Rapid Gradient Echo	page 50
MRI	Magnetic Resonance Imaging	page 23
mRNA	messenger ribonucleid acid	page 23
MSN	Medium spiny neuron	page 26
NECTAR	Neuroreceptor regulation of brain structure and function	page 46
NIFTI	Neuroimaging Informatics Technology	page 56
OLA	olanzapine 7.5mg treatment group	page 49
PANSS	Positive and Negative Syndrome Scale	page 111
PCA	Principal Component Analysis	page 55
PCASL	Pseudo-continuous arterial spin labelling	page 50
PD	pharmacodynamic	page 24
PET	Positron Emission Tomography	page 23
PK	pharmacokinetic	page 24
poly(I:C)	Polyinosinic:polycytidylic acid	page 35
QUIT	Quantitative imaging Tool	page 75
RF	radiofrequency	page 50
RNAseq	RNA sequencing	page 42
ROI	Region of Interest	page 51
SD	standard deviation	page 49
SGAs	Second Generation Antipsychotics	page 25
SNR	Signal-to-noise ratio	page 50
SPECT	Single Photon Emission Computed Tomography	page 27
SPM	Statistical Parametric Mapping	page 50
SPSS	Statistical Package for Social Sciences	page 53
TE	Echo time	page 75
tedana	TE-Dependent ANAlysis	page 77
TFCE	Threshold-Free Cluster Enhancement	page 78

TI	Inversion time	page 74
T_{max}	peak level of plasma concentration	page 50
TR	Repetition time	page 111
VBM	Voxel Based Morphometry	page 31
WM	White matter	page 50

1 Introduction

In my introduction, I will first introduce the class of drugs called 'antipsychotics', their clinical use, side effects and pharmacodynamic properties. Even though antipsychotics have been largely characterised for the treatment of psychosis in terms of clinical response and side effects, their effect on brain physiology and how this relates to treatment is less clear. A deeper understanding of these effects is crucial to uncover biological mechanisms driving their clinical efficacy as well as their side effects. I will review clinical neuroimaging studies along with evidence from pre-clinical and experimental medicine studies on the effects of antipsychotic medication with a focus on the effect of dopamine D2 receptors (D_2R) blockade in brain structure and function. In particular, I will review studies investigating the effect of D_2R blockade on brain tissue and volume, brain perfusion and functional connectivity (FC). One important limitation of clinical neuroimaging studies done in patients with psychosis (often chronically medicated patients) is that results are biased by disease state and trait. One possible strategy to overcome these limitations is to integrate results from cross-sectional or longitudinal studies in non-medicated patients with pharmacological experiments in healthy volunteers using neuroimaging. However, pharmacological neuroimaging studies in healthy volunteers have their limitations too. One limitation stands on the fact that Magnetic Resonance Imaging (MRI) measures are not able to capture neurochemical changes related to drug pharmacodynamics. Nonetheless, drug effects on MRI signals have often been interpreted as the result of dose-dependent enhanced or reduced pre- or post-synaptic activity due to the action of the drug on its targets (Khalili-Mahani et al., 2017). For example, the effects of antipsychotics on brain structure and function have often been tacitly attributed to D_2R blockade which is considered the main mechanism of action of this class of drugs for clinical treatment, although many antipsychotics have high affinity for other receptors. However, since MRI does not measure neuronal activity directly, linking neuro-receptor binding with MRI signal change requires a degree of conjecture. For these reasons, despite the body of evidence, the neurochemical mechanisms underlying structural and functional brain changes after antipsychotic administration remain unclear. Recently, different authors (Dukart et al., 2018; Hansen et al., 2022) have attempted to fill this gap of knowledge with the use of multimodal approaches that combine functional MRI (fMRI) measures with measures of target receptors in the brain

(e.g., Positron Emission Tomography (PET), *post-mortem* autoradiography, brain mRNA expression). In my introduction, I will review these studies and discuss the rationale of this approach linking pharmacokinetics and pharmacodynamic properties of the drugs (i.e., PK/PD model). During my PhD, I was able to assess the validity of this approach by testing the spatial association of antipsychotic main effects in healthy volunteers on brain perfusion against D_2R protein density and *DRD2* mRNA expression spatial profile (Chapter 2). The integration of human brain transcriptomics with neuroimaging data has been made possible thanks to the release of the Allen Human Brain Atlas (AHBA) (Hawrylycz et al., 2012) which contains mRNA expression measures for >20,000 genes covering the whole brain and, critically, in a standard stereotaxic space. In recent years many different methods have been used to integrate this data set with brain imaging data, although this endeavour has lacked harmony in terms of the workflow of data processing and subsequent analyses. In this introduction, I will also discuss the main issues in need of a thorough examination when integrating the AHBA with neuroimaging which have a significant impact on reproducibility. In my PhD, these considerations guided the methodological work to test the spatial association between the main effect of antipsychotics in Cerebral Blood Flow (CBF) and mRNA expression data.

Whilst previous pharmacological MRI studies have shown that acute single exposure to D_2R antagonism is associated with alterations in brain structure and function, it remains unknown if these are an acute response to neuroreceptor modulation that normalises with repeated D_2R antagonism, or if an effect remains detectable after sustained D_2R blockade at clinically relevant doses. In addition, it is unknown whether prolonged blockade of D_2R in healthy volunteers is associated with brain structural and functional alterations which single-dose studies have not revealed. In my PhD, I have attempted to fill this gap by investigating the effect of sustained D_2R blockade on brain structure and function in a double-blind randomized, crossover, placebo control study in healthy volunteers taking daily doses of amisulpride at clinically relevant doses for one week.

Finally, in this Introduction, I will also provide a brief description of the 3 studies of my PhD and a full explanation of their rationale. Parts of the introduction are based on my published papers on spatial profiling of antipsychotic effect on brain perfusion to D_2R brain distribution (Selvaggi et al. (2019) and Appendix A); on the integration of whole brain transcriptome with neuroimaging data (Selvaggi et al. (2021) and Appendix B); on the differences in CBF

between non-medicated first-episode psychosis patients (FEP) and healthy controls (HC) (Selvaggi et al. (2022) and Appendix C).

1.1 Antipsychotics

As suggested by the name itself, antipsychotics are drugs whose main indication is the treatment of psychosis. However, antipsychotics are also used in many other disorders like bipolar disorder (i.e., treatment of mania with or without psychotic symptoms), Alzheimer's disease or other dementias (to treat behavioural disturbances) and even in children with neurodevelopmental disorders associated with severe behavioural symptoms (Taylor et al., 2021). They are traditionally grouped into two main sub-classes: first-generation antipsychotics (FGAs) and second-generation antipsychotics (SGAs) (Leucht, Corves, et al., 2009). FGAs are also called "typical" or "conventional" antipsychotics. Both names refer to the fact that these drugs were the first to be proven effective in patients with schizophrenia. The very first drug of this class was chlorpromazine (a phenothiazine derivative with histaminergic properties) whose discovery dates back to the '50s (Lehmann & Hanrahan, 1954). Further studies revealed that chlorpromazine and other drugs of this class like haloperidol (developed by Paul Janssen, (Janssen, 1967)) were able not only to reduce psychotic symptoms but also caused a clinical condition characterized by severe psychomotor slowing, affective blunting and quieting. This condition was named "*neurolepsis*" (or "*catalepsis*") and, as a result, antipsychotics started to be named also as "neuroleptics". The pharmacological mechanism underlying efficacy in psychosis and side effects, including *neurolepsis*, was uncovered only a couple of decades later. Indeed, in the 1970s studies demonstrated that the key pharmacological property of all neuroleptics was their antagonism to D_2R (Burt et al., 1977). Given this evidence, a dysfunction in the dopaminergic system (mainly in the mesolimbic pathway) was hypothesized as a plausible pathophysiological mechanism of schizophrenia: the so-called "dopamine hypothesis". This model posits that schizophrenia is caused by an increased release of dopamine in the brain (hyper-dopaminergic state; (Snyder, 1976). The model progressed towards reviews and reconceptualization. Thanks to the analysis of *post-mortem* data, metabolites and imaging data, the dopamine hypothesis gained regional specificity. In particular, these studies showed that schizophrenia was not the result of a simple excess of dopaminergic transmission in the whole brain, but rather the effect of a regional-specific dopamine dysfunction: prefrontal hypo-dopaminergic

state and subcortical hyper-dopaminergic state (Abi-Dargham, 2004; Davis et al., 1991). The model received other updates in more recent years (Howes & Kapur, 2009). Recent advances in neuroimaging techniques have revealed that the dopaminergic dysfunction in schizophrenia is greatest in the nigrostriatal pathways as opposed to the mesolimbic pathway and in particular in the dorsal striatum (also called associative striatum) which is an integrative hub connected with both the cortex and the midbrain (McCutcheon et al., 2019). It has been proposed that psychotic symptoms arise from a combination of enhanced spontaneous phasic dopamine signalling and reduced adaptive release which increases the signal-to-noise ratio in the associative striatum in front of relevant stimuli (Maia & Frank, 2017). In the associative striatum, connections between medium spiny neurons (MSNs) of the direct and indirect pathways facilitate the signal integration and suppression of undesirable behaviour. In schizophrenia, the excess of dopamine release impairs this mechanism leading to altered behaviour such as aberrant salience, abnormal perceptions, and cognitive and negative symptoms. (McCutcheon et al., 2019). D_2R-blockade counteracts dopamine overactivity and enhances the suppressing activity of the indirect (i.e., no-go) MSN pathway. However, as antipsychotics do not have regional specificity desirable behaviours are suppressed along with undesirable ones (Kharkwal et al., 2016). Indeed D_2R-antagonism is a key mechanism responsible for antipsychotics' therapeutic efficacy but also for their side effects. The most important side effects caused by D_2R blockade are *neurolepsis*, prolactin increase with related sexual dysfunction and extrapyramidal symptoms (EPS). *Neurolepsis* has been already described above. Patients treated with FGAs usually present blunted affect, anhedonia, and cognitive deficits. Despite the similarity in the phenomenological presentation, these effects, are distinct from the primary negative symptoms and are usually dose-dependent. These symptoms are also known as "secondary negative symptoms" and they have been associated with D_2R blockade in the nucleus accumbens and the dopamine mesocortical pathway (Kirschner et al., 2017; Peralta et al., 2000). The antagonism of D_2R in the dopamine tuberoinfundibular pathway is responsible instead for the increase of prolactin plasma levels caused by FGAs. This condition is associated with galactorrhoea, amenorrhea, infertility, sexual dysfunction, weight gain and demineralization of bones, especially in postmenopausal women (Kapur & Remington, 2001). The most frequent side effects of FGAs are EPS. EPS include a variety of movement disorders very similar to those seen in Parkinson's disease: tremor, dystonia (spasm and persistent muscle contraction), rigidity, akathisia (motor

restlessness), and bradykinesia (slow movements). Although it cannot be properly classified as an EPS, tardive dyskinesia is also included in the group of motor side effects associated with antipsychotic treatment. Tardive dyskinesia is characterized by jerky movements, usually of the tongue or facial muscles (i.e., facial grimacing, chewing, etc.) and has been associated with prolonged exposure to FGAs. All EPS are thought to be caused by D_2R blockade in the nigrostriatal dopaminergic pathway (Farde et al., 1992). FGAs differ in potency (i.e., the amount of drug required to produce a pharmacological effect) and pharmacodynamic profile. Some FGAs have alternative targets responsible for side effects different from those related to D_2R blockade. For example, chlorpromazine and promazine are also histamine-1 (H_1) receptor blockers causing drowsiness, sedation and orthostatic hypotension (Peroutka & Synder, 1980). Some FGAs have also anticholinergic properties causing dry mouth, blurred vision, constipation, urinary retention, and cognitive dysfunction via muscarinic receptors (M_1) blockade (Georgiou et al., 2021; Joshi et al., 2021; Ozbilen & Adams, 2009).

SGAs are also called "atypical" antipsychotics because they have peculiar clinical and pharmacological properties that distinguish SGAs from FGAs (Leucht, Komossa, et al., 2009). Clinically, SGAs differ from FGAs mainly for their side effect profiles. SGAs tend to cause fewer EPS than FGAs, however, they are associated with a higher incidence of weight gain and diabetes and increased cardio-metabolic risk as compared with FGAs (Leucht et al., 2013). Pharmacologically, SGAs differ from FGAs because they all are serotonin-2A receptor ($5HT_2AR$) antagonists in addition to D_2R antagonists (Meltzer, 1988), and show peculiar pharmacological properties such as higher selectivity for the mesolimbic pathway and fast dissociation at D_2Rs (de Bartolomeis et al., 2015; Kapur & Mamo, 2003; Kapur & Seeman, 2001; Kapur et al., 1999). Serotoninergic neurons modulate the activity of dopaminergic neurons either directly with the action of postsynaptic $5HT_2AR$ on dopamine neurons or indirectly via the action of $5HT_2AR$ on interneurons. In particular, the $5HT_2AR$ acts as a modulator of dopamine release via its action on dopaminergic neurons (Auclair et al., 2004; Dewey et al., 1995; Porras et al., 2002). This mechanism is thought to explain clinical differences between FGAs and SGAs. PET and Single Photon Emission Computed Tomography (SPECT) studies revealed that patients with schizophrenia receiving SGAs had less D_2R occupancy in the striatum and fewer EPS than patients treated with FGAs (Bernardo et al., 2001; Gefvert et al., 2001; Stone et al., 2009). $5HT_2AR$ antagonism is also

thought to explain the reduction of other common side effects of FGAs like secondary negative symptoms (Fusar-Poli et al., 2015) and hyperprolactinemia (Hanssens et al., 2008). Classic hallucinogens like lysergic acid (LSD) and psilocybin which are all $5HT_2AR$ agonists can produce hallucinations and delusions as a consequence of the downstream effect on dopamine and glutamate release which are reverted by the administration of $5HT_2AR$ antagonists (Cumming et al., 2021). In this model, $5HT_2AR$ antagonism may reduce positive symptoms by reducing glutamate release in pyramidal neurons of the cortex and therefore lowering the downstream stimulation on the dopamine mesolimbic pathway (Aghajanian & Marek, 2000; Vollenweider et al., 1998). However, clinical trials with pure $5HT_2AR$ antagonist agents failed to demonstrate efficacy in reducing psychotic symptoms in patients with Schizophrenia (Ebdrup et al., 2011) indicating that D_2R blockade is critical for the treatment of this disorder. In conclusion, SGAs, with their $5HT_2AR$ antagonist property have a more complex mechanism of action than FGAs with actions on positive, negative (albeit modest) and cognitive symptoms and a significant reduction of EPS and hyperprolactinemia. Although SGAs cause fewer EPS and hyperprolactinemia than FGAs, they are not free from side effects. All SGAs are associated with weight gain, obesity, diabetes, dyslipidaemia, and therefore increased cardio-metabolic risk (Correll et al., 2009; Pillinger et al., 2020). The mechanism underlying this effect is thought to be related to increased appetite possibly caused by H_1 receptors and serotonin-2C receptor ($5HT_2CR$) antagonism, however, the mechanisms driving peripheral insulin resistance and dyslipidaemia have not been fully characterized (Elman et al., 2006). Some SGAs, in addition to $5HT_2AR$ antagonism, have another key pharmacological property that distinguishes them from FGAs. This is the case with drugs like aripiprazole which are D_2R partial agonists (DPAs). DPAs bind D_2R not causing full blockade (like FGAs) or stimulation (like agonists or dopamine itself). In particular, DPAs bind D_2R activating signal transduction to be intermediate between full and no output depending on the amount of dopamine present in the synaptic space (Lieberman, 2004). Another property of DPAs is fast dissociation from D_2R (Kapur & Seeman, 2001). Because of these mechanisms, DPAs can reduce positive symptoms reducing D_2R hyperactivity, without causing significant EPS because they do not completely antagonize D_2R. Although DPAs are commonly considered SGAs, some authors called this group of antipsychotics also "third-generation antipsychotics" (Mailman & Murthy, 2010).

1.2 The effect of antipsychotics on brain structure

1.2.1 Studies in patients with psychosis

Meta-analyses of longitudinal studies conclude that patients with psychosis show a decline in brain volume and thickness during the course of the treatment, particularly in the frontal and temporal lobes (Moncrieff & Leo, 2010; Navari & Dazzan, 2009; Smieskova et al., 2009). Some meta-analyses and large cross-sectional studies also found an association between grey matter reduction and cumulative antipsychotic exposure, suggesting a possible causal link between antipsychotic exposure and grey matter loss (Fusar-Poli et al., 2013; Haijma et al., 2013; Huhtaniska et al., 2017; van Erp et al., 2018). However, grey matter loss has also been associated with disease states such as duration of illness, disease severity and the number of relapses (Andreasen et al., 2013; Ho et al., 2011; van Erp et al., 2018). In addition, non-medicated and drug-naïve patients also show grey matter reduction as compared with HC (Fusar-Poli et al., 2012). Disentangling the direct effects of antipsychotic drugs on brain structure and disease state is challenging. For example, individuals with greater illness severity or treatment-resistant patients may require higher doses of antipsychotics, both of which could be associated with a greater degree of brain adaptations, both functionally and structurally.

Authors	Type of Study	Results
Moncrieff and Leo (2010)	Meta-analysis, n ~ 650	Progressive reduction of brain size and enlargement of brain spaces in people who are taking antipsychotics drug
Navari and Dazzan (2009)	Meta-analysis, cross-sectional and longitudinal studies	Global volumetric reductions, greater in frontal and temporal lobes, with greater association with typical than with atypical antipsychotics.
Smieskova et al. (2009)	Meta-analysis, cross-sectional and longitudinal studies	Typical and atypical antipsychotics associated with reduced frontal and temporal lobe volume.
van Erp et al. (2018)	Multi-centre, n ~ 4500	Regional cortical thickness negative correlated with medication, disease severity, and duration
Haijma et al. (2013)	Meta-analysis, n ~ 18 000	Gray matter cortical reductions but subcortical increases associated with longer illness duration and higher dose of medication.
Fusar-Poli et al. (2012)	Meta-analysis, n ~ 800	General grey matter reductions in drug naïve subjects
Fusar-Poli et al. (2013)	Meta-analysis, n ~ 1800, follow-up ~ 72 weeks	Gray matter volume decreases associated with cumulative antipsychotic exposure

Huhtaniska et al. (2017)	Meta-analysis, *n* ~ 700, follow-up > 2 years	Gray matter volume decreases, and basal ganglia increases associated with cumulative antipsychotic exposure
Ho et al. (2011)	Longitudinal, *n* ~ 200, follow-up ~7 years	Gray matter decreases associated with cumulative antipsychotic exposure.
Andreasen et al. (2013)	Longitudinal, *n* ~ 200, follow-up ~7 years	Decreases of total and regional (e.g., frontal) cerebral volume associated with number of relapses and cumulative antipsychotic exposure
Chopra, Fornito, et al. (2021)	Longitudinal, randomized, controlled, triple-blinded, n ~ 90, follow-up 6 months	Increased volume in the pallidum at 3 months associated with greater reduction in symptom severity. No differences at 12 months.
Andersen et al. (2020)	Longitudinal, HC parallel control group, FEP= 21, HC= 23, follow-up 6 weeks	Increased striatal volume (right caudate nucleus and right putamen) correlated with amisulpride plasma levels.
Voineskos et al. (2020)	Longitudinal, randomized, double blind, n ~ 80, follow-up 36 weeks	Reduction in cortical thickness in patient treated with olanzapine as compared with the ones in the placebo arm.

Table 1. Collected evidence on the association between brain grey matter alteration and treatment with antipsychotics in patients with psychosis.

Andersen et al. (2020) investigated in a longitudinal study the effect of 6 weeks of amisulpride in a cohort of antipsychotic naïve, first-episode schizophrenia patients paralleled with a healthy control group. They restricted their investigation to basal ganglia volume changes reporting a significant increase in grey matter volume in both the right caudate nucleus and the right putamen as compared with controls. Interestingly the changes also correlated with amisulpride plasma levels but not with D_2R occupancy evaluated with SPECT. Notably mean amisulpride dose was relatively low (~200 mg) and achieved on average ~40% D_2R occupancy in the striatum which is below the therapeutic range for antipsychotic efficacy (Kapur et al., 2000).

Placebo-controlled studies in patients are difficult to design because of ethical concerns. Nonetheless, results from two placebo-controlled trials have been published over the last few years. Voineskos et al. (2020) found in a 36-week placebo-controlled trial in patients with psychotic depression a reduction in cortical thickness in patients treated with olanzapine as compared with the placebo arm. No changes were found in cortical surface area, subcortical volumes, and fractional anisotropy (FA). Notably, patients were randomly assigned to the active or placebo arm after having reached remission of both psychosis and depression in a previous trial with a combination of olanzapine and sertraline. The study did not address any specific effect of the antidepressant medication which further limits the generalizability of the findings. Chopra, Fornito, et al. (2021) investigated in antipsychotic naïve FEP the effects of

SGAs (risperidone or paliperidone) against placebo in 6 months. Both active and placebo arms received psychosocial therapy. The two groups were also paralleled with a longitudinal cohort of HC. At 3 months, the authors found an increase in pallidal grey matter volume in patients treated with antipsychotics, a reduction in the placebo arm and no changes in the HC cohort. In addition, a greater increase in pallidal volume was associated with a greater reduction in symptom severity. However, pallidal volume normalized in both active and placebo arms after 12 months. Even though the results of these studies partially fit with the results of uncontrolled longitudinal studies, a direct comparison of the two placebo-controlled studies reveals inconsistent results (i.e., pallidal grey matter increase vs. no change in the basal ganglia). This inconsistency may reflect differences in the study design, patient characteristics, treatment regime and other disease states, or other possible technical confounding variables (see below section 1.2.4). In addition, as the evidence comes from few, small placebo-controlled studies it is not possible to draw definitive conclusions. More studies and meta-analyses are therefore needed to control for a possible publication bias which skews the literature to positive results obtained in small studies.

1.2.2 Single-dose studies in healthy volunteers

One way to isolate disease effects from the direct effect of D_2R blockade on brain structure is to implement experimental studies in healthy volunteers. At the time of writing the present thesis, two studies investigated the effect of single-dose administration on brain volume and structure in healthy volunteers. Tost et al. (2010) investigated in seven antipsychotic naïve healthy male volunteers the effect of a large acute haloperidol intravenous challenge (5mg per 70kg of body weight) on brain volumes. The authors found using Voxel-Based Morphometry (VBM) a decrease in the volume of the ventral putamen with partial recovery after one half-life interval of the drug (24 hours). These results were not replicated by other authors (Hawkins et al., 2018) who investigated the effect of an oral single dose of different antipsychotics (i.e., haloperidol 3mg, olanzapine 7.5mg, risperidone 0.5mg and 2mg) in a randomised, placebo-controlled, crossover study in male healthy volunteers. The authors found no change in brain volume across sessions and used different volumetric analysis techniques. Interestingly, the authors complemented their results, also reporting no effects of acute antipsychotic challenge on quantitative T1 relaxometry maps which returns more information on brain microstructure as compared with standard T1-weighted maps. The two

studies report inconsistent results, which might be related to the different routes of administration (intravenous vs. acute challenge), the dose of the drug (5mg/70kg vs. 3mg fixed oral) and the different study designs (uncontrolled vs. placebo-controlled).

1.2.3 Pre-clinical studies

The collected evidence of pre-clinical studies of animal exposure to D_2R blockade indicates an effect of reduction of brain volumes. In particular, models of chronic exposure to haloperidol and olanzapine in both normal rats (Drazanova et al., 2019; Vernon et al., 2014; Vernon et al., 2012; Vernon et al., 2011) and non-human primates (Dorph-Petersen et al., 2005) showed a reduction in brain volume in the frontal and parietal cortex. Andersson et al. (2002) found, together with decreased cortical volumes, also increased caudate-putamen volumes in adult rats chronically treated with haloperidol and clozapine whereas olanzapine-treated animals showed a reduction in striatal volumes. These results have been later replicated in mice (Guma et al., 2018). Interestingly, mice lacking D_2R did not show brain alterations after antipsychotic exposure highlighting the specific role of D_2R blockade on structural brain alterations induced by antipsychotics (Guma et al., 2018). To date, only one pre-clinical study (Fujimoto et al., 1987) investigated the effect of acute challenge of antipsychotic on quantitative T1 relaxation time, finding an increase in T1 in the striatum of dogs receiving intravenously a 20mg dose of haloperidol using a very low spatial resolution as compared with current standards. The results of this study have never been replicated.

1.2.4 Limitations of brain volumetric studies

An important, but seldom carefully considered, limitation of brain volumetric MRI studies is that MRI does not return a direct measure of brain volume or structure. MRI images are made from changes in intensity as a function of proton relaxation times (i.e., T1, T2) which may be influenced by several physiological, pathological, pharmacological, and artefactual factors. In other words, changes or differences in brain volumes assessed with structural MRI might represent just epiphenomena of different biochemical or physical effects not necessarily linked with the pathophysiological process under investigation (Weinberger & Radulescu, 2016). In addition, alterations of brain morphometry (i.e., volume, thickness, etc.) may not necessarily be interpreted as the result of a neurodegenerative process. Microstructural changes can manifest in changes in the volume or thickness of brain structure

during neurodevelopment or other neuroplastic processes. For example, Natu et al. (2019) have shown that differences in brain myelination during neurodevelopment can lead to apparent alterations of cortical thickness because of changes in T1 depending on the variation of the amount of myelin in the tissue. Another example is the change in CBF induced by pharmacological challenges which may masquerade as brain volumetric changes (Franklin et al., 2013). This possibility, however, did not receive confirmation in a subsequent placebo-controlled study in healthy volunteers, where acute exposure to a single dose of antipsychotic was associated with increased CBF in the basal ganglia without significant changes in either T1 or brain volumes (Hawkins et al., 2018). Since it is virtually impossible to systematically control all possible confounding factors in cross-sectional case-control MRI studies, some authors have recommended caution when interpreting results reporting brain volumetric changes suggesting to replace expression as "cortical thinning", "atrophy", "tissue loss", etc. with more neutral statements such as "differences in MRI measurements" (Weinberger & Radulescu, 2016, 2021). At the same time, technological advantages can offer the opportunity to increase our biological understanding of changes in MRI signals by integrating T1-weighted sequences with other MRI measures such as CBF and quantitative T1 mapping (Hawkins et al., 2018).

1.3 The effect of antipsychotics on brain perfusion

1.3.1 Studies in patients with psychosis

Altered brain perfusion has been implicated in the neurobiology of psychosis, initially with PET studies with $[^{15}O]H_2O$ which reported hypoperfusion in frontal, anterior cingulate, temporal, and parietal cortices (Goozee et al., 2014; Hill et al., 2004). Longitudinal PET studies with $[^{15}O]H_2O$ showed that drug naïve FEP, had greater perfusion in the basal ganglia after treatment with antipsychotics (Lahti et al., 2005; Miller et al., 1997; Miller et al., 2001). More recently, Arterial Spin Labelling (ASL) utilizing MRI, has been used to measure CBF. ASL studies in people with chronic schizophrenia, treated with antipsychotics, show reduced CBF in frontal, parietal and occipital regions and increased CBF in the basal ganglia (Aghajanian & Marek, 2000; Legind et al., 2019; Liu et al., 2012; Oliveira et al., 2018; Pinkham et al., 2011; Pinkham et al., 2015), though the basal ganglia findings have not been consistently replicated (Ota et al., 2014; Zhu et al., 2017). Thus, there is evidence for cortical

hypoperfusion in chronic schizophrenia, but it is unclear from these studies when this occurs in the development of the disorder. Studies in clinical high-risk for psychosis (CHR-P) individuals have reported increased CBF in basal ganglia and hippocampus (Allen et al., 2018; Allen et al., 2016; Modinos, Egerton, et al., 2018). Increased hippocampal perfusion in CHR-P individuals has also been found with gadolinium-enhanced MRI (Schobel et al., 2013). These findings indicate that CBF alterations may occur early in the development of psychosis, though, because most CHR-P subjects do not go on to develop psychosis, it is unclear how specific they are to psychosis. To date, only one study has investigated cerebral perfusion using ASL in FEP patients (Kindler et al., 2018). This study found increased perfusion in basal ganglia and reduced CBF in the frontal cortex in people with FEP, all of whom were taking antipsychotic medication. Given the collected literature it is therefore unclear what is the extent of the interaction between antipsychotic effects on CBF and alterations in brain perfusion related to pathophysiology.

1.3.2 Single-dose studies in healthy volunteers

Early evidence in humans of increased striatal CBF after antipsychotic administration comes from PET [^{15}O] H_2O studies (Mehta et al., 2003). Similar results were also obtained in more recent studies using ASL. In particular, Fernandez-Seara et al. (2011), reported increased CBF in the striatum and thalamus in healthy volunteers after a single oral dose of 10 mg of metoclopramide. Handley et al. (2013) showed that both single oral doses of haloperidol 3mg and aripiprazole 10mg increased CBF in the striatum in healthy volunteers with a larger effect size for haloperidol. Consistently, Hawkins et al. (2018) found in an oral single-dose study in healthy male controls that haloperidol 3mg, and risperidone 2mg and 0.5mg increased striatal CBF compared to placebo. Michels et al. (2016) reported increased CBF in several brain regions including the striatum, the insula, and the prefrontal and parietal cortex in healthy volunteers after a single dose of quetiapine 100mg even though these results should be considered with caution as they were not corrected for multiple comparisons. Viviani et al. (2013) investigated the effect of repeated daily oral doses of amisulpride 200mg after a period of 7 days on CBF assessed with ASL in healthy male volunteers. They found that relative to placebo, amisulpride 200mg was associated with a large significant cortical reduction in CBF particularly in the prefrontal lobes and a modest increased perfusion in the basal ganglia (albeit not corrected for multiple comparisons). Notably, amisulpride, as other benzamides

(e.g., sulpiride), at low doses as the one used in the study by Viviani et al. (2013), shows a selective modulation of dopamine release in the dopaminergic mesolimbic pathway acting preferentially on pre-synaptic D_2R (i.e., D_2R short isoform) (Pani & Gessa, 2002). Taken together these studies indicate that, independently from the drug used, acute D_2R-blockade is associated with increased perfusion in the basal ganglia. The result by Viviani et al. (2013) does not allow us to draw a definite conclusion on whether the effects persist after sustained D_2R-blockade within a therapeutic range desirable for antipsychotic efficacy (i.e. at least 60% of post-synaptic D_2R occupancy) (Kapur et al., 2000).

1.3.3 Pre-clinical studies

Results of pre-clinical studies, investigating the effect of D_2R blockade induced by antipsychotics on brain perfusion are mixed. Nordquist et al. (2008) reported a dose-dependent reduction in perfusion as assessed with ASL in the piriform cortex, perirhinal cortex, nucleus accumbens and amygdala and a trend towards an increase in the dorsal striatum in rats receiving an acute intraperitoneal injection of 1 to 30mg of aripiprazole. Notably, these changes were not absolute CBF changes but normalized to whole brain perfusion. These results were not replicated after chronic (30 days) exposure to aripiprazole of poly(I:C) exposed rats (i.e., an animal model of neurodevelopmental disorder) (Drazanova et al., 2018). Another animal ASL study (Drazanova et al., 2019) investigated the effect of acute and chronic (8 weeks) exposure to olanzapine in rats reporting a reduction of CBF in the sensorimotor cortex and no change in the hippocampus and piriform cortex. No other brain regions were specifically tested in this study.

A much larger pre-clinical literature has linked dopamine function and modulation of dopamine receptors (including D_2R) to neurovascular coupling and changes in haemodynamic-related MRI signals (Chen et al., 2005; Choi et al., 2006; Mandeville et al., 2011; Schwarz et al., 2004). Mandeville et al. (2013) recapitulated this literature and put forward a physiological model linking the fMRI temporal response in the basal ganglia to variation in dopamine release and modulation of dopamine receptors such as enhanced dopamine release and endogenous stimulation of post-synaptic D_2R produced a dose-dependent reduction in MR haemodynamic response of the basal ganglia. The authors also proposed that modulation at dopamine D_1 receptors (D_1R) and D_2R by agonist and antagonist can alter this relationship depending on the affinity and occupancy at the target receptor

(Mandeville et al., 2013). In line with the proposed model, the same group found, using simultaneous PET/MR, a monotonic increase in regional Cerebral Blood Volume (CBV) following injection of an increasing dose of the D_2R antagonist radiotracer [^{11}C] raclopride in the striatum of two male rhesus macaques (Sander et al., 2013). Interestingly, [^{11}C] raclopride non-displaceable binding potential (BP_{ND}) changes reflecting changes in D_2R receptor occupancy, correlated with the amplitude of hemodynamic changes (i.e., CBV): the higher the dose the larger CBV increase; and in time: BP_{ND} variation and changes in CBV showed similar temporal profiles. The same group also found an inverse relationship between receptor occupancy and CBV with the selective D_2R agonist quinpirole in male rhesus macaques (i.e., CBV decrease in the face of dose-dependent increase of receptor occupancy) (Sander et al., 2016). Overall, the collected pre-clinical evidence supports a neurovascular coupling mechanism linking MR haemodynamic changes and D_2R pharmacological modulation in the basal ganglia, although stronger evidence has been reported in studies in non-human primates as compared with murine models. To date, these findings have not been translated to humans.

1.4 The effect of antipsychotics on functional connectivity

1.4.1 Studies in patients with psychosis

Alterations in brain connectivity patterns at rest have been largely investigated in patients with psychosis compared to HC with consolidated evidence of alterations within cortico-striatal-thalamic loop circuits (Anticevic et al., 2014; Avram et al., 2020; Horga et al., 2016; Sabaroedin et al., 2023; Sarpal, Argyelan, et al., 2016). However, as previously discussed, cross-sectional studies in patients are not able to disentangle between disease and treatment effects. Few studies have investigated the effect of antipsychotic treatment using longitudinal designs. Lui et al. (2010) investigated the effect of 6 weeks of antipsychotic treatment on FC in antipsychotic-naïve patients with schizophrenia. They found that, as compared with baseline, patients showed increased synchronous brain activity (as evaluated with amplitude of low-frequency fluctuations, ALFF) in several brain regions including the frontal gyrus, the superior and inferior parietal lobule, the medial frontal cortex and the caudate. In addition, using both seed-based and Independent Component Analysis (ICA) approaches, the authors found a widespread reduction of FC between these brain regions after treatment with antipsychotics. Interestingly, in comparison with matched HC, patients showed decreased

ALFF when naïve only in the prefrontal cortex and increased ALFF in the caudate and putamen after treatment. These results are in line with CBF findings described in the previous section suggesting that the local effects in the basal ganglia, expected because of the high density of receptors present, might be accompanied by non-local effects in the cortex in key brain regions relevant for psychotic disorders such as the frontal and parietal cortices. Sarpal et al. (2015) directly investigated the effects of antipsychotic treatment (i.e., 12 weeks of either aripiprazole or risperidone at clinically effective doses) on cortico-striatal connectivity in FEP with a longitudinal study design. They performed a seed-based connectivity analysis on resting state fMRI data segmenting the basal ganglia in 12 seeds (6 by hemisphere). They found no differences between FEP and controls at baseline. They reported significantly increased connectivity between the seed in the right ventral caudate and the left thalamus and the right nucleus accumbens in FEP associated with treatment response such as patients with better clinical outcomes had increased connectivity between the dorsal striatum and the prefrontal cortex and decreased connectivity between the ventral striatum and posterior regions. Notably, FEP were not naïve at baseline, albeit treated for less than 2 weeks. Other studies investigated the effect of antipsychotic treatment in longitudinal designs on thalamocortical connectivity reporting an increased connectivity over time (Berge et al., 2022; Chan et al., 2022; Chopra, Francey, et al., 2021; Duan et al., 2020). Finally, other authors found, using longitudinal designs, changes in FC over time in patients with psychosis only as a function of treatment response (Duan et al., 2020; Kraguljac et al., 2016; Lin et al., 2021) while others identified normalization of abnormal connectivity patterns present at baseline (Abbott et al., 2013; Anticevic et al., 2015; Guo et al., 2017; Keedy et al., 2009; Nejad et al., 2012; Sambataro et al., 2010; Snitz et al., 2005; van Veelen et al., 2011). To sum up, the evidence converges to changes in FC between cortical and subcortical regions in patients with psychosis after treatment. These results also highlight that antipsychotic treatment might be associated with non-local effects through the modulation of the function of brain regions innervated by D_2R such as the striatum and the thalamus. However, as discussed for other imaging modalities, these studies do not allow us to fully disentangle net treatment effects from disease states and traits associated with changes in neurobiology and other sources of clinical heterogeneity.

1.4.2 Single-dose studies in healthy volunteers

FMRI experiments in healthy volunteers also reported altered FC in the basal ganglia. Along with the structural findings reported in section 1.2.2, Tost et al. (2010) found functional decoupling (i.e., negative FC) between the striatum and the motor cortex after an acute intravenous challenge with haloperidol 5mg per 70kg in seven healthy volunteers. Interestingly, the authors also report that cortico-striatal dysconnectivity within the motor circuit was also associated with slower reaction time during a motor activation task. This effect subsequently normalized after one-half life of the drug. It should be noted, however, that this study adopted a serial pharmacological MRI experiment without placebo-controlled sessions. Cole, Oei, et al. (2013) in a placebo-controlled, randomised, parallel-group resting-state fMRI study in healthy male volunteers receiving a single dose of levodopa 100mg or haloperidol 3mg, found a linear trend (levodopa > placebo > haloperidol) of altered cortico-subcortical FC. As regards D_2R blockade, the authors found that the haloperidol-treated group had reduced FC between the posterior default-mode network and the midbrain, between the frontoparietal network and the dorsal caudate, between the fronto-insular network and the ventral striatum and between the frontoparietal network and the thalamus. In a re-analysis of the same datasets using ICA the same authors reported a decreased connectivity in the haloperidol group as compared with placebo between the basal ganglia and the motor cortex, while the antero-centric default-mode network (DMN) showed greater connectivity with the precentral and middle frontal gyri and lower connectivity with the supramarginal gyrus in the haloperidol group as compared with placebo (Cole, Beckmann, et al., 2013). Grimm et al. (2020) performed a similar study using a cross-over design in healthy volunteers of both sexes receiving a single dose of either levodopa 125mg, amisulpride 200mg or placebo. The authors reported that D_2R blockade was associated with an increased FC between the putamen and the precuneus and between the nucleus accumbens and the supplemental motor cortex. Amisulpride administration was also associated with reduced seed-based connectivity from the substantia nigra to the postcentral gyrus and the cerebellum. Altered FC within the cortico-striatal-thalamic loop has also been reported in single-dose experimental studies in healthy volunteers using task-based fMRI (Diaconescu et al., 2010; Honey et al., 2003). To the best of my knowledge, only one study (Metzger et al., 2015) has investigated the effect of repeated daily doses of antipsychotics on FC in healthy volunteers. In this study, the authors investigated, in a randomized, double-

blind, placebo-controlled crossover study, the effects on resting-state FC after one week of daily doses of either reboxetine 4mg, amisulpride 200mg or placebo. They found that, as compared with placebo, 7 days of daily doses of amisulpride was associated with increased ALFF in the putamen which correlated with amisulpride plasma levels. In addition, the authors also reported a widespread pattern of altered FC after amisulpride as compared with placebo which included the locus coeruleus, the amygdala, the substantia nigra and the nucleus accumbens. However, it is important to highlight that their results were reported without correction for multiple comparisons. Moreover, as discussed earlier in section 1.3.2, the use of the dose of 200mg of amisulpride might not be sufficient to achieve a level of post-synaptic D_2R blockade that allows an adequate translation of these results at the clinical level. Overall, the existing literature indicates that acute exposure to D_2R blockade alters cortico-subcortical FC. However, it is still unclear how these alterations are related to behavioural effects and how results after acute challenge compare with sustained D_2R antagonism.

1.4.3 Pre-clinical studies

The pre-clinical literature on the effect of D_2R blockade on FC is scarce. To the best of my knowledge, only one study investigated the effect of a single dose of haloperidol 1mg/kg on FC using resting-state fMRI in rats using a placebo-controlled design (Gass et al., 2013). The authors found a decrease in FC between the substantia nigra and several brain regions such as the frontal and cingulate cortex, the motor cortex, and the ventral pallidum. This animal study further confirms the human evidence on perturbation of the cortico-nigro-striatal network after D_2R blockade.

1.5 Effects on brain structure and function and antipsychotic pharmacodynamic: the PK/PD model

The main goal of pharmacological MRI is to identify the effects of drug administration on brain structure and function. Over the last few years, the use of MRI in pharmacology research has become increasingly important as a tool to assess drug brain penetration, investigate the relationship between brain response and clinical outcome and assist go-no-go decisions in the drug development process (Nathan et al., 2014; Schwarz et al., 2011). Pharmacological MRI has also delivered important results for neuroscience allowing the investigation of drug-induced modulation of specific pathways and brain networks in

controlled experimental settings (Khalili-Mahani et al., 2017). However, as discussed previously, one limitation of pharmacological MRI studies relies on the nature of the MRI signals which do not allow a direct link between brain effects and drug mechanism of action. Receptor occupancy theory posits that the magnitude of the drug response is a function of receptor availability (Clark, 1937). In other words, incremental changes in functional response correspond to increments of the fraction of receptors bound. This relationship also depends on specific characteristics of each compound, such as dissociation or affinity constant (K_d) (Ploeger et al., 2009) as in the following equations:

$$[D] + [R] \underset{K_d}{\leftrightarrow} [DR] \rightarrow Effect$$

Equation [1]: Receptor occupancy theory (Clark, 1937)

$$K_d = \frac{[D][R]}{[DR]}$$

Equation [2]: Dissociation or affinity constant

MRI measures such as T1 relaxation time and MRI signals based on haemodynamic changes (e.g., Blood-Oxygen-Level-Dependent signal (BOLD), CBV, CBF) are not able to measure neuronal activity directly or to directly detect the biochemical mechanism of drug-receptor binding. Therefore, in the absence of a direct link between drug binding and MRI effects, the interpretation of the results in pharmacological MRI studies in the context of drug pharmacokinetics (PK) and pharmacodynamics (PD) is often relegated to speculations. Applied pharmacology often integrates PK data (i.e., drug-concentration time series in the system after drug administration) with PD effects (i.e., the observed effect corresponding to drug concentration) in unified models called pharmacokinetic/pharmacodynamic (PK/PD) models to identify dose-concentration-response relationships and subsequently develop predictive models (Meibohm & Derendorf, 1997). Several pharmacological MRI studies have investigated the relationship between variations in drug concentration and brain functional effects including PK modelling in neuroimaging analysis. Using this approach it has been possible to create PK profiles of the brain functional response of different compounds such

as ketamine (De Simoni et al., 2013; Doyle et al., 2013), psilocybin (Carhart-Harris et al., 2012; Preller et al., 2020), tetrahydro-cannabidiol (THC) (Klumpers et al., 2012) and anaesthetics (Becerra et al., 2006). Another approach to explore the PK/PD relationship in pharmacological MRI is to enhance molecular specificity of drug effects in the brain by integrating data from other modalities (e.g., PET, SPECT, post-mortem autoradiography, post-mortem mRNA, or protein assays, etc.) that allows an estimate of receptor distribution in the brain. Under the assumption, justified by the receptor occupancy model, that drugs exert their effects in brain regions that have higher target receptor density or higher affinity or higher binding potential, it is possible to characterise brain topography of drug effects by evaluating the association between drug effects and receptor distribution in the brain. This approach has been recently proposed to investigate the brain functional effect of different drugs (Dipasquale et al., 2020; Dipasquale et al., 2019; Dukart et al., 2018; Wong et al., 2022). Even though the spatial architecture of protein distribution in the brain is typically consistent across individuals (Hawrylycz et al., 2012), between-subjects variation in receptor density within the same brain region is not negligible (Farde et al., 1995) and may drive inter-individual differences in drug brain effects. In addition, drug distribution and elimination are heavily influenced by several physiological factors such as age, sex, body weight, water, fat composition of the tissue, etc., which further contribute to inter-individual variability in drug response. Therefore, individualized receptor profile mapping together with detailed PK information is necessary to generate PK/PD models that are generalizable at the level of the individual. As described in section 1.3.2 for the case of antipsychotics and changes in CBF related to D_2R-blockade, PK/PD models have been investigated in preclinical studies (Mandeville et al., 2013; Sander et al., 2013; Sander et al., 2016) but still, a full translation in humans is lacking. Detailed PK/PD modelling of antipsychotic effects on brain structure and function can enhance our understanding of biological mechanisms underlying between-subject variability in clinical response and side effects which are both important goals in psychiatry research.

1.6 Integration of neuroimaging analysis with whole brain transcriptome data

The release of the AHBA (Hawrylycz et al., 2012) offered the opportunity to integrate novel measures of brain target distribution with neuroimaging data. The AHBA is a free-access multimodal dataset (Shen et al., 2012) containing comprehensive genome-wide whole-brain

microarray transcriptomic, structural MRI and histological information obtained from six healthy adult human donors. The atlas features the expression levels of >20,000 genes profiled by ~60,000 microarray probes in different brain regions that are spatially resolved in the standard Montreal Neurological Institute (MNI) coordinates system which allows a one-to-one spatial matching with neuroimaging data (Shen et al., 2012). Transcriptomic data from the AHBA is associated with T1-weighted images (McColgan et al., 2018), T1-weighted/T2-weighted ratio images (Ritchie et al., 2018), cortical thickness (Shin et al., 2018), diffusion-weighted MRI images (Forest et al., 2017; Romme et al., 2017), PET data (Beliveau et al., 2017; Komorowski et al., 2020; Rizzo, Veronese, Heckemann, et al., 2014), fMRI networks and FC measures (Hawrylycz et al., 2015; Richiardi et al., 2015). Since the AHBA publication in 2012, several authors developed distinct pipelines to process AHBA data and match them with brain images. Notably, AHBA data analysis is a non-trivial task because different choices could be made in the various analysis steps required to integrate mRNA expression measures with imaging data. Analysis of complex data is at higher risk of poor reproducibility without standardization of methods. Five sources of variability in AHBA data analysis can potentially impact the results: i) probe selection, ii) spatial mapping of samples, iii) data normalization and between-donors variability, iv) region selection, and v) statistics.

Probe selection

In the AHBA, mRNA expression for each gene is measured with multiple probes (on average 2.0 ± 1.4 probes per gene). Therefore, it becomes important to define a unique mRNA profile that is representative of each gene. Even though the AHBA documentation suggests data filtering strategies based on the intensity of the signal compared with background noise, (http://human.brain-map.org/static/docs), to date there is no consensus on which is the best method for probe selection when 2 or more probes pass this threshold for the same gene. Many different strategies have been proposed for probe selection including filtering against background noise or comparison against the expression of housekeeping genes (French & Paus, 2015), consistency measures (e.g., correlations between probes) (Burt et al., 2018), and distribution-based measures (e.g., by discarding probes showing the highest variance (Richiardi et al., 2015) or the least skewed distribution (Rizzo et al., 2016)). Other authors did not select any probe and instead utilized all available probes (Rizzo, Veronese, Tonietto,

et al., 2014) or created a unique profile by simply averaging their expression (Ritchie et al., 2018). Another method that has been proposed for probe selection is to compare microarray data with RNA sequencing (RNAseq) data which offers higher sensitivity and specificity as compared with the microarray technique. However, the implementation of this method is limited by the fact that RNAseq data in AHBA is available only for two donors (and for a limited number of samples). Finally, another relevant issue is that the AHBA contains not-annotated probes and there is a risk that probes currently assigned to a specific gene in the AHBA could need re-annotation given the continuous updates of the public sequencing databases (Romero-Garcia et al., 2018).

Spatial mapping of samples

The Allen Institute, before dissection, acquired whole-brain T1-weighted MRI images from each donor which were subsequently registered in standard MNI space, such that mRNA samples across brain regions could be identified using native and MNI coordinates. In addition, each sample is associated with an anatomical ID. Even though a common standard space allows a one-to-one matching between mRNA expression and imaging signals, the distribution of AHBA sampling is sparser and more discrete than voxel-wise images that are commonly used in neuroimaging. One possible solution that has been proposed to overcome this issue is to implement a region-based segmentation approach where the whole AHBA dataset is resolved into discrete brain regions using a reference atlas (French & Paus, 2015). This approach has two main drawbacks: i) the transcriptomic-imaging integration is highly dependent on the atlas adopted, and ii) it might be possible that samples are inaccurately assigned to a different brain region that is close to the one where the sample was taken originally. To mitigate these problems, other authors took advantage of the detailed anatomical annotations of the AHBA instead of using external atlases (Cioli et al., 2014). The AHBA provides, along with each tissue sample, anatomical annotations (called anatomical IDs). These annotations are offered at two different resolutions: coarse level (26 regions) and structure level (169 regions). Brain images can then be resampled in the AHBA space identifying each transcriptomic sample and its corresponding imaging sample. Works that use the AHBA anatomical annotations have the advantage that they work on a common parcellation framework that is provided by the AHBA and that is closer to the raw data, even though it does not always match segmentations typically used in imaging analysis. Finally,

another important source of variability is related to the fact that donors differ in each region regarding both the number and position of the samples.

Region selection

Related to the previous point, several different strategies have also been used to select brain regions used to carry out correlation analysis of AHBA data with imaging datasets. For instance, some authors limited the analyses to cortical regions (Richiardi et al., 2015) whereas other authors performed cross-correlations in the whole brain, including both cortical and subcortical areas (Beliveau et al., 2017). Variance in gene expression has been reported to be different between cortical and subcortical regions (Hawrylycz et al., 2015) and therefore the inclusion or the exclusion of subcortical areas from the analysis could potentially lead to different degrees of inconsistency in the results depending on the homogeneity of mRNA expression across brain regions. In addition, AHBA sampling covered only the left hemisphere for four donors whereas for two donors both hemispheres were covered. Given the fact that the impact of lateralization on specific gene sets and specific brain regions is still unknown, this issue must be considered when performing region selection. Finally, as discussed before, brain regions can have quite a substantially different number of samples, questioning whether there should be a minimum number of samples defining the mRNA expression of a particular region to be chosen for the analysis. Irrespective of the number of samples, brain regions also differ in terms of spatial extension. Large regions are expected to show higher variability in gene expression, as they are more likely to encompass sub-regions characterized by different gene expression patterns (Vertes et al., 2016).

Data normalization and between-donor variability

AHBA data comes from the post-mortem brains of 6 different donors. The donors are 5 males and 1 female, the age range is 24–57 years and they have different ethnic backgrounds (3 Caucasians, 2 African Americans, 1 Latin). Donors also differ in many other characteristics: cause of death, post-mortem intervals, brain pH, tissue cytoarchitectural integrity, RNA quality, number of sampling, sampling sites, number and type of probes used for each gene (http://human. brain-map.org/static/docs). While preserving this information might be valuable for analysis within the AHBA data, between-donor variability must be minimized when AHBA data is aggregated for cross-comparison with external imaging

datasets. Even though recommendations have been proposed (Arnatkeviciute et al., 2019), there is still no consensus on normalization strategies.

Statistics

Another relevant point of disagreement between studies is which statistical test is used to correlate AHBA mRNA expression measures with imaging data. Most authors employed Spearman rank correlation analysis given the fact that AHBA data pooled from all the donors and all the regions does not follow a normal distribution for most of the genes (French & Paus, 2015; Komorowski et al., 2020). However, other authors employed the General Lineal Model and Pearson correlation (Beliveau et al., 2017; Veronese et al., 2016). Generally, normality should be always checked beforehand or non-parametric testing should be used as a countercheck. Another correlational strategy that has been proposed to control for inter-subject heterogeneity is the use of multivariate correlations where mRNA data from different donors is weighted to reflect biological variability (Rizzo et al., 2016). Another important issue when assessing the spatial association between neuroimaging data and AHBA transcriptomics is the statistical assumption of covariance stationarity of the measures between brain regions. However this assumption not always is reflected in the data and this can lead to inflated statistics and spurious results (Burt et al., 2020). Different approaches based on spatial permutation have been proposed to minimise this risk (Markello et al., 2021; Vasa et al., 2018).

1.7 The rationale of the studies and PhD projects description

The overall aim of this thesis is to provide a more detailed understanding of the effects of clinically relevant D_2R blockade on brain structure and function trying to disentangle disease from treatment effects. Despite a large body of literature, several aspects of dopaminergic modulation of brain structure and function remain unclear. While this literature has demonstrated changes in cerebral perfusion, it was not known how these changes across the entire brain could be understood through predictions from receptor occupancy theory and if similar effects would occur with sustained D_2R blockade. In addition, it remains unclear whether between-subject differences in PK and drug occupancy can explain differences in drug functional effects in vivo in humans. Moreover, the evidence for structural changes is not generally supported by single-dose studies using doses in the clinical range but has been

shown in longitudinal studies in patients, which are uncontrolled. A multimodal placebo-control study with sustained D_2R blockade could fill this gap of knowledge. Finally, to understand the effects of psychosis on perfusion, unaffected by medication, a study in an unmedicated cohort is required.

The three specific aims of this thesis are therefore:

1) Clarify the link between brain changes and D_2R occupancy in line with preclinical PK/PD models.
2) Investigate how changes in brain structure and function observed in experimental studies in healthy volunteers after single-dose administration compare with experimental designs of sustained D_2R blockade, thus in a dosing regimen close to the clinical practice.
3) Considering the strong evidence of altered CBF in the basal ganglia after D_2R blockade, investigate CBF in non-medicated patients with psychosis to disentangle medication and disease effects.

To investigate these aspects, my PhD included three projects: spatial profiling of antipsychotic effect on brain perfusion to D_2R distribution, the NEuroreCepTor regulation of brAin structuRe and function (NECTAR) study, and the investigation of brain perfusion in antipsychotic-free FEP patients.

1.7.1 Spatial profiling of antipsychotic effect on brain perfusion to D_2R brain distribution

This project aims to investigate the spatial association between changes in CBF after single-dose administration and normative distribution of D_2R following the principles of the drug receptor theory discussed in section 1.5. I developed a neuroimaging analysis workflow that integrates ASL data with other datasets informative of D_2R distribution in the brain such as PET templates using radioligands with D_2R affinity and mRNA data from the AHBA. Critically, as discussed in section 1.6, the use of post-mortem mRNA data required thorough consideration of the analysis pipelines and comparison between methods (Selvaggi et al. (2021) and Appendix B).

1.7.2 The NECTAR study

The NECTAR study is a within-subject, cross-over, double-blinded, placebo-controlled experimental medicine study in healthy volunteers. Participants received either daily doses of the D_2R antagonist amisulpride (400mg) or placebo for a period of one week followed by placebo or started with placebo and then received amisulpride. A washout period of at least 10 days (or >5 half-lives of the drug/active metabolites) has been used between sessions. MRI was acquired at three time points: baseline and at the end of each ACTIVE or PLACEBO session. For a small subset of the sample, also [^{11}C] PHNO PET was acquired at baseline and at the end of the ACTIVE session to explore between-subjects variability in the relationship between D_2R and MRI effects. To the best of my knowledge, this is the very first experimental medicine study in healthy volunteers that investigates the effect of sustained D_2R blockade on brain structure and function integrating data from different imaging modalities acquired in one experimental setting. In my PhD, I investigated the effect of a week of D_2R blockade with amisulpride 400mg on brain volumes, quantitative T1 maps, and CBF as assessed with ASL and cortico-striatal FC measures using resting-state fMRI. I also sought to explore the relationship between MRI effects (when present) and D_2R spatial distribution (applying the methods developed in the previous study) and between-subjects variability D_2R occupancy.

1.7.3 Brain perfusion in antipsychotic-free FEP patients

Finally, considering the strong evidence of the relationship between changes in CBF in the basal ganglia and D_2R blockade, also corroborated by the result of this thesis I also sought to investigate differences in brain perfusion using ASL between non-medicated FEP and HC to disentangle medication and disease effects. Notably, this is the first study investigating differences in brain perfusion between patients with psychosis and healthy control using ASL as previous studies investigated CBF differences cross-sectionally in medicated patients.

2 Spatial profiling of antipsychotic effect on brain perfusion to D2R brain distribution

2.1 My contribution

At the start of my PhD, the full dataset was already acquired. I developed, with the help of my second supervisor Dr. Ottavia Dipasquale and Dr. Mattia Veronese, the entire analysis framework. I also performed pre-processing of ASL data with the advice of Dr. Fernando Zelaya and extracted both protein density and mRNA expression profiles from the AHBA. While extracting mRNA profiles, I also extensively reviewed the literature to evaluate different methods to process the AHBA dataset. This review highlighted that different processing pipelines could potentially lead to different results. I discussed these considerations with my first supervisor Prof. Mitul Mehta, with Dr. Mattia Veronese and with Prof. Federico Turkheimer. The result of this discussion guided the application of the AHBA dataset in this project and led to a publication that highlights the potential risks of reproducibility when integrating the AHBA dataset with neuroimaging data which confirmed that the methods applied were appropriate (Selvaggi et al. (2021) and Appendix B). I also performed all statistical analyses for the spatial association tests. I interpreted the data with the help of my 2 supervisors and Dr. Mattia Veronese. Finally, I drafted the manuscript for publication (Selvaggi et al. (2019) and Appendix A). I also presented these results at 2 international conferences as an oral presentation.

2.2 Aims and hypothesis of the study

The present work aimed to test in humans whether CBF changes induced by a single dose of different antipsychotics co-varies with measures of D_2R distribution. In particular, I employed two datasets from healthy volunteers (Hawkins et al., 2018) to evaluate the spatial correlation between CBF variation in the placebo vs. antipsychotic comparison against the population-based receptor density profiles derived from human PET scans using the high-affinity D_2R antagonist [^{18}F] Fallypride. I also investigated the same relationship at the gene expression level using *post-mortem* mRNA expression measures of the *DRD2* gene (the gene coding for D_2R) extracted from the AHBA (Hawrylycz et al., 2012). Brain mRNA expression variation across brain regions is associated with resting-state fMRI networks

suggesting that brain hemodynamic response may be linked to the architecture of the human brain transcriptome (Hawrylycz et al., 2015; Richiardi et al., 2015). Here, brain microarray mRNA expression data was chosen as a proxy for protein-level receptor density in the human brain. While post-transcriptional events may alter the relationship between gene expression and protein synthesis (Liu et al., 2016), brain mRNA expression maps have been shown to predict in vivo protein levels as measured with PET (Beliveau et al., 2017; Rizzo, Veronese, Heckemann, et al., 2014). Following the receptor occupancy theory and the neurovascular coupling model suggested by pre-clinical studies and described in the introduction (Mandeville et al., 2013; Sander et al., 2013), I hypothesized that there would be a detectable linear relationship between the main effects of antipsychotics on CBF measures and D_2R receptor density profiles evaluated at the protein and gene expression level. Even though brain microarray mRNA expression data from the AHBA is noisier and more discrete than the PET BP_{ND} maps (because of the limited number of samples), I expected CBF increases after antipsychotics to be linearly associated also with *DRD2* mRNA expression spatial profiles. However, given the fact that mRNA expression only approximates cellular protein levels due to post-transcriptional regulatory mechanisms, I predict microarray data to explain less variance in CBF changes than PET-derived maps.

2.3 Methods

2.3.1 Participants and study design

Data were collected as part of a project approved by the National Research Ethics Service Committee London – Brent. Details about participants, protocol and study design have been described in detail by Hawkins et al. (2018). Briefly, forty-two healthy male subjects were enrolled in a double-blind, placebo-controlled, randomised, fully counterbalanced, three-session crossover design. Participants were randomised into two equal parallel study groups (Group 1 age mean/standard deviation (SD) 27.6/6.9; Group 2 age mean/SD 28.3/6.3). In the first group, participants received a placebo, 7.5 mg of olanzapine (OLA), or 3 mg of haloperidol (HAL) on each study day. In the second group, participants received a placebo, 0.5 or 2 mg risperidone (lowRIS and highRIS respectively). All but lowRIS dosages were chosen to achieve on average at least 60% of D_2R receptor occupancy (Kapur et al., 2000; Tauscher et al., 2004). On dosing day, participants followed a standardised regime. The MRI scan was performed at the time of the predicted peak level of plasma concentration of the

drug after oral administration (T_{max}): approximately 5 h after drug administration for Group 1 and 2 h for Group 2 (de Greef et al., 2011; Midha et al., 1989). Study days were seven days apart to allow washout between sessions. After the final visit, a follow-up phone call was made to monitor potential adverse events related to the study drugs.

2.3.2 MRI acquisition and pre-processing

Scans were acquired using a GE MR750 3-T scanner and a 12-channel head coil. A T2-weighted image (Field of View (FOV)= 240 mm, TR/TE= 4380/46.992 ms, 320x256x156 matrices, slice thickness= 2 mm) was acquired during the first visit and then used for the pre-processing of ASL images (see below). A T1-weighed Magnetization Prepared – RApid Gradient Echo (MPRAGE) scan was also acquired (on the second visit): FOV= 270 mm, TR/TE/TI= 7.312/3.016/400 ms, 256x256x156 matrix, slice thickness= 1.2 mm) for normalization purposes. Measurement of CBF was carried out using a 3D pseudo-continuous ASL (3D-PCASL) sequence. Labelling of arterial blood was achieved with a 1500ms train of Hanning-shaped radiofrequency (RF) pulses in the presence of a net magnetic field gradient along the flow direction (the z-axis of the magnet). After a post-labelling delay of 1525ms, a whole brain volume was read using a 3D inter-leaved "stack-of-spirals" Fast Spin Echo readout consisting of 8 interleaved spiral arms in the in-plane direction, with 512 points per spiral interleave (TE/TR= 11ms/4968 ms). 60 slice-partitions of 3mm thickness were defined in the 3D readout. The in-plane FOV was 240×240 mm. The sequence used four background suppression pulses to minimise static tissue signal at the time of image acquisition. The combination of flow-driven adiabatic inversion of the PCASL pulse, plus background suppression, yields a substantial increase in the signal-to-noise ratio (SNR) of ASL, of up to 50%. Therefore, only four pairs of control-labelled images are required to produce reliable perfusion-induced signal differences (Alsop et al., 2015). The mean perfusion weighted difference image was derived from the average of the difference of the four control-label pairs. Voxel-wise CBF was computed by dividing this mean difference image by a proton density (image acquired at the end of the sequence, using identical readout parameters). This computation was done according to the formula suggested in the ASL consensus article (Alsop et al., 2015). The New Segment tool in Statistical Parametric Mapping (SPM) was used to create grey matter, white matter (WM), and cerebrospinal (CSF) images from each T1 image. These then entered the Diffeomorphic Anatomical

Registration Through Exponentiated Lie Algebra toolbox (DARTEL) to create a study-specific template and set of flow fields to later transform each subject's ASL data into standard space (Ashburner & Friston, 2005, 2011). The T2-weighted images were also co-registered with the T1 images. Each raw proton density image was then co-registered with the T2 image. The parameters for this transformation were then applied to the CBF maps (as they were already in alignment with the proton density image) before their normalization using DARTEL flow fields. Finally, the normalized CBF maps were smoothed using a 6 mm full width at half maximum (FWHM) kernel. Global CBF values were extracted using the MarsBar toolbox (http://marsbar.sourceforge.net) and the default whole-brain mask provided in SPM. A group-wide paired t-test was performed in SPM for each drug vs. placebo comparison. Grey matter CBF was added as a covariate of no interest in the model to account for peripheral (global) drug effects and between-subjects variability in the global brain perfusion (Handley et al., 2013; Viviani et al., 2013; Viviani et al., 2009). Contrast images (e.g., DRUG>PLACEBO and PLACEBO<DRUG) were then segmented by using the Desikan-Killiany Atlas (Desikan et al., 2006) to extract ΔCBF profiles.

2.3.3 Receptor density profile

Figure 1 shows the general framework of the analysis. D_2R profiles were extracted from an independent [^{18}F]-Fallypride PET template built by averaging six BP_{ND} whole-brain maps acquired in six right-handed males aged 18-45 who did not participate in the study (Dunn et al., 2010). Participants had no history of head injury, neurological disease, psychosis or learning disability and were free of medication. After a complete description of the study, written informed consent was obtained from participants according to local ethical procedures. Scanning was conducted on a GE VCT (BGO) PET scanner. Participants received a low-dose CT scan (10mA) for attenuation correction. List mode 3D acquisition commenced for 80 minutes, then 90 minutes, following a 10-minute rest period. Scan duration was in line with what was recommended to achieve equilibrium (Slifstein et al., 2010; Vernaleken et al., 2011). A bolus of 250 mBq radiolabelled [^{18}F]-Fallypride diluted up to 10ml with normal saline was given intravenously over 10 seconds and flushed with 10ml normal saline. Scans were reconstructed as non-attenuation corrected PET images (to preserve anatomical information) and realigned, followed by the formation of a mean image for transformation to the SPM PET template. Regional D_2R BP_{ND} was then calculated using

the simplified reference region tissue model (Lammertsma et al, 1996) implemented in MATLAB. [^{18}F]-Fallypride is a D_2R receptor antagonist, and it is a well-established PET radiotracer in the study of D_2-like receptor distribution in the brain (Mukherjee et al., 2002). The [^{18}F]-Fallypride template was segmented with the Desikan-Killiany Atlas (Desikan et al., 2006) and for each of the 85 Regions of Interest (ROI) of the template, the voxel-wise mean BP_{ND} value was extracted with the *fslmeants* function implemented in the Functional Software Library suite (FSL, FMRIB, Oxford, UK). Conventional parametric modelling of regional BP_{ND} was performed by using the cerebellum as the reference region (Ichise et al., 2003). Therefore, both left and right cerebellar ROIs (namely "rh_cerebellum_cortex" and "lh_cerebellum_cortex") were excluded from correlation analyses with CBF profiles. D_2R PET radiotracers differ in signal-to-noise ratio (Mukherjee et al., 1999). For instance, [^{11}C] - Raclopride has fast in-vivo kinetics and lower affinity as compared with other PET ligands (Hall et al., 1988). For this reason, it can reliably quantify receptor availability in brain regions densely populated by D_2Rs such as the striatum. By contrast, other D_2R radiotracers such as [^{11}C]-FLB 457 and [^{18}F]-Fallypride have higher affinity and signal-to-noise ratio. This allows more reliable quantification in extra-striatal areas where D_2R density is much lower than the striatum (Narendran et al., 2011; Slifstein et al., 2010). To compare the contribution of striatal vs. extra-striatal regions to this association, a [^{11}C]-Raclopride template was segmented with the Desikan-Killiany Atlas (Desikan et al., 2006) using the same approach used with the [^{18}F]-Fallypride template. Here I also excluded cerebellar ROIs because parametric modelling of regional BP_{ND} was performed using the cerebellum as the reference region.

2.3.4 CBF profiles

CBF profiles were obtained from maps of CBF changes at the group level. For each antipsychotic, a group-wide paired t-test was performed in SPM for each drug vs. placebo. Grey matter total blood flow was added as a covariate of no interest in the model to account for peripheral (global) drug effects and between-subjects variability in the global brain perfusion (Handley et al., 2013; Viviani et al., 2013; Viviani et al., 2009). For each antipsychotic, the main effect of the drug was tested using group voxel-wise paired t-tests with cluster-level Family-Wise Error (FWE) correction (alpha= 0.05, cluster defining threshold= 0.001) as implemented in SPM. Also, to provide a quantification of striatal CBF increase after antipsychotic exposure, a paired t-test was performed for each drug vs. placebo

comparison on CBF extracted from an ROI encompassing the whole striatum. In addition, for each contrast and each subject percent of CBF change was calculated using the following equation: $CBF_{\%change} = \frac{CBF_{DRUG} - CBF_{PLACEBO}}{CBF_{PLACEBO}} \times 100$. In agreement with previous studies (Handley et al., 2013; Hawkins et al., 2018), I identified statistically significant increases in CBF after drug administration (against placebo) and have thus focussed on this contrast in the remainder of this work. Therefore, DRUG>PLACEBO contrast maps for each antipsychotic were segmented by using the Desikan-Killiany (Desikan et al., 2006) using the same approach used for the extraction of receptor profiles. This resulted in 85 ΔCBF profiles measuring the antipsychotic-induced increase of CBF in each ROI. For consistency with the receptor profile data, I carried out correlation analyses excluding the two cerebella ROIs.

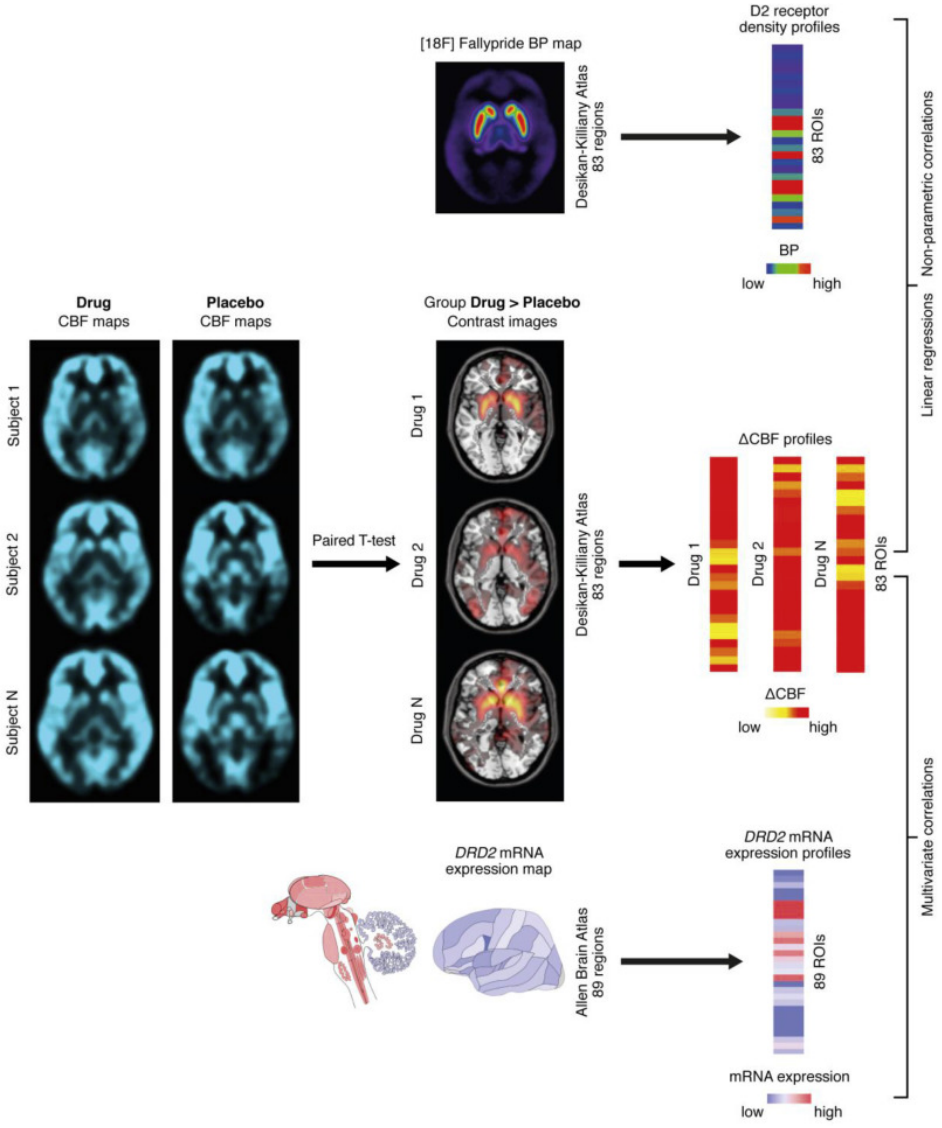

Figure 1. The general framework of the analysis. Group-level map showing the main effect of the drug was computed for each antipsychotic. The resulting maps and the [^{18}F]-Fallypride PET template were segmented

into 83 ROIs by using the Desikan-Killiany Atlas (Desikan et al., 2006). For each ROI, ΔCBF profiles and [^{18}F]-Fallypride BP_{ND} template values were extracted and then correlated. *DRD2* gene brain microarray mRNA expression values were extracted from AHBA data (http://human.brain-map.org) (Shen et al., 2012). The MENGA software (http://www.nitrc.org/projects/menga/) (Rizzo et al., 2016) was used to extract *DRD2* mRNA expression profiles which then entered multivariate correlation analysis against ΔCBF profiles.

2.3.5 Statistical analysis for the ΔCBF/receptor density profiles correlations

To test the associations between ΔCBF profiles (derived for each antipsychotic) and D_2R density profiles, linear regression models as implemented in the Statistical Package for Social Sciences (SPSS) were used (IBM, SPSS Statistics, Version 23). The normal distribution of the residuals of the regression models was tested by the Shapiro-Wilk test. BP_{ND} data were transformed using a natural logarithmic function (ln) so that the residuals conformed to a normal distribution. For all linear regression models, Mahalanobis distance and Cook's distance were computed to explore the presence of multivariate outliers and estimate the presence of highly influential data points. To identify multivariate outliers, Mahalanobis distance values were compared to a chi-square distribution with degrees of freedom equal to the number of variables (two in this case) with p= 0.001 (Finch, 2012). Any data point with Cook's distance higher than 1 was considered a highly influential outlier and excluded from the analysis (Cook & Weisberg, 1982). To further control for the effect of extreme observation I also used the bias-corrected accelerated bootstrap technique as implemented in SPSS (Efron et al., 1994) with 10,000 resamples. Non-parametric Spearman's correlations between ΔCBF profiles and receptor BP_{ND} profiles were also performed as a countercheck. In addition, to account for spatial autocorrelation effects, a spatial permutation test has been applied to compare the empirical correlation between BP_{ND} and ΔCBF maps to a set of null correlations generated by randomly rotating (N= 10,000) the spherical projection of the cortical parcellation of the spatial maps before projecting it back on brain surface preserving both spatial contiguity and hemispheric symmetry (Vasa et al., 2018). For subcortical ROIs, a set of random maps (N= 10,000) was generated using permutation. Subcortical ROI sets were integrated with the cortical sets to generate a null distribution of 10,000 correlations which was used to compare the empirical correlation. Moreover, Fisher's r-to-z transformation was performed to test the pairwise significance of the difference between correlation coefficients of ΔCBF profiles between different antipsychotics. The asymptotic covariance method was adopted to account for the fact that correlations had one variable in common.

2.3.6 mRNA profiles and genetic correlations

The AHBA dataset consists of 6 healthy donors 5 males, and 1 female, age: 42.5 ± 13.4, range 24– 57 years) with ~30000 gene expression profiles sampled throughout the brain. Expression values for each probe were normalized using the guidance provided by the AHBA website. For each donor, sample data for all probes were converted into z-score (using mean and standard deviation as normalization factors within a given subject) which were then used for all the analyses. Antipsychotics' contrast images (DRUG>PLACEBO) were resampled in the AHBA space. Then, each CBF image sample was spatially matched with the corresponding genomic AHBA sample within a search window of a sphere of 5mm radius centred on the MNI coordinates of the AHBA sample. *DRD2* gene brain microarray mRNA expression values were extracted from AHBA data (http://human.brain-map.org) by using the Multimodal Environment for Neuroimaging and Genomic Analysis (MENGA) toolbox (http://www.nitrc.org/projects/menga/) (Rizzo et al., 2016). The same toolbox was used to carry out correlations with the ΔCBF profiles of each antipsychotic. First, both the CBF contrast image and AHBA data were segmented using the list of structures (N= 169) provided by the AHBA. A subset of 89 structures (ROIs), each containing at least one genomic sample for all the six AHBA brains (donors), was selected to perform correlations between ΔCBF profiles and gene expression. For each donor, sample data were converted from their original log2 intensity in z-scores using mean and standard deviation as a normalization factor for a given subject. This was done to minimize bias related to inter-donor variability in the AHBA dataset. For the *DRD2* gene, a unique profile was obtained by selecting the probe whose expression values were highly consistent across donors. Distributions of expression values for all the probes were evaluated across donors, retaining the probe with the most symmetric and least skewed distribution. In the case of multiple samples within the same ROI, the average between samples within the ROI was calculated (Rizzo et al., 2016). After completing the matching and the extraction of ΔCBF and gene expression profiles, two different correlations were performed: 1) between-donors correlation or gene auto-correlation returning the biological variability of the spatial profile of mRNA expression between donors (the higher the gene autocorrelation the lower the heterogeneity in mRNA expression spatial profile between donors); 2) correlation between each gene expression and the ΔCBF by ROIs also called cross-correlation. A Principal Component Analysis (PCA) on mRNA expression measures of the 6 AHBA donors was performed

beforehand to extract the component that accounted for at least 95% of the total variance in the mRNA expression data. In particular, the PCA was performed on an 89 x 6 matrix (89 ROIs by 6 donors) and represented a consistent spatial mRNA expression profile across all donors. This component was then used in the regression model against CBF profiles. Significance was assessed with a bootstrapping approach resulting in a chance likelihood of the correlation coefficient expressed as a percentage. More specifically, ROIs were permuted within donors repeating the correlation between the PCA component and CBF profiles 1000 times, to obtain a measure of the likelihood that the correlation found was different from chance level. A multivariate spatial correlation using MENGA was also performed between *DRD2* gene expression profiles and [^{18}F]-Fallypride BP_{ND} maps. As for protein density profile analysis, Fisher's r-to-z transformation was performed to test the pairwise significance of the difference between correlation coefficients of ΔCBF profiles between different antipsychotics and between PET and mRNA profiles.

To test reproducibility between AHBA data processing and spatial matching methods (see section 1.8, Appendix B and Selvaggi et al. (2021)), correlations between *DRD2* mRNA expression and ΔCBF were performed also with voxel-wise, whole-brain mRNA expression maps obtained from the AHBA using variogram models (Gryglewski et al., 2018). Briefly, this method employs a spatial analysis where variogram models and Gaussian Process Regression are used to predict gene expression measures in locations that were not originally sampled in the AHBA. The output of this method consists of voxel-wise maps for each gene. For further details about AHBA data processing and variogram models please refer to the original publication (Gryglewski et al., 2018). Gene expression maps were already created and released as freely downloadable NIFTI images by the authors. I downloaded the *DRD2* mRNA expression map (http://www.meduniwien.ac.at/neuroimaging/mRNA.html). This image was already in standard space according to the MNI templates; therefore no normalization was needed. *DRD2* mRNA expression image was segmented into 83 ROIs using the Desikan-Killiany Atlas and *DRD2* mRNA expression values were extracted for each ROI. *DRD2* mRNA expression values were then correlated with ΔCBF profiles extracted from the same ROIs. Linear models within SPSS (IBM, SPSS Statistics, Version 23) were evaluated. ΔCBF profiles were the dependent variable and *DRD2* mRNA expression was the independent variable.

2.4 Results

2.4.1 The main effect of antipsychotics on CBF

The group paired t-tests revealed that all antipsychotics but olanzapine, produced a statistically significant increase of CBF in the striatum. HAL>PLA t-contrast revealed a significant cluster in the left putamen (k= 755, pFWE cluster-level corrected= 0.041; $t_{(1,19)}$= 5.78; peak MNI coordinates: -26 -6 -6). OLA>PLA t-contrast revealed a significant cluster in the right parietal cortex (Brodmann Area (BA) 39; k= 456, pFWE cluster-level corrected= 0.001; $t_{(1,19)}$= 5.77; peak MNI coordinates: 34 -71 51) and in the right parahippocampal gyrus (k= 421, pFWE cluster-level corrected= 0.015; $t_{(1,19)}$= 4.98; peak MNI coordinates: 24 6 -30). lowRIS>PLA t-contrast revealed a significant cluster in the left caudate (k= 1692, pFWE cluster-level corrected< 0.001; $t_{(1,19)}$= 5.49; peak MNI coordinates: -11 11 -15). highRIS>PLA t-contrast revealed a significant cluster in the left caudate (k= 7664, pFWE cluster-level corrected<0.001; $t_{(1,19)}$= 8.63; peak MNI coordinates: -13 8 9). None of the DRUG<PLA t-contrast revealed statistically significant clusters. Figure 2 shows sections of the brain overlaid with FWE cluster-level corrected t-contrast.

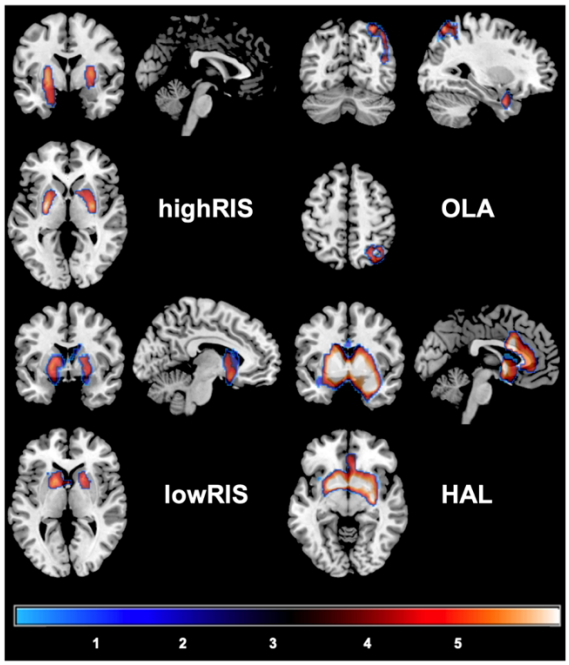

Figure 2. DRUG>PLACEBO t-contrast images (FWE cluster-level corrected, cluster defining threshold= 0.001). The colour bar indicates the t values of the paired t-test. HAL: haloperidol; OLA: olanzapine; lowRIS: risperidone 0.5mg; highRIS: risperidone 2mg.

Paired t-test on CBF in the whole striatum showed increased perfusion (as compared with PLACEBO) after HAL ($t_{(20)}$= 3.65, p= 0.002, Cohen's d= 0.78, average CBF % change= 8.8%), after lowRIS ($t_{(20)}$= 3.11, p= 0.005, Cohen's d= 0.68, average CBF % change= 5.5%) and after highRIS ($t_{(20)}$= 3.11, p= 0.005, Cohen's d= 0.68, average CBF % change= 7.1%). No statistically different changes in striatal perfusion were found after OLA (p= 0.68).

2.4.2 CBF changes with D_2R profile correlations

All antipsychotic ΔCBF profiles significantly correlated with [^{18}F]-Fallypride BP_{ND} template values (Table 2 and Figure 3). HAL ΔCBF had the strongest correlation with [^{18}F]-Fallypride BP_{ND} template (R_{linear}= 0.78) followed by RIS (R_{linear}= 0.73 and R_{linear}= 0.72 for lowRIS and highRIS respectively) and OLA (R_{linear}= 0.48). Results from linear models and non-parametric Spearman correlations were consistent. In all linear regressions, none of the data points was identified as a highly influential outlier (all Cook's distances< 1) or multivariate outliers (all Mahalanobis distances p> 0.01). Results were retained after 10,000 resamples (all bootstrapped p< 0.01).

DRUG>PLA contrast	[^{18}F]-Fallypride BP_{ND} template				*DRD2* mRNA expression	
	R_{linear}	p_{linear}	rho	p	R	Chance likelihood
HAL	+0.78	p < 0.001	+0.61	p < 0.001	+0.34	0%
OLA	+0.48	p < 0.001	+0.51	p < 0.001	+0.21	0%
lowRIS	+0.73	p < 0.001	+0.76	p < 0.001	+0.43	0%
highRIS	+0.72	p < 0.001	+0.61	p < 0.001	+0.45	2%

Table 2. Summary of the correlations of ΔCBF profiles D_2R profiles ([^{18}F]-Fallypride BP_{ND} template) and of genomic multivariate cross-correlations of antipsychotics' ΔCBF profiles with *DRD2* mRNA expression profiles.

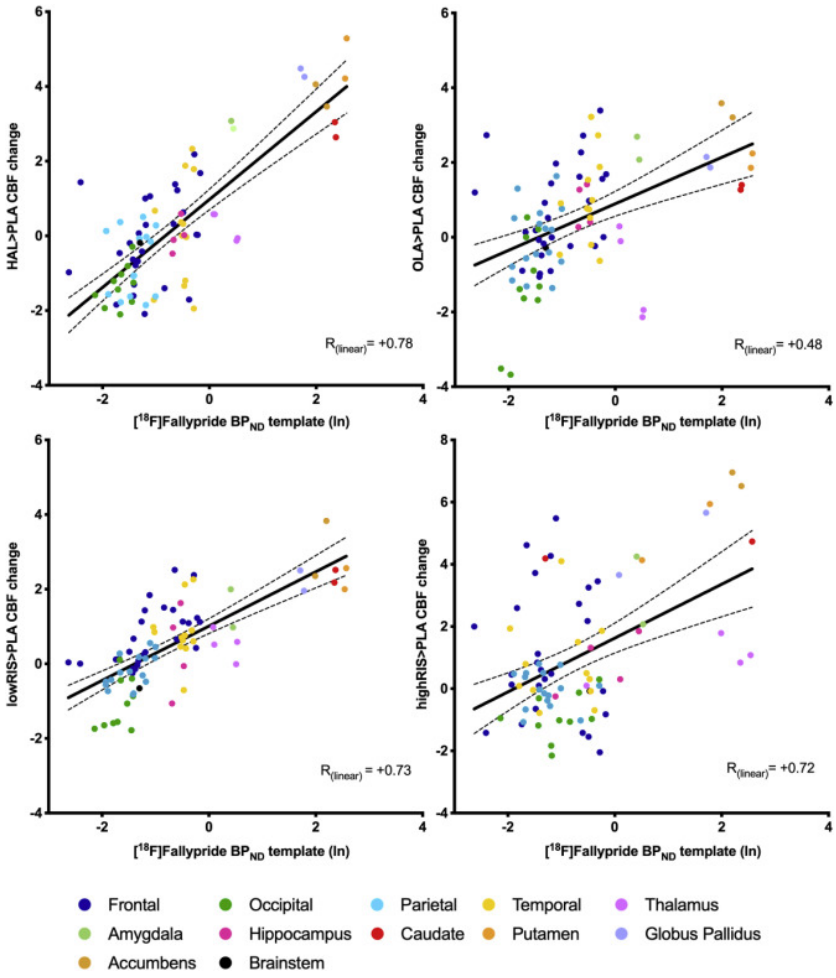

Figure 3. Scatterplots of ΔCBF/receptor density profiles correlations. Top row: scatterplot of the correlation between HAL ΔCBF profiles and [^{18}F]-Fallypride BP_{ND} template (left) and of the correlation between OLA ΔCBF profiles and [^{18}F]-Fallypride BP_{ND} template (right). Bottom row: scatterplot of the correlation between lowRIS ΔCBF profiles and [^{18}F]-Fallypride BP_{ND} template (left) and of the correlation between highRIS ΔCBF profiles and [^{18}F]-Fallypride BP_{ND} template (right). Dashed lines indicate 95% confidence bands.

Results were retained after correcting for the spatial autocorrelation effects (Vasa et al., 2018). Table 3 reports the results of this analysis.

	empirical correlation	p-value
HALPLA		
Spearman	0.5796	0.0006
Pearson	0.7623	<0.0002
OLAPLA		
Spearman	0.5403	0.0005
Pearson	0.5284	0.0002
lowRISPLA		
Spearman	0.7547	<0.0002
Pearson	0.7584	<0.0002
highRISPLA		
Spearman	0.6417	0.0002
Pearson	0.7455	<0.0002

Table 3. Summary of the correlations of ΔCBF profiles and D_2R profiles ([^{18}F]-Fallypride BP_{ND} template) considering spatial autocorrelation effects.

To compare striatal vs. extra-striatal contributions to this association, I also performed correlations between ΔCBF and receptor density profiles by extracting BP_{ND} values from a [^{11}C]-Raclopride PET template. [^{11}C]-Raclopride is a tracer with a lower affinity for D_2R compared to [^{18}F]-Fallypride and thus areas of lower D_2R density have lower specific activity. I found a weaker correlation with the [^{11}C]-Raclopride BP_{ND} template as compared with the [^{18}F]-Fallypride BP_{ND} template. All antipsychotic ΔCBF profiles significantly linearly correlated with [^{11}C]-Raclopride BP_{ND} values (Figure 4). Similarly to [^{18}F]-Fallypride analysis, HAL ΔCBF had the strongest correlation with [^{11}C]-Raclopride BP_{ND} (R_{linear}= +0.63) followed by RIS (R_{linear}= +0.55 and R_{linear}= +0.59 for lowRIS and highRIS respectively) and OLA (R_{linear}= +0.28). Results from linear models and non-parametric Spearman correlations were largely consistent. Interestingly, the strength of associations was weaker for [^{11}C]-Raclopride as compared with [^{18}F]-Fallypride.

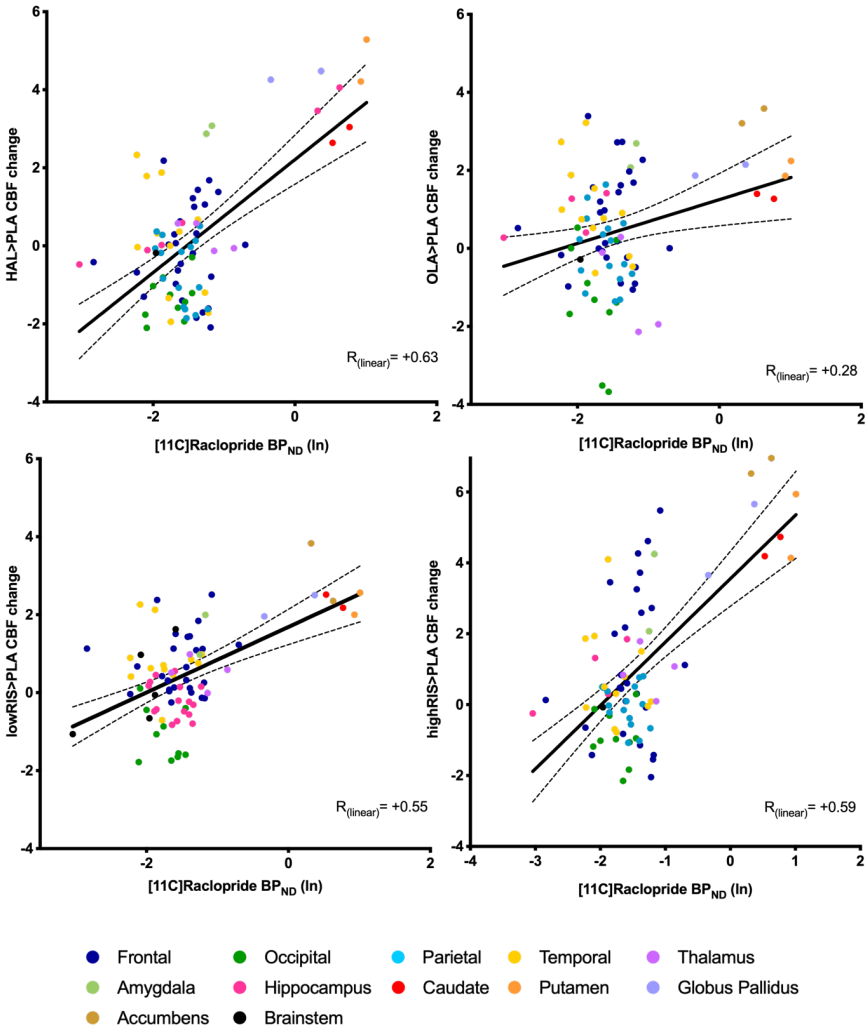

Figure 4. Top row: scatterplot of the correlation between HAL ΔCBF profiles and [^{11}C]-Raclopride BP_{ND} (left) and of the correlation between OLA ΔCBF profiles and [^{11}C]-Raclopride BP_{ND} (right). Bottom row: scatterplot of the correlation between lowRIS ΔCBF profiles and [^{11}C]-Raclopride BP_{ND} (left) and of the correlation between highRIS ΔCBF profiles and [^{11}C]-Raclopride BP_{ND} (right). Dashed lines indicate 95% confidence bands. HAL: haloperidol, OLA: olanzapine, lowRIS: low dose of risperidone, highRIS: high dose of risperidone.

2.4.3 mRNA expression correlations

The average correlation coefficient (R^2) of the genomic autocorrelation analysis for the *DRD2* gene was 0.575 (SD= 0.058) for the six donors. This result indicated good stability between donors of *DRD2* mRNA expression spatial profile (Rizzo et al., 2016). For the different antipsychotic drugs, the correlation coefficients were all positive and statistically significant (Figure 5) and significantly lower than those obtained for the PET template (PET R^2 range= 0.20–0.60; mRNA PET R^2 range= 0.04–0.20; pairwise-comparisons all $p<0.05$).

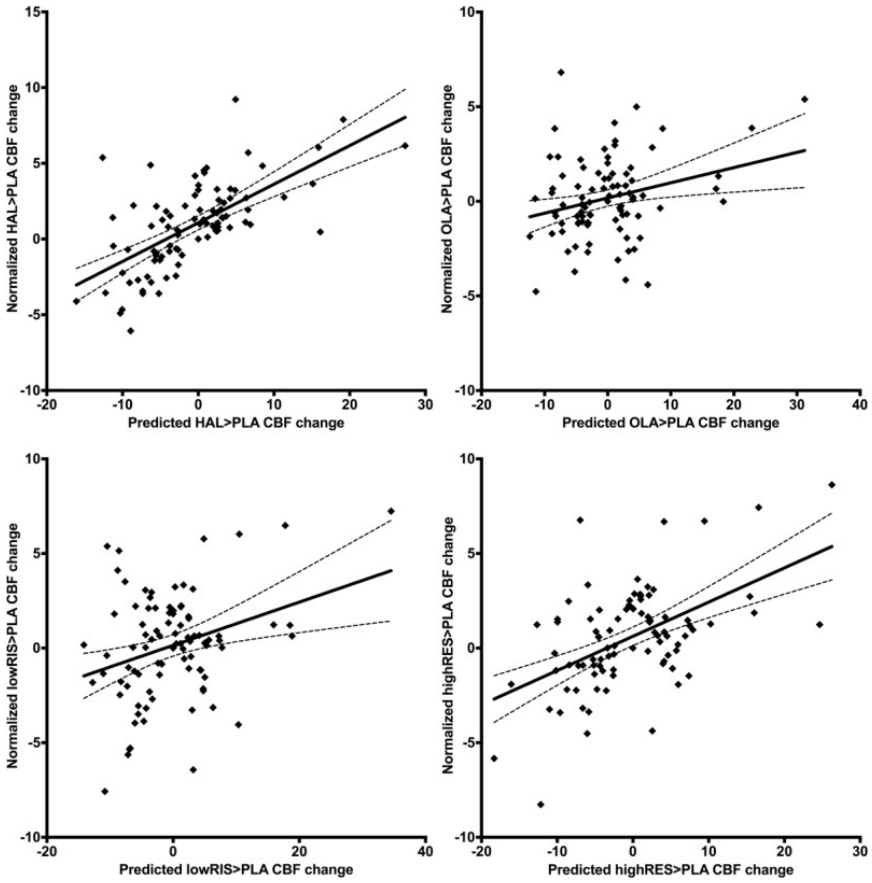

Figure 5. Scatterplots of the genomic correlation. For all scatterplots on the y-axis normalized DRUG>PLACEBO CBF changes and on the x-axis DRUG>PLACEBO CBF changes predicted by the first Principal Component of the mRNA expression measures of the 6 AHBA donors. Top right: HAL; Top left: OLA; Bottom right: lowRIS; Bottom left: highRIS. Dashed lines indicate 95% confidence bands.

Similar results were obtained using the variogram approach (Gryglewski et al., 2018). ΔCBF profiles for all antipsychotics were linearly correlated with *DRD2* mRNA profiles evaluated with this method (R_{HAL}= 0.25; R_{OLA}= 0.38; R_{lowRIS}= 0.19; $R_{highRIS}$= 0.58; all $p<0.05$). Notably, the correlations obtained with this method were consistent with the ones obtained using the MENGA software and reported in the main text. This additional analysis confirms that the association between *DRD2* mRNA expression values extracted from the AHBA is low to moderate. In addition, the consistency of the two mRNA analyses suggests that it is unlikely that different strategies in AHBA processing might have biased the results. *DRD2* mRNA expression data was directly correlated with [^{18}F]-Fallypride BP_{ND} (average R= 0.32 +/- 0.09). This result is in line with previous findings which have already shown low to

moderate correlations between *DRD2* mRNA expression data of the AHBA and PET BP_{ND} D_2R (Rizzo et al., 2016).

2.4.4 Differential strength of association between ΔCBF and receptor density profiles

The rank of order and R_{linear} values matched the variation in affinity with D_2R (NIMH Psychoactive Drug Screening Program https://pdsp.unc.edu/databases/kidb.php), such that the stronger the association between ΔCBF profiles and D_2R densities the lower the Ki (Table 2 and Figure 6). In the pairwise correlation comparisons, I found significant differences for HAL vs. OLA (z= 5.46), lowRIS vs. OLA (z= 4.19) and vs. highRIS vs. OLA (z= 3.90) (all p< 0.01, Bonferroni corrected, Figure 6). All the other comparisons were not significant. As for the correlation with [^{18}F]-Fallypride values, genomic mRNA expression correlations qualitatively mirrored Ki differences between antipsychotics at D_2R. However, none of the pairwise comparisons between correlation coefficients between antipsychotics was statistically significant after correction for multiple comparisons.

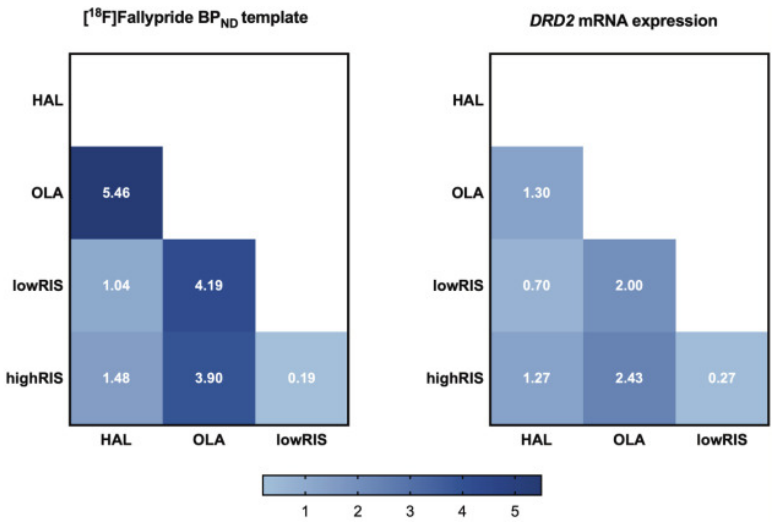

Figure 6. Differential strength of association between ΔCBF and D_2R profiles. Heat maps showing z-values for the pairwise comparison of correlations. The colour bar indicates z-scores. On the left correlations with [^{18}F]-Fallypride BP_{ND} template values, and the right correlations with mRNA microarray data from the ABA. HAL: haloperidol, OLA: olanzapine, lowRIS: low dose of risperidone, highRIS: high dose of risperidone. The following tests were performed HAL vs. OLA, HAL vs. lowRIS, HAL vs. highRIS, lowRIS vs. OLA, highRIS vs. OLA, and highRIS vs. lowRIS.

2.5 Discussion

The present study aimed to investigate the spatial relationship between the effects of single clinically effective doses of antipsychotics on CBF and receptor distribution profiles in the brain as indexed by [^{18}F]-Fallypride BP_{ND} values extracted from a template map and brain *DRD2* mRNA expression profiles. Consistently with my hypothesis, I found that for all compounds there was a spatial coupling between drug-induced CBF changes and D_2R density profiles (at both protein and gene expression levels). In addition, I found that mRNA data explained less variance in CBF changes than PET derived map.

Receptor Density Profiles

The spatial association between CBF changes induced by all antipsychotics and receptor brain spatial distribution of D_2R matches earlier evidence in non-human primates showing large CBF increases after injection of the D_2R antagonist PET tracer [^{11}C]-Raclopride in brain regions with high D_2R density (Sander et al., 2013). This suggests that the relationship between the physiological response to D_2R antagonist and D_2R availability described in preclinical models (Sander et al., 2013) might also exist in vivo in humans. Furthermore, I have shown that the relationship between CBF increases after antipsychotic administration also matched [^{18}F]-Fallypride BP_{ND} template values in extra-striatal ROIs significantly populated by D_2R such as the thalamus and the amygdala, even though they show lower BP_{ND} template values as compared with striatal ROIs. These results extend earlier evidence (Sander et al., 2013) and suggest that the linear coupling between CBF response to dopaminergic drugs and D_2R concentration might also be a valid model outside the striatum. This interpretation is also supported by the weaker correlation of ΔCBF with [^{11}C]-Raclopride BP_{ND} template as compared with [^{18}F]-Fallypride BP_{ND} template. However, it must be acknowledged that correlations between ΔCBF profiles and D_2R profiles extracted from the [^{11}C]-Raclopride might have been biased by the lack of reliable extra-striatal D_2R binding. Of note, in Sander et al. (2013) the functional measure was CBV instead of CBF. However, given the tight association between CBV changes and CBF changes (Ito, Ibaraki, et al., 2005; Ito, Kanno, et al., 2005), I believe this difference will not affect the interpretation of my findings.

Microarray mRNA expression data

I found that for all antipsychotics, the ΔCBF profiles also correlated with microarray mRNA expression data extracted from the AHBA. All genomic correlations were positive and therefore in the same direction as [^{18}F]-Fallypride BP_{ND} template linear models. Notably, microarray mRNA expression measures explained less variance in ΔCBF than [^{18}F]-Fallypride BP_{ND} template values. This is consistent with my hypothesis motivated by the existence of a large variability between mRNA expression and protein synthesis due to post-transcriptional regulation mechanisms (Liu et al., 2016). My findings are consistent with previous works that have linked the spatial architecture of the brain transcriptome to the brain structure (McColgan et al., 2018; Shin et al., 2018), function (Hawrylycz et al., 2015; Richiardi et al., 2015) and in vivo measures of brain proteins (Gryglewski et al., 2018; Rizzo et al., 2016; Rizzo, Veronese, Tonietto, et al., 2014; Veronese et al., 2016). Here I could show that *post-mortem* brain mRNA expression data may potentially be used to also map variations in MRI functional response to drug stimulation. However, such mapping has still many limitations to be addressed to adopt it extensively in the context of pharmacological-MRI studies. For instance, it might be difficult to use mRNA expression mapping in neurotransmitter systems where protein synthesis is highly dependent on post-transcriptional regulation mechanisms (e.g., the serotonin system) (Beliveau et al., 2017; Rizzo et al., 2016). While further studies are needed to fully validate this mRNA expression-MRI approach, it might be especially valuable for profiling the functional effects of drugs with poorly characterized or unknown targets. Interestingly, as for the correlation with receptor density profiles, the rank order of correlations between ΔCBF and *DRD2* mRNA expression measures mirrored affinity profiles of the compounds, although these differences were only numerical. It is worth noting that the variance explained by genomic correlation was lower than the PET correlations which might have reduced the chance of detecting any significant difference in the pairwise comparison between the correlation coefficients. These findings represent further evidence supporting the hypothesized PK/PD model of the antipsychotic effect of CBF measures (Mandeville et al., 2013). Indeed, I was able to show that quantitative measures of the brain functional effect of antipsychotics (i.e., CBF changes) are directly associated with receptor density measures. However, intrinsic limitations of the AHBA dataset should be considered when evaluating mRNA/ΔCBF relationships. First, the number of available AHBA donors is limited (N= 6) and therefore only approximates population-

level brain mRNA expression templates. However, despite this limitation, AHBA data can predict brain protein densities (Gryglewski et al., 2018; Rizzo et al., 2016; Rizzo, Veronese, Tonietto, et al., 2014; Veronese et al., 2016) and other neuroimaging measures. Another limitation is that different approaches have been proposed to analyse this dataset (e.g., French and Paus (2015); Gryglewski et al. (2018)). The fact that different strategies in AHBA dataset processing could affect the reproducibility of the findings is under debate (Arnatkeviciute et al., 2019; Selvaggi et al., 2021). I have also analysed the mRNA/ΔCBF correlations using a different method that employs whole-brain voxel-wise mRNA expression maps obtained from variograms (Gryglewski et al., 2018). The results of this analysis were comparable with the analysis performed in MENGA. Therefore, I believe that it is unlikely that this methodological issue could have biased these results.

Differential strength of association between ΔCBF and receptor density profiles

The correlation strength between ΔCBF and receptor density measured with PET varied between the different antipsychotics tested. One possible interpretation of this difference might be related to the differential affinities of these compounds to D_2R (Dukart et al., 2018). These results seem to be in line with this hypothesis. The strengths of the association were higher for antipsychotics with a higher affinity for D_2R. In particular, HAL was the drug with the highest correlation coefficient and the lowest Ki, whereas OLA showed the lowest correlation coefficient and the highest Ki. Both lowRIS and highRIS were in the middle between HAL and OLA. Another possible interpretation might be related to the different secondary affinities between the drugs. For instance, for compounds with a high affinity to $5HT_2AR$ like risperidone and olanzapine, part of the effect on CBF might also be linked with a mechanism different from D_2R blockade (Goozee et al., 2014). Both olanzapine and risperidone as well as other second-generation antipsychotics (e.g., aripiprazole) showed decreases in CBF especially in cortical areas with a mechanism that is possibly mediated by $5HT_2AR$ (Handley et al., 2013; Lahti et al., 2005). I did not find differences in correlations between the two different doses of risperidone, even though they do show different effect sizes in CBF increase. This might indicate that the coupling between the measurable physiological effects and target receptor distribution can be detected regardless of the dose of the compound if that dose can produce detectable functional effects. Nonetheless, differences in the brain disposition of antipsychotics have been reported in previous studies

(Kornhuber et al., 2006; Rodda et al., 2006). In particular, animal data suggested that antipsychotics (including the ones considered in the present work) show different blood-brain barrier penetration and brain clearance leading to dissimilar spatial distribution in the brain (Loryan et al., 2016). Even though these dissimilarities have been reported to be only moderate (Loryan et al., 2016), brain disposition is a factor to be considered in addition to receptor affinity when linking the pharmacodynamics of each antipsychotic with receptor occupancy. Therefore, without maps of brain deposition variation, conclusions regarding the D_2R affinities and strength of associations between receptors and CBF are necessarily incomplete.

Limitations

Some limitations need to be considered for the present study. First, we used population-based profiles of D_2R density as the spatial architecture of D_2R is typically consistent across individuals (Rizzo, Veronese, Heckemann, et al., 2014; Veronese et al., 2016). For example, the striatum always has a higher D_2R density than the thalamus which in turn has higher D_2R density than the cortex. However, variance in density between individuals within the same brain region (Farde et al., 1995) may drive inter-individual differences in the drug functional response. Individualized receptor profile mapping is, therefore, necessary to bring more precision to the method and to further validate the present findings. Nevertheless, normative atlases for protein and mRNA expressions have proven useful in many different applications, suggesting that the core spatial architecture of the brain receptor systems is consistent across individuals (Gryglewski et al., 2018; Rizzo, Veronese, Heckemann, et al., 2014; Veronese et al., 2016). In addition, I considered only local effects by matching CBF changes and D_2R density measures with the same ROIs. However, studies in patients and healthy volunteers showed that antipsychotics also produce changes in FC suggesting the existence of downstream effects that were not included in my analyses (Cole, Oei, et al., 2013). As discussed above, increases in CBF after acute antipsychotic challenges have been usually interpreted as the result of neuronal metabolic changes due to D_2R blockade. D_2-like receptors are also present in perivascular astrocytes and endothelial cells modulating brain hemodynamic changes. However, these receptors are mainly D_3R and not D_2R (Choi et al., 2006). Together with the knowledge that the affinity of these compounds for D_2R is higher than for D_3R, we expect the change in CBF to be mainly neuronal in origin. In addition, both

risperidone and olanzapine, but not haloperidol, act as antagonists at $5HT_2AR$ (Meltzer, 1988). Blockade of $5HT_2AR$ on smooth-muscle cells of brain arteries has been shown to induce relative vasodilation in animal models (i.e. blocking vasoconstriction caused by the endogenous ligand serotonin) (Kovacs et al., 2012). Therefore, the degree to which these non-neuronal effects contribute to the associations described here is not known. Finally, I believe that the limited sample size offered by the AHBA (N= 6) could have undermined the power of detecting a linear relationship between mRNA data and CBF changes. This factor could also be an alternative explanation of the difference I found between mRNA and PET correlations with CBF.

3 The NECTAR Study

3.1 My contribution

When I started my PhD a first draft of the NECTAR study protocol had already been produced. Under the close supervision of my first supervisor and in collaboration with Dr. Tiago Reis Marques and Prof. Oliver Howes I contributed to the first draft to refine study procedures and optimise MRI methods, including expanding the MRI methods to include quantitative T1 mapping, multi echo-resting state fMRI and PCASL protocols. The updated protocol was submitted to the attention of the local ethical committee, and I was the lead for the study team with Dr. Tiago Reis Marques in liaison with the ethical committee and responding to any comments. Before recruitment, I was responsible for designing and implementing standardized study procedures including medical assessments, blood sampling, detailed Case Report Forms (CRF), implementation of MRI sequences, digital cognitive assessments and recruiting platform. This activity has been performed with the help of Dr. Uzma Zahid and under the supervision of Dr. Tiago Reis Marques. I liaised with the Pharmacy Manufacturing Unit, Guy's and St Thomas' NHS Foundation Trust and with the Pharmacy Department, Maudsley Hospital, South London and Maudsley NHS Foundation for drug manufacturing and dispensing respectively. I also liaised with Invicro Ltd. for PET scan procedures and with Bioaffinity for laboratory testing. In collaboration with Dr. Uzma Zahid and Dr. Martin Osugo, I recruited participants for the study also carrying out study visits, medical assessments, and safety monitoring. I pre-processed and analysed MRI data and in particular structural MRI sequences, Arterial Spin Labelling data and multi-echo resting-state fMRI data under the supervision of my second supervisor Dr. Ottavia Dipasquale. Dr Tobias Wood assisted me in the analysis of quantitative T1 data. I also analysed PET data and performed PK/PD modelling with the supervision of Dr. Mattia Veronese. I interpreted the results with the help of my 2 supervisors and with the additional contribution of Dr. Tiago Reis Marques, Dr. Mattia Veronese and Prof. Oliver Howes. I also submitted a conference abstract which has been accepted as a poster presentation at two international conferences.

3.2 Aims

As discussed in the Introduction, while the effect of acute single-dose exposure to D_2R antagonism has been associated with alteration in brain structure and function (even though results are not consistent in structural studies), it remains unclear if these are acute responses to D_2R receptors blockade which normalizes with repeated doses. Similarly, it is unknown whether sustained D_2R receptor antagonism at clinically relevant doses is associated with alterations in brain structure and function not seen in single-dose studies. Determining these effects is critical to understanding the role of D_2R modulation on brain structure and function and in disentangling disease states and traits from direct pharmacological effects. In this study, I aimed to investigate the effect of sustained D_2R blockade on brain structure and function. I aimed to investigate the effect of sub-chronic D_2R antagonism on brain volume and T1 changes as assessed with quantitative T1 mapping, CBF as assessed with ASL, and cortico-striatal connectivity as assessed with resting-state fMRI. In addition, I aimed to explore the PK/PD relationship by investigating the association between brain changes and between-subject variability in D_2R measured with PET imaging with [^{11}C]-PHNO and drug peripheral levels. With these aims a within-subject, cross-over, double-blinded, placebo-controlled study design in healthy individuals was conducted.

In the study, participants received daily doses of either amisulpride 400mg or placebo for 7 days. The 400mg dose was chosen as previous studies have shown that it can achieve at least 60% of D_2R occupancy and therefore antipsychotic effects in patients with psychosis (Sparshatt et al., 2009; Vernaleken et al., 2004). MRI assessments were performed at baseline (before dosing) and after one week of amisulpride and after 1 week of placebo. A washout period of at least 10 days was used between sessions to minimize any carry-over effects.

Despite previous attempts to investigate the effects of sub-chronic antipsychotic exposure on brain structure and function in healthy volunteers (Metzger et al., 2015; Viviani et al., 2013), to the best of my knowledge, this is the first study to investigate the effects of sustained D_2R blockade on brain structure and function in healthy volunteers at clinically relevant doses with a multimodal approach. Therefore, directional hypotheses on brain effects are

based on the limited findings from single-dose studies and uncontrolled studies in patients described in the Introduction. The main hypotheses were:

1) Exposure to one week of D_2R antagonism will not produce significant alterations in brain volume and T1 signal (Hawkins et al., 2018)
2) Exposure to one week of D_2R antagonism will produce a significant increase in brain perfusion in brain regions with a high density of D_2R such as the basal ganglia (Handley et al., 2013; Hawkins et al., 2018; Selvaggi et al., 2019)
3) Sustained D_2R blockade in the basal ganglia will also produce non-local effects such as altered cortico-striatal FC. Based on earlier evidence, I hypothesize a functional decoupling between the striatum and cortical regions such as the motor cortex and the executive network (Cole, Oei, et al., 2013; Tost et al., 2010)

Exploratory hypotheses:

1) Changes in brain structure and function will be associated with inter-individual variation in antipsychotic plasma levels and/or D_2R occupancy as assessed with PET
2) Sustained D_2R blockade will produce extrapyramidal symptoms associated with brain structural and/or functional effects.

3.3 Methods

3.3.1 Participants

Healthy male and female participants were recruited through King's College London Research Volunteer Recruitment Circular e-mail and online platforms. Inclusion criteria were: i) age 18-65 years old; ii) no diagnosis of Parkinson's, Huntington or any movement disorder (excluding tics); iii) no diagnosis of schizophrenia, schizophreniform or any psychotic disorder; iv) sufficient understanding of the nature of the study and any hazards of participating in it; v) ability to communicate satisfactorily with the investigator and to participate in and comply with the requirements of, the entire study; vi) willingness to give written consent to participate after reading the information and consent form, and after having the opportunity to discuss the study with the investigator or their delegate; vii) capacity to provide informed consent, as judged by an investigator. Exclusion criteria were: i) history of significant neurological disorder (including significant head trauma or significant

loss of consciousness, Parkinson's disease, epilepsy, dementia, Huntington's or other disorder that may be sensitive to dopamine modulation) or significant medical disorder; ii) family history of Schizophrenia or Psychotic disorders; ii) any absolute contraindications to dopamine agonists or antagonists; iii) previous significant use of dopamine agonists or antagonists; iii) any absolute contraindications to MRI imaging studies, including, but not limited to, the presence of an implanted electronic device (such as cardiac pacemaker) or presence of metal implants; iv) pregnancy and/or breast-feeding; v) substance dependence/abuse other than to cigarettes and caffeine; vi) suicide risk or other significant safety risk as judged by the patient's psychiatrist or study physician; vii) participation in a clinical study of unlicensed medicines within the previous 30 days; viii) clinically relevant abnormal findings at the screening assessment as judged significant by the principal investigator; ix) presence of other acute or chronic illness or history of chronic illness sufficient to invalidate the volunteer's participation in the study or make it unnecessarily hazardous and judged significant by the principal investigator; x) the likelihood that the subject will not comply with study requirements; xi) objection by a General Practitioner, or another doctor responsible for their treatment, to the volunteer entering the study. All participants provided valid and written informed consent to participate in the study. The study was approved by the West London & GTAC Research Ethics Committee.

3.3.2 Study design and procedures

A randomised, double-blind, placebo-controlled, within-arm cross-over study design was adopted. Figure 7 summarizes the study design and procedures. Participants were randomised to receive either amisulpride for a period of one week followed by placebo or placebo for a week and then amisulpride. A washout period of at least 10 days (>5 half-lives of the drug/active metabolites, amisulpride half-life= 12 hours) has been used in between arms, to minimize any carry-over effects. To improve drug tolerability participants were instructed to take the pills at night, approximately 30 minutes before going to sleep. To further promote drug tolerability doses were gradually titrated: first day 200mg, second day 300mg, and third to seventh day 400mg. For each day the number of pills taken by participants was the same for both amisulpride and placebo arms to maintain blind.

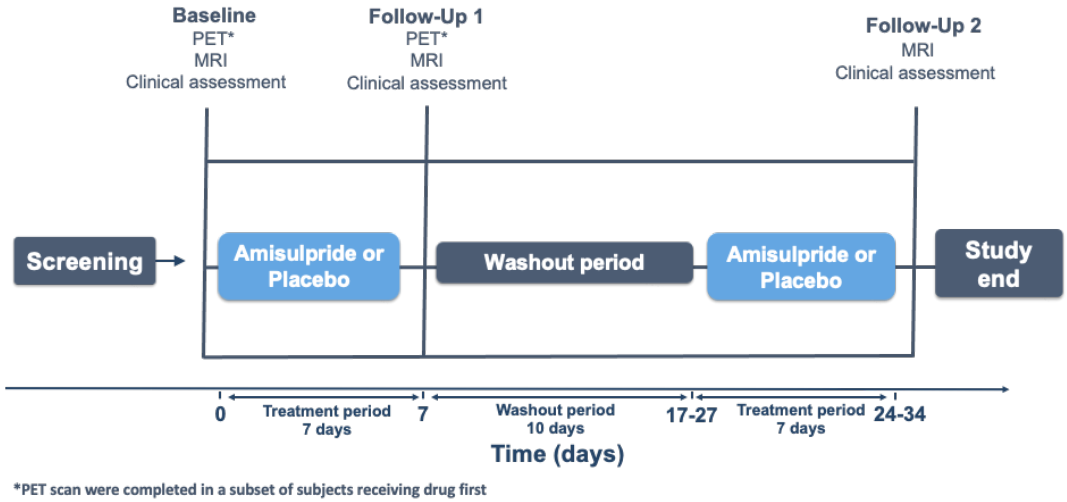

Figure 7. Study design. After screening and consenting participants entered a double-blind, randomised, crossover study design in which they received either amisulpride 400mg for one week or placebo. Sessions were separated by a washout period of at least 10 days to minimize any carry-over effect. After screening three visits were conducted for each participant: baseline visit before receiving any medication, Follow-up 1 at the end of the first week and Follow-up 2 at the end of the second week.

Participants received a phone call to explain the study and were invited to a screening visit. The screening included checking the inclusion and exclusion criteria and signing informed consent. A 12-lead ECG was performed to rule out QTc prolongation and other cardiac problems before starting the drug administration. Vital signs, full clinical examination and laboratory testing were also conducted during the screening visit. Urine drug screening and pregnancy tests were also performed during the screening visit. All clinical assessments performed during the screening visit were repeated at each study visit (e.g., Baseline visit, follow-up 1 and follow-up 2 visits). Clinical examination at baseline and follow-up visits included evaluation of EPS using the Extrapyramidal Symptom Rating Scale (ESRS) (Chouinard & Margolese, 2005). Baseline visits also included MRI brain imaging and [^{11}C]-PHNO PET brain imaging. MRI and [^{11}C]-PHNO PET scans were conducted on the same day. Only a subsample of participants was randomly allocated to have both the MRI and the PET scan at baseline. To maintain the double-blind, for participants allocated to have both PET and MRI, clinical evaluations were performed by researchers who were not aware of MRI and PET allocations. In addition, it is worth highlighting that, apart from clinical evaluations, the rest of the measures taken in this study (e.g., MRI, PET, laboratory tests) were objective measures taken in a standardized fashion which are unlikely to be influenced by blinding. Moreover, all participants consented to all the procedures of the study, including

the possibility of having both the PET and MRI which allocation occurred randomly across participants. Nonetheless, all analyses included also order as a nuisance covariate to further control also statistically for order effects. Baseline visits were performed before the administration of the first dose of study medication (within 28 days). On day 1 participants were dosed. After dose administration, they were monitored for approximately 3 hours for any potential side effects. Participants were then given oral medication for the following week and received detailed instructions and safety recommendations. On the morning following the last dose of the drug or placebo (follow-up 1, FU1), participants had the second MRI brain imaging and the second [^{11}C]-PHNO PET brain imaging (if allocated). Participants were assessed using the same clinical and laboratory assessments used at baseline, including drug urine tests. Blood laboratory testing included amisulpride plasma levels. Participants randomly allocated to receive both MRI and [^{11}C]-PHNO PET scans were also allocated to receive the drug first, so they had [^{11}C]-PHNO PET scans only at baseline and FU1 visits. After the FU1 visit, participants entered a period of wash-out between crossovers of at least 10 days. Participants then crossed over to receive either amisulpride or placebo for another week (7 days). The procedures for the second week were identical to the ones for the first week of treatment. On the morning following the final dose of drug or placebo, the participants returned for the final visit (Follow-up 2, FU2 visit) which included MRI scans, clinical and laboratory assessments with amisulpride plasma levels, including drug urine test MRI and [^{11}C]-PHNO PET scanning was conducted at the same time of day per session when possible.

3.3.3 PK analysis

Amisulpride plasma levels were evaluated for all participants at both FU1 and FU2 visits. Evaluation of amisulpride plasma levels was used to assess participants' compliance with study procedures. Independent sample t-test and Spearman correlations were used to test the difference in amisulpride plasma level between males and females and the association with body weight respectively given the known effect of these variables in drug pharmacokinetics including amisulpride (Bowskill et al., 2012; Glatard et al., 2020).

3.3.4 Extrapyramidal symptoms analysis

Between-session differences in EPS were evaluated using the total ESRS score (Chouinard & Margolese, 2005). A paired t-test was used to test differences in the total ESRS score between ACTIVE and PLACEBO sessions. As for all other measures, subjects with no detectable amisulpride plasma levels were excluded from the analysis. One additional subject was excluded from the analysis because of missing data, leaving a sample of 24 subjects for which EPS were tested.

3.3.5 MRI Acquisition

MRI was acquired using a Siemens 3T Prisma scanner.

Structural MRI

The MP2RAGE sequence was used to derive T1-weighted and quantitative T1 maps. Briefly, the MP2RAGE sequence is a refinement of the MPRAGE sequence that combines two MPRAGE acquisitions, interleaved at different inversion times (TI), and creates a homogeneous T1-weighted contrast with an intrinsic correction of B_1 inhomogeneities and reduced residual proton density and T2* weighting. From the MP2RAGE sequence also T1 relaxation times can be derived to build quantitative T1 maps which have been shown to have high within- and between-subjects reproducibility (Marques et al., 2010). The following acquisition parameters were used: voxel size= 1mm^3, slice thickness= 1mm, FOV= 256mm, matrix= 256x256 mm, TR= 5000 ms, TE= 2.98 ms, flip angle 1= 4 deg, flip angle 2= 5 deg, TI 1= 707 ms, TI 2= 2500 ms. No fat or water suppression was implemented.

ASL

Measurement of regional CBF was carried out using a 3D pseudo-continuous ASL (3D-PCASL) sequence and the following parameters: bolus duration= 1800 ms, inversion time= 3600ms, FOV= 220 mm, TR= 4000ms, TE= 13.32ms, slice thickness= 3 mm, resolution 1.7 x 1.7 x 3 mm, acquisition time= 4 minutes 42 s. Eight control-label pairs were used to derive a perfusion-weighted difference image. The sequence included background and fat suppression for optimal reduction of the static tissue signal. The sequence also included a perfusion calibration (M0) scan with TR= 5,000 ms to compute the CBF map in standard physiological units (ml blood/100 g tissue/min) (Alsop et al., 2015; Wang et al., 2005).

Resting-state fMRI

Resting-state functional MRI data were obtained at rest in all sessions using a multi-echo echo-planar imaging (EPI) sequence. Briefly, this acquisition method consists in acquiring fMRI data at multiple echo times (TE) for each volume. The method takes advantage of the dependence of the BOLD signal with TE to separate BOLD-like components (which according to the neurovascular coupling model reflect neuronal activity) from non-BOLD-like ones (which are likely artefactual components related to movement, field inhomogeneity, cardiac and respiratory pulse, etc.) (Kundu et al., 2013). Resting-state fMRI using multi-echo acquisitions has shown several advantages as compared with standard single-echo acquisitions, including SNR increase due to the combination of echoes, better signal recovery in brain areas typically affected by signal drop- and access to denoising strategies which outperform standard denoising techniques typically used in single-echo acquisitions (Dipasquale et al., 2017; Kundu et al., 2012). The following acquisition parameters were used: TR= 2510 ms, TE1= 15 ms, TE2= 27.6 ms, TE3= 40.1 ms, resolution: 1.7 x 1.7 x 3 mm, slice thickness= 3 mm, 42 slices, 206 volumes, flip-angle= 90 degrees, FOV= 220 mm.

3.3.6 MRI pre-processing

Before starting with pre-processing, the images from all sequences, subjects and sessions were visually inspected to identify major artefacts. Subjects having artefactual or corrupted images in at least one session were discarded from subsequent analysis (see below).

Structural MRI

The regularized method (O'Brien et al., 2014) as implemented in the QUantitative Imaging Tool (QUIT, http://github.com/spinicist/QUIT) was used to produce T1-weighted and quantitative T1 maps from MP2RAGE acquisitions. T1-weighted images were preprocessed following the standard processing pipeline for VBM analysis as implemented in SPM. Briefly, T1-weighted images were segmented to generate grey and WM images which were later used to derive nonlinear deformations to warp grey and WM images in MNI space (Ashburner & Friston, 2000, 2005). T1-weighted images were resampled at 2 mm isotropic resolution and spatially smoothed using a 6 mm FWHM Gaussian kernel. T1-weighted images were also processed using the standard FreeSurfer (version 6.0.0) image analysis suite

pipeline (using the recon-all command) to perform cortical and subcortical volumetric segmentation. Briefly, this step included motion correction, removal of non-brain tissue using a hybrid watershed/surface deformation procedure, automated Talairach transformation, segmentation of the subcortical WM and deep grey matter volumetric structures, intensity normalization, tessellation of the grey matter-white matter boundary, automated topology correction, and surface deformation following intensity gradients to optimally place the grey/white and grey/cerebrospinal fluid borders at the location where the greatest shift in intensity defines the transition to the other tissue class (Dale et al., 1999; Fischl & Dale, 2000; Fischl et al., 1999). The Desikan-Killiany cortical parcellation (Desikan et al., 2006) and the subcortical parcellation (Fischl et al., 2002) provided in FreeSurfer were used to derive volumetric measures (in mm^3) of cortical and subcortical ROIs for both hemispheres (N= 95). A study-specific template representing the average T1-weighted anatomical image across subjects was built using baseline structural scans and Advanced Normalization Tools (ANTs) (Avants et al., 2011). This template has been used to improve the coregistration of T1, CBF, and resting-state fMRI images to MNI space. Before co-registration and warping all T1 maps were skull-stripped with Brain Extraction Tool (BET) as implemented in FSL (Smith, 2002). For each participant and session, T1 maps were co-registered to their corresponding baseline T1-weighted image and then normalized to the study-specific template before warping to standard MNI space. T1 maps were resampled at 1 mm isotropic resolution and spatially smoothed using a 3 mm FWHM Gaussian kernel.

ASL

Quantified CBF maps for each subject and session were skull-stripped with BET as implemented in FSL (Smith, 2002), co-registered to their corresponding baseline structural scan, normalized to the study-specific T1-weighted template and subsequently warped to standard MNI space and resampled to a 2 mm^3 isotropic resolution using ANTs (Avants et al., 2011). Finally, CBF images were spatially smoothed using a 6 mm FWHM Gaussian kernel.

Resting-state fMRI

First, for each participant and session framewise displacement (FD) was also calculated (Power et al., 2014) on the first echo. Subjects with at least one session with FD> 0.3 mm

were discarded from subsequent analyses. The Analysis of Functional NeuroImages (AFNI) software (afni_proc.py, version 21.3.04) (Cox, 1996) and the TE-Dependent ANAlysis (*tedana*) (version 0.0.10, https://doi.org/10.5281/zenodo.6461353) Python library were used to pre-process resting-state multi-echo fMRI data (Kundu et al., 2013; Kundu et al., 2012). First, volume re-alignment, time series de-spiking and slice time correction were performed for each session. After these steps data entered the *tedana* workflow where they were optimally combined (OC) (i.e., signal across echoes were combined using a weighted average) (Kundu et al., 2013), and de-noised to remove motion artefacts and other non-BOLD sources of noise. Briefly, Principal Component Analysis (PCA) was used to reduce the data dimensionality of the OC data by decomposing it into component maps and time series. Next, the dimensionally reduced and optimally combined data entered a TE-dependent ICA to identify and remove TE-independent (i.e., non-BOLD components). The independent component time series were fit to the pre-processed time series from each of the three echoes to generate ICA weights for each echo. These weights were then fitted to the linear TE-dependence and TE-independence models to generate F-statistics and component-level κ and ρ values, which respectively indicate BOLD and non-BOLD weightings. The κ and ρ metrics were then used to identify non-BOLD-like components which were regressed out of the optimally combined dataset as noise regressors to produce a denoised dataset (Kundu et al., 2015; Kundu et al., 2013). WM and CSF masks were obtained from the segmentation of each subject and session T1-weighted structural images and eroded to minimize partial volume effects. For all sessions, both masks were co-registered to each individual's functional volumes to extract the mean WM and CSF signals, which were regressed out of the denoised datasets. Data was then temporally filtered with a high-pass temporal filter with a cut-off frequency of 0.005 Hz, co-registered to its corresponding T1-weighted structural scan, normalized to the study-specific template, resampled to an isotropic resolution of $2mm^3$ and warped to standard MNI-152 space. Finally, images were spatially smoothed using a 6 mm FWHM Gaussian kernel.

3.3.7 MRI analysis

T1-weighted images

For each cortical and subcortical parcellation, a paired t-test on the volumetric measures estimated by Freesurfer was performed in R (version 4.2.2, https://www.R-project.org/).

Only grey matter ROIs were selected (N= 87). False Discovery Rate (FDR) correction was applied to correct for multiple comparisons. Standard VBM voxel-wise analysis was performed in SPM. A paired t-test with order (i.e., ACTIVE first or PLACEBO first) as a covariate of no interest was performed. FWE correction at both cluster and voxel levels, as implemented in SPM, was applied (Friston et al., 1994). Both ACTIVE>PLACEBO and ACTIVE<PLACEBO contrasts were tested.

T1 maps

Both ROI and voxel-wise analyses were performed on T1 maps. T1 mean signal from whole grey matter, bilateral caudate, putamen and ventral striatum ROIs were evaluated. For each bilateral ROI a repeated measure Analysis of Covariance (ANCOVA) with order (i.e., ACTIVE first or PLACEBO first) as a covariate of no interest was performed. Bonferroni correction was used to correct for multiple comparisons (alpha= 0.05/4= 0.0125). ROI analyses were performed in JASP (version 0.14.1, https://jasp-stats.org). A voxel-wise non-parametric paired t-test at the grey matter level with order as a covariate of no interest was performed in FSL randomise (Winkler et al., 2014) with Threshold-Free Cluster Enhancement (TFCE) correction and 5000 permutations (Smith & Nichols, 2009). Both ACTIVE>PLACEBO and ACTIVE<PLACEBO contrasts were tested.

CBF maps

Both ROI and voxel-wise analyses were performed on CBF images. Using the same grey matter and bilateral ROIs described previously, total CBF, assessed within the grey matter, and regional CBF values from bilateral caudate, putamen and nucleus accumbens were extracted. A repeated measure ANCOVA with order as a covariate of no interest was used to assess between-session differences in the total CBF. For each bilateral ROI a repeated measure ANCOVA with order and grey matter (global) CBF as a covariate of no interest was performed. Bonferroni correction was used to correct for multiple comparisons (alpha= 0.05/3= 0.016). ROI analyses were performed in JASP (version 0.14.1, https://jasp-stats.org). Similarly to the voxel-wise analysis on T1 maps a voxel-wise non-parametric paired t-test with order (i.e., drug first or placebo first) and global CBF as covariates of no interest was performed for CBF maps in FSL randomise (Winkler et al., 2014) with TFCE correction and 5000 permutations (Smith & Nichols, 2009). Both ACTIVE>PLACEBO

and ACTIVE<PLACEBO contrasts were tested. Global CBF was added as a covariate of no interest in the model in both ROI and voxel-wise analyses to account for peripheral drug effects and between-subject variability in global brain perfusion as done in previous works (Handley et al., 2013; Selvaggi et al., 2019; Viviani et al., 2009, 2013). A paired t-test without global CBF as a covariate of no interest was also performed for both ROI and voxel-wise analysis.

Similarly to the study described in Chapter 2 group-level ACTIVE>PLACEBO and ACTIVE<PLACEBO contrast images were segmented into cortical and subcortical ROIs using the Desikan-Killiany Atlas (Desikan et al., 2006) to extract ΔCBF profiles. The same pipeline described in Chapter 2 was used to test the associations between regional ΔCBF profiles and D_2R density profiles. In addition, to test the association between significant changes in CBF and EPS absolute CBF was extracted from the significant cluster in the voxel-wise CBF analysis, using the *fslmeants* function. Spearman correlation was used to test the association between the CBF changes and changes in total ESRS (i.e., EPS severity).

Resting-state fMRI

To investigate the effects of D_2R blockade on cortico-striatal connectivity I performed a seed-based FC analysis in the resting-state fMRI sample using the two-step multiple regression analysis (also known as *dual regression)* as implemented in FSL (Nickerson et al., 2017; Smith et al., 2014). The three striatal subdivisions (i.e., sensorimotor, limbic, and executive) of the Oxford-GSK-Imanova Probabilistic Striatal Connectivity Atlas were used as seeds (Tziortzi et al., 2014). Briefly, binarised masks of the three striatal subdivisions were used in the first step of a two-step multiple regression analysis as a set of spatial regressors to fit BOLD fluctuations across voxels in resting state fMRI to the dominant fluctuation in each of the striatal maps. In the second step, the subject-specific time series estimated in the first step were used as temporal regressors in a second multiple regression analysis to estimate the subject-specific FC spatial maps for both ACTIVE and PLACEBO sessions. For each seed, the group-level FC images, derived by averaging the FC maps across subjects and sessions, were first visually inspected to check whether the analysis produced the expected FC patterns (Tziortzi et al., 2014). Three separate paired t-tests (i.e., one for each striatal subdivision), were performed using FSL randomise (Winkler et al., 2014) with TFCE correction and 5000 permutations (Smith & Nichols, 2009). Order was used in the tests as a

covariate of no interest and both ACTIVE>PLACEBO and ACTIVE<PLACEBO contrast were tested for each seed. Bonferroni correction was applied on top of the TFCE correction to correct for the number of tests performed (2 contrasts x 3 seeds= 6; alpha= 0.05/6= 0.008). To explore the relationship between FC results and CBF results, for each subject and each session I estimated the mean CBF and FC signals from the significant clusters in the ASL and resting state fMRI analyses using the *fslmeants* function. Spearman correlation was then used to test the association between CBF and FC. To explore the association between the significant FC changes and EPS the raw signal was extracted from the peak of the significant clusters in the resting state fMRI analysis, using the *fslmeants* function. Spearman correlation was also used to test the association between the ACTIVE-PLACEBO differences in FC changes and the ACTIVE-PLACEBO differences in total ESRS.

3.3.8 PET acquisition and quantification

PET images were acquired using a Siemens Biograph HiRez XVI PET scanner (Siemens Healthcare, Erlangen, Germany). A low-dose computed tomography scan was first obtained for attenuation and model-based scatter correction followed by the injection of a single intravenous bolus of 0.020–0.029 μg/kg [^{11}C]-PHNO. Dynamic emission data were acquired continuously for 90 minutes after the administration of the radiotracer. The dynamic images were then reconstructed using a filtered back-projection algorithm into 31 frames (8×15s, 3×60s, 5×120s, 15×300s) with a 128 matrix, a zoom of 2.6 and a trans axial Gaussian filter of 5 mm. PET images were analysed using MATLAB version 2015b and an automatic analysis pipeline implemented in MIAKAT (release 4.2.6) (Gunn et al., 2016). The ICBM152 high-resolution structural MRI template in MNI space was non-linearly warped to the high-resolution T1-weighted MRI of each participant using SPM. The derived deformation parameters were then applied to the Martinez striatal atlas, which defines the anatomical extents of the limbic (ventral), associative and sensorimotor striatal regions of interest (ROIs) in MNI space (Egerton et al., 2010; Martinez et al., 2003), and the atlas used in Tziortzi et al. (2011) to define a cerebellar ROI to be used as the reference region. The application of deformation parameters brings the ROIs into the native space of each subject's MRI scan. The MRI was then downsampled to the PET resolution (2 mm^3). A frame-by-frame registration process on a single frame of reference was used for motion correction for dynamic PET images. Individual averaged PET images were then co-registered to their respective

MRIs using rigid body co-registration. Regional time activity curves (TACs) were obtained by applying individual parcellations to the realigned dynamic images. The outcome measure of interest was BP_{ND} of [^{11}C]-PHNO:

$$BP_{ND} = \frac{f_{ND} B_{avail}}{K_D}$$

Equation [3]: non-displaceable binding potential

where B_{avail} is the proportion of D_2R available to be bound by [^{11}C]-PHNO (i.e., the fraction of receptors not bound by endogenous synaptic dopamine), f_{ND} is the free fraction of [^{11}C]-PHNO in the brain and $\frac{1}{K_D}$ the affinity of the ligand for the target. BP_{ND} was obtained by kinetic modelling with a simplified reference tissue model (Gunn et al., 1997; Lammertsma & Hume, 1996). The whole cerebellum was used as a reference region due to its low content of dopaminergic neurons (Egerton et al., 2010; Kumakura & Cumming, 2009). For each subject, I measured the magnitude of amisulpride-induced D_2R blockade (i.e., D_2R occupancy) bilaterally in each striatal sub-region. Specifically, this was quantified as the reduction in BP_{ND} from the baseline condition ($BP_{ND}^{Baseline}$) to the post-amisulpride condition ($BP_{ND}^{Amisulpride}$), expressed as a percentage of $BP_{ND}^{Baseline}$:

$$\Delta BP_{ND} = 100 \times \frac{BP_{ND}^{Baseline} - BP_{ND}^{Amisulpride}}{BP_{ND}^{Baseline}} \%$$

Equation [4]: Amisulpride receptor occupancy

3.3.9 PK/PD analysis

To explore whether changes in CBF induced by amisulpride were associated with inter-individual differences in amisulpride plasma levels and D_2R occupancy, following the preclinical models in rhesus macaques (Sander et al., 2013), I implemented a PK/PD model to quantitatively link amisulpride plasma levels, D_2R blockade and CBF changes. Amisulpride plasma levels were collected on one single occasion at FU1 and FU2 visits. Since only one PK sample per session was collected in this study, it was not possible to fully

characterize a PK model based on the available data. Amisulpride pharmacokinetic properties have been well described using a one-compartment open model with first-order absorption and elimination (Glatard et al., 2020; Huang et al., 2021):

$$C_p(t) = \frac{Dose \cdot k_a}{{}^{V}/_{F} \cdot \left(k_a - {}^{CL}/_{V}\right)} \cdot \left(e^{\frac{CL}{V}t} - e^{k_a \cdot t}\right)$$

Equation [5]: Amisulpride pharmacokinetic one-compartment model

where $Dose$ is the amount of drug taken, F the bioavailability, ${}^{V}/_{F}$ (L) the apparent central volume, k_a $({}^{1}/_{h})$ the absorption rate constant, ${}^{CL}/_{V}$ $({}^{L}/_{h})$ the elimination constant rate defined as the ratio between oral clearance ${}^{CL}/_{F}$ $\left({}^{L}/_{h}\right)$ and the apparent central volume. Since only one blood sample per subject was available, it was not possible to directly estimate these parameters for this population. To model the pharmacokinetics of amisulpride after a repeated dose administration, model parameters taken from previous studies conducted using amisulpride doses comparable with the one in our study were used (Glatard et al., 2020; Huang et al., 2021. The results obtained by the simulation were compared with the measured data and those reported in the literature by experiments with similar doses. The simulation was carried out using the MATLAB toolbox Simbiology. The classic Hill equation was used to describe the relationship between drug plasma concentration and receptor occupancy. This equation is a direct model and assumes that free drug concentration equilibrates rapidly between the plasma, free brain, and target-bound compartments:

$$E = \frac{E_{max} \cdot C_p}{EC_{50} + C_p}$$

Equation [6]: Hill equation

Where C_p is the plasma concentration of the drug and EC_{50} is the drug plasma concentration that achieves 50% of receptor occupancy. PET receptor occupancy data were available for only four subjects, so the model was first used to estimate the population EC_{50} parameters

using the receptor occupancy that was measured with PET and the plasma concentration at the time of the PET scan. Once the model parameters were estimated, the Hill equation was used to predict the receptor occupancy for all the other subjects who did not perform the PET scans, by using measured plasma drug concentration. Preclinical models (Mandeville et al., 2013; Sander et al., 2013) have linked variation in cerebral blood volume (CBV) after D_2R blockade with D_2R occupancy using the following equation which was adapted to this case study:

$$\Delta CBV = -N_2 \cdot B_{max,2} \cdot \vartheta(0)_{DA} \cdot \vartheta_{AM}$$

Equation [7]: Neurovascular coupling model linking D_2R occupancy with variation in CBV

where positive variation in CBV (ΔCBV) relates with amisulpride occupancy ($\vartheta_{AM)}$, basal dopamine occupancy ($\vartheta(0)_{DA}$), and the local receptor density $B_{max,2}$ via an inhibitory neurovascular coupling constant (N_2) estimated for D_2R antagonists (Sander et al., 2013) Previous studies have demonstrated that CBV and CBF are linked by a power law relationship (Grubb et al., 1974; Ito, Ibaraki, et al., 2005):

$$CBV = c \cdot CBF^{\beta}$$

Equation [8]: Power law relationship linking CBV with CBF

Combining Equation 7 with Equation 8, I obtained the following relationship between CBF changes and receptor occupancy:

$$\Delta CBF = \alpha \cdot \vartheta_{AM}^{b}$$

Equation [9]: Relationship between CBF and receptor occupancy

where $\alpha = \frac{-N_2 \cdot B_{max,2} \cdot \vartheta(0)_{DA}}{c}$ is a parameter that includes all the constant values inside the model by Sander et al. (2013), b is the inverse of the parameter β and ϑ_{AM}^{b} is the amisulpride receptor occupancy. I finally tested whether this relationship was able to fit changes in CBF and receptor occupancy data in bilateral putamen and caudate ROIs in this dataset. Both absolute CBF and

relative-to-global CBF (i.e., absolute CBF after regressing out grey matter CBF) differences were tested. All available PK data were used in this analysis including those collected in participants lost at follow-up, but for which detectable amisulpride plasma levels were available (N= 28). Five subjects were excluded because of missing data regarding the time of sampling and/or the time the last dose was taken. Therefore available data for 23 participants were included in this analysis.

3.4 Results

3.4.1 Sample characteristics

Thirty-seven participants passed screening procedures, were enrolled in the study, and received the first dose of either amisulpride or placebo. Seven participants dropped out after enrolment and dosing. All but one participant who dropped out from the study had adverse events (AEs) possibly/probably related to drug administration. All but 7 participants who completed the study had AEs possibly/probably related to drug administration. All AEs were mild to moderate, were followed up and resolved with no interventions. No serious AEs were reported. Table 4 lists all AEs possibly/probably related to amisulpride administration that were observed in the study and their frequency.

AE	Number of participants
sedation	20
restlessness	13
impaired concentration	6
anxiety	4
nausea	4
disturbed sleep	4
headache	3
blurred vision	3
dizziness	2
rigidity	2
akathisia	2
increased appetite	1
breast pain	1
constipation	1
dystonia	1

Table 4. The frequency of AEs possibly/probably related to amisulpride administration observed in the study.

Five participants had no detectable amisulpride plasma levels in the ACTIVE session and, therefore were excluded from all analyses as compliance with the study procedure was compromised. The final sample, therefore, included 25 subjects (15 females, age range: 19-56 years, mean: 26.6 years, SD ± 7.7 years). For each imaging modality, some subjects were excluded because of corrupted or artefactual acquisitions or because of protocol unavailability. Two subjects had corrupted MP2RAGE acquisitions (files were corrupted at the time of transferring them from the MRI to the scanner), so T1 and brain volume analyses were performed in a subsample of 23 participants (14 females, age range: 19-56 years, mean: 26.8 years, SD ± 8.1 years). PCASL was not acquired for 4 subjects because of protocol unavailability (the protocol was discontinued by the scanner manufacturer), so CBF analysis was performed in a subsample of 21 participants (11 females, age range: 19-56 years, mean: 27.2 years, SD ± 8.3 years). Multi-echo resting-state fMRI was not acquired for 5 participants because of protocol unavailability. One participant was discarded from the resting-state dataset because of highly artefactual acquisition (signal drop in the frontal lobe) and three participants were discarded because of FD> 3mm in at least one session. Therefore, resting-state analyses were performed in a subsample of 16 participants (11 females, age range: 19-56 years, mean: 27.7 years, SD ± 8.8 years). Finally, complete baseline and follow-up [^{11}C]-PHNO scans were acquired in 4 participants who also had completed MRI sessions and detectable amisulpride plasma levels (1 female, age range: 22-56 years, mean: 31.5 years, SD ± 16.4 years).

3.4.2 Extrapyramidal symptoms analysis

Paired t-test on total ESRS scores revealed, higher EPS in the ACTIVE session as compared with the PLACEBO session ($mean(SD)_{ACTIVE}$= 4.2(5.39), $mean(SD)_{PLACEBO}$= 0.25(0.37), $t_{1,23}$= 3.55, p= 0.002, Cohen's d= 0.73). Table 5 shows the frequency of severity of EPS in the sample based on the first subscale of the ESRS (Chouinard & Margolese, 2005).

Severity	Number of subjects	Percent
absent	10	42%
mild	8	33%
moderate	4	17%
severe	2	8%

Table 5. The frequency of EPS severity as evaluated with the ESRS.

3.4.3 PK analysis

The mean (± SD) drug plasma concentration was 291 (± 187) µg/L. T-test revealed that there was no statistical difference (p= 0.995) in plasma concentration between female and male participants, even though the mean plasma concentration for females (343 ± 229) was numerically higher than for males (234 ± 114). The average (± SD) weight was 71 Kg (± 14). Spearman rank correlation revealed that there was no statistical correlation of both weight and age with plasma concentration (rho= -0.168, p= 0.39).

3.4.4 D_2R occupancy analysis

I found an average (± SD) D_2R occupancy (ΔBP_{ND}) of 57.1% in the caudate (± 8.5%) and 49.4% in the putamen (± 5.3%). Figure 8 shows parametric maps indicating average voxel-wise D_2R occupancy achieved in the study.

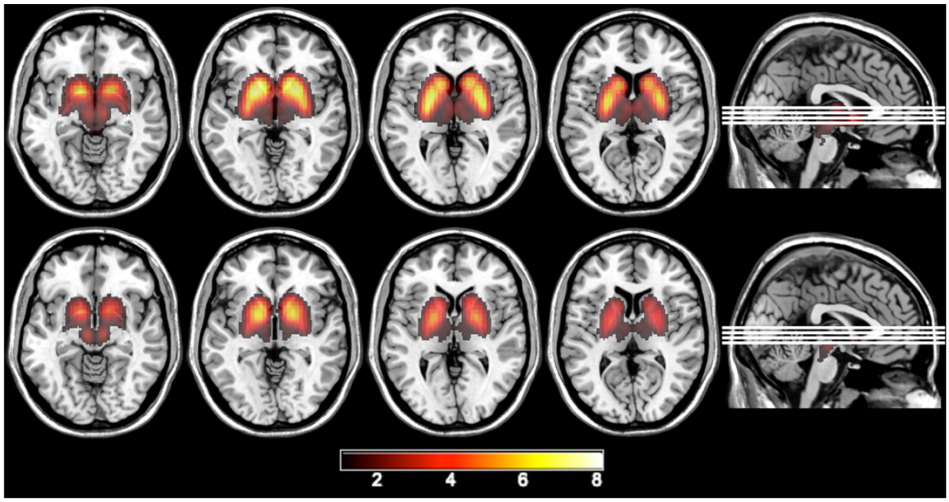

Figure 8. Parametric maps showing average BP_{ND} for BASELINE (top row) and ACTIVE (bottom row) sessions and indicating average voxel-wise receptor occupancy achieved in the study.

3.4.5 Brain volume analysis

FreeSurfer ROI analysis

No differences in total grey matter volume were found between ACTIVE and PLACEBO conditions ($t_{(1,24)}$= 0.005, p= 0.99). No FDR-corrected differences between ACTIVE and PLACEBO conditions were found. Table 5 reports the full statistics of this analysis. Paired t-test revealed two areas significantly different before correction for multiple comparisons: the right frontal pole ($t_{(1,24)}$= -2.81, $p_{uncorrected}$= 0.01) and in left putamen ($t_{(1,24)}$= +2.95, $p_{uncorrected}$= 0.01). Post-hoc repeated measure ANCOVA including order (i.e., ACTIVE or PLACEBO first) did not return any significant difference between ACTIVE and PLACEBO conditions in both the right frontal pole ($F_{(1,23)}$= 2.03. p= 0.16, -ve t above) and left putamen ($F_{(1,23)}$= 0.1, p= 0.75).

Brain Region	t	Confidence Interval	Standard Error	p-value (uncorrected)	p-value (FDR corrected)
Cortical					
Left banks of the superior temporal sulcus	0.32	-72.48±98.32	41.38	0.76	0.98
Left caudal anterior cingulate cortex	0.18	-54.62±65.02	28.99	0.86	0.98
Left caudal middle frontal cortex	0.72	-81.6±167.84	60.43	0.49	0.98
Left cuneus	0.46	-43.48±68.12	27.04	0.66	0.98
Left entorhinal cortex	0.74	-52.76±110.68	39.6	0.48	0.98
Left frontal pole	0.36	-35.07±49.47	20.48	0.73	0.98
Left fusiform gyrus	1.8	-18.95±275.99	71.45	0.09	0.98
Left inferior parietal gyrus	-0.41	-203.25±137.09	82.45	0.7	0.98
Left inferior temporal gyrus	-0.47	-312.76±196.76	123.44	0.65	0.98
Left insula	0.25	-127.86±162.1	70.25	0.81	0.98
Left isthmus cingulate	-0.06	-45.63±43.39	21.57	0.96	0.98
Left lateral occipital cortex	0.84	-119.16±280.44	96.81	0.42	0.98
Left lateral orbitofrontal cortex	-0.85	-386.87±161.51	132.85	0.41	0.98
Left lingual gyrus	-0.64	-155.44±82.72	57.7	0.54	0.98
Left medial orbitofrontal cortex	-0.56	-290.26±167.54	110.91	0.59	0.98
Left middle temporal gyrus	-1.11	-650.02±197.54	205.33	0.29	0.98
Left paracentral gyrus	1.31	-53.91±241.03	71.45	0.21	0.98

Left para-hippocampal gyrus	1.88	-6.49±136.17	34.56	0.08	0.98
Left pars opercularis	-0.41	-101.59±67.99	41.09	0.69	0.98
Left pars orbitalis	0.07	-66.94±71.42	33.52	0.95	0.98
Left pars triangularis	-0.05	-62.31±59.51	29.51	0.97	0.98
Left pericalcarine	-0.68	-51.01±25.97	18.65	0.51	0.98
Left postcentral gyrus	0.36	-177.35±251.75	103.96	0.73	0.98
Left posterior cingulate	-0.09	-76.92±71	35.84	0.94	0.98
Left precentral cortex	0.85	-111.29±266.33	91.48	0.41	0.98
Left precuneus	0.48	-91.13±146.33	57.53	0.64	0.98
Left rostral anterior cingulate	0.44	-96.36±147.88	59.17	0.67	0.98
Left rostral middle frontal gyrus	0.29	-186.56±246.4	104.89	0.78	0.98
Left superior frontal gyrus	0.71	-241.16±492.2	177.67	0.49	0.98
Left superior parietal gyrus	0.15	-156.85±181.09	81.87	0.89	0.98
Left superior temporal gyrus	-0.62	-247.3±134.18	92.42	0.55	0.98
Left supramarginal gyrus	-0.23	-203.82±163.26	88.93	0.83	0.98
Left temporal pole	-1.15	-117.91±33.99	36.8	0.27	0.98
Left transverse temporal gyrus	0.55	-17.53±30.17	11.56	0.59	0.98
Right banks of the superior temporal sulcus	-0.34	-72.89±52.65	30.42	0.75	0.98
Right caudal anterior cingulate cortex	0.43	-39.21±59.53	23.92	0.68	0.98
Right caudal middle frontal cortex	-0.07	-159.38±149.7	74.88	0.95	0.98
Right cuneus	1.16	-24.94±88.22	27.42	0.26	0.98
Right entorhinal cortex	0.87	-47.4±116.44	39.69	0.4	0.98
Right frontal pole	-2.81	-87.2±-13.29	17.91	0.01	0.43
Right fusiform gyrus	0.27	-169.27±218.15	93.86	0.8	0.98
Right inferior parietal gyrus	0.8	-162.81±366.01	128.11	0.44	0.98
Right inferior temporal gyrus	-0.73	-645±311.16	231.64	0.48	0.98
Right insula	-0.1	-222.44±202.52	102.95	0.93	0.98
Right isthmus cingulate	1.93	-2.82±79.94	20.05	0.07	0.98
Right lateral occipital cortex	-0.34	-203.36±146.24	84.7	0.74	0.98
Right lateral orbitofrontal cortex	-0.36	-405.92±286.48	167.74	0.73	0.98
Right lingual gyrus	-0.77	-157.04±71.76	55.43	0.45	0.98
Right medial orbitofrontal cortex	1.17	-45.9±165.02	51.1	0.26	0.98
Right middle temporal gyrus	-1.14	-659.97±192.53	206.53	0.27	0.98
Right paracentral gyrus	1.01	-30.18±87.94	28.62	0.33	0.98
Right para-hippocampal gyrus	0.33	-45.33±62.21	26.06	0.75	0.98

Right pars opercularis	-0.39	-155.89±106.45	63.56	0.71	0.98
Right pars orbitalis	-1.18	-230.44±63.4	71.19	0.26	0.98
Right pars triangularis	-1.22	-181.61±47.29	55.46	0.24	0.98
Right pericalcarine	1.45	-16.88±95.04	27.11	0.17	0.98
Right postcentral gyrus	0.98	-65.44±182.08	59.97	0.35	0.98
Right posterior cingulate	-0.93	-141.14±54.02	47.28	0.37	0.98
Right precentral cortex	0.76	-144.51±311.47	110.47	0.46	0.98
Right precuneus	1.35	-29.72±141.4	41.46	0.2	0.98
Right rostral anterior cingulate	0.14	-60.85±69.57	31.6	0.9	0.98
Right rostral middle frontal gyrus	-1.16	-562.78±157.98	174.61	0.26	0.98
Right superior frontal gyrus	1	-140.64±403.04	131.72	0.33	0.98
Right superior parietal gyrus	0.38	-135.48±196.04	80.31	0.71	0.98
Right superior temporal gyrus	-0.5	-151.41±93.01	59.21	0.63	0.98
Right supramarginal gyrus	0.49	-109.42±175.98	69.14	0.64	0.98
Right temporal pole	1.97	-3.22±125.62	31.22	0.07	0.98
Right transverse temporal gyrus	1.24	-11.6±45.92	13.94	0.24	0.98
Subcortical					
Brain Stem	0.16	-191.41±222.13	100.18	0.88	0.98
Left Accumbens	0.16	-22.73±26.47	11.92	0.88	0.98
Left Amygdala	-0.41	-67.48±45.31	27.33	0.69	0.98
Left Caudate	0.83	-20.73±48.15	16.69	0.42	0.98
Left Cerebellum Cortex	-0.05	-488.36±465.84	231.16	0.97	0.98
Left Hippocampus	-1.3	-73.01±16.64	21.72	0.21	0.98
Left Pallidum	-0.02	-34.46±33.82	16.54	0.99	0.99
Left Putamen	2.95	25.14±142.53	28.45	0.01	0.43
Left Thalamus	0.19	-146.11±175.67	77.96	0.86	0.98
Left Ventral Diencephalon	1.14	-39.43±134.98	42.26	0.27	0.98
Right Accumbens	0.79	-15.9±35.47	12.45	0.44	0.98
Right Amygdala	-0.07	-49.21±46.22	23.12	0.95	0.98
Right Caudate	1.69	-21.3±208.1	55.58	0.11	0.98
Right Cerebellum Cortex	-0.28	-707.65±542.25	302.8	0.79	0.98
Right Hippocampus	0.72	-42.75±87.72	31.61	0.49	0.98
Right Pallidum	0.69	-71.14±141.69	51.56	0.51	0.98
Right Putamen	1.63	-24.35±205.27	55.63	0.12	0.98
Right Thalamus	-1.78	-255.52±19.34	66.59	0.09	0.98
Right Ventral Diencephalon	1.35	-22.27±106.08	31.1	0.2	0.98

Table 6. Summary statistics of the analysis of differences between ACTIVE and PLACEBO on FreeSurfer volumetric estimates for each cortical and subcortical parcellation. The direction of the numerical difference is given by the sign of the t value. For +ve t-value the contrast is ACTIVE>PLACEBO and for -ve t values ACTIVE<PLACEBO.

Voxel-wise analysis

VBM analysis did not reveal FWE-corrected significant results in both DRUG>PLACEBO and DRUG<PLACEBO contrasts.

3.4.6 Quantitative T1 analysis

ROI analysis

No significant effect of the session was found in the three pre-selected *a priori-defined* ROIs. Table 6 and Figure 9 report the statistics of these analyses.

ROI	DRUG	Mean	SD	p-value
Nucleus Accumbens	PLACEBO	1.266	0.030	0.79
	ACTIVE	1.269	0.028	
Caudate	PLACEBO	1.405	0.055	0.40
	ACTIVE	1.402	0.064	
Putamen	PLACEBO	1.038	0.027	0.37
	ACTIVE	1.041	0.028	

Table 7. Summary statistics of the ROI subcortical analyses on T1 values (seconds). SD: standard deviation.

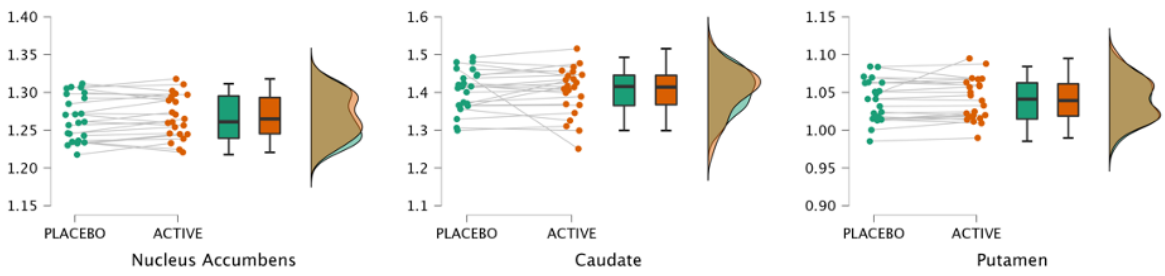

Figure 9. Raincloud plots of the differences in T1 values between ACTIVE and PLACEBO conditions in the three pre-selected a priori ROIs.

Voxel-wise analysis

Voxel-wise analysis on T1 maps revealed no significant effects in both ACTIVE>PLACEBO and ACTIVE<PLACEBO contrasts.

3.4.7 CBF analysis

Global CBF

No significant differences between ACTIVE and PLACEBO conditions in global CBF (ml/100g/min) were found (mean ± SD, ACTIVE: 41.6 ± 5.9, PLACEBO: 43.2 ± 8.3, p value= 0.23).

ROI analysis

Repeated measure ANCOVA with order and global CBF as covariate of no interest revealed a significant increase in regional CBF in all bilateral *a priori* defined ROIs in the ACTIVE condition as compared with the PLACEBO condition (nucleus accumbens: F= 12.8, η_p^2= 0.42, p= 0.002, average % CBF increase= 5.5%; caudate: F= 17.4, η_p^2= 0.49, p< 0.001, average % CBF increase= 6.9%; putamen: F= 26.9, η_p^2= 0.59, p< 0.001, average % CBF increase= 7.4%). All results survived Bonferroni correction for multiple testing (alpha= 0.05/3= 0.016). Figure 10 summarizes the results of the ROI analysis on CBF data. Repeated measure ANCOVA with order but not global CBF as a covariate of no interest did not reveal statistically significant differences between ACTIVE and PLACEBO (all p> 0.15).

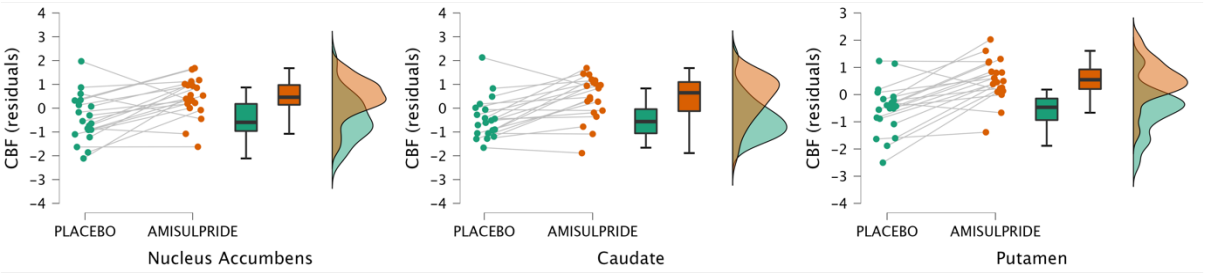

Figure 10. Raincloud plots of the differences in CBF (residuals) between ACTIVE and PLACEBO conditions in the three pre-selected a priori ROIs.

Voxel-wise analysis

Voxel-wise paired t-test with order and global CBF as a covariate of no interest revealed a significant increase in CBF bilaterally in caudate and putamen in the ACTIVE>PLACEBO contrast. The opposite contrast (i.e., ACTIVE<PLACEBO) did not reveal any significant clusters. Figure 11 shows the results of the voxel-wise analysis. Table 8 reports local maxima statistics of the voxel-wise analysis. The analysis without global CBF as a covariate of no interest did not reveal any statistically significant result in both ACTIVE>PLACEBO and ACTIVE<PLACEBO contrasts.

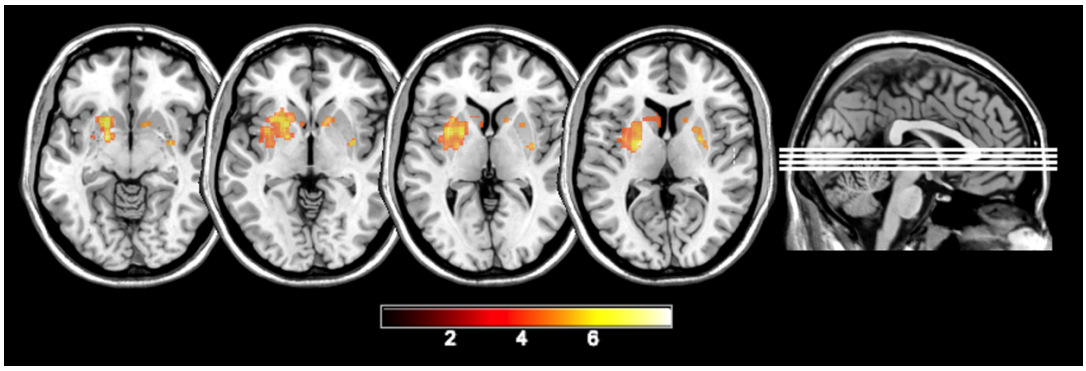

Figure 11. Brain sections showing increased CBF in the ACTIVE relative to the PLACEBO condition in bilateral clusters encompassing the caudate and the putamen (TFCE-corrected clusters). The colour bar indicates t-statistics.

Cluster Index	t	MNI coordinates (x, y, z) in mm			Brain region
1	6.72	26	-2	10	right putamen
1	5.98	32	-6	-6	right putamen
1	5.79	34	-6	2	right putamen
1	5.67	20	6	16	right caudate
1	5.15	12	10	-12	right nucleus accumbens
1	5.15	12	12	0	right caudate
2	8.01	-22	-6	10	left putamen
2	7.33	-18	0	-6	left globus pallidus
2	7.18	-32	4	2	left putamen
2	7.1	-20	12	-6	left putamen
2	6.92	-24	14	-4	left putamen
2	6.61	-22	4	2	left putamen

Table 8. Local maxima statistics of the voxel-wise non-parametric paired t-test on CBF data (ACTIVE>PLACEBO contrast). Only TFCE-corrected clusters are reported.

Spatial mapping to receptor density profiles

The analysis of the spatial correlation between D_2R density and ΔCBF returned a significant positive linear association between ΔCBF and D_2R density profiles (rho= 0.4, p= 0.02). Results were retained also after controlling for spatial autocorrelation effects.

Association with EPS

Spearman correlation did not indicate an association between relative CBF changes in the voxel-wise significant cluster and total ESRS scores (rho= -0.35, p= 0.137).

3.4.8 PK/PD model

The pharmacokinetic simulation returned a model that was able to correctly predict the kinetics of amisulpride after repeated doses with the concentration being in line with previous reports (Bowskill, Patel, Handley, & Flanagan, 2012; Bressan et al., 2003; Meisenzahl et al., 2008; Puech, Fleurot, & Rein, 1998). Moreover, the majority of the subjects fell inside the simulated concentration curves showing that the data were in agreement with the plasma concentration measured in previous studies (Figure 12). The subjects outside the range were considered outliers and not considered for further analysis.

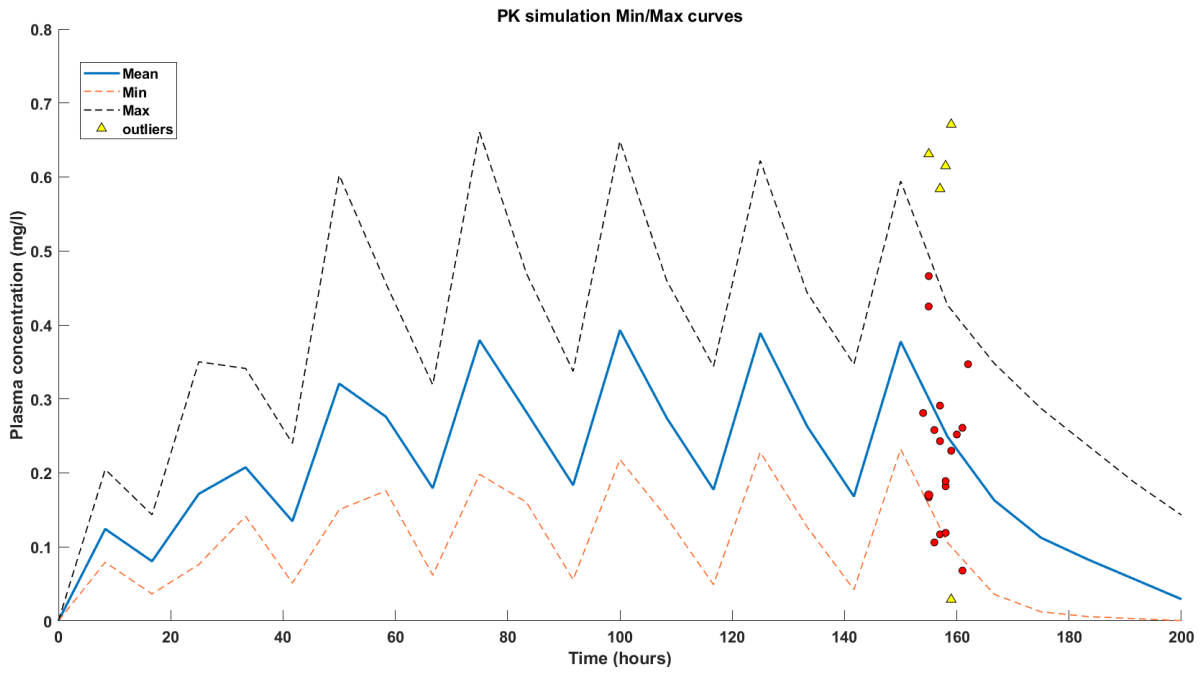

Figure 12. Maximum, minimum, and mean curves obtained with PK simulation. Red dots and yellow triangles indicate the participants' data. Red dots indicate participants whose amisulpride plasma levels fell within the expected range. Yellow triangles indicate participants whose amisulpride plasma levels were outliers for the given distribution.

The fitting of PET receptor occupancy data returned a EC_{50} value of 182.1 ng/ml for the putamen and 117.7 ng/ml for the caudate, in line with previous findings (Vernaleken et al., 2004). Given the plasma concentration of amisulpride across subjects, simulated receptor occupancy ranged from 11.6 to 86.9% for the putamen and from 16.9 to 91.1% for the caudate. The mean+/-SD of amisulpride receptor occupancy was 52.9+/-17.7% for the putamen and 62.3+/-17.2% for the caudate and in agreement with the expected D_2R occupancy of the drug with the given dosage (Vernaleken et al., 2004). Figure 13 shows the results of the receptor occupancy simulation.

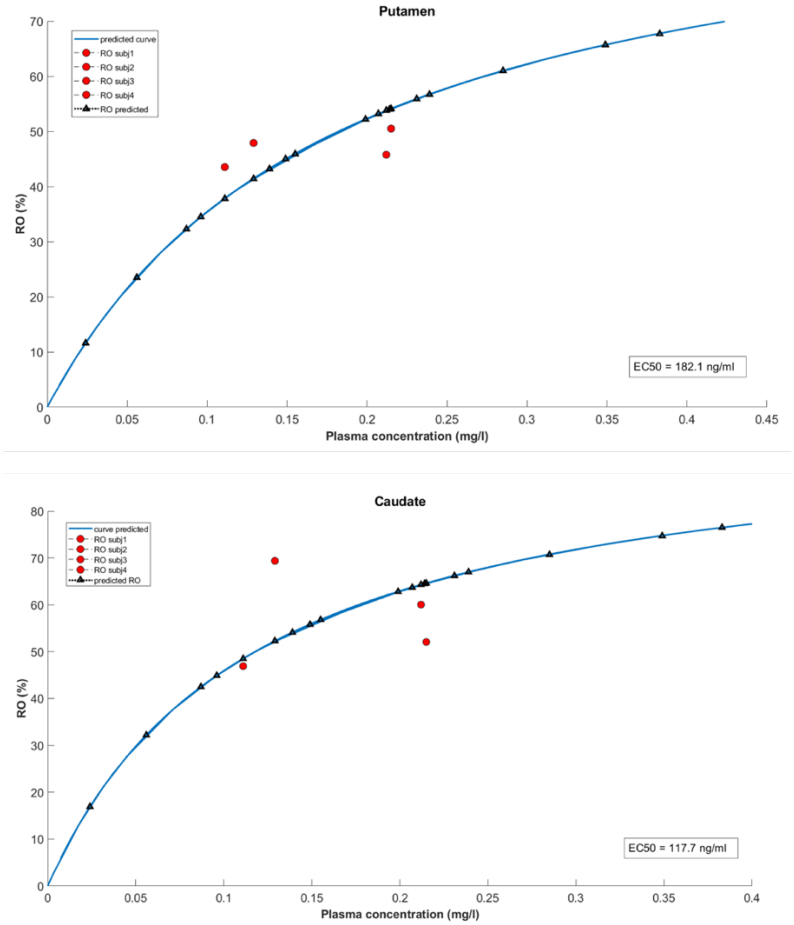

Figure 13. Results of the receptor occupancy simulation for the putamen (top) and the caudate (bottom). The blue line indicates the predicted relationship between plasma amisulpride levels (mg/l) and receptor occupancy

(RO). Red circles indicate true data (RO calculated in this study), and black triangles indicate predicted receptor occupancy corresponding to true amisulpride plasma level for all the subjects who did not have PET scans.

Figure 14 shows the relationship between amisulpride receptor occupancies and ΔCBF changes for the putamen and the caudate. The models were statistically significant for both the putamen *(*F= 19.2, p< 0.001*)* and the caudate (F= 8.25, p-value< 0.01). The exponent b of the power law model (Equation 5) was 1.66 and 1.82 for the putamen and the caudate, respectively and both were in line with previous preclinical findings in primates (Sander et al., 2013). Taken together these results indicate that the model proposed by (Sander et al., 2013) was able to fit ΔCBF changes and receptor occupancy in this dataset.

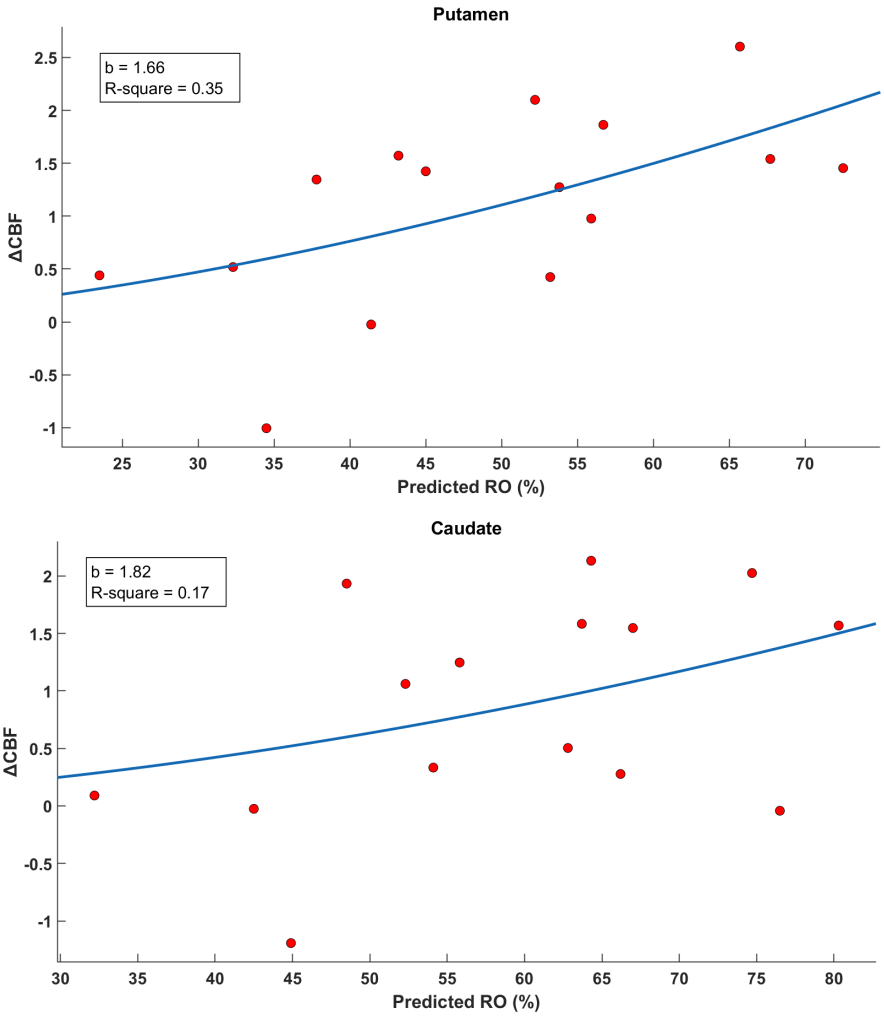

Figure 14. ΔCBF vs. amisulpride receptor occupancy for the putamen (top) and the caudate (bottom). Data show a monotonically increasing relationship (p< 0.001). RO: receptor occupancy.

3.4.9 Functional connectivity analysis

Figure 15 shows the group-average FC maps for each striatal seed. The group-average FC maps closely matched the expected FC networks for the three probabilistic striatal subdivisions of the Oxford-Imanova Atlas (Tziortzi et al., 2014).

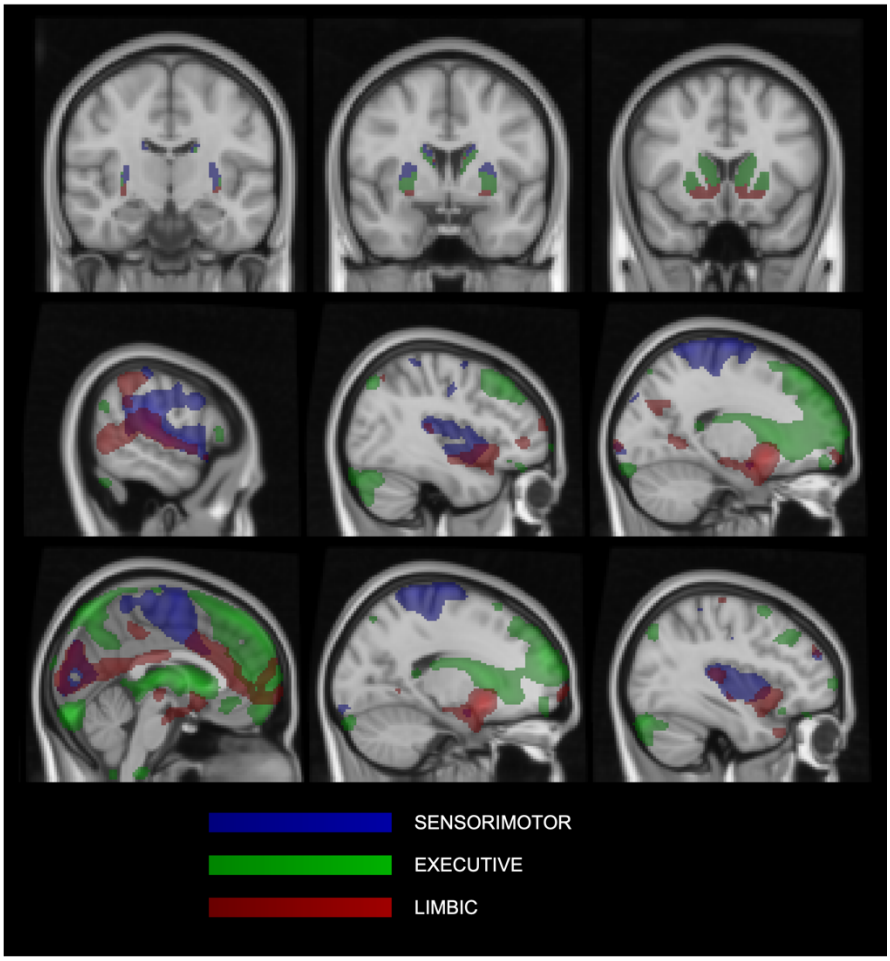

Figure 15. Top row: striatal probabilistic subdivisions as in the Oxford-Imanova atlas (Tziortzi et al., 2014). Central and bottom rows: group-average (for both ACTIVE and PLACEBO sessions) FC networks for each striatal subdivision. The colour legend applies to all rows, blue: sensorimotor, green: executive, red: limbic.

Paired t-tests in *randomise* revealed a significant TFCE-corrected cluster (p= 0.008) for the ACTIVE<PLACEBO contrast in the sensorimotor network, which was located in the left motor cortex (Figure 16). Table 10 reports the local maxima statistics of this analysis. No

significant TFCE-corrected clusters were found in the opposite (i.e., ACTIVE>PLACEBO) contrast, nor in limbic and executive FC networks in both contrasts.

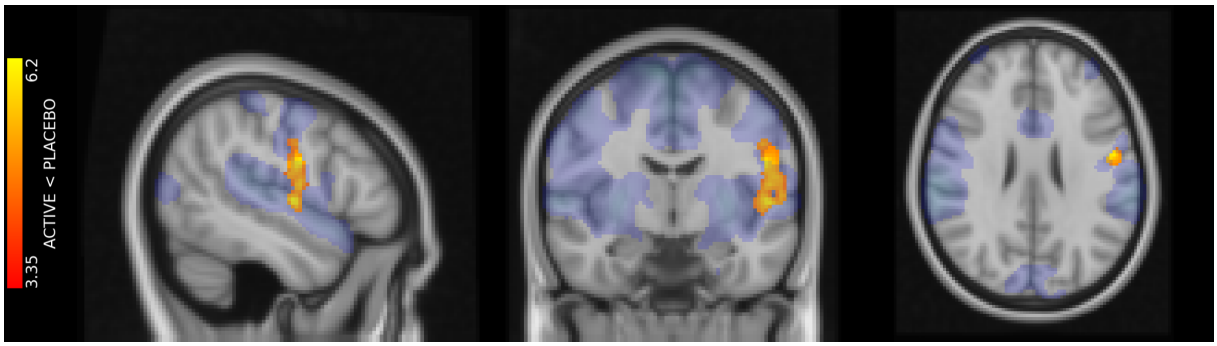

Figure 16. Brain sections showing decreased (ACTIVE<PLACEBO) FC between the sensorimotor subdivision of the striatum and the primary motor cortex after amisulpride. The colour bar indicates t statistics. In light blue overlay of the group-average sensorimotor FC network.

Cluster Index	t	MNI coordinates (x, y, z) in mm			Brain region
1	7.75	-58	0	0	left supplementary motor area (BA 6)
1	6.61	-54	0	18	left supplementary motor area (BA 6)
1	6.34	-60	-10	6	left primary motor cortex (BA 4)
1	6.23	-44	-10	32	left primary motor cortex (BA 4)
1	6.18	-50	-6	24	left supplementary motor area (BA 6)
1	6.09	-58	-12	14	left primary sensory cortex (BA 1)
2	9.3	-54	10	-8	left superior temporal gyrus (BA 22)

Table 9. Local maxima statistics of the voxel-wise non-parametric paired t-test on FC within the sensorimotor network (ACTIVE>PLACEBO contrast). Only TFCE-corrected clusters are reported. BA: Brodmann Area.

Association with CBF

Spearman correlation did not indicate an association between CBF changes in the striatum and FC changes in the motor cortex using both absolute (rho= 0.04, p= 0.89) and relative-to-global CBF (rho= 0.144, p= 0.59).

Association with EPS

Spearman correlation indicated a significant negative association between FC changes in the peak voxel in Broadman Area 6 (MNI coordinates: -58 0 0) and EPS changes such as subjects with a greater reduction in cortico-striatal FC in the ACTIVE conditions also showed greater

EPS after one week of amisulpride 400mg daily doses (rho= -0.54, p= 0.037). Figure 17 reports the scatterplot of this association.

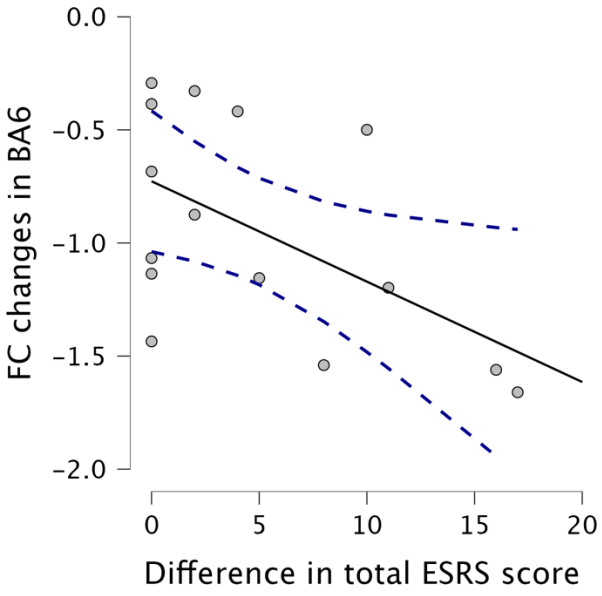

Figure 17. Scatterplot showing the association between-sessions FC differences in the peak significant voxel in Broadman Area 6 (BA6, MNI coordinates: -58 0 0) and between-session difference in total ESRS score. Both differences were computed by subtracting PLACEBO from ACTIVE session values.

3.5 Discussion

Overall, the results of my analyses supported the main hypothesis of the study. In particular, they indicate that sustained D_2R blockade produces functional alterations in the striatum in the absence of structural changes. In addition, my findings also provide preliminary evidence of an association between CBF changes in the striatum induced by antipsychotics and inter-individual variability in D_2R occupancy. Moreover, functional alterations were associated with EPS developed after antipsychotic administration.

Effect of sustained D_2R blockade on brain structure

I did not find differences in either brain volume or quantitative T1-signal between amisulpride and placebo conditions. FreeSurfer ROI analysis revealed differences between amisulpride and placebo conditions in the right frontal pole and the left putamen. However, these effects were not significant after correction for multiple comparisons indicating that they were likely spurious results.

These negative findings are in line with previous studies in HC using single-dose administration of antipsychotics (Hawkins et al., 2018) and in contrast with earlier reports of changes in T1 (Fujimoto et al., 1987) and grey matter volume (Tost et al., 2010) after acute intravenous injection of haloperidol in dogs and humans respectively. However, a direct comparison between our study and the studies by Fujimoto et al. (1987) and Tost et al. (2010) is complicated by the different routes of administration. In particular, acute intravenously administered doses (Fujimoto et al., 1987; Tost et al., 2010) produce large and rapid increases in drug plasma levels as compared with the oral repeated-dose regime with first-pass metabolism and steady-state equilibrium used in the present study and typical clinical dosing regimens. For example, acute intravenous administration of high doses of antipsychotics could produce physiological changes (both locally and systemically) that alter the biophysical environment and could consequently have an impact on the MRI measurement even in the absence of real changes in tissue characteristics such as microstructure composition or volume. In other words, several other transient processes could explain the alterations in MRI signal interpreted as apparent "structural" changes in these studies such as changes in cell microstructure, cell and tissue hydration, changes in iron content, activation of microglia, transient tissue remodelling as a consequence of systemic effects (Weinberger & Radulescu, 2016, 2021) which might manifest only in these particular experimental conditions and not in oral exposures like in our study and in Hawkins et al. (2018). Critically, in this study, I investigated the effect of D_2R blockade on brain structure adding to standard volumetric analysis on T1-weighted data also quantitative T1 mapping as the outcome measure. As discussed in the introduction, quantitative T1 mapping is more informative on brain microstructure as compared with standard T1-weighted images (Franklin et al., 2013; Marques et al., 2010; Salgado-Pineda et al., 2006). Indeed, T1-weighted images are qualitative measures that are heavily dependent on acquisition protocols which limits reproducibility and could also be influenced by several "non-structural" factors that alter the magnetic resonance properties of the tissue (e.g., T1 relaxation time) such as differences in the water content, changes in iron content, myelination, or microglial activation (Cousins et al., 2013; Deoni, 2011; Franklin et al., 2013; Salgado-Pineda et al., 2006). Therefore, the absence of an effect of sustained D_2R blockade on quantitative mapping provides a within-study validation of the negative findings in brain volume based on T1-weighted images.

Thus, the findings of my structural analysis showed that there were no differences in structural morphometrics, and also no differences in quantitative T1 values which influence the T1-weighted mapping approach that is commonly used. This extends earlier evidence of single-dose studies in healthy volunteers with clinically relevant doses (Hawkins et al., 2018), indicating that sustained D_2R blockade in healthy volunteers, obtained with repeated administration of D_2R antagonists, is not associated with changes detectable with both T1 mapping techniques and T1-weighted morphometric. This indicates that both acute and sustained D_2R blockade at clinically relevant doses that achieve antipsychotic effects in patients with psychosis do not produce a pharmacological effect in brain structural morphometrics as detectable by current MRI techniques in healthy individuals. Critically the present findings and the one in Hawkins et al. (2018) were found in randomised, within-subjects and placebo-controlled experiments as opposed to previous results obtained in serial experiments without a placebo-control session (Tost et al., 2010).

A very limited number of clinical studies with placebo-controlled designs have investigated the effects of antipsychotics on brain structure in patients with psychosis. While this scarcity is justifiable by ethical concerns, recently the results from two randomized placebo-controlled studies in patients have been published. Voineskos et al. (2020) found, in a 36-week placebo-controlled study in patients with psychotic depression a reduction in cortical thickness in patients treated with olanzapine as compared with the placebo arm. Notably, patients were not naïve to antipsychotic treatment as they were randomly assigned to the active or placebo arm after having reached remission of both psychosis and depression in a previous trial with a combination of olanzapine and sertraline. Chopra, Fornito, et al. (2021) investigated in antipsychotic naïve FEP the effects of SGAs (risperidone or paliperidone) against placebo in 6 months. The two groups were also paralleled with a longitudinal cohort of healthy volunteers. At 3 months, the authors found an increase in pallidal grey matter volume in patients treated with antipsychotics, a reduction in the placebo arm and no changes in the HC cohort. However, pallidal volume normalized in both active and placebo arms after 12 months. As discussed in the Introduction, the two studies reported inconsistent results which might be explained by different study designs, patient characteristics, treatment regimes and other disease states.

The results presented here are also inconsistent with these placebo-controlled studies in patients (Chopra, Fornito, et al., 2021; Voineskos et al., 2020). However, it should be noted,

that both investigations examined a much longer exposure (i.e., 3-9 months) as compared with the exposure tested in this study (i.e., one week). So, one possible interpretation of our findings in the context of the clinical evidence might suggest that tissue remodelling induced by D_2R blockade might require longer exposure (i.e., at least more than one week) to produce detectable changes in MRI signals currently used for the investigation of brain structure. This hypothesis might be sustained also by pre-clinical studies in rodents and non-human primates which have found reduced grey matter volumes after chronic antipsychotic administration (with an exposure approximately equivalent to as much as 2 human years) (Dorph-Petersen et al., 2005; Vernon et al., 2012; Vernon et al., 2011). This hypothesis is also coherent with the findings of Andersen et al. (2020) who reported increased striatal volume in FEP after 6 weeks of treatment with a low dose of amisulpride. However, their investigation was not paralleled by careful investigation of T1 and CBF so it might be possible that their findings were just "apparent" morphometric changes. In light of the inconsistencies and the limitations of the clinical study, the present negative findings add to the current debate on the effect on the brain structure of exposure to antipsychotics, showing that one week of D_2R blockade in HC, so in the absence of disease state and trait effects, does not produce alteration in MRI signals usually interpreted as brain "structural" changes. Future placebo-controlled clinical studies in patients with psychosis with higher control of confounding factors as compared with previous studies (e.g., heterogeneity in diagnosis, treatment, dosing regime, previous exposure, etc.) and maybe placebo-controlled studies in healthy control with longer exposure as compared to the one used in this study might further clarify the role of antipsychotic exposure on brain remodelling and how it interacts with disease effects. However, it must be acknowledged that studies in HC with D_2R blockade exposure longer than one week might be difficult to perform in reason of ethical concerns about the risk-benefit ratio for participants. In addition, the present study suggests that future longitudinal clinical studies could add to standard brain morphometric analyses based also quantitative T1 mapping to dampen down the highlighted risk to interpret as "structural" changes alterations of MRI signals unrelated to actual brain remodelling processes (Weinberger & Radulescu, 2016, 2021).

Effect of sustained D_2R blockade on brain perfusion

Both ROI and voxel-wise analyses indicated increased CBF in the striatum with a larger effect size in the putamen as compared with other striatal subdivisions. These results extend previous evidence from single-dose studies in healthy volunteers (Fernandez-Seara et al., 2011; Handley et al., 2013; Hawkins et al., 2018; Mehta et al., 2003) indicating that also sustained D_2R blockade is associated with increased perfusion in the striatum. Interestingly, similarly to Hawkins et al. (2018) I found increased CBF in the absence of changes in T1 relaxometry metrics, further suggesting that changes in brain perfusion induced by antipsychotics are not likely to drive brain volumetric changes (or apparent changes) as hypothesized by previous reports (Franklin et al., 2013). My findings might appear in contrast with the results reported by Viviani et al. (2013), which showed that a repeated daily oral dose of amisulpride 200mg for 7 days was associated with a large significant cortical reduction in CBF and a modest (and not corrected for multiple comparisons) increase in the striatum. In this study, I found a robust increase in CBF in the basal ganglia in the absence of cortical reduction. This apparent discrepancy might be reconciled by taking into account that in this study we used a higher amisulpride dose (i.e., 400mg) which achieves on average approximately 60% of D_2R occupancy in the striatum which is within the therapeutic range required for the treatment of psychotic symptoms (Kapur et al., 2000; Vernaleken et al., 2004). Therefore the use of a higher dose of amisulpride with a higher occupancy of D_2R could explain the larger effect size of CBF change in the striatum in our study as compared with previous reports. This interpretation is also coherent with preclinical models suggesting a direct monotonic relationship between D_2R occupancy and neurovascular coupling (Mandeville et al., 2013; Sander et al., 2013) confirmed by the PK/PD analysis performed here. The absence of cortical effects in our study is more difficult to reconcile with the findings by Viviani et al. (2013), but a possible explanation might rely upon the different doses as well. As discussed in the introduction, amisulpride, as other benzamides (e.g., sulpiride), at low doses, shows a selective modulation of dopamine release acting preferentially on pre-synaptic D_2R/D_3R auto-receptors (Pani & Gessa, 2002; Schoemaker et al., 1997). Given the hypothesized indirect monotonic relationship between dopamine release and CBV via D_2R agonism (Mandeville et al., 2013; Sander et al., 2016) it might be possible that at low dose amisulpride could produce a reduction in CBV and CBF which is not detectable at higher doses where the antagonism at post-synaptic D_2R/D_3R blockade is prevalent.

In this study, I was able to detect increased perfusion in the striatum after sustained D_2R blockade after regressing out global perfusion as a covariate of no interest whereas these effects did not reach statistical significance without the inclusion of this covariate in the model. However, it should be noted that absolute CBF and relative-to-global CBF are not necessarily interchangeable or collinear measures (see this issue discussed in greater detail in Chapter 4) and therefore a careful interpretation of the findings in this context is important. The regression of global perfusion in CBF analyses is an approach that has been adopted in many studies to minimize between-subjects and between-session variability and has been shown to increase sensitivity in within-subject designs in both PET and ASL experiments (Boellaard, 2009; Viviani et al., 2009). In the specific context of studies investigating the effect of antipsychotic exposure on CBF, most authors reported differences between the two metrics with larger effect sizes obtained in global-perfusion-regressed models as compared with absolute CBF estimations also in the absence of differences in global perfusion between conditions as in this study (Fernandez-Seara et al., 2011; Handley et al., 2013; Hawkins et al., 2018; Viviani et al., 2013). Previous studies have shown dose-dependent relative CBF changes after drug administration in the absence of absolute changes (Black et al., 2000), suggesting that changes in relative CBF might better capture "neuronal" effects of drug exposure as opposed to absolute CBF which might be more heavily affected by non-neuronal (e.g., vascular) effects. My results are therefore in line with previous findings as regards CBF metrics and with this hypothesis. In addition, it is important to highlight that, even though amisulpride has a high affinity for D_2R/D_3R receptors, it also shows non-negligible affinities for serotonin receptors such as $5HT_2BR$ and $5HT_7R$ (Abbas et al., 2009). Antagonism at serotonin receptors (including $5HT_2BR$ and $5HT_7R$) has been associated with relative vasodilation due to the blockade of the sympathetic tone induced by the endogenous ligand serotonin (Kovacs et al., 2012; Launay et al., 2002; Ullmer et al., 1995). Even though in this study I did not find a significant difference in whole grey matter CBF between sessions on average grey matter perfusion was lower in the amisulpride as compared with the placebo condition (amisulpride: 41.6 ± 5.9, placebo: 43.2 ± 8.3). Therefore, as previously discussed, it might be possible that in this study the inclusion of the global perfusion as a covariate might have further increased sensitivity by partially regressing out non-neuronal effects. Interestingly, a similar pattern of differential effect sizes between absolute and relative-to-global CBF has been observed in previous studies using single-dose administration of other

antipsychotics with affinity to serotonin receptors such as olanzapine, risperidone and aripiprazole (Handley et al., 2013; Hawkins et al., 2018). Also, D_3R mediate non-neuronal changes in CBF being present in astroglial cells where D_3R agonism has been shown to produce vasoconstriction (Choi et al., 2006). Amisulpride has a strong affinity for both D_2R and D_3R receptors as an antagonist, therefore the contribution of non-neuronal effects on CBF mediated by D_3R represents an important factor contributing to the observed CBF increase due to vasodilation. In this study, I found the largest increase in CBF in striatal regions such as the putamen and the caudate in which the relative concentration of D_2R prevails over D_3R as compared with other regions such as the ventral striatum, the globus pallidus and the substantia nigra (Smart et al., 2020; Tziortzi et al., 2011). Therefore, even though the D_3R-mediated effect on CBF should be considered an important confounding factor in this study, the spatial distribution of the effects found in this study suggests that it is unlikely that my findings have been completely driven by non-neuronal mechanisms.

I also found a spatial association between CBF changes induced by amisulpride and D_2R spatial distribution profiles as indexed by the [^{18}F]-Fallypride BP_{ND} template map. These findings extend the ones reported in Chapter 2 (Selvaggi et al., 2019) indicating that a spatial match exists also between D_2R distribution in the brain and CBF changes induced by sustained D_2R blockade induced by antipsychotics. Also here data shows that the relationship between CBF increases after antipsychotic administration also matched D_2R profiles in extra-striatal ROIs, significantly populated by D_2R such as the thalamus and the amygdala, even though they show lower BP_{ND} template values as compared with striatal ROIs further suggesting that the hypothesized neurovascular coupling model (Mandeville et al., 2013; Sander et al., 2013) might also be valid outside the striatum. However as discussed in Chapter 2, spatial matching, being based on a population-based profile of D_2R density, does not take into account between-subject variability in D_2R within the same brain region (Farde et al., 1995) which might drive inter-individual differences in drug response.

PK/PD model

To explore how between-subjects variability in D_2R relates to differences in CBF changes after D_2R blockade, I investigated the relationship between D_2R occupancy and CBF changes. However, since in this study [^{11}C]-PHNO PET scans were allocated only to a limited number of participants, I did not have a number of complete datasets (i.e., both

longitudinal PET [^{11}C]-PHNO and ASL scans) to achieve a sufficient power to detect such a relationship in the whole sample. For this reason, a PK/PD predictive framework was developed to overcome these limitations. First, I verified using a simulation that measured amisulpride plasma levels in each participant conformed to a repeated dose administration PK model described in the literature. I found that most of the subjects had amisulpride plasma levels falling inside the range of concentration predicted by the literature-based model (Bowskill et al., 2012; Bressan et al., 2003; Meisenzahl et al., 2008; Puech et al., 1998). The results of the receptor occupancy analyses were in line with what was expected from previous studies investigating D_2R occupancy by amisulpride in humans (la Fougere et al., 2005; Martinot et al., 1996; Vernaleken et al., 2004). Amisulpride plasma levels were used to predict unknown D_2R occupancy for the remaining subjects through the Hill equation. I obtained receptor occupancy predictions, given the corresponding amisulpride plasma levels, that were also in line with previous reports (Sparshatt et al., 2009). Finally, the relationship between predicted receptor occupancy and observed CBF changes after amisulpride in our dataset was significantly fitted by the neurovascular coupling model described in non-human primates (Sander et al., 2013). Model fit indicated a monotonically increasing relationship between CBF changes and D_2R occupancy in the caudate and the putamen such as higher D_2R occupancy was associated with higher CBF increase in the amisulpride as compared with the placebo condition. To the best of my knowledge, this is the very first time that this relationship has been detected in vivo in humans. However, it must be acknowledged that the present findings were obtained using a combination of real and simulated data. Future studies with a methodology with higher sensitivity and precision (e.g., simultaneous PET/MR) could refine the evidence presented here. In addition, future studies could also test the stability of this neurovascular coupling model to different D_2R antagonists with different affinities to D_2R and other receptors such as serotonin receptors and with different brain penetration mechanisms (Hartter et al., 2003; Sekhar et al., 2019). Establishing a detailed PK/PD relationship in drug studies could open a variety of useful clinical and experimental applications. Taking the example examined in the present thesis, if future human studies could demonstrate with sufficient reproducibility and specificity the link between D_2R occupancy and consequent CBF change following D_2R blockade, it might be possible in principle to index D_2R occupancy in patients with psychosis with MRI signals with maybe higher precision than currently available methods and while avoiding exposure

to noxious effects such as injected radioactivity or more importantly side effects associated with a D_2R occupancy above the therapeutic window of antipsychotics (Kapur et al., 2000; Nord & Farde, 2011). Another interesting clinical application of the present findings might be to test whether such neurovascular coupling exists in patients with psychosis, how it compares with the physiological one and how it relates to treatment response and side effects.

Effect of sustained D_2R blockade on functional connectivity

Seed-based FC analyses revealed a functional uncoupling (i.e., reduced functional connectivity) between the sensorimotor subdivision of the striatum and the primary motor cortex after sustained D_2R blockade with amisulpride. No significant effects were detected in cortico-striatal FC with the limbic and executive striatal seeds. My results are difficult to match with inconsistent evidence coming from longitudinal studies in FEP showing either reduced functional connectivity between the striatum and frontal and parietal cortices (Lui et al., 2010) or increased cortico-thalamic FC (Sarpal et al., 2015). However, as already discussed, the interpretation of drug effects in clinical longitudinal studies is complicated by disease state and traits, and other factors that affect most studies (e.g. non-randomisation to treatment, lack of placebo control) which do not allow us to fully elucidate treatment effects. My results better match and extend evidence from earlier reports of single-dose administration of antipsychotics showing a reduced FC between the striatum and parietal regions including the motor cortex (Cole, Beckmann, et al., 2013; Cole, Oei, et al., 2013; Tost et al., 2010), by showing that a cortico-striatal functional uncoupling within the motor circuit is present also after sustained D_2R blockade. Grimm et al. (2020) reported increased FC between the striatum and the motor cortex after a single dose of amisulpride 200mg which is in apparent contrast with my findings. However, as already discussed previously, amisulpride at low doses acts preferentially on pre-synaptic D_2R/D_3R auto-receptors modulating dopamine release as opposed to higher doses where it acts preferentially as an antagonist at post-synaptic D_2R/D_3R (Pani & Gessa, 2002; Schoemaker et al., 1997). Thus, this dose-dependent dual mechanism of action might explain the opposite findings between this study and the one by Grimm et al. (2020).

I was able to show that functional uncoupling between the sensorimotor subdivision of the striatum and the motor cortex also correlated with the severity of EPS after amisulpride administration. My findings extend earlier evidence which showed an association between

functional uncoupling within the motor cortico-striatal loop and motor impairment evaluated as delayed reaction time in a motor task following intravenous acute injection of haloperidol in seven healthy participants (Tost et al., 2010) indicating that this relationship also exists after sustained D_2R blockade with oral, repeated doses of a D_2R antagonist. Interestingly, in this study reduced FC between the dorsal striatum and the motor cortex after sustained D_2R blockade, was associated with EPS which represents more profound motor impairments as compared with delayed response in a motor task. Critically, these results are coherent with current knowledge on the role of D_2R in striatal MSN of the indirect pathway which are interconnected with the motor cortex (Borra et al., 2021; Martel & Galvan, 2022; Wall et al., 2013) and participate in motor control. Indeed, pre-clinical studies have shown that chronic blockade of D_2R alters neuronal plasticity in the dorsal striatum reducing the excitability of the indirect pathway and in turn altering the balance of striatal functional connections (Cazorla et al., 2014; Cazorla et al., 2012; Chan et al., 2012). As stated in the introduction, the most frequent and perhaps most disabling side effect associated with chronic D_2R blockade in patients with psychosis are EPS. Here I was able to identify a pattern of brain MRI signal alterations after sustained D_2R blockade in healthy volunteers which were associated with EPS which might be tested as a potential biomarker for EPS in clinical studies.

Finally, even though the significant cluster found in the CBF analysis, and the sensorimotor seed used in the FC analysis overlapped in the dorsal striatum (i.e., posterior putamen), I did not find an association between both absolute and relative CBF changes and FC changes induced by amisulpride. Considering the tight association between CBV, CBF and the BOLD signal (Buxton et al., 2004) this might indicate that the changes in FC found in this study were not affected by changes in striatal perfusion induced by amisulpride.

Strength and limitations

One strength of this study is that I tested the effect of repeated doses of antipsychotics in healthy volunteers on brain structure and function using a multimodal approach that combined different advanced (e.g., quantitative T1 mapping, multi-echo fMRI) MRI sequences with *in vivo* D_2R estimation using PET and with detailed clinical evaluations. To the best of my knowledge, this kind of study is unprecedented. In addition, the use of clinically relevant doses of antipsychotics (i.e., a dose that achieves at least 60% of D_2R

occupancy) is of particular interest for the possible translation of the findings in the clinical setting. Moreover, another strength is the adoption of a rigorous counterbalanced within-subject study design which overcomes the limitations of previous studies using longitudinal uncontrolled designs (Tost et al., 2010). The extensive use of non-parametric testing and careful control for false positives in multiple testing which sometimes undermines the reproducibility of neuroimaging studies (Eklund et al., 2016) is another strength. However, this study has some limitations that must be acknowledged to correctly interpret the results. First, the counterbalanced approach of the study design implied that not all ACTIVE conditions longitudinally followed the PLACEBO conditions. While this approach has the advantage of controlling for order effects, it could be argued that changes present in the ACTIVE conditions could be carried over into later sessions. However, considering that longitudinal single-dose studies have shown that antipsychotic effects are reversible (Hawkins et al., 2018; Tost et al., 2010), I believe that the separation of sessions by a wash-out period of at least 5 amisulpride half-lives has been sufficient to protect from carry-over effects. This is further sustained by the fact that all our findings were robust to the inclusion of order as a covariate of no interest and therefore not limited to one order. In addition, even though PET and MRI were acquired on the same day, they were not acquired at the same times which might have undermined the power to explore the between-subjects variability in the PK/PD model. Moreover, as previously stated, my findings were based on a combination of real and simulated data. Future studies using simultaneous PET/MR might be able to remove this source of variance, therefore, increasing the sensitivity and specificity of the PK/PD model.

4 Brain perfusion in non-medicated FEP patients

4.1 My contribution

At the start of my PhD, the full dataset was already acquired. I performed the pre-processing of ASL data with the advice of Dr. Fernando Zelaya. I integrated the clinical data with the neuroimaging data with the help of Dr. Sameer Jauhar. I also performed all statistical analyses. I interpreted the data with the help of Dr. Sameer Jauhar, Prof. Oliver Howes and my first supervisor Prof. Mitul Mehta. Finally, I drafted the manuscript for publication (Selvaggi et al. (2022) and Appendix C).

4.2 Aims and hypothesis of the study

ASL studies in people with chronic Schizophrenia, treated with antipsychotics, show reduced CBF in frontal, parietal and occipital regions and increased CBF in the basal ganglia (Legind et al., 2019; Liu et al., 2012; Oliveira et al., 2018; Pinkham et al., 2011) though the basal ganglia findings have not been consistently replicated (Ota et al., 2014; Zhu et al., 2017). Thus, there is evidence for cortical hypoperfusion in chronic schizophrenia, but it is unclear from these studies when this occurs in the development of the disorder. The results of previous chapters of the present thesis indicate, in line with evidence from pre-clinical studies (Sander et al., 2013) and other experimental studies (Handley et al., 2013; Hawkins et al., 2018; Mehta et al., 2003), that acute blockade of D_2R is associated with an increased CBF in the basal ganglia and also that the increased perfusion in the basal ganglia persists after sustained D_2R blockade in healthy volunteers. Thus, I aimed to determine if CBF is altered in FEP patients who are free from antipsychotic medication. Based on prior results of this thesis and previous studies in medicated FEP (Kindler et al., 2018), I hypothesized that antipsychotic-free FEP would show lower absolute CBF in the frontal cortex while keeping CBF in the striatum within physiological ranges. In addition, while previous cross-sectional investigations have shown associations between altered CBF and severity of psychotic symptoms in Schizophrenia (Kindler et al., 2018), it is unknown if brain perfusion before treatment (therefore not influenced by antipsychotic medication) is associated with subsequent symptomatic improvement with antipsychotic treatment. Thus, I aimed to

explore this association in a prospective study of patients who went on to receive antipsychotic treatment.

4.3 Methods

4.3.1 Study Participants

Study participants were recruited from FEP teams within South London and Maudsley NHS Foundation Trust (Fusar-Poli et al., 2020) and Central and West London NHS Trust. All participants provided informed written consent. For both groups' exclusion criteria were history of head trauma, dependence on illicit drugs, any significant medical co-morbidity (minor illnesses such as seasonal allergies were permitted) and contraindication to MRI scanning.

Baseline study

The inclusion criteria for the patient group were psychotic disorder according to ICD-10 criteria (World Health Organization et al., 1992) in the first episode of illness. Age and sex-matched healthy volunteers were recruited through local advertisements from the same geographical areas. Inclusion criteria for HC were: no personal history of psychiatric illness (assessed using the Structured Clinical Interview for the Diagnostic and Statistical Manual for Mental Disorders (DSM), First (2014)) and no history of psychotropic medication use. All patients were antipsychotic-naïve or antipsychotic-free for at least 6 weeks for oral antipsychotics or 6 months for depot antipsychotics (Jauhar et al., 2019). The sample included nine antipsychotic-naïve and 12 antipsychotic-free patients. All but one patient included in the baseline study was not taking other psychotropic medication (i.e., antidepressants, mood stabilizers, benzodiazepines) at the time of the MRI scan. Only one patient was taking antidepressant medication (sertraline) at the time of the MRI scan (Viviani et al., 2012).

Follow-up study

Inclusion criteria for the patient group were: psychotic disorder according to ICD-10 criteria (World Health Organization et al., 1992); in the first episode of illness; and antipsychotic-free or -naïve or minimally treated (taking antipsychotics at minimal effective dose for less than 2 weeks, (Agid et al., 2003; Levine & Leucht, 2012). All patients were clinically assessed

at baseline and reassessed after taking antipsychotic treatment, at a therapeutic dose as specified in the Maudsley Prescribing Guidelines (Taylor et al., 2021), for a minimum of 4 weeks. All patients were in stable treatment at follow-up after titration. Clinical measures were rated at baseline and follow-up using the Positive and Negative Syndrome Scale (PANSS) (Kay et al., 1989). Patients received follow-up for at least 6 months to determine if there had been a subsequent response in patients who showed non-response at 4 weeks (duration to follow-up in months 24.73 ± 16.89) (Jauhar et al., 2019). Subjects with psychosis were classified by antipsychotic exposure as antipsychotic-naïve, antipsychotic-free (prior oral antipsychotic medication but free of treatment for at least 6 weeks (oral) or 6 months (depot, if relevant)) or minimally treated (taking antipsychotic medication for 2 weeks or less). The sample included seven antipsychotic-naïve, four antipsychotic-free and three minimally treated with antipsychotics.

4.3.2 MRI acquisition and pre-processing

MRI acquisition

Scans were acquired using a GE MR750 3-T scanner and a 12-channel head coil. A T1-weighted MPRAGE scan was also acquired (FOV= 260 mm; TE= 2.8 ms; TR= 6.98ms; 256×256 matrix; slice thickness= 1.2 mm, flip angle = 11) for normalization purposes. A T2-weighted image (FOV= 240 mm; TE= 54.68 ms; repetition time = 4380 ms; 320 × 320 matrix; slice thickness= 4 mm) was also acquired and used for the pre-processing of ASL images (see below). Measurement of CBF was carried out using a 3D-PCASL sequence. Labelling of arterial blood was achieved with a 1,500 ms train of Hanning-shaped RF pulses in the presence of a net magnetic field gradient along the flow direction (the z-axis of the magnet). After a post-labelling delay of 1525ms, a whole brain volume was read using a 3D inter-leaved "stack-of-spirals" Fast Spin Echo readout, consisting of 8 interleaved spiral arms in the in-plane direction, with 512 points per spiral interleave (TE/TR= 11 ms/4968 ms; 60 slice-partitions of 3mm thickness were defined in the 3D readout). The in-plane FOV was 240×240 mm. The spiral sampling of k-space was re-gridded to a rectangular matrix with an approximate in-plane resolution of 3.6mm. The sequence used four background suppression pulses to minimise static tissue signal at the time of image acquisition. The combination of flow-driven adiabatic inversion of the PCASL pulse, plus background suppression, yields a substantial increase in the SNR of ASL, of up to 50%. Therefore, only

four pairs of control-labelled images are required to produce reliable perfusion-induced signal differences. The mean perfusion weighted difference image was derived from the average of the difference of the four Control-Label pairs. The entire acquisition time of the 3D-PCASL sequence was 6:08 min.

Pre-processing

Proton density images were used to obtain a quantification of absolute CBF in standard physiological units (ml blood/100g tissue/min) using the formula suggested in the ASL consensus paper (Alsop et al., 2015). The unified segmentation algorithm as implemented in SPM (Ashburner & Friston, 2005) was used to create grey matter, WM and CSF images from each T1-weighted image and to create a set of flow fields to later transform each subject's T1-weighted and ASL data into standard space. The T2-weighted images were co-registered with the T1-weighted images. Each raw proton density image was then co-registered with the T2 image. The parameters for this transformation were then applied to the CBF maps (as they were already in alignment with the proton density image) before their normalization. The addition of these two co-registration steps helped us to achieve a better alignment between CBF and T1-weighted images which prevented distortions during normalization. Images were resampled to 2 mm isotropic voxels and normalized into standard MNI space. Finally, the normalized CBF maps were smoothed using a 6 mm full FWHM kernel. Normalized T1-weighted images were also smoothed using a 6 mm FWHM kernel.

4.3.3 Statistical analysis

Demographics

Demographic characteristics (i.e., age, sex) were compared between FEP and HC using χ^2 or independent sample t-tests for categorical and continuous data respectively.

ROI analysis

Absolute CBF values in the whole grey matter and each ROI were extracted using spatially normalized individual grey matter images and the WFU-Pickatlas ROIs with the MarsBar toolbox (http://marsbar.sourceforge.net). Based on previous findings (Allen et al., 2016; Kindler et al., 2018), the following bilateral ROIs were selected as the primary ROIs: the frontal cortex (size= 61 104 mm), the hippocampus (size= 15 024 mm) and the striatum (size=

36 816 mm). For comparisons with the same investigations (Allen et al., 2016; Kindler et al., 2018), I also explored differences between FEP and HC in relative-to-global perfusion CBF. For each ROI a linear regression model was performed with absolute CBF in the ROI as the dependent variable and global grey matter CBF as the independent variable. For each linear regression in each ROI, unstandardized residuals were computed.

To test the primary hypothesis that FEP would show reduced absolute CBF in the frontal cortex and increased CBF in the striatum and hippocampus, a repeated measure ANOVA was used with "ROI" as the within-subject factor and "GROUP" as the between-subject factor. Tukey HSD test has been used for *post hoc* pairwise comparison. An independent sample t-test was used to test absolute CBF in the whole grey matter to determine if there was a global group difference in CBF. Cohen's d has been computed to obtain estimates of effect size. To test differences in relative-to-global CBF, absolute CBF unstandardized residual against global grey matter CBF were entered as dependent variables in a repeated measure ANOVA with "ROI" as the within-subject variable and "GROUP" as the between-subjects variable. Tukey HSD has been used for *post hoc* pairwise comparison. Even though groups were matched by age and sex, to further control for age and sex effects I performed two separate sensitivity analyses by adding age and sex as a covariate of no interest in ANCOVA models.

Voxel-wise analysis

Differences in absolute CBF were also tested in whole-brain voxel-wise analyses. Based on recent recommendations (Eklund et al., 2016), I performed a non-parametric analysis as implemented in FSL randomise (Winkler et al., 2014) and TFCE (Smith & Nichols, 2009) with 5000 permutations to create a non-parametric null distribution and calculate a 5% significance threshold. I also tested relative-to-global-perfusion CBF differences between FEP and HC in voxel-wise analysis using FSL randomise by including global grey matter CBF as a nuisance covariate in the model.

Structural analysis

To check whether results could be influenced by differences in grey matter volume differences between FEP and HC, standard VBM analysis as implemented in SPM was performed on pre-processed T1-weighted images to determine if there were volumetric

differences between groups. Voxel-wise independent sample t-test as implemented in SPM was performed to assess differences in grey matter volume between FEP and controls. Grey matter, WM and CSF images of each participant were combined to obtain estimates of total intracranial volume (ICV). In addition, T1-weighted images were processed using FreeSurfer (version 7.1.1, http://surfer.nmr.harvard.edu) image analysis suite to produce measures of cortical thickness estimates using the FreeSurfer automated brain segmentation process (recon-all) (Fischl et al., 2002; Fischl et al., 1999). An FWHM Gaussian kernel of 10mm was applied. Vertex-wide independent sample t-test was performed for both left and right hemispheres to assess differences in cortical thickness between FEP and controls. Both FEP>HC and FEP<HC contrast were analysed. Cluster-level correction for multiple comparisons was implemented with −log 10(p)value= 3 as cluster-defining threshold and alpha= 0.05. I performed additional analyses to further control for partial volume effects. In particular, I performed: i) ANOVA with grey matter absolute CBF as the dependent variable, "GROUP" (i.e., FEP, HC) as the between-subject variable and whole grey matter volume as a covariate of no interest; ii) Pearson correlations between grey matter volume estimates and absolute CBF extracted from pre-defined ROIs. An independent sample t-test was used to test differences in ICV between FEP and HC.

Correlation with PANSS change

Percentage changes in PANSS were calculated, adjusting for minimum scores (% change in total PANSS= [((baseline score – 30) – (follow-up score – 30))/(baseline score – 30)] × 100) (Leucht et al., 2005). To explore the association between baseline CBF and improvement in symptoms, linear regression analysis was performed between both baseline absolute and relative-to-global CBF values from the primary ROIs and percentage change in total PANSS. For each linear regression model, Bonferroni correction was applied for the number of ROI tested (alpha= 0.05/3= 0.016). For all linear regression models, Mahalanobis distance and Cook's distance were computed to examine the presence of multi-variate outliers and to estimate the presence of highly influential data points. To identify multivariate outliers, Mahalanobis distance values were compared to a χ^2 distribution with degrees of freedom equal to the number of variables (two in this case) with p= 0.001 (Finch, 2012). Any data point with Cook's distance higher than 1 was considered a highly influential outlier and excluded from the analysis as recommended (Cook & Weisberg, 1982). To further test the

robustness of the analysis by reducing the effect of extreme observations, I used the bias-corrected accelerated bootstrap technique with 10,000 resamples (Efron et al., 1994). I have also tested the association between CBF (both absolute and relative-to-global) with PANSS positive and negative subscales changes. Percentage changes in PANSS positive and negative were calculated, adjusting for minimum scores (% change in positive/negative PANSS= [((baseline score – 7) – (follow-up score – 7))/ (baseline score – 7)] * 100) (Leucht et al., 2005).

Bayesian hypothesis testing

In light of the limited sample size of the study, I paralleled the standard hypothesis testing method (p-value approach) with Bayesian hypothesis testing to verify that non-significant results support evidence of absence of effects or absence of evidence (Keysers et al., 2020). All analyses were performed in JASP (version 0.14.1, https://jasp-stats.org). In particular, to assess evidence of an interaction between absolute CBF in ROIs and groups I performed a Bayesian Repeated Measure ANOVA with ROI as a repeated measure and GROUP as a between-subjects factor. The comparison was performed against the null model and Bayes Factor (BF) BF_{10} was selected as the output measure. Similarly, I also performed a Bayesian Independent Sample t-test for each ROI. Results are reported using the one-tailed BF_{10} (FEP<HC). Effect size estimates are reported as median posterior probability with a 95% credibility interval. Bayes factor robustness check was also performed.

4.4 Results

4.4.1 Baseline study

Demographics

Twenty-one people with FEP (mean age ± SD, 24.85 ± 3.85, three females) and 22 HC (23.45 ± 3.21, eight females) were included in the baseline study. HC and FEP groups did not significantly differ in age (t=1.29, p=0.3) or sex (χ^2= 2.8, p= 0.1).

	FEP, n= 21	HC, n= 22	p-value
Age (mean ± SD)	24.85 ± 3.85	23.45 ± 3.21	0.3
Sex (M/F)	18/3	14/8	0.1
Education (years, mean ± SD)	14.4 ± 2.1	15.68 ± 2.6	0.1
PANSS Total baseline (mean ± SD)	70.7 ± 18.6	-	-
PANSS Positive baseline (mean ± SD)	13.7 ± 4.4	-	-
PANSS Negative baseline (mean ± SD)	13.4 ± 6.3	-	-
Antipsychotic naïve (%)	43%	-	-
Antipsychotic-free (%)	57%	-	-
Minimal antipsychotic treatment (%)	0%	-	
Smoking status (never/past/current)	13/2/6	12/6/4	0.3
Substance use (never/past/current)	17/3/1	15/3/4	0.4
Alcohol (never/past/current)	11/2/8	9/1/12	0.5
Ethnicity (white/black/asian/others)	4/6/5/6	4/13/3/2	-

Table 10. Summary of demographic and clinical characteristics of the baseline study sample.

Absolute CBF

Absolute whole brain CBF was significantly lower in FEP (mean ± SD, 27.642 ± 59.52) as compared to HC (mean ± SD, 32.334 ± 43.75) ($t_{(1,41)}$= −2.94, p= 0.005, Cohen's d= 0.89). Results did not change after the removal of the participant receiving antidepressants at the time of the scan (p< 0.001). For the ANOVA including all ROIs, there was a significant main effect of GROUP ($F_{(1)}$= 4.74, p= 0.035) and a significant ROI × GROUP interaction ($F_{(1.55)}$= 3.89, p= 0.032 after Greenhouse–Geisser correction) on absolute CBF. Tukey HSD *post hoc* test revealed significantly lower absolute CBF in the frontal cortex in FEP as compared to HC ($t_{(1,41)}$= −2.75, p= 0.009, Cohen's d= 0.84) with no statistically significant differences between FEP and HC in the hippocampus ($t_{(1,41)}$=−1.5, p= 0.13) or striatum ($t_{(1,41)}$=−1.4, p= 0.1). Results did not change after the removal of the participant receiving antidepressants at the time of the scan (p< 0.001). Figure 19 shows absolute CBF values in the three ROIs (i.e., frontal cortex, hippocampus, and striatum). I conducted an exploratory analysis separating the patients into antipsychotic-naïve and antipsychotic-free sub-groups (Figure 20). ANOVA of grey matter CBF revealed a significant effect of GROUP (F= 4.258, p= 0.021). Tukey HSD *post hoc* pairwise comparison revealed a significant difference between HC and

antipsychotic-free (p= 0.049) and a trend towards a significant difference between HC and antipsychotic-naïve (p= 0.069). No statistical difference was found between antipsychotic-free and -naïve patients (p= 0.997). Repeated measure ANOVA revealed no statistically significant ROI by GROUP interaction (F= 2.2, p= 0.09, after Greenhouse-Geisser correction).

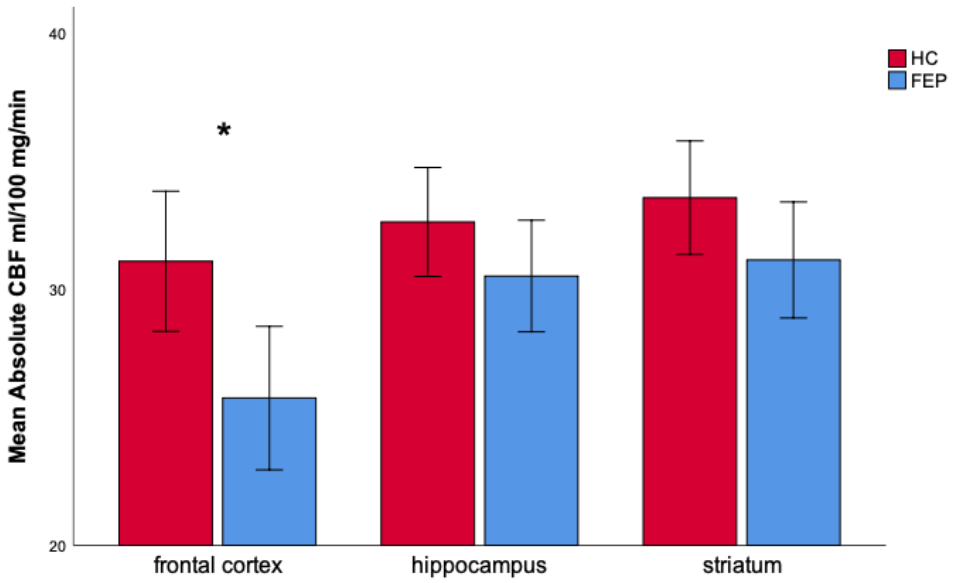

Figure 18. Absolute CBF in the selected a priori ROIs. There were significant main effects of GROUP and ROI, and a significant GROUP by ROI interaction (p= 0.032, Greenhouse-Geisser correction). Post-hoc testing showed that CBF was significantly lower in the frontal cortex (Cohen's *d*= 0.84, p= 0.009) but not in the other regions in patients with FEP relative to controls. FEP: first episode psychosis, HC: healthy controls. Asterisks (*) indicated significant tests. Bars indicate 95% confidence intervals.

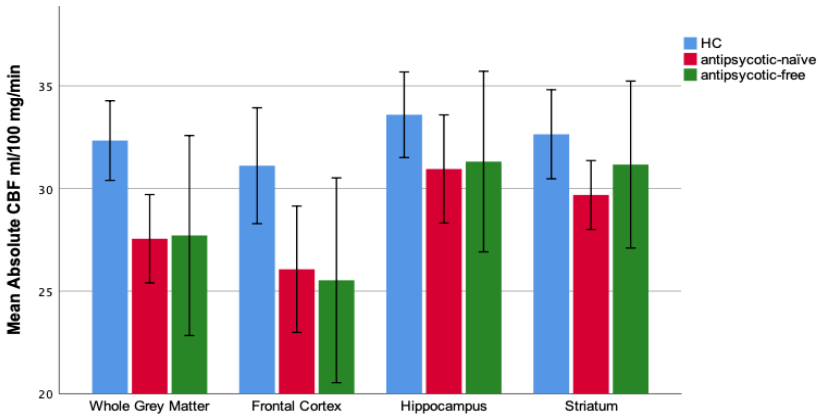

Figure 19. Absolute CBF differences between healthy controls (HC), antipsychotic-naïve and antipsychotic-free patients. Bars indicate 95% confidence intervals.

ANOVA on whole grey matter CBF with GROUP as a between-subject factor and SEX as a covariate of no interest revealed a significant main effect of GROUP (p= 0.008), a significant main effect of SEX (p= 0.042), but a non-significant GROUP x sex interaction (p= 0.97). Repeated measure ANOVA with ROI as a within-subject factor, GROUP as a between-subject factor and sex as a covariate of no interest revealed a significant ROI x GROUP interaction (p= 0.017 Greenhouse-Geisser corrected), and non-significant ROI x SEX and ROI x SEX x GROUP interactions (p= 0.243 and p= 0.142 respectively, Greenhouse-Geisser corrected). ANOVA on whole grey matter CBF with GROUP as a between-subject factor and age as a covariate of no interest revealed a significant main effect of GROUP (p= 0.012) and a non-significant main effect of age (p= 0.14). Repeated measure ANOVA with ROI as a within-subject factor, GROUP as a between-subject factor and age as a covariate of no interest revealed a significant ROI x GROUP interaction (p= 0.04 Greenhouse-Geisser corrected), a non-significant ROI x age interactions (p= 0.97 and p= 0.142 respectively, Greenhouse-Geisser corrected).

Relative-to-global CBF

There was a trend towards a significant main effect of GROUP (F= 3.9, p= 0.054), but no significant main effect of ROI (p= 0.85) or significant ROI x GROUP interaction (p= 0.23) on relative CBF.

CBF whole-brain voxel-wise analysis

Figure 21 shows whole-brain voxel-wise differences (p< 0.05, TFCE-corrected) between FEP and HC. The direct voxel-wise comparison revealed significantly lower CBF in FEP compared to HC in widespread cortical areas including frontal, parietal and occipital areas. The opposite contrast (i.e., HC<FEP) did not reveal any significant clusters. Whole brain voxel-wise analysis of relative-to-global CBF did not reveal any TFCE-corrected cluster in either FEP>HC or FEP < HC contrasts.

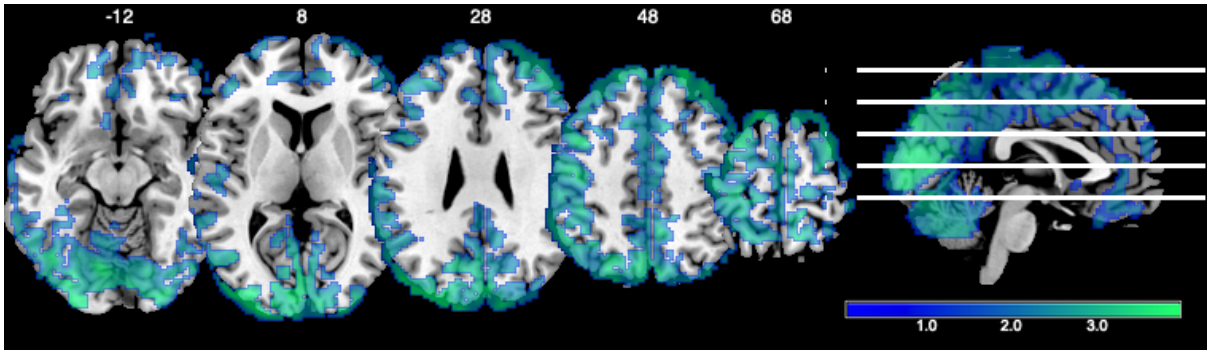

Figure 20. Brain sections showing significantly lower absolute CBF in FEP relative to HC in the frontal, parietal and occipital cortex (TFCE-corrected clusters). The colour bar indicates t-statistics.

Bayesian hypothesis testing

Bayesian Repeated Measure ANOVA provided evidence for an effect of group (BF_{incl}= 4.385) and a GROUP x ROI interaction (BF_{incl}= 5.707). Figure 21 shows posterior distribution plots for both effects. This analysis further provides evidence of an interaction between ROI and GROUP in absolute CBF.

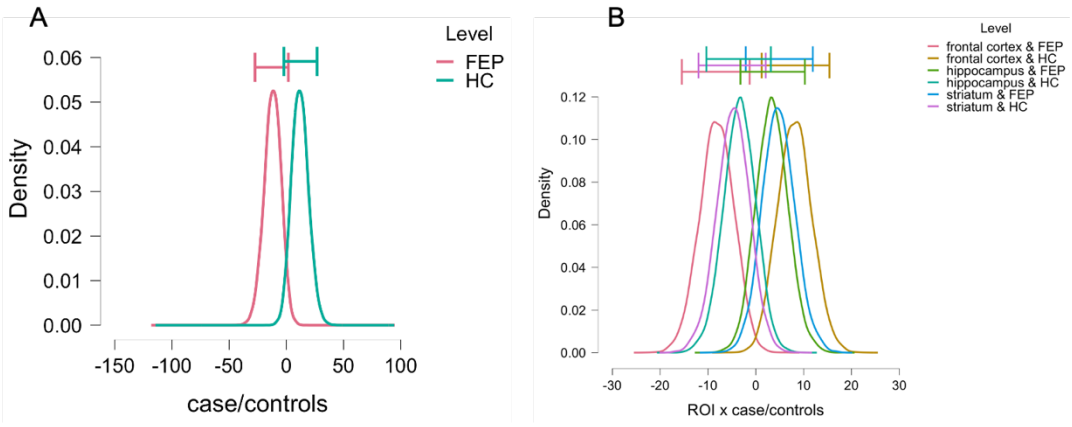

Figure 21. Posterior distribution plots for the main effect of group (A) and ROI by GROUP interaction (B).

Furthermore, given the evidence of an ROI x GROUP interaction and a significant difference between FEP and HC in the frontal cortex, but not in the striatum and hippocampus, I also performed a Bayesian Independent Sample t-test for each ROI. Results are reported using the one-tailed BF_{10} (FEP<HC). Effect size estimates are reported as median posterior probability with a 95% credibility interval. Bayes factor robustness check was also performed. Results revealed moderate to strong evidence of reduction of absolute

CBF in the frontal cortex (BF_{-0}= 10.93, median posterior probability= -0.716, 95%, CI= [-1.344, -0.158]), whereas the data suggest inconclusive evidence for a reduction in the hippocampus (BF_{-0}= 1.423, median posterior probability= -0.41, 95%, CI= [-0.975, -0.036]) and striatum (BF_{-0}= 1.167, median posterior probability= -0.379, 95%, CI= [-0.934, -0.030]). Overall, the results suggest that there is moderate to strong evidence in favour of reduced absolute CBF in FEP as compared with HC in the frontal cortex. Instead, even though the data tend to the null hypothesis in both hippocampus and striatum H_0 and H_1 are equally likely in the sample. However, results from the sequential analysis show that increasing sample size would increase evidence for reduced absolute CBF in the frontal cortex in FEP as compared with HC, but not in the hippocampus and striatum. Figure *22* summarizes the results of these analyses.

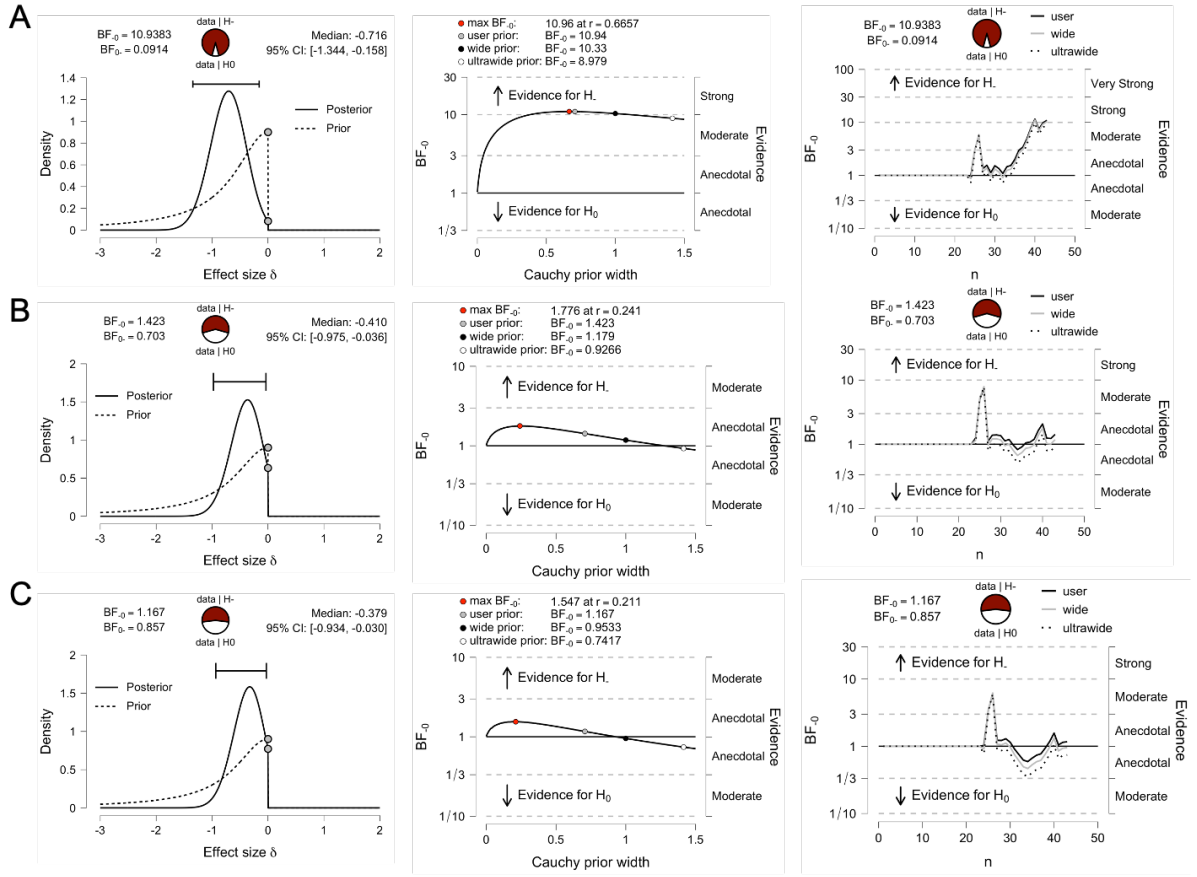

Figure 22. Results of the Bayes independent sample t-test in the frontal cortex (A), hippocampus (B), and striatum (C). The first column shows plots of priors and posteriors of each t-test together with the median and CI of the effect size. The second column shows absolute CBF in each ROI as a function of effect size priors. The third column shows the results of the Sequential Analysis that returns the accumulation of evidence with increasing sample size.

Structural analysis

FEP and HC did not differ in total grey matter volume ($t_{(1,41)}$= −1.8, p= 0.08) or total ICV ($t_{(1,41)}$= 0.95, p= 0.96). Voxel-wise VBM analysis did not reveal any significant differences in grey matter volume between FEP and HC. FreeSurfer analysis did not reveal any significant cluster of cortical thickness differences between FEP and HC. ANCOVA on grey matter absolute CBF revealed a significant effect of GROUP (F= 7.67, p= 0.008) and a non-significant effect of grey matter volume (F= 0.14, p= 0.9). No significant correlations were found between grey matter volume estimates and absolute CBF in the whole grey matter (r= 0.13, p= 0.39), frontal cortex (r= 0.16, p= 0.29), striatum (r= 0.004, p= 0.98) and hippocampus (r= 0.05, p= 0.74).

4.4.2 Follow-up study

Demographics

Fourteen patients with FEP (23.85 ± 3.77, four female) were included in the follow-up study. Eleven patients also took part in the baseline study (Table 12).

	FEP, n= 14	**p-value**
Age (mean ± SD)	23.85 ± 3.77	-
Sex (M/F)	10/4	-
PANSS Total baseline (mean ± SD)	75.42 ± 18.2	-
PANSS Positive baseline (mean ± SD)	20.21± 6.19	-
PANSS Negative baseline (mean ± SD)	15.57 ± 6.5	-
PANSS Total follow-up (mean ± SD)	58.7 ± 19.22	-
PANSS Positive follow-up (mean ± SD)	13.9 ± 5.5	-
PANSS Negative follow-up (mean ± SD)	14.5 ± 7.1	-
PANSS Total change (mean ± SD)	32.6 ± 33.1	0.02
PANSS Positive change (mean ± SD)	9.4 ± 9.1	0.01
PANSS Negative change (mean ± SD)	5.9 ± 9.3	0.29
Antipsychotic naïve (%)	50%	-
Antipsychotic-free (%)	29%	-
Minimal antipsychotic treatment (%)	21%	-
Smoking status (never/past/current)	6/4/4	-
Substance use (never/past/current)	7/4/3	-
Alcohol (never/past/current)	6/3/5	-
Ethnicity (white/black/asian/others)	1/4/4/5	-

Table 11. Summary of demographics and clinical characteristics of the follow-up study sample.

Correlations between baseline CBF and PANSS change

There were no significant associations between absolute CBF extracted from the ROIs and percentage change in total PANSS score (p> 0.32). However, relative-to-global CBF in the frontal cortex correlated positively with the percentage change in total PANSS (Figure 18; r= 0.67, p= 0.008). In all linear regression models, none of the data points was identified as an influential outlier (all Cook's distances< 1) or multivariate outliers (all Mahalanobis distances p>0.001). Results were retained after applying a bias-corrected accelerated bootstrap technique with 10,000 resamples (bootstrapped p= 0.05). In addition, Spearman rank correlations yielded similar results to linear regression analysis (Spearman rho= 0.574, p= 0.032). I found that % positive PANSS change was not associated with absolute CBF (all p> 0.323) and relative-to-global CBF (all p> 0.093) in all ROIs (i.e., grey matter, frontal cortex, striatum, hippocampus). I found that % negative PANSS change was not associated with absolute CBF (all p> 0.857) and relative-to-global CBF (all p> 0.515) in all ROIs (i.e., grey matter, frontal cortex, striatum, hippocampus).

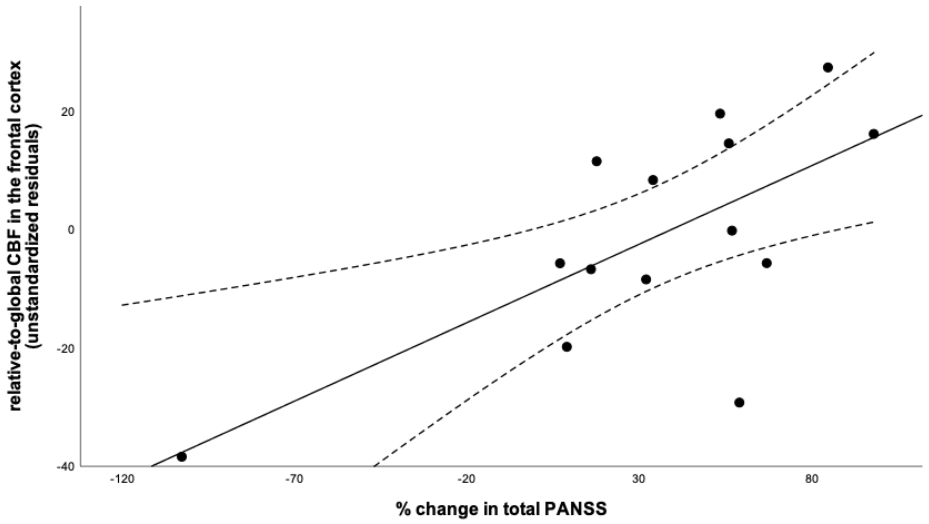

Figure 23. Scatterplot showing significant correlations between relative-to-global frontal CBF at baseline and percentage improvement in total PANSS with subsequent treatment (r= 0.57, p= 0.05).

Given the known effect of antipsychotics on CBF, I have also performed a sensitivity analysis in the follow-up sample to test the association between relative-to-global CBF in the frontal cortex with PANSS total change after removing patients minimally treated at baseline (N=

3). The analysis revealed and confirmed an effect in the same direction as the main analysis, although this result was not formally significant (r= 0.46, p= 0.07). The results of this sub-analysis along with the fact that the subjects removed in this sub-analysis were receiving antipsychotic treatment at a minimal effective dose for less than two weeks before the baseline scan suggest that it is unlikely that the inclusion of minimally treated patients in the follow-up sample could have biased the result of this analysis.

4.5 Discussion

I found absolute CBF was significantly lower in the frontal cortex but not striatum or hippocampus in people with FEP free of antipsychotic medication. My whole brain analyses found significantly lower perfusion in the patients in additional cortical areas, including the parietal and occipital cortices. Lower perfusion and metabolism of the frontal cortex at rest is a replicated finding in chronic Schizophrenia (Bullmore et al., 1999; Weinberger & Berman, 1988) demonstrated using various neuroimaging techniques including SPECT, [^{18}F]-FDG and [^{15}O]-H_2O PET, BOLD signal and recently with ASL (Hill et al., 2004; Kindler et al., 2015). Interestingly previous studies using PET and SPECT in unmedicated FEP revealed reduced cortical perfusion and metabolism (Brewer et al., 2007; Molina et al., 2005). My results corroborate and extend this evidence by showing the existence of lower frontal cortical absolute perfusion in FEP without the potential confound of antipsychotic treatment, using MRI. In addition, my exploratory whole-brain analyses indicate cortical hypoperfusion extends beyond the frontal cortex, including both parietal and occipital cortices. This extends evidence that the function of these regions is altered during cognitive tasks in Schizophrenia (Calderone et al., 2013; Hahn et al., 2018) to show perfusion is also altered early in the illness course. In contrast to findings in antipsychotic-treated patients and people at clinical risk of psychosis (Allen et al., 2016; Kindler et al., 2018), I found no significant difference in absolute and relative-to-global CBF in the striatum or hippocampus relative to controls. When these results are considered alongside the preclinical (Mandeville et al., 2013; Sander et al., 2013) and experimental (Handley et al., 2013; Hawkins et al., 2018; Shcherbinin et al., 2015; Viviani et al., 2013) evidence that antipsychotics increase striatal perfusion, with a mechanism possibly mediated by D_2R (Selvaggi et al. (2019), see also Chapter 2 and Chapter 3 of the present thesis), this could indicate that previous evidence of higher striatal CBF in people with Schizophrenia taking antipsychotics might be explained

by D_2R blockade. Longitudinal studies are required to confirm preliminary evidence (Goozee et al., 2014) suggesting that treatment with antipsychotics does increase striatal perfusion in patients.

I did not find any differences in the hippocampus in either absolute or relative-to-global perfusion, in contrast to findings in people at clinical risk of psychosis. Taken with my findings in the frontal cortex, this could suggest that there is a progression of pathophysiological alterations from the hippocampus before the onset of psychosis to the frontal cortex with the development of illness. However, it should be recognized that not all subjects at clinical risk develop psychosis and longitudinal studies with repeated scanning are required to test if there are changes in hypoperfusion during the development of psychosis.

Relative-to-global CBF in the frontal cortex at presentation explained approximately 40% of the variance in subsequent response to antipsychotic treatment, such that patients with higher relative-to-global CBF showed higher symptom improvement with treatment. These results extend prior evidence that response to antipsychotic treatment in FEP is associated with FC (Sarpal, Argyelan, et al., 2016), D_2R availability (Wulff et al., 2015), and dopamine synthesis capacity (Jauhar et al., 2019) to suggest that relative frontal perfusion could potentially contribute to a biomarker for antipsychotic response in FEP (Veronese et al., 2021). I did not find correlations between relative-to-global CBF in the striatum and hippocampus and PANSS change. However, given the lower CBF in several cortical regions in patients, it might be possible that cortical regions other than the frontal cortex are also linked to treatment response, but the test was underpowered to detect these relationships. I did not find correlations between absolute CBF and PANSS change, suggesting that changes in local perfusion relative to whole brain perfusion are best able to capture variability in clinical response. I found that antipsychotic-free FEP shows lower absolute CBF in cortical regions but no significant difference in relative-to-global CBF. Treatment response was associated with relative-to-global frontal CBF but not with absolute CBF. The absence of group differences in relative-to-global CBF is consistent with my whole brain findings that indicate that there is lower absolute CBF in other cortical regions, mainly driven by lower CBF in parietal and occipital cortices as compared with controls. On the other hand, subcortical CBF (i.e., striatal, and hippocampal) seems to be unaltered in patients relative to controls (see Bayes Factor testing). Thus, taken together, these findings suggest an imbalance between cortical and subcortical blood flow early in Schizophrenia. The

association between relative-to-global CBF (but not absolute CBF) with treatment response might seem counterintuitive. However, this finding might be less difficult to interpret considering the direct association between the two variables. Patients with larger improvement in symptoms (i.e., greater symptoms reduction) were those with relatively lower alterations in frontal CBF as compared with the rest of the cortex (i.e., higher relative-to-global frontal CBF), suggesting that patients with more marked frontal hypofunction are less responsive to treatment with D_2R antagonists. This extends other evidence of frontal dysfunction in patients whose illness does not respond to D_2R antagonism (Howes & McCutcheon, 2017; Howes et al., 2017; Mouchlianitis et al., 2016; Potkin et al., 2020). This interpretation is also coherent with recent reports indicating neurovascular uncoupling in brain regions such as the frontal cortex in Schizophrenia (Sukumar et al., 2020).

Strengths and limitations

Strengths of this study include the inclusion of people with FEP free from antipsychotic medication, and longitudinal measures in FEP patients. A methodological strength of the study is the evaluation of both absolute and relative-to-global CBF. Previous studies in CHR-P and FEP have used one metric without reporting the other (Allen et al., 2018; Allen et al., 2016; Kindler et al., 2018; Modinos, Egerton, et al., 2018). However, my results suggest that antipsychotic-free FEP show different patterns of alteration in absolute and relative-to-global CBF. Therefore, I advise that future studies should include both metrics to facilitate comparisons. Previous works testing CBF differences in chronic Schizophrenia as compared with HC using ASL have shown variability in grey matter perfusion across individuals (Chen et al., 2022; Parkes et al., 2004; Pinkham et al., 2011). In this study, I used a 3D-PCASL with background suppression which offers a non-invasive, efficient, and highly reproducible tool to investigate brain perfusion as compared with other ASL methods (Alsop et al., 2015; Chen et al., 2022). PCASL sequences have shown higher test-retest reliability as compared with other MRI sequences (such as BOLD task or resting state fMRI) used to identify biomarkers in psychosis (Holiga et al., 2018). In addition, PCASL has shown good test-retest reliability (Intraclass coefficient (ICC) range: 0.63–0.83; Holiga et al. (2018)), and is comparable with PET [^{18}F]-DOPA (ICC range: 0.42–0.94; Egerton et al. (2010)), which has been proposed as a potential biomarker for treatment stratification in psychosis (Veronese et al., 2021). I obtained absolute CBF values on average of 40–50 ml/100 g tissue/minute in

grey matter in healthy volunteers which are at the lower range of previous investigations using pulsed ASL and/or other scanner manufacturers (Alsop et al., 2015). In our study, we used a post-labelling approach and background suppression protocol that was slightly slower than the one recommended by the ASL white paper (Alsop et al., 2015), which could account for the slightly lower CBF values we obtained. However, I did not find artefactual hyperperfusion regions in my analysis, suggesting that the post-labelling delay had no major effect on data quality. One potential issue in the imaging analysis could be the influence of partial volume effects given structural brain alterations in FEP (Brugger & Howes, 2017). However, I did not find group differences in grey matter volume, total ICV and cortical thickness, suggesting that partial volume effects are unlikely to explain our results, although we cannot completely rule out a contribution of partial volume effects to our findings. Demographic heterogeneity of the sample is thought to be an important factor contributing to variability across individuals. Age and sex have been strongly associated with CBF variability (Liu et al., 2012; Viviani et al., 2009). The groups were very similar in mean age and sex distribution. Nevertheless, to check for any influence of these, we conducted further analyses including these as covariates. The results remained essentially unchanged when sex and age were added as covariates of no interest, suggesting these are not influencing our findings. Body-mass index, caffeine intake or nicotine consumption immediately before scanning could be other sources of variability. In common with prior studies in psychosis (Davies et al., 2019; Modinos, Simsek, et al., 2018; Overton et al., 2020), I did not control for these. However, the two groups did not differ in terms of smoking status, alcohol intake and substance use, which suggests that both caffeine intake and nicotine consumption might be similar between groups. Nevertheless, we cannot exclude group differences in the use of these substances influencing our findings and further studies matching for intake on these would be useful. In addition, it should be recognized that the frontal ROI is larger than the hippocampal and striatal ROIs. This may result in a higher SNR for the frontal region over these other regions, and consequently, greater sensitivity to detect group differences. However, SNR estimates and sensitivity analyses both suggest that it is unlikely that ROI size has affected our results. Furthermore, in the follow-up study patients were treated in a naturalistic design. Thus, these findings do not provide information about the specific effects of antipsychotic treatment. Finally, although the baseline study constituted a larger cohort than that previously reported in FEP (Kindler et al., 2018) given the relatively modest sample

size, further studies are needed to test the generalisability of our findings to other cohorts and settings.

Implications and future directions

Frontal dysfunction is one of the key mechanisms thought to contribute to the pathophysiology of psychosis (Howes & Murray, 2014; McCutcheon et al., 2020; Weinberger & Berman, 1988). These findings indicate that frontal hypoperfusion is present early in the development of the disorder and in unmedicated patients and are consistent with these models and other markers of frontal hypofunction in SCZ (Howes & McCutcheon, 2017; Onwordi et al., 2020; Osimo et al., 2019). In addition, given the close link between CBF and brain metabolism (Riederer et al., 2018), our results are in line with the evidence of increased lactate levels and pH (Dogan et al., 2018; Du et al., 2014) and mitochondrial dysfunction in SCZ (Prince et al., 1999; Rajasekaran et al., 2015) suggesting that altered brain oxidative capacity could be the pathophysiological substrate underlying abnormal brain function in psychosis. In addition, these results indicate that alterations in brain perfusion at presentation are associated with subsequent antipsychotic response suggesting that brain perfusion could be used to help predict future clinical response. Previous evidence suggested antipsychotics may normalize brain metabolism (Buchsbaum et al., 2009); however recently some authors have proposed that this normalization might not be sustainable in some patients (Turkheimer et al., 2020). Future longitudinal studies are therefore needed to understand the effect of antipsychotic treatment on brain metabolism in psychosis.

5 Discussion

In this chapter, I will summarise my results discussing them in relation to the overall rationale and main hypotheses of my PhD. I will discuss the potential clinical implications of my findings in the context of the treatment of patients with psychosis along with possible future directions. This chapter will not discuss in detail each of my findings in the context of existing literature which has been already extensively discussed in each of the main chapters.

One of the main goals of my PhD was to link brain changes evaluated with MRI induced by antipsychotics to plausible neurochemical mechanisms such as D_2R blockade bridging the gap between PK and PD. First, I conducted a study (Chapter 2) that revealed that the brain topology of CBF changes induced by a single dose of antipsychotics in healthy volunteers was associated with the spatial distribution of D_2R in the brain as evaluated using PET D_2R population-based templates and *DRD2* mRNA expression data from the AHBA. Interestingly, the spatial coupling between ΔCBF and D_2R profiles varied between the different antipsychotics tested, possibly reflecting differential affinities. My first project, therefore, provided evidence of an association between the functional effect of antipsychotics (i.e., perfusion changes) and the distribution of their target receptors (i.e., D_2R) in striatal and extra-striatal regions. This link between neurotransmitter target and haemodynamic change supported the translation in humans of the proposed preclinical model indicating the existence of neurovascular coupling mechanisms linked with D_2R occupancy (Sander et al., 2013; Sander et al., 2016). However, in this study, I was not able to assess how between-subject variability in D_2R occupancy relates to CBF changes after antipsychotic administration.

In my second project (Chapter 3) I aimed to specifically address this issue in a study of sustained blockade of D_2R. In this study, I was able to test the association between CBF changes after sustained D_2R in healthy volunteers (taking daily doses of amisulpride 400mg for one week) with between-subject variability in amisulpride plasma levels and D_2R occupancy as assessed with [^{11}C]-PHNO PET. As only a subset of participants had complete MRI and PET scans, data was likely underpowered to detect a relationship between D_2R occupancy and CBF changes. Therefore, I developed a PK/PD framework that was able to

predict from available PK data D_2R occupancy estimates that were in line with previous amisulpride receptor occupancy studies (Sparshatt et al., 2009). I was then able to fit D_2R occupancy data and CBF changes using the model proposed by Sander et al. (2013) in the caudate and the putamen. These results provided evidence in humans that a monotonically increasing relationship between changes in brain perfusion and D_2R occupancy by antagonists exists not just between brain regions but also between subjects. Interestingly, while these findings represent the first in human evidence of such a relationship, these might also extend the model based on acute single-dose D_2R blockade (Sander et al., 2013) to sustained D_2R blockade achieved with repeated doses in a steady state equilibrium. This is particularly relevant for the potential translation of the findings as this route of administration recreates a PK scenario which is much closer to the one observed in patients taking antipsychotics chronically as compared with experimental designs. However, future studies are needed to confirm these associations in humans as my results are based on a mixture of real and simulated data.

In light of the strong evidence of D_2R blockade being associated with increased CBF, especially in the basal ganglia (Handley et al., 2013; Hawkins et al., 2018; Mehta et al., 2003; Viviani et al., 2013) it remains unclear to which extent alterations in brain perfusion described in patients with psychosis are related to pathophysiological processes or rather a consequence of pharmacological treatment. Therefore another aim of my PhD was to try to disentangle between medication and disease effects in brain perfusion. Previous studies using ASL in medicated FEP and chronic schizophrenia showed a reduction in cortical perfusion and an increase in CBF in the basal ganglia as compared with healthy controls (Kindler et al., 2015; Kindler et al., 2018; Legind et al., 2019; Liu et al., 2012; Oliveira et al., 2018; Ota et al., 2014; Pinkham et al., 2011; Pinkham et al., 2015). In my third project (Chapter 4) I investigated CBF differences between FEP free from antipsychotic medication and HC assessing both absolute and relative-to-global CBF. In the same project, I also investigated the association between baseline CBF and treatment response in a partially nested follow-up study as an exploratory aim. I found a significantly lower absolute CBF in the frontal cortex and no differences in the striatum or hippocampus. Whole brain voxel-wise analysis revealed widespread cortical reductions in absolute CBF in large cortical clusters that encompassed occipital, parietal and frontal cortices. I did not find differences in relative-to-global CBF in

the selected region of interest and voxel-wise analysis. Finally, relative-to-global frontal CBF was correlated with the percentage change in total PANSS after antipsychotic treatment. In contrast to findings in antipsychotic-treated patients, in this study, I did not find CBF differences in the striatum between antipsychotic-free FEP and healthy controls. Considering these findings alongside the consolidated evidence (also supported by the results of the present thesis) that antipsychotics do increase striatal perfusion with a plausible mechanism associated with D_2R occupancy, my results point toward the fact that previous evidence of higher striatal CBF in people with schizophrenia taking antipsychotics might be considered a direct effect of medication linked with D_2R blockade. Longitudinal studies in antipsychotic naïve FEP might clarify to which extent D_2R blockade increases CBF in patients and how this relates to psychosis pathophysiology. By the time of writing the present PhD thesis Bojesen et al. (2023) published their paper investigating CBF differences in antipsychotic naïve FEP as compared with healthy controls and longitudinal changes after six weeks of treatment with variable doses of aripiprazole (5mg to 20mg). At baseline, they replicated the findings reported in the present thesis with no significant differences in striatal perfusion between antipsychotic-free FEP and healthy controls. Interestingly, longitudinal analysis revealed that after six weeks of treatment with aripiprazole, FEP had increased CBF in the striatum as compared with a matched longitudinal cohort of healthy controls. The authors also explored the association between CBF changes and symptom improvement reporting no associations between changes in striatal and thalamic perfusion and changes in the PANSS scale. This might indicate that changes in striatal perfusion might not be related to pathophysiological changes linked with symptom severity. Together with the results of the experiment conducted in my PhD which shows that striatal perfusion increases in HC after single and repeated doses of antipsychotics (Chapter 2 and Chapter 3), this might further suggest that changes in striatal perfusion in patients with psychosis might be more likely a direct pharmacological consequence of D_2R blockade rather than the effect of a pathophysiological process. In addition, in my study in antipsychotic-free FEP, I found that baseline cortical perfusion was associated with subsequent treatment response (Chapter 4) suggesting that changes in other brain regions are more likely to reflect changes in disease states as compared with changes in regions such as the basal ganglia which might be more susceptible to pharmacological effect of the local D_2R blockade. Future multimodal imaging longitudinal studies in patients could confirm this hypothesis and also test its validity in the

context of different antipsychotics with different receptor affinity profiles and mechanisms of action. In addition, both my study nor the one by Bojesen et al. (2023) did not differentiate between patients with affective (i.e., bipolar or psychotic depression, schizoaffective disorder) and non-affective psychosis (i.e., first-episode schizophrenia or schizophreniform disorder). Future longitudinal studies might also disentangle the effect of disease traits (i.e., differential diagnosis) on cerebral perfusion and how it interacts with treatment effects.

While this thesis provides further evidence on the link between D_2R blockade and CBF increases after antipsychotic exposure, the cellular mechanisms underlying this association remain unclear. CBF is continuously regulated to meet the high metabolic demands of the brain tissue, through the response to local changes in neuronal activity (i.e., neurovascular coupling) (Attwell et al., 2010), but also through other mechanisms such as i) the response of cerebral vessels to changes in perfusion pressure (i.e., autoregulation); ii) the vascular reactivity to vasoactive stimuli (e.g., carbon dioxide (CO2)); and iii) the endothelium responses (Claassen et al., 2021). Some authors (Goozee et al., 2014) have speculated that increased CBF after antipsychotic exposure might reflect greater metabolic demand as a consequence of synapsis processes related to D_2R antagonism in line with the neurovascular coupling model. Indeed, most brain energy is used for synaptic transmission, with the largest ATP consumption happening post-synaptically to pump out ions mediating synaptic currents followed by pre-synaptic processes such as ATPase pumps (e.g., sodium-, calcium- and vacuolar proton-ATPase pumps) and vesicle trafficking. Also, astrocytes contribute to the metabolic demand of the brain with ATP largely used to extrude Na^+ (Attwell & Laughlin, 2001; Harris et al., 2012). Animal models suggested that CBV and CBF responses follow a dopamine-mediated function such as changes in CBF are the result of the relative balance between D_1R-mediated excitation and D_2R-mediated inhibition (Mandeville et al., 2013). Indeed D_1R and D_2R produce opposing effects post-synaptically by stimulating or inhibiting the adenylate cyclase by interacting with protein $G\alpha_s$ and protein $G\alpha_i$ respectively. This model is supported by the experimental evidence that D_1R agonism increases perfusion in the basal ganglia whereas antagonism decreases it (Choi et al., 2006; Mandeville et al., 2011; Marota et al., 2000), and D_2R agonist and antagonist produce changes in the opposite direction (Chen et al., 2005; Sander et al., 2013; Sander et al., 2016). In non-human primates and humans, where the striatum contains a similar density of D_1R and D_2R receptors

(Cumming, 2011), changes in D_2R availability are thought to explain large variations in dopamine-mediated CBV/CBF response as a result of the higher affinity of dopamine for D_2R as compared to D_1R (Marcellino et al., 2012). As a result, D_2R antagonist is thought to displace dopamine at D_2R shifting the D_1R/D_2R balance toward excitation. Therefore, the increase of CBF in the basal ganglia after D_2R blockade might reflect increased activity perhaps particularly in D_1 MSN (Kharkwal et al., 2016; McCutcheon et al., 2019). The functional uncoupling between the striatum and the motor cortex and its association with EPS discussed in Chapter 3 might support this hypothesis. Also, pre-synaptic mechanisms might contribute to the neurovascular response associated with D_2R blockade. For instance, antagonism at pre-synaptic D_2R autoreceptors induces dopamine release which could potentiate the neurovascular response associated with excitation of the post-synaptic terminal and also increase the metabolic demand of the pre-synaptic terminal due to increased vesicle trafficking (Sander et al., 2013; Stamford et al., 1988). In addition, also blockade of postsynaptic D_2R increases dopamine release through the feedback mechanisms which could also contribute to the increase in the energy demand of the presynaptic terminal (Cumming et al., 1997). Notably, these mechanisms are not mutually exclusive, therefore they all might contribute synergistically to the CBF increase following the D_2R blockade. A further complication of this model is that the magnitude of the CBF response may also depend on the amount of dopamine present in the synaptic space as well as interindividual variability in dopamine synthesis capacity and release. This might be particularly relevant for antipsychotics with partial agonism properties (e.g., aripiprazole) and in patients with psychosis who have elevated dopamine release as a trait. Furthermore, it is not possible to exclude that this CBF response might be also influenced by non-neuronal mechanisms such as the dopaminergic modulation of the brain microvasculature, endothelium and astrocytes. Indeed stimulation of D_1R on smooth muscle cells produces vasodilation with increased CBV and stimulation of D_3R on astrocytes produces vasoconstriction and CBV decreases (Choi et al., 2006). Even though these non-neuronal effects are less likely to be produced by a direct effect of D_2Rs due to their lower density on microvessels and astrocytes relative to D_1Rs and D_3Rs, it might be possible that D_2R blockade might indirectly interact with these mechanisms by altering dopamine release. In addition, non-neuronal mechanisms could partially contribute to the CBF response of antipsychotics with a high affinity for D_3R such as amisulpride. Moreover, blockade of $5HT_2AR$ on smooth-muscle cells of brain arteries has

been shown to induce relative vasodilation (i.e., blocking vasoconstriction caused by the endogenous ligand serotonin) (Kovacs et al., 2012). Therefore other non-neuronal mechanisms might influence the CBF response to antipsychotics which are both serotonin and dopamine antagonists such as SGAs.

Finally, another aim of the present thesis was to investigate how changes in brain structure and function observed in experimental studies in healthy volunteers after single-dose administration compare with experimental studies of sustained D_2R blockade, thus in a dosing regimen close to the clinical practice. This aim fits in the ongoing debate on the consequences of long-term exposure to antipsychotic medication on brain structure and function (Correll et al., 2018; Fountoulakis & Stahl, 2022; Lawrie, 2022), which is complicated by the difficulties in teasing apart disease states and traits from medication effects and is also facing criticisms related to the correct biological interpretation of changes detected using MRI (Weinberger & Radulescu, 2016, 2021). To address this goal I have investigated the effects of sustained D_2R blockade in a double-blinded, randomized, crossover, placebo-controlled study in healthy volunteers who received either amisulpride 400mg or a placebo daily for seven days. I found that, while sustained D_2R blockade did not induce structural changes, as showed in the result of T1 signal and volume, it was associated with increased CBF in the striatum and reduced FC between the dorsal striatum and the motor cortex. Interestingly, FC changes were also associated with EPS such as a greater reduction in FC was associated with greater EPS. CBF findings have been already extensively discussed above. The analysis of structural metrics revealed that one week of D_2R blockade with oral administration of antipsychotic was not associated with changes in T1 signal and brain morphometrics. While my results suggest that it is unlikely that antipsychotic administration induces an alteration of brain structure, at least in the short term, they do not allow to draw any conclusions on long-term exposure. It might be possible that a longer exposure (e.g., > 1 week) is needed to allow tissue remodelling processes which have been hypothesized to explain structural changes observed in longitudinal studies in patients with psychosis (Chopra, Fornito, et al., 2021; Voineskos et al., 2020). This hypothesis is coherent with findings in pre-clinical studies in rodents and non-human primates which have found reduced cortical grey matter volumes after chronic antipsychotic administration and reversible increase of striatal volume (with an exposure approximately equivalent to as much

as 2 human years) (Dorph-Petersen et al., 2005; Vernon et al., 2012; Vernon et al., 2011). The results by Andersen et al. (2020) of increased striatal volume after 6 weeks of low dose of amisulpride in antipsychotic naïve FEP are also in favour of this hypothesis. The cellular mechanisms that could underly these alterations in brain structural metrics are largely unknown. Animal studies have not provided evidence of neuronal loss *per se* after antipsychotic exposure, while loss of the neuropil has been observed including alterations of astrocyte and microglial cell density and morphology (Konopaske et al., 2007; Vernon et al., 2014). However, it is still unknown whether this represents a homeostatic response or an ongoing, detrimental inflammatory process (Amato et al., 2017; Cotel et al., 2015; Turkheimer et al., 2020). As previously stated, it is difficult to directly compare the findings from clinical studies with my findings as they were obtained in a well-controlled experiment in healthy volunteers, i.e., in the absence of all the confounding factors that accompany clinical studies (e.g., disease state and trait, between-subjects differences in medications and doses, comorbidity, substance abuse, etc.). Nonetheless, considering the inconsistencies and the limitations of the clinical studies, the present negative findings add to the current debate on the effect on the brain structure of exposure to antipsychotics, showing that one week of D_2R blockade in healthy controls, in the absence of disease state and trait effects, does not produce any alteration in MRI signals usually interpreted as brain "structural" changes. Future placebo-controlled clinical studies in patients with psychosis with higher control of confounding factors as compared with previous studies (e.g., heterogeneity in diagnosis, treatment, dosing regime, previous exposure, etc.) might further clarify the role of antipsychotic exposure on brain remodelling and how it interacts with disease effects. Critically, the addition of the evaluation of short-term effects (e.g., acute or one-week exposure) in future longitudinal studies in patients could also significantly contribute to disentangle disease from treatment effects and further confirm the hypothesis advanced here.

My negative findings in brain morphometrics are further corroborated by a parallel careful examination of changes in T1 relaxometry. The vast majority of studies investigating alterations in "brain structure" typically rely on the segmentation of images into tissue types based on the distribution of T1-weighted intensity values and *a priori* probabilistic tissue maps. This is the common approach implemented by the widely used software SPM (i.e., VBM) and FreeSurfer (Ashburner & Friston, 2000, 2005; Fischl et al., 2002). However T1-

weighted images are qualitative measures heavily dependent on acquisition protocols, which limits reproducibility and could also be influenced by several "non-structural" factors altering the magnetic resonance properties of the tissue such as differences in the water content (Duning et al., 2005; Franklin et al., 2013; Kempton et al., 2011; Weinberger & Radulescu, 2016). The recent advances in quantitative T1 relaxometry mapping allow an absolute measure of T1 relaxation time, which is voxel-wise and can be acquired within a typical MRI protocol. Because the measure is quantitative, it is also more easily comparable between time points and represents a more informative measure of microstructural changes as compared with T1-weighted images (Draganski & Kherif, 2013; Draganski et al., 2014; Sagi et al., 2012). Notably, T1 (and T2) relaxation times highly depend on the concentration of macro-molecules such as proteins, phospholipids, polysaccharides and fat as well as on the amount of water bound to macro-molecules (e.g., bound water protons tend to have shorter T1 and T2) (Akber, 1996, 2008; Black et al., 2000; Edzes & Samulski, 1977; James, 1977; Knauss et al., 1996). Antipsychotic exposure has been associated with alterations which might modify the water composition of brain tissue even in the short term such as changes in CBV and CBF (Franklin et al., 2013; Hawkins et al., 2018; Sander et al., 2013) or other neuroadaptation mechanisms such as inflammation (Amato et al., 2017; Cotel et al., 2015). In my study sustained D_2R blockade was not associated with changes in either T1-weighted volumetric analysis or T1 relaxometry maps indicating that it is very unlikely that one week of D_2R blockade is associated with alterations in brain microstructure detectable with current MRI techniques at standard 3T resolution. A multimodal approach such as the one used in the study (Chapter 3) might enhance the specificity of clinical studies investigating brain "structural" changes in patients with psychosis.

However, in the absence of any detectable tissue remodelling effects, sustained D_2R blockade in healthy volunteers was associated with functional changes. I found that sustained D_2R blockade was associated with reduced FC between the dorsal striatum and the motor cortex. As for other imaging modalities, FC results of this thesis, are difficult to compare with clinical longitudinal studies because of the high heterogeneity that typically characterizes these investigations. Lui et al. (2010), in their study in antipsychotic-free FEP, found, after 6 weeks of treatment with SGAs, a widespread reduction in network-level functional connectivity (i.e., changes in FC between networks) that was correlated to increased regional

ALFF. None of the changes were associated with changes in symptom severity. Notably, when they paralleled longitudinal changes in patients with HC, they found reduced FC between the striatum and frontal cortices. However, they did not explore differences in cortico-striatal connectivity between striatal subdivisions. Sarpal et al. (2015) specifically investigated changes in cortico-striatal FC in antipsychotic-free FEP after 12 weeks of treatment with either risperidone or aripiprazole. In contrast with Lui et al. (2010), they did not find a reduction in FC when comparing follow-up scans with HC in a paired manner, but instead, they found that, in the absence of longitudinal differences with controls, patients with better clinical improvement had higher positive FC changes between the associative striatum and the prefrontal cortex, between the ventral striatum and the hippocampus, and between the ventral putamen and the insula. Both studies did not report altered FC between the striatum and the motor cortex, putting my results in a position of apparent contrast with the findings of those clinical studies. However, as already discussed, clinical and methodological heterogeneity (e.g., medication status at baseline, different diagnoses, duration of follow-up, etc.) might explain this discrepancy. In this context, of particular interest are the results by Lui et al. (2010), in which alterations in FC, observed at baseline in FEP as compared with HC, normalized after treatment (e.g., in the frontoparietal network). This might indicate that D_2R blockade might have different effects on FC in the presence of alterations in FC at baseline due to pathophysiological processes that occurred before antipsychotic exposure. Similarly, the same pathophysiological alterations might interact with the effects of D_2R blockade on physiological (i.e., normal) brain networks producing a mixed effect in which pathological processes are difficult to separate from pure pharmacological effects. The consistent evidence of a cortico-striatal functional uncoupling within the motor circuit after a single dose (Cole, Beckmann, et al., 2013; Cole, Oei, et al., 2013; Tost et al., 2010) and repeated dose (the present thesis) administration of antipsychotics in HC might support this hypothesis. Duration to follow-up might be another possible explanation for the inconsistency between clinical and experimental studies in healthy volunteers. For example, alterations in FC within the cortico-striatal motor loop might be particularly manifest after short-term exposure as opposed to long-term exposure when the occurrence of structural and functional remodelling processes might create a more complex picture.

The FC analysis also highlighted the functional uncoupling between the striatum and the motor cortex as a neural correlate of EPS observed after one week of D_2R blockade. Interestingly, this association between neural alteration and behavioural effects after antipsychotic administration has been already shown after acute injection of haloperidol in healthy volunteers (Tost et al., 2010). Notably, here I was able to investigate a similar research question but using a different experimental setting characterized by repeated daily oral doses of antipsychotics for one week, a randomized placebo-controlled study design and state-of-the-art clinical evaluation of EPS. Therefore, the results of my PhD further suggest that alterations in cortico-striatal connectivity might merit further investigations to establish and validate a potential biomarker for antipsychotic side effects in patients with schizophrenia.

Future directions

Overall the results of my PhD show that the integration between imaging modalities could have an added value in addressing research questions that are not easily addressable by studies involving just one modality. Each imaging method has its advantages and disadvantages and specificity to particular neurobiological processes. For example, PET has provided excellent quantitative mapping of drug binding to neuro-receptors. However, this approach is expensive, inapplicable in large studies, impractical when a drug targets multiple receptor sites and poorly informative on drug functional effects. Similarly, structural and functional MRI have their drawbacks hinged on the biophysical nature of MRI markers which complicate the interpretation of findings at the molecular level and are also prone to artefactual effects. Taken together the results of my PhD might encourage future clinical and pharmacological applications of multimodal imaging.

Future drug studies could highly benefit from the adoption of multimodal approaches such as the one used in this thesis. Here I showed that the combination of PET with MRI (which could be even tightly integrated by acquiring simultaneous PET/MRI signals) could be a powerful way of demonstrating how the functional effects of drugs are associated with major receptor targets. Beyond the full validation of the neurovascular coupling model to D_2R in humans, future studies might also investigate the association between functional effects and other antipsychotic targets such as serotonin receptors or different actions to D_2R such as

partial agonism (e.g., aripiprazole, brexpiprazole, etc.). A more challenging but intriguing application might be also to characterize antipsychotics PK/PD relationship in a dose-dependent fashion such as different effects might be associated with different target occupancy achieved at different doses (e.g., pre-synaptic D_2R in the case of amisulpride, D_2R vs. $5HT_2A$ in the case of olanzapine or risperidone, etc). This method could also be applied to novel antipsychotics to enhance the translation in humans of PK/PD investigations that are usually performed in pre-clinical studies. Also, the approach might not necessarily be limited to compounds that directly bind to receptor targets, as it could also be used to investigate downstream effects (McCutcheon et al., 2021; Rogeau et al., 2022).

As shown here, multimodal approaches could also bridge the gap between drug actions at target receptors and behavioural effects (Uchida et al., 2011). The investigation of brain functional effects linked with receptor occupancy could increase our understanding of neurobiological mechanisms driving treatment response and side effects. This might be particularly relevant to elucidate between-subject variability in drug response. The search for biomarkers is a longstanding issue in neuroimaging research applied to psychiatry (Dazzan, 2014; Kraguljac et al., 2021; Rubio et al., 2021; Sarpal, Lencz, et al., 2016; Tregellas, 2014; Wylie et al., 2016). Neuroimaging biomarkers have been thought of as a possible tool to guide clinical decision-making to deliver a precision medicine approach to patients and therefore reduce the costs of ineffective treatment and long-term side effects (Linden & Fallgatter, 2009). However, issues related to clinical and biological heterogeneity and technical reproducibility have heavily limited the concrete translation of different neuroimaging measures into clinically useful biomarkers (Kapur et al., 2012). It has been proposed that for a neuroimaging biomarker to be successful it should focus on clinically relevant questions, have a close link with biological mechanisms and pathophysiological processes and have a high predictive value in both experimental and clinical settings (Abi-Dargham & Horga, 2016). This thesis shows that the effect of D_2R blockade exerted by antipsychotics on brain function is linked with well-established biological and pharmacological mechanisms and is associated with highly disabling side effects experienced by patients with psychosis such as EPS. From this evidence, future multimodal longitudinal imaging investigations in patients with psychosis could establish the validity of these findings as biomarkers. For example, future studies could identify a proxy for D_2R occupancy based on CBF data and a predictive

model for EPS which could guide the clinician to narrow the antipsychotic treatment within the known "therapeutic window" of D_2R blockade (Kapur et al., 2000). In addition, similar multimodal investigation could link D_2R occupancy with other behavioural alterations putatively associated with functional domains. Some examples might include positive symptoms and salience processing, negative symptoms and reward processing, and cognitive deficits and working memory.

6 Conclusion

My whole PhD project highlights the importance of investigating the effects of antipsychotics on brain structure and function to generate knowledge to be translated into clinical settings. In my PhD, I was able to show that D_2R blockade produces alterations in striatal perfusion in healthy controls, within a plausible PK/PD framework. These alterations were absent in patients free from antipsychotic medications, thus suggesting that these alterations are likely pharmacological effects. In addition, I found evidence supporting the potential role of altered cortico-striatal connectivity as a potential biomarker for EPS which are among the most distressing side effects experienced by patients with psychosis taking antipsychotic treatment. Finally, the use of a multimodal approach allowed me to directly link functional effects with neurochemical mechanisms. The results of my PhD strongly encourage this effort in neuroimaging research, especially in pharmacological MRI, to overcome the natural limitations of the MRI signal, enhance biological plausibility and reduce the degree of conjecture when interpreting results. This would dramatically improve our understanding of the effects of pharmacological treatment on brain structure and function. A more in-depth understanding of these effects is crucial to better explain pathophysiological mechanisms and between-subjects variability in response.

References

Abbas, A. I., Hedlund, P. B., Huang, X. P., Tran, T. B., Meltzer, H. Y., & Roth, B. L. (2009). Amisulpride is a potent 5-HT7 antagonist: relevance for antidepressant actions in vivo. *Psychopharmacology (Berl)*, *205*(1), 119-128. https://doi.org/10.1007/s00213-009-1521-8

Abbott, C. C., Jaramillo, A., Wilcox, C. E., & Hamilton, D. A. (2013). Antipsychotic drug effects in schizophrenia: a review of longitudinal FMRI investigations and neural interpretations. *Curr Med Chem*, *20*(3), 428-437. https://doi.org/10.2174/0929867311320030014

Abi-Dargham, A. (2004). Do we still believe in the dopamine hypothesis? New data bring new evidence. *Int J Neuropsychopharmacol*, *7 Suppl 1*, S1-5. https://doi.org/10.1017/S1461145704004110

Abi-Dargham, A., & Horga, G. (2016). The search for imaging biomarkers in psychiatric disorders. *Nat Med*, *22*(11), 1248-1255. https://doi.org/10.1038/nm.4190

Aghajanian, G. K., & Marek, G. J. (2000). Serotonin model of schizophrenia: emerging role of glutamate mechanisms. *Brain Res Brain Res Rev*, *31*(2-3), 302-312. https://doi.org/10.1016/s0165-0173(99)00046-6

Agid, O., Kapur, S., Arenovich, T., & Zipursky, R. B. (2003). Delayed-onset hypothesis of antipsychotic action: a hypothesis tested and rejected. *Arch Gen Psychiatry*, *60*(12), 1228-1235. https://doi.org/10.1001/archpsyc.60.12.1228

Akber, S. F. (1996). NMR relaxation data of water proton in normal tissues. *Physiol Chem Phys Med NMR*, *28*(4), 205-238. https://www.ncbi.nlm.nih.gov/pubmed/9153797

Akber, S. F. (2008). Water proton relaxation times of pathological tissues. *Physiol Chem Phys Med NMR*, *40*, 1-42. https://www.ncbi.nlm.nih.gov/pubmed/20070038

Allen, P., Azis, M., Modinos, G., Bossong, M. G., Bonoldi, I., Samson, C., Quinn, B., Kempton, M. J., Howes, O. D., Stone, J. M., Calem, M., Perez, J., Bhattacharayya, S., Broome, M. R., Grace, A. A., Zelaya, F., & McGuire, P. (2018). Increased Resting Hippocampal and Basal Ganglia Perfusion in People at Ultra High Risk for Psychosis: Replication in a Second Cohort. *Schizophr Bull*, *44*(6), 1323-1331. https://doi.org/10.1093/schbul/sbx169

Allen, P., Chaddock, C. A., Egerton, A., Howes, O. D., Bonoldi, I., Zelaya, F., Bhattacharyya, S., Murray, R., & McGuire, P. (2016). Resting Hyperperfusion of the Hippocampus, Midbrain, and Basal Ganglia in People at High Risk for Psychosis. *Am J Psychiatry*, *173*(4), 392-399. https://doi.org/10.1176/appi.ajp.2015.15040485

Alsop, D. C., Detre, J. A., Golay, X., Gunther, M., Hendrikse, J., Hernandez-Garcia, L., Lu, H., MacIntosh, B. J., Parkes, L. M., Smits, M., van Osch, M. J., Wang, D. J., Wong, E. C., & Zaharchuk, G. (2015). Recommended implementation of arterial spin-labeled perfusion MRI for clinical applications: A consensus of the ISMRM perfusion study group and the European consortium for ASL in dementia. *Magn Reson Med*, *73*(1), 102-116. https://doi.org/10.1002/mrm.25197

Amato, D., Beasley, C. L., Hahn, M. K., & Vernon, A. C. (2017). Neuroadaptations to antipsychotic drugs: Insights from pre-clinical and human post-mortem studies. *Neurosci Biobehav Rev*, *76*(Pt B), 317-335. https://doi.org/10.1016/j.neubiorev.2016.10.004

Andersen, H. G., Raghava, J. M., Svarer, C., Wulff, S., Johansen, L. B., Antonsen, P. K., Nielsen, M. O., Rostrup, E., Vernon, A. C., Jensen, L. T., Pinborg, L. H., Glenthoj, B. Y., & Ebdrup, B. H. (2020). Striatal Volume Increase After Six Weeks of Selective Dopamine D(2/3) Receptor Blockade in First-Episode, Antipsychotic-Naive Schizophrenia Patients. *Front Neurosci*, *14*, 484. https://doi.org/10.3389/fnins.2020.00484

Andersson, C., Hamer, R. M., Lawler, C. P., Mailman, R. B., & Lieberman, J. A. (2002). Striatal volume changes in the rat following long-term administration of typical and atypical antipsychotic drugs. *Neuropsychopharmacology*, *27*(2), 143-151. https://doi.org/10.1016/S0893-133X(02)00287-7

Andreasen, N. C., Liu, D., Ziebell, S., Vora, A., & Ho, B. C. (2013). Relapse duration, treatment intensity, and brain tissue loss in schizophrenia: a prospective longitudinal MRI study. *Am J Psychiatry*, *170*(6), 609-615. https://doi.org/10.1176/appi.ajp.2013.12050674

Anticevic, A., Cole, M. W., Repovs, G., Murray, J. D., Brumbaugh, M. S., Winkler, A. M., Savic, A., Krystal, J. H., Pearlson, G. D., & Glahn, D. C. (2014). Characterizing thalamo-cortical disturbances in schizophrenia and bipolar illness. *Cereb Cortex*, *24*(12), 3116-3130. https://doi.org/10.1093/cercor/bht165

Anticevic, A., Hu, X., Xiao, Y., Hu, J., Li, F., Bi, F., Cole, M. W., Savic, A., Yang, G. J., Repovs, G., Murray, J. D., Wang, X. J., Huang, X., Lui, S., Krystal, J. H., & Gong, Q. (2015). Early-course

unmedicated schizophrenia patients exhibit elevated prefrontal connectivity associated with longitudinal change. *J Neurosci*, *35*(1), 267-286. https://doi.org/10.1523/JNEUROSCI.2310-14.2015
Arnatkeviciute, A., Fulcher, B. D., & Fornito, A. (2019). A practical guide to linking brain-wide gene expression and neuroimaging data. *Neuroimage*, *189*, 353-367. https://doi.org/10.1016/j.neuroimage.2019.01.011
Ashburner, J., & Friston, K. J. (2000). Voxel-based morphometry--the methods. *Neuroimage*, *11*(6 Pt 1), 805-821. https://doi.org/10.1006/nimg.2000.0582
Ashburner, J., & Friston, K. J. (2005). Unified segmentation. *Neuroimage*, *26*(3), 839-851. https://doi.org/10.1016/j.neuroimage.2005.02.018
Ashburner, J., & Friston, K. J. (2011). Diffeomorphic registration using geodesic shooting and Gauss-Newton optimisation. *Neuroimage*, *55*(3), 954-967. https://doi.org/10.1016/j.neuroimage.2010.12.049
Attwell, D., Buchan, A. M., Charpak, S., Lauritzen, M., Macvicar, B. A., & Newman, E. A. (2010). Glial and neuronal control of brain blood flow. *Nature*, *468*(7321), 232-243. https://doi.org/10.1038/nature09613
Attwell, D., & Laughlin, S. B. (2001). An energy budget for signaling in the grey matter of the brain. *J Cereb Blood Flow Metab*, *21*(10), 1133-1145. https://doi.org/10.1097/00004647-200110000-00001
Auclair, A., Drouin, C., Cotecchia, S., Glowinski, J., & Tassin, J. P. (2004). 5-HT2A and alpha1b-adrenergic receptors entirely mediate dopamine release, locomotor response and behavioural sensitization to opiates and psychostimulants. *Eur J Neurosci*, *20*(11), 3073-3084. https://doi.org/10.1111/j.1460-9568.2004.03805.x
Avants, B. B., Tustison, N. J., Song, G., Cook, P. A., Klein, A., & Gee, J. C. (2011). A reproducible evaluation of ANTs similarity metric performance in brain image registration. *Neuroimage*, *54*(3), 2033-2044. https://doi.org/10.1016/j.neuroimage.2010.09.025
Avram, M., Brandl, F., Knolle, F., Cabello, J., Leucht, C., Scherr, M., Mustafa, M., Koutsouleris, N., Leucht, S., Ziegler, S., & Sorg, C. (2020). Aberrant striatal dopamine links topographically with cortico-thalamic dysconnectivity in schizophrenia. *Brain*, *143*(11), 3495-3505. https://doi.org/10.1093/brain/awaa296
Becerra, L., Harter, K., Gonzalez, R. G., & Borsook, D. (2006). Functional magnetic resonance imaging measures of the effects of morphine on central nervous system circuitry in opioid-naive healthy volunteers. *Anesth Analg*, *103*(1), 208-216, table of contents. https://doi.org/10.1213/01.ane.0000221457.71536.e0
Beliveau, V., Ganz, M., Feng, L., Ozenne, B., Hojgaard, L., Fisher, P. M., Svarer, C., Greve, D. N., & Knudsen, G. M. (2017). A High-Resolution In Vivo Atlas of the Human Brain's Serotonin System. *J Neurosci*, *37*(1), 120-128. https://doi.org/10.1523/JNEUROSCI.2830-16.2016
Berge, D., Lesh, T. A., Smucny, J., & Carter, C. S. (2022). Improvement in prefrontal thalamic connectivity during the early course of the illness in recent-onset psychosis: a 12-month longitudinal follow-up resting-state fMRI study. *Psychol Med*, *52*(13), 2713-2721. https://doi.org/10.1017/S0033291720004808
Bernardo, M., Parellada, E., Lomena, F., Catafau, A. M., Font, M., Gomez, J. C., Lopez-Carrero, C., Gutierrez, F., Pavia, J., & Salamero, M. (2001). Double-blind olanzapine vs. haloperidol D2 dopamine receptor blockade in schizophrenic patients: a baseline-endpoint. *Psychiatry Res*, *107*(2), 87-97. https://doi.org/10.1016/s0925-4927(01)00085-3
Black, K. J., Hershey, T., Gado, M. H., & Perlmutter, J. S. (2000). Dopamine D(1) agonist activates temporal lobe structures in primates. *J Neurophysiol*, *84*(1), 549-557. https://doi.org/10.1152/jn.2000.84.1.549
Boellaard, R. (2009). Standards for PET image acquisition and quantitative data analysis. *J Nucl Med*, *50 Suppl 1*, 11S-20S. https://doi.org/10.2967/jnumed.108.057182
Bojesen, K. B., Glenthoj, B. Y., Sigvard, A. K., Tangmose, K., Raghava, J. M., Ebdrup, B. H., & Rostrup, E. (2023). Cerebral blood flow in striatum is increased by partial dopamine agonism in initially antipsychotic-naive patients with psychosis. *Psychol Med*, 1-11. https://doi.org/10.1017/S0033291723000144
Borra, E., Rizzo, M., Gerbella, M., Rozzi, S., & Luppino, G. (2021). Laminar Origin of Corticostriatal Projections to the Motor Putamen in the Macaque Brain. *J Neurosci*, *41*(7), 1455-1469. https://doi.org/10.1523/JNEUROSCI.1475-20.2020
Bowskill, S. V., Patel, M. X., Handley, S. A., & Flanagan, R. J. (2012). Plasma amisulpride in relation to prescribed dose, clozapine augmentation, and other factors: data from a therapeutic drug monitoring service, 2002-2010. *Hum Psychopharmacol*, *27*(5), 507-513. https://doi.org/10.1002/hup.2256
Bressan, R. A., Erlandsson, K., Jones, H. M., Mulligan, R., Flanagan, R. J., Ell, P. J., & Pilowsky, L. S. (2003). Is regionally selective D2/D3 dopamine occupancy sufficient for atypical antipsychotic

effect? an in vivo quantitative [123I]epidepride SPET study of amisulpride-treated patients. *Am J Psychiatry*, *160*(8), 1413-1420. https://doi.org/10.1176/appi.ajp.160.8.1413

Brewer, W. J., Yucel, M., Harrison, B. J., McGorry, P. D., Olver, J., Egan, G. F., Velakoulis, D., & Pantelis, C. (2007). Increased prefrontal cerebral blood flow in first-episode schizophrenia following treatment: longitudinal positron emission tomography study. *Aust N Z J Psychiatry*, *41*(2), 129-135. https://doi.org/10.1080/00048670601109899

Brugger, S. P., & Howes, O. D. (2017). Heterogeneity and Homogeneity of Regional Brain Structure in Schizophrenia: A Meta-analysis. *JAMA Psychiatry*, *74*(11), 1104-1111. https://doi.org/10.1001/jamapsychiatry.2017.2663

Buchsbaum, M. S., Haznedar, M., Newmark, R. E., Chu, K. W., Dusi, N., Entis, J. J., Goldstein, K. E., Goodman, C. R., Gupta, A., Hazlett, E., Iannuzzi, J., Torosjan, Y., Zhang, J., & Wolkin, A. (2009). FDG-PET and MRI imaging of the effects of sertindole and haloperidol in the prefrontal lobe in schizophrenia. *Schizophr Res*, *114*(1-3), 161-171. https://doi.org/10.1016/j.schres.2009.07.015

Bullmore, E., Brammer, M., Williams, S. C., Curtis, V., McGuire, P., Morris, R., Murray, R., & Sharma, T. (1999). Functional MR imaging of confounded hypofrontality. *Hum Brain Mapp*, *8*(2-3), 86-91. https://doi.org/10.1002/(SICI)1097-0193(1999)8:2/3<86::AID-HBM3>3.0.CO;2-S

Burt, D. R., Creese, I., & Snyder, S. H. (1977). Antischizophrenic drugs: chronic treatment elevates dopamine receptor binding in brain. *Science*, *196*(4287), 326-328. https://doi.org/10.1126/science.847477

Burt, J. B., Demirtas, M., Eckner, W. J., Navejar, N. M., Ji, J. L., Martin, W. J., Bernacchia, A., Anticevic, A., & Murray, J. D. (2018). Hierarchy of transcriptomic specialization across human cortex captured by structural neuroimaging topography. *Nat Neurosci*, *21*(9), 1251-1259. https://doi.org/10.1038/s41593-018-0195-0

Burt, J. B., Helmer, M., Shinn, M., Anticevic, A., & Murray, J. D. (2020). Generative modeling of brain maps with spatial autocorrelation. *Neuroimage*, *220*, 117038. https://doi.org/10.1016/j.neuroimage.2020.117038

Buxton, R. B., Uludag, K., Dubowitz, D. J., & Liu, T. T. (2004). Modeling the hemodynamic response to brain activation. *Neuroimage*, *23 Suppl 1*, S220-233. https://doi.org/10.1016/j.neuroimage.2004.07.013

Calderone, D. J., Martinez, A., Zemon, V., Hoptman, M. J., Hu, G., Watkins, J. E., Javitt, D. C., & Butler, P. D. (2013). Comparison of psychophysical, electrophysiological, and fMRI assessment of visual contrast responses in patients with schizophrenia. *Neuroimage*, *67*, 153-162. https://doi.org/10.1016/j.neuroimage.2012.11.019

Carhart-Harris, R. L., Erritzoe, D., Williams, T., Stone, J. M., Reed, L. J., Colasanti, A., Tyacke, R. J., Leech, R., Malizia, A. L., Murphy, K., Hobden, P., Evans, J., Feilding, A., Wise, R. G., & Nutt, D. J. (2012). Neural correlates of the psychedelic state as determined by fMRI studies with psilocybin. *Proc Natl Acad Sci U S A*, *109*(6), 2138-2143. https://doi.org/10.1073/pnas.1119598109

Cazorla, M., de Carvalho, F. D., Chohan, M. O., Shegda, M., Chuhma, N., Rayport, S., Ahmari, S. E., Moore, H., & Kellendonk, C. (2014). Dopamine D2 receptors regulate the anatomical and functional balance of basal ganglia circuitry. *Neuron*, *81*(1), 153-164. https://doi.org/10.1016/j.neuron.2013.10.041

Cazorla, M., Shegda, M., Ramesh, B., Harrison, N. L., & Kellendonk, C. (2012). Striatal D2 receptors regulate dendritic morphology of medium spiny neurons via Kir2 channels. *J Neurosci*, *32*(7), 2398-2409. https://doi.org/10.1523/JNEUROSCI.6056-11.2012

Chan, C. S., Peterson, J. D., Gertler, T. S., Glajch, K. E., Quintana, R. E., Cui, Q., Sebel, L. E., Plotkin, J. L., Shen, W., Heiman, M., Heintz, N., Greengard, P., & Surmeier, D. J. (2012). Strain-specific regulation of striatal phenotype in Drd2-eGFP BAC transgenic mice. *J Neurosci*, *32*(27), 9124-9132. https://doi.org/10.1523/JNEUROSCI.0229-12.2012

Chan, S. Y., Brady, R. O., Lewandowski, K. E., Higgins, A., Ongur, D., & Hall, M. H. (2022). Dynamic and progressive changes in thalamic functional connectivity over the first five years of psychosis. *Mol Psychiatry*, *27*(2), 1177-1183. https://doi.org/10.1038/s41380-021-01319-3

Chen, J., Xue, K., Yang, M., Wang, K., Xu, Y., Wen, B., Cheng, J., Han, S., & Wei, Y. (2022). Altered Coupling of Cerebral Blood Flow and Functional Connectivity Strength in First-Episode Schizophrenia Patients With Auditory Verbal Hallucinations. *Front Neurosci*, *16*, 821078. https://doi.org/10.3389/fnins.2022.821078

Chen, Y. C., Choi, J. K., Andersen, S. L., Rosen, B. R., & Jenkins, B. G. (2005). Mapping dopamine D2/D3 receptor function using pharmacological magnetic resonance imaging. *Psychopharmacology (Berl)*, *180*(4), 705-715. https://doi.org/10.1007/s00213-004-2034-0

Choi, J. K., Chen, Y. I., Hamel, E., & Jenkins, B. G. (2006). Brain hemodynamic changes mediated by dopamine receptors: Role of the cerebral microvasculature in dopamine-mediated neurovascular coupling. *Neuroimage*, *30*(3), 700-712. https://doi.org/10.1016/j.neuroimage.2005.10.029

Chopra, S., Fornito, A., Francey, S. M., O'Donoghue, B., Cropley, V., Nelson, B., Graham, J., Baldwin, L., Tahtalian, S., Yuen, H. P., Allott, K., Alvarez-Jimenez, M., Harrigan, S., Sabaroedin, K., Pantelis, C., Wood, S. J., & McGorry, P. (2021). Differentiating the effect of antipsychotic medication and illness on brain volume reductions in first-episode psychosis: A Longitudinal, Randomised, Triple-blind, Placebo-controlled MRI Study. *Neuropsychopharmacology*, *46*(8), 1494-1501. https://doi.org/10.1038/s41386-021-00980-0

Chopra, S., Francey, S. M., O'Donoghue, B., Sabaroedin, K., Arnatkeviciute, A., Cropley, V., Nelson, B., Graham, J., Baldwin, L., Tahtalian, S., Yuen, H. P., Allott, K., Alvarez-Jimenez, M., Harrigan, S., Pantelis, C., Wood, S. J., McGorry, P., & Fornito, A. (2021). Functional Connectivity in Antipsychotic-Treated and Antipsychotic-Naive Patients With First-Episode Psychosis and Low Risk of Self-harm or Aggression: A Secondary Analysis of a Randomized Clinical Trial. *JAMA Psychiatry*, *78*(9), 994-1004. https://doi.org/10.1001/jamapsychiatry.2021.1422

Chouinard, G., & Margolese, H. C. (2005). Manual for the Extrapyramidal Symptom Rating Scale (ESRS). *Schizophr Res*, *76*(2-3), 247-265. https://doi.org/10.1016/j.schres.2005.02.013

Cioli, C., Abdi, H., Beaton, D., Burnod, Y., & Mesmoudi, S. (2014). Differences in human cortical gene expression match the temporal properties of large-scale functional networks. *PLoS One*, *9*(12), e115913. https://doi.org/10.1371/journal.pone.0115913

Claassen, J., Thijssen, D. H. J., Panerai, R. B., & Faraci, F. M. (2021). Regulation of cerebral blood flow in humans: physiology and clinical implications of autoregulation. *Physiol Rev*, *101*(4), 1487-1559. https://doi.org/10.1152/physrev.00022.2020

Clark, A. J. (1937). *General pharmacology*. Julius Springer. http://www.springer.com/gb/

Cole, D. M., Beckmann, C. F., Oei, N. Y., Both, S., van Gerven, J. M., & Rombouts, S. A. (2013). Differential and distributed effects of dopamine neuromodulations on resting-state network connectivity. *Neuroimage*, *78*, 59-67. https://doi.org/10.1016/j.neuroimage.2013.04.034

Cole, D. M., Oei, N. Y., Soeter, R. P., Both, S., van Gerven, J. M., Rombouts, S. A., & Beckmann, C. F. (2013). Dopamine-dependent architecture of cortico-subcortical network connectivity. *Cereb Cortex*, *23*(7), 1509-1516. https://doi.org/10.1093/cercor/bhs136

Cook, R. D., & Weisberg, S. (1982). *Residuals and influence in regression*. Chapman and Hall. http://digitool.hbz-nrw.de:1801/webclient/DeliveryManager?pid=2300268&custom_att_2=simple_viewer http://www.gbv.de/dms/hbz/toc/ht000074796.pdf

Correll, C. U., Manu, P., Olshanskiy, V., Napolitano, B., Kane, J. M., & Malhotra, A. K. (2009). Cardiometabolic risk of second-generation antipsychotic medications during first-time use in children and adolescents. *JAMA*, *302*(16), 1765-1773. https://doi.org/10.1001/jama.2009.1549

Correll, C. U., Rubio, J. M., & Kane, J. M. (2018). What is the risk-benefit ratio of long-term antipsychotic treatment in people with schizophrenia? *World Psychiatry*, *17*(2), 149-160. https://doi.org/10.1002/wps.20516

Cotel, M. C., Lenartowicz, E. M., Natesan, S., Modo, M. M., Cooper, J. D., Williams, S. C., Kapur, S., & Vernon, A. C. (2015). Microglial activation in the rat brain following chronic antipsychotic treatment at clinically relevant doses. *Eur Neuropsychopharmacol*, *25*(11), 2098-2107. https://doi.org/10.1016/j.euroneuro.2015.08.004

Cousins, D. A., Aribisala, B., Nicol Ferrier, I., & Blamire, A. M. (2013). Lithium, gray matter, and magnetic resonance imaging signal. *Biol Psychiatry*, *73*(7), 652-657. https://doi.org/10.1016/j.biopsych.2012.09.029

Cox, R. W. (1996). AFNI: software for analysis and visualization of functional magnetic resonance neuroimages. *Comput Biomed Res*, *29*(3), 162-173. https://doi.org/10.1006/cbmr.1996.0014

Cumming, P. (2011). Absolute abundances and affinity states of dopamine receptors in mammalian brain: A review. *Synapse*, *65*(9), 892-909. https://doi.org/10.1002/syn.20916

Cumming, P., Ase, A., Laliberte, C., Kuwabara, H., & Gjedde, A. (1997). In vivo regulation of DOPA decarboxylase by dopamine receptors in rat brain. *J Cereb Blood Flow Metab*, *17*(11), 1254-1260. https://doi.org/10.1097/00004647-199711000-00014

Cumming, P., Scheidegger, M., Dornbierer, D., Palner, M., Quednow, B. B., & Martin-Soelch, C. (2021). Molecular and Functional Imaging Studies of Psychedelic Drug Action in Animals and Humans. *Molecules*, *26*(9). https://doi.org/10.3390/molecules26092451

Dale, A. M., Fischl, B., & Sereno, M. I. (1999). Cortical surface-based analysis. I. Segmentation and surface reconstruction. *Neuroimage*, *9*(2), 179-194. https://doi.org/10.1006/nimg.1998.0395

Davies, C., Paloyelis, Y., Rutigliano, G., Cappucciati, M., De Micheli, A., Ramella-Cravaro, V., Provenzani, U., Antoniades, M., Modinos, G., Oliver, D., Stahl, D., Murguia, S., Zelaya, F., Allen, P., Shergill, S., Morrison, P., Williams, S., Taylor, D., McGuire, P., & Fusar-Poli, P. (2019). Oxytocin modulates hippocampal perfusion in people at clinical high risk for psychosis. *Neuropsychopharmacology*, *44*(7), 1300-1309. https://doi.org/10.1038/s41386-018-0311-6

Davis, K. L., Kahn, R. S., Ko, G., & Davidson, M. (1991). Dopamine in schizophrenia: a review and reconceptualization. *Am J Psychiatry*, *148*(11), 1474-1486. https://doi.org/10.1176/ajp.148.11.1474

Dazzan, P. (2014). Neuroimaging biomarkers to predict treatment response in schizophrenia: the end of 30 years of solitude? *Dialogues Clin Neurosci*, *16*(4), 491-503. https://doi.org/10.31887/DCNS.2014.16.4/pdazzan

de Bartolomeis, A., Tomasetti, C., & Iasevoli, F. (2015). Update on the Mechanism of Action of Aripiprazole: Translational Insights into Antipsychotic Strategies Beyond Dopamine Receptor Antagonism. *CNS Drugs*, *29*(9), 773-799. https://doi.org/10.1007/s40263-015-0278-3

de Greef, R., Maloney, A., Olsson-Gisleskog, P., Schoemaker, J., & Panagides, J. (2011). Dopamine D2 occupancy as a biomarker for antipsychotics: quantifying the relationship with efficacy and extrapyramidal symptoms. *AAPS J*, *13*(1), 121-130. https://doi.org/10.1208/s12248-010-9247-4

De Simoni, S., Schwarz, A. J., O'Daly, O. G., Marquand, A. F., Brittain, C., Gonzales, C., Stephenson, S., Williams, S. C., & Mehta, M. A. (2013). Test-retest reliability of the BOLD pharmacological MRI response to ketamine in healthy volunteers. *Neuroimage*, *64*, 75-90. https://doi.org/10.1016/j.neuroimage.2012.09.037

Deoni, S. C. (2011). Magnetic resonance relaxation and quantitative measurement in the brain. *Methods Mol Biol*, *711*, 65-108. https://doi.org/10.1007/978-1-61737-992-5_4

Desikan, R. S., Segonne, F., Fischl, B., Quinn, B. T., Dickerson, B. C., Blacker, D., Buckner, R. L., Dale, A. M., Maguire, R. P., Hyman, B. T., Albert, M. S., & Killiany, R. J. (2006). An automated labeling system for subdividing the human cerebral cortex on MRI scans into gyral based regions of interest. *Neuroimage*, *31*(3), 968-980. https://doi.org/10.1016/j.neuroimage.2006.01.021

Dewey, S. L., Smith, G. S., Logan, J., Alexoff, D., Ding, Y. S., King, P., Pappas, N., Brodie, J. D., & Ashby, C. R., Jr. (1995). Serotonergic modulation of striatal dopamine measured with positron emission tomography (PET) and in vivo microdialysis. *J Neurosci*, *15*(1 Pt 2), 821-829. https://doi.org/10.1523/JNEUROSCI.15-01-00821.1995

Diaconescu, A. O., Menon, M., Jensen, J., Kapur, S., & McIntosh, A. R. (2010). Dopamine-induced changes in neural network patterns supporting aversive conditioning. *Brain Res*, *1313*, 143-161. https://doi.org/10.1016/j.brainres.2009.11.064

Dipasquale, O., Martins, D., Sethi, A., Veronese, M., Hesse, S., Rullmann, M., Sabri, O., Turkheimer, F., Harrison, N. A., Mehta, M. A., & Cercignani, M. (2020). Unravelling the effects of methylphenidate on the dopaminergic and noradrenergic functional circuits. *Neuropsychopharmacology*, *45*(9), 1482-1489. https://doi.org/10.1038/s41386-020-0724-x

Dipasquale, O., Selvaggi, P., Veronese, M., Gabay, A. S., Turkheimer, F., & Mehta, M. A. (2019). Receptor-Enriched Analysis of functional connectivity by targets (REACT): A novel, multimodal analytical approach informed by PET to study the pharmacodynamic response of the brain under MDMA. *Neuroimage*, *195*, 252-260. https://doi.org/10.1016/j.neuroimage.2019.04.007

Dipasquale, O., Sethi, A., Lagana, M. M., Baglio, F., Baselli, G., Kundu, P., Harrison, N. A., & Cercignani, M. (2017). Comparing resting state fMRI de-noising approaches using multi- and single-echo acquisitions. *PLoS One*, *12*(3), e0173289. https://doi.org/10.1371/journal.pone.0173289

Dogan, A. E., Yuksel, C., Du, F., Chouinard, V. A., & Ongur, D. (2018). Brain lactate and pH in schizophrenia and bipolar disorder: a systematic review of findings from magnetic resonance studies. *Neuropsychopharmacology*, *43*(8), 1681-1690. https://doi.org/10.1038/s41386-018-0041-9

Dorph-Petersen, K. A., Pierri, J. N., Perel, J. M., Sun, Z., Sampson, A. R., & Lewis, D. A. (2005). The influence of chronic exposure to antipsychotic medications on brain size before and after tissue fixation: a comparison of haloperidol and olanzapine in macaque monkeys. *Neuropsychopharmacology*, *30*(9), 1649-1661. https://doi.org/10.1038/sj.npp.1300710

Doyle, O. M., De Simoni, S., Schwarz, A. J., Brittain, C., O'Daly, O. G., Williams, S. C., & Mehta, M. A. (2013). Quantifying the attenuation of the ketamine pharmacological magnetic resonance imaging response in humans: a validation using antipsychotic and glutamatergic agents. *J Pharmacol Exp Ther*, *345*(1), 151-160. https://doi.org/10.1124/jpet.112.201665

Draganski, B., & Kherif, F. (2013). In vivo assessment of use-dependent brain plasticity--beyond the "one trick pony" imaging strategy. *Neuroimage*, *73*, 255-259; discussion 265-257. https://doi.org/10.1016/j.neuroimage.2012.08.058

Draganski, B., Kherif, F., & Lutti, A. (2014). Computational anatomy for studying use-dependant brain plasticity. *Front Hum Neurosci*, *8*, 380. https://doi.org/10.3389/fnhum.2014.00380
Drazanova, E., Kratka, L., Vaskovicova, N., Skoupy, R., Horska, K., Babinska, Z., Kotolova, H., Vrlikova, L., Buchtova, M., Starcuk, Z., Jr., & Ruda-Kucerova, J. (2019). Olanzapine exposure diminishes perfusion and decreases volume of sensorimotor cortex in rats. *Pharmacol Rep*, *71*(5), 839-847. https://doi.org/10.1016/j.pharep.2019.04.020
Drazanova, E., Ruda-Kucerova, J., Kratka, L., Horska, K., Demlova, R., Starcuk, Z., Jr., & Kasparek, T. (2018). Poly(I:C) model of schizophrenia in rats induces sex-dependent functional brain changes detected by MRI that are not reversed by aripiprazole treatment. *Brain Res Bull*, *137*, 146-155. https://doi.org/10.1016/j.brainresbull.2017.11.008
Du, F., Cooper, A. J., Thida, T., Sehovic, S., Lukas, S. E., Cohen, B. M., Zhang, X., & Ongur, D. (2014). In vivo evidence for cerebral bioenergetic abnormalities in schizophrenia measured using 31P magnetization transfer spectroscopy. *JAMA Psychiatry*, *71*(1), 19-27. https://doi.org/10.1001/jamapsychiatry.2013.2287
Duan, X., Hu, M., Huang, X., Su, C., Zong, X., Dong, X., He, C., Xiao, J., Li, H., Tang, J., Chen, X., & Chen, H. (2020). Effect of Risperidone Monotherapy on Dynamic Functional Connectivity of Insular Subdivisions in Treatment-Naive, First-Episode Schizophrenia. *Schizophr Bull*, *46*(3), 650-660. https://doi.org/10.1093/schbul/sbz087
Dukart, J., Holiga, S., Chatham, C., Hawkins, P., Forsyth, A., McMillan, R., Myers, J., Lingford-Hughes, A. R., Nutt, D. J., Merlo-Pich, E., Risterucci, C., Boak, L., Umbricht, D., Schobel, S., Liu, T., Mehta, M. A., Zelaya, F. O., Williams, S. C., Brown, G., . . . Sambataro, F. (2018). Cerebral blood flow predicts differential neurotransmitter activity. *Sci Rep*, *8*(1), 4074. https://doi.org/10.1038/s41598-018-22444-0
Duning, T., Kloska, S., Steinstrater, O., Kugel, H., Heindel, W., & Knecht, S. (2005). Dehydration confounds the assessment of brain atrophy. *Neurology*, *64*(3), 548-550. https://doi.org/10.1212/01.WNL.0000150542.16969.CC
Dunn, J. T., Baker, S. X., Stone, J., Cleij, M., Marsden, P. K., O'Doherty, M., & Reed, L. J. (2010). Differential Occupancy of Striatal Versus Extrastriatal Dopamine D2/D3 Receptors by the Typical Antipsychotic Haloperidol in Man Measured Using I [18f]-Fallypride Pet. *Journal of Psychopharmacology*, *24*, A33-A33. <Go to ISI>://WOS:000281115000093
Ebdrup, B. H., Rasmussen, H., Arnt, J., & Glenthoj, B. (2011). Serotonin 2A receptor antagonists for treatment of schizophrenia. *Expert Opin Investig Drugs*, *20*(9), 1211-1223. https://doi.org/10.1517/13543784.2011.601738
Edzes, H. T., & Samulski, E. T. (1977). Cross relaxation and spin diffusion in the proton NMR or hydrated collagen. *Nature*, *265*(5594), 521-523. https://doi.org/10.1038/265521a0
Efron, B., Tibshirani, R., Taylor, & Francis. (1994). *An introduction to the bootstrap*. Chapman & Hall/CRC. http://ed-primo.hosted.exlibrisgroup.com/openurl/44UOE/44UOE_services_page?u.ignore_date_coverage=true&rft.mms_id=9924225647302466
Egerton, A., Demjaha, A., McGuire, P., Mehta, M. A., & Howes, O. D. (2010). The test-retest reliability of 18F-DOPA PET in assessing striatal and extrastriatal presynaptic dopaminergic function. *Neuroimage*, *50*(2), 524-531. https://doi.org/10.1016/j.neuroimage.2009.12.058
Eklund, A., Nichols, T. E., & Knutsson, H. (2016). Cluster failure: Why fMRI inferences for spatial extent have inflated false-positive rates. *Proc Natl Acad Sci U S A*, *113*(28), 7900-7905. https://doi.org/10.1073/pnas.1602413113
Elman, I., Borsook, D., & Lukas, S. E. (2006). Food intake and reward mechanisms in patients with schizophrenia: implications for metabolic disturbances and treatment with second-generation antipsychotic agents. *Neuropsychopharmacology*, *31*(10), 2091-2120. https://doi.org/10.1038/sj.npp.1301051
Farde, L., Hall, H., Pauli, S., & Halldin, C. (1995). Variability in D2-dopamine receptor density and affinity: a PET study with [11C]raclopride in man. *Synapse*, *20*(3), 200-208. https://doi.org/10.1002/syn.890200303
Farde, L., Nordstrom, A. L., Wiesel, F. A., Pauli, S., Halldin, C., & Sedvall, G. (1992). Positron emission tomographic analysis of central D1 and D2 dopamine receptor occupancy in patients treated with classical neuroleptics and clozapine. Relation to extrapyramidal side effects. *Arch Gen Psychiatry*, *49*(7), 538-544. https://doi.org/10.1001/archpsyc.1992.01820070032005
Fernandez-Seara, M. A., Aznarez-Sanado, M., Mengual, E., Irigoyen, J., Heukamp, F., & Pastor, M. A. (2011). Effects on resting cerebral blood flow and functional connectivity induced by

metoclopramide: a perfusion MRI study in healthy volunteers. *Br J Pharmacol*, *163*(8), 1639-1652. https://doi.org/10.1111/j.1476-5381.2010.01161.x

Finch, W. H. (2012). Distribution of variables by method of outlier detection. *Frontiers in Psychology*, *3*. https://doi.org/ARTN 211
10.3389/fpsyg.2012.00211

First, M. B. (2014). DSM-5 and paraphilic disorders. *J Am Acad Psychiatry Law*, *42*(2), 191-201. https://www.ncbi.nlm.nih.gov/pubmed/24986346

Fischl, B., & Dale, A. M. (2000). Measuring the thickness of the human cerebral cortex from magnetic resonance images. *Proc Natl Acad Sci U S A*, *97*(20), 11050-11055. https://doi.org/10.1073/pnas.200033797

Fischl, B., Salat, D. H., Busa, E., Albert, M., Dieterich, M., Haselgrove, C., van der Kouwe, A., Killiany, R., Kennedy, D., Klaveness, S., Montillo, A., Makris, N., Rosen, B., & Dale, A. M. (2002). Whole brain segmentation: automated labeling of neuroanatomical structures in the human brain. *Neuron*, *33*(3), 341-355. https://doi.org/10.1016/s0896-6273(02)00569-x

Fischl, B., Sereno, M. I., & Dale, A. M. (1999). Cortical surface-based analysis. II: Inflation, flattening, and a surface-based coordinate system. *Neuroimage*, *9*(2), 195-207. https://doi.org/10.1006/nimg.1998.0396

Forest, M., Iturria-Medina, Y., Goldman, J. S., Kleinman, C. L., Lovato, A., Oros Klein, K., Evans, A., Ciampi, A., Labbe, A., & Greenwood, C. M. T. (2017). Gene networks show associations with seed region connectivity. *Hum Brain Mapp*, *38*(6), 3126-3140. https://doi.org/10.1002/hbm.23579

Fountoulakis, K. N., & Stahl, S. M. (2022). The effect of first- and second-generation antipsychotics on brain morphology in schizophrenia: A systematic review of longitudinal magnetic resonance studies with a randomized allocation to treatment arms. *J Psychopharmacol*, *36*(4), 428-438. https://doi.org/10.1177/02698811221087645

Franklin, T. R., Wang, Z., Shin, J., Jagannathan, K., Suh, J. J., Detre, J. A., O'Brien, C. P., & Childress, A. R. (2013). A VBM study demonstrating 'apparent' effects of a single dose of medication on T1-weighted MRIs. *Brain Struct Funct*, *218*(1), 97-104. https://doi.org/10.1007/s00429-012-0385-6

French, L., & Paus, T. (2015). A FreeSurfer view of the cortical transcriptome generated from the Allen Human Brain Atlas. *Front Neurosci*, *9*, 323. https://doi.org/10.3389/fnins.2015.00323

Friston, K. J., Worsley, K. J., Frackowiak, R. S., Mazziotta, J. C., & Evans, A. C. (1994). Assessing the significance of focal activations using their spatial extent. *Hum Brain Mapp*, *1*(3), 210-220. https://doi.org/10.1002/hbm.460010306

Fujimoto, T., Nakano, T., Fujii, M., Okada, A., Harada, K., Yokoyama, Y., Uchida, T., Tsuji, T., Igata, A., & Asakura, T. (1987). Changes in proton T1 in dog brains due to the administration of haloperidol. *Magn Reson Imaging*, *5*(6), 469-474. https://doi.org/10.1016/0730-725x(87)90381-x

Fusar-Poli, P., Lai, S., Di Forti, M., Iacoponi, E., Thornicroft, G., McGuire, P., & Jauhar, S. (2020). Early Intervention Services for First Episode of Psychosis in South London and the Maudsley (SLaM): 20 Years of Care and Research for Young People. *Front Psychiatry*, *11*, 577110. https://doi.org/10.3389/fpsyt.2020.577110

Fusar-Poli, P., Papanastasiou, E., Stahl, D., Rocchetti, M., Carpenter, W., Shergill, S., & McGuire, P. (2015). Treatments of Negative Symptoms in Schizophrenia: Meta-Analysis of 168 Randomized Placebo-Controlled Trials. *Schizophr Bull*, *41*(4), 892-899. https://doi.org/10.1093/schbul/sbu170

Fusar-Poli, P., Radua, J., McGuire, P., & Borgwardt, S. (2012). Neuroanatomical maps of psychosis onset: voxel-wise meta-analysis of antipsychotic-naive VBM studies. *Schizophr Bull*, *38*(6), 1297-1307. https://doi.org/10.1093/schbul/sbr134

Fusar-Poli, P., Smieskova, R., Kempton, M. J., Ho, B. C., Andreasen, N. C., & Borgwardt, S. (2013). Progressive brain changes in schizophrenia related to antipsychotic treatment? A meta-analysis of longitudinal MRI studies. *Neurosci Biobehav Rev*, *37*(8), 1680-1691. https://doi.org/10.1016/j.neubiorev.2013.06.001

Gass, N., Schwarz, A. J., Sartorius, A., Cleppien, D., Zheng, L., Schenker, E., Risterucci, C., Meyer-Lindenberg, A., & Weber-Fahr, W. (2013). Haloperidol modulates midbrain-prefrontal functional connectivity in the rat brain. *Eur Neuropsychopharmacol*, *23*(10), 1310-1319. https://doi.org/10.1016/j.euroneuro.2012.10.013

Gefvert, O., Lundberg, T., Wieselgren, I. M., Bergstrom, M., Langstrom, B., Wiesel, F., & Lindstrom, L. (2001). D(2) and 5HT(2A) receptor occupancy of different doses of quetiapine in schizophrenia: a PET study. *Eur Neuropsychopharmacol*, *11*(2), 105-110. https://doi.org/10.1016/s0924-977x(00)00133-4

Georgiou, R., Lamnisos, D., & Giannakou, K. (2021). Anticholinergic Burden and Cognitive Performance in Patients With Schizophrenia: A Systematic Literature Review. *Front Psychiatry*, *12*, 779607. https://doi.org/10.3389/fpsyt.2021.779607

Glatard, A., Guidi, M., Delacretaz, A., Dubath, C., Grosu, C., Laaboub, N., von Gunten, A., Conus, P., Csajka, C., & Eap, C. B. (2020). Amisulpride: Real-World Evidence of Dose Adaptation and Effect on Prolactin Concentrations and Body Weight Gain by Pharmacokinetic/Pharmacodynamic Analyses. *Clin Pharmacokinet*, *59*(3), 371-382. https://doi.org/10.1007/s40262-019-00821-w

Goozee, R., Handley, R., Kempton, M. J., & Dazzan, P. (2014). A systematic review and meta-analysis of the effects of antipsychotic medications on regional cerebral blood flow (rCBF) in schizophrenia: association with response to treatment. *Neurosci Biobehav Rev*, *43*, 118-136. https://doi.org/10.1016/j.neubiorev.2014.03.014

Grimm, O., Kopfer, V., Kupper-Tetzel, L., Deppert, V., Kuhn, M., de Greck, M., & Reif, A. (2020). Amisulpride and l-DOPA modulate subcortical brain nuclei connectivity in resting-state pharmacologic magnetic resonance imaging. *Hum Brain Mapp*, *41*(7), 1806-1818. https://doi.org/10.1002/hbm.24913

Grubb, R. L., Jr., Raichle, M. E., Eichling, J. O., & Ter-Pogossian, M. M. (1974). The effects of changes in PaCO2 on cerebral blood volume, blood flow, and vascular mean transit time. *Stroke*, *5*(5), 630-639. https://doi.org/10.1161/01.str.5.5.630

Gryglewski, G., Seiger, R., James, G. M., Godbersen, G. M., Komorowski, A., Unterholzner, J., Michenthaler, P., Hahn, A., Wadsak, W., Mitterhauser, M., Kasper, S., & Lanzenberger, R. (2018). Spatial analysis and high resolution mapping of the human whole-brain transcriptome for integrative analysis in neuroimaging. *Neuroimage*, *176*, 259-267. https://doi.org/10.1016/j.neuroimage.2018.04.068

Guma, E., Rocchetti, J., Devenyi, G. A., Tanti, A., Mathieu, A., Lerch, J. P., Elgbeili, G., Courcot, B., Mechawar, N., Chakravarty, M. M., & Giros, B. (2018). Regional brain volume changes following chronic antipsychotic administration are mediated by the dopamine D2 receptor. *Neuroimage*, *176*, 226-238. https://doi.org/10.1016/j.neuroimage.2018.04.054

Gunn, R., Coello, C., & Searle, G. (2016). Molecular Imaging And Kinetic Analysis Toolbox (MIAKAT) - A Quantitative Software Package for the Analysis of PET Neuroimaging Data. *Journal of Nuclear Medicine*, *57*. <Go to ISI>://WOS:000442211003086

Gunn, R. N., Lammertsma, A. A., Hume, S. P., & Cunningham, V. J. (1997). Parametric imaging of ligand-receptor binding in PET using a simplified reference region model. *Neuroimage*, *6*(4), 279-287. https://doi.org/10.1006/nimg.1997.0303

Guo, W., Liu, F., Chen, J., Wu, R., Li, L., Zhang, Z., & Zhao, J. (2017). Olanzapine modulation of long- and short-range functional connectivity in the resting brain in a sample of patients with schizophrenia. *Eur Neuropsychopharmacol*, *27*(1), 48-58. https://doi.org/10.1016/j.euroneuro.2016.11.002

Hahn, B., Robinson, B. M., Leonard, C. J., Luck, S. J., & Gold, J. M. (2018). Posterior Parietal Cortex Dysfunction Is Central to Working Memory Storage and Broad Cognitive Deficits in Schizophrenia. *J Neurosci*, *38*(39), 8378-8387. https://doi.org/10.1523/JNEUROSCI.0913-18.2018

Haijma, S. V., Van Haren, N., Cahn, W., Koolschijn, P. C., Hulshoff Pol, H. E., & Kahn, R. S. (2013). Brain volumes in schizophrenia: a meta-analysis in over 18 000 subjects. *Schizophr Bull*, *39*(5), 1129-1138. https://doi.org/10.1093/schbul/sbs118

Hall, H., Kohler, C., Gawell, L., Farde, L., & Sedvall, G. (1988). Raclopride, a new selective ligand for the dopamine-D2 receptors. *Prog Neuropsychopharmacol Biol Psychiatry*, *12*(5), 559-568. https://doi.org/10.1016/0278-5846(88)90001-2

Handley, R., Zelaya, F. O., Reinders, A. A., Marques, T. R., Mehta, M. A., O'Gorman, R., Alsop, D. C., Taylor, H., Johnston, A., Williams, S., McGuire, P., Pariante, C. M., Kapur, S., & Dazzan, P. (2013). Acute effects of single-dose aripiprazole and haloperidol on resting cerebral blood flow (rCBF) in the human brain. *Hum Brain Mapp*, *34*(2), 272-282. https://doi.org/10.1002/hbm.21436

Hansen, J. Y., Shafiei, G., Markello, R. D., Smart, K., Cox, S. M. L., Norgaard, M., Beliveau, V., Wu, Y., Gallezot, J. D., Aumont, E., Servaes, S., Scala, S. G., DuBois, J. M., Wainstein, G., Bezgin, G., Funck, T., Schmitz, T. W., Spreng, R. N., Galovic, M., . . . Misic, B. (2022). Mapping neurotransmitter systems to the structural and functional organization of the human neocortex. *Nat Neurosci*, *25*(11), 1569-1581. https://doi.org/10.1038/s41593-022-01186-3

Hanssens, L., L'Italien, G., Loze, J. Y., Marcus, R. N., Pans, M., & Kerselaers, W. (2008). The effect of antipsychotic medication on sexual function and serum prolactin levels in community-treated schizophrenic patients: results from the Schizophrenia Trial of Aripiprazole (STAR) study (NCT00237913). *BMC Psychiatry*, *8*, 95. https://doi.org/10.1186/1471-244X-8-95

Harris, J. J., Jolivet, R., & Attwell, D. (2012). Synaptic energy use and supply. *Neuron*, *75*(5), 762-777. https://doi.org/10.1016/j.neuron.2012.08.019

Hartter, S., Huwel, S., Lohmann, T., Abou El Ela, A., Langguth, P., Hiemke, C., & Galla, H. J. (2003). How does the benzamide antipsychotic amisulpride get into the brain?--An in vitro approach comparing amisulpride with clozapine. *Neuropsychopharmacology*, *28*(11), 1916-1922. https://doi.org/10.1038/sj.npp.1300244

Hawkins, P. C. T., Wood, T. C., Vernon, A. C., Bertolino, A., Sambataro, F., Dukart, J., Merlo-Pich, E., Risterucci, C., Silber-Baumann, H., Walsh, E., Mazibuko, N., Zelaya, F. O., & Mehta, M. A. (2018). An investigation of regional cerebral blood flow and tissue structure changes after acute administration of antipsychotics in healthy male volunteers. *Hum Brain Mapp*, *39*(1), 319-331. https://doi.org/10.1002/hbm.23844

Hawrylycz, M., Miller, J. A., Menon, V., Feng, D., Dolbeare, T., Guillozet-Bongaarts, A. L., Jegga, A. G., Aronow, B. J., Lee, C. K., Bernard, A., Glasser, M. F., Dierker, D. L., Menche, J., Szafer, A., Collman, F., Grange, P., Berman, K. A., Mihalas, S., Yao, Z., . . . Lein, E. (2015). Canonical genetic signatures of the adult human brain. *Nat Neurosci*, *18*(12), 1832-1844. https://doi.org/10.1038/nn.4171

Hawrylycz, M. J., Lein, E. S., Guillozet-Bongaarts, A. L., Shen, E. H., Ng, L., Miller, J. A., van de Lagemaat, L. N., Smith, K. A., Ebbert, A., Riley, Z. L., Abajian, C., Beckmann, C. F., Bernard, A., Bertagnolli, D., Boe, A. F., Cartagena, P. M., Chakravarty, M. M., Chapin, M., Chong, J., . . . Jones, A. R. (2012). An anatomically comprehensive atlas of the adult human brain transcriptome. *Nature*, *489*(7416), 391-399. https://doi.org/10.1038/nature11405

Hill, K., Mann, L., Laws, K. R., Stephenson, C. M., Nimmo-Smith, I., & McKenna, P. J. (2004). Hypofrontality in schizophrenia: a meta-analysis of functional imaging studies. *Acta Psychiatr Scand*, *110*(4), 243-256. https://doi.org/10.1111/j.1600-0447.2004.00376.x

Ho, B. C., Andreasen, N. C., Ziebell, S., Pierson, R., & Magnotta, V. (2011). Long-term antipsychotic treatment and brain volumes: a longitudinal study of first-episode schizophrenia. *Arch Gen Psychiatry*, *68*(2), 128-137. https://doi.org/10.1001/archgenpsychiatry.2010.199

Holiga, S., Sambataro, F., Luzy, C., Greig, G., Sarkar, N., Renken, R. J., Marsman, J. C., Schobel, S. A., Bertolino, A., & Dukart, J. (2018). Test-retest reliability of task-based and resting-state blood oxygen level dependence and cerebral blood flow measures. *PLoS One*, *13*(11), e0206583. https://doi.org/10.1371/journal.pone.0206583

Honey, G. D., Suckling, J., Zelaya, F., Long, C., Routledge, C., Jackson, S., Ng, V., Fletcher, P. C., Williams, S. C., Brown, J., & Bullmore, E. T. (2003). Dopaminergic drug effects on physiological connectivity in a human cortico-striato-thalamic system. *Brain*, *126*(Pt 8), 1767-1781. https://doi.org/10.1093/brain/awg184

Horga, G., Cassidy, C. M., Xu, X., Moore, H., Slifstein, M., Van Snellenberg, J. X., & Abi-Dargham, A. (2016). Dopamine-Related Disruption of Functional Topography of Striatal Connections in Unmedicated Patients With Schizophrenia. *JAMA Psychiatry*, *73*(8), 862-870. https://doi.org/10.1001/jamapsychiatry.2016.0178

Howes, O. D., & Kapur, S. (2009). The dopamine hypothesis of schizophrenia: version III--the final common pathway. *Schizophr Bull*, *35*(3), 549-562. https://doi.org/10.1093/schbul/sbp006

Howes, O. D., & McCutcheon, R. (2017). Inflammation and the neural diathesis-stress hypothesis of schizophrenia: a reconceptualization. *Transl Psychiatry*, *7*(2), e1024. https://doi.org/10.1038/tp.2016.278

Howes, O. D., McCutcheon, R., Agid, O., de Bartolomeis, A., van Beveren, N. J., Birnbaum, M. L., Bloomfield, M. A., Bressan, R. A., Buchanan, R. W., Carpenter, W. T., Castle, D. J., Citrome, L., Daskalakis, Z. J., Davidson, M., Drake, R. J., Dursun, S., Ebdrup, B. H., Elkis, H., Falkai, P., . . . Correll, C. U. (2017). Treatment-Resistant Schizophrenia: Treatment Response and Resistance in Psychosis (TRRIP) Working Group Consensus Guidelines on Diagnosis and Terminology. *Am J Psychiatry*, *174*(3), 216-229. https://doi.org/10.1176/appi.ajp.2016.16050503

Howes, O. D., & Murray, R. M. (2014). Schizophrenia: an integrated sociodevelopmental-cognitive model. *Lancet*, *383*(9929), 1677-1687. https://doi.org/10.1016/S0140-6736(13)62036-X

Huang, S., Li, L., Wang, Z., Xiao, T., Li, X., Liu, S., Zhang, M., Lu, H., Wen, Y., & Shang, D. (2021). Modeling and Simulation for Individualized Therapy of Amisulpride in Chinese Patients with Schizophrenia: Focus on Interindividual Variability, Therapeutic Reference Range and the Laboratory Alert Level. *Drug Des Devel Ther*, *15*, 3903-3913. https://doi.org/10.2147/DDDT.S327506

Huhtaniska, S., Jaaskelainen, E., Heikka, T., Moilanen, J. S., Lehtiniemi, H., Tohka, J., Manjon, J. V., Coupe, P., Bjornholm, L., Koponen, H., Veijola, J., Isohanni, M., Kiviniemi, V., Murray, G. K., & Miettunen, J. (2017). Long-term antipsychotic and benzodiazepine use and brain volume changes in schizophrenia: The Northern Finland Birth Cohort 1966 study. *Psychiatry Res Neuroimaging*, *266*, 73-82. https://doi.org/10.1016/j.pscychresns.2017.05.009

Ichise, M., Liow, J. S., Lu, J. Q., Takano, A., Model, K., Toyama, H., Suhara, T., Suzuki, K., Innis, R. B., & Carson, R. E. (2003). Linearized reference tissue parametric imaging methods: application to [11C]DASB positron emission tomography studies of the serotonin transporter in human brain. *J Cereb Blood Flow Metab*, *23*(9), 1096-1112. https://doi.org/10.1097/01.WCB.0000085441.37552.CA

Ito, H., Ibaraki, M., Kanno, I., Fukuda, H., & Miura, S. (2005). Changes in the arterial fraction of human cerebral blood volume during hypercapnia and hypocapnia measured by positron emission tomography. *J Cereb Blood Flow Metab*, *25*(7), 852-857. https://doi.org/10.1038/sj.jcbfm.9600076

Ito, H., Kanno, I., & Fukuda, H. (2005). Human cerebral circulation: positron emission tomography studies. *Ann Nucl Med*, *19*(2), 65-74. https://doi.org/10.1007/BF03027383

James, T. L. (1977). Measurements of water proton NMR spin-lattice relaxation time in the rotating frame (T1p) for studying motions in solutions of giant macro-molecules and supramolecular particles (T2 virus). *Physiol Chem Phys*, *9*(2), 161-166. https://www.ncbi.nlm.nih.gov/pubmed/601108

Janssen, P. A. (1967). The pharmacology of haloperidol. *Int J Neuropsychiatry*, *3*, Suppl 1:10-18. https://www.ncbi.nlm.nih.gov/pubmed/4293129

Jauhar, S., Veronese, M., Nour, M. M., Rogdaki, M., Hathway, P., Turkheimer, F. E., Stone, J., Egerton, A., McGuire, P., Kapur, S., & Howes, O. D. (2019). Determinants of treatment response in first-episode psychosis: an (18)F-DOPA PET study. *Mol Psychiatry*, *24*(10), 1502-1512. https://doi.org/10.1038/s41380-018-0042-4

Joshi, Y. B., Thomas, M. L., Braff, D. L., Green, M. F., Gur, R. C., Gur, R. E., Nuechterlein, K. H., Stone, W. S., Greenwood, T. A., Lazzeroni, L. C., MacDonald, L. R., Molina, J. L., Nungaray, J. A., Radant, A. D., Silverman, J. M., Sprock, J., Sugar, C. A., Tsuang, D. W., Tsuang, M. T., . . . Light, G. A. (2021). Anticholinergic Medication Burden-Associated Cognitive Impairment in Schizophrenia. *Am J Psychiatry*, *178*(9), 838-847. https://doi.org/10.1176/appi.ajp.2020.20081212

Kapur, S., & Mamo, D. (2003). Half a century of antipsychotics and still a central role for dopamine D2 receptors. *Prog Neuropsychopharmacol Biol Psychiatry*, *27*(7), 1081-1090. https://doi.org/10.1016/j.pnpbp.2003.09.004

Kapur, S., Phillips, A. G., & Insel, T. R. (2012). Why has it taken so long for biological psychiatry to develop clinical tests and what to do about it? *Mol Psychiatry*, *17*(12), 1174-1179. https://doi.org/10.1038/mp.2012.105

Kapur, S., & Remington, G. (2001). Dopamine D(2) receptors and their role in atypical antipsychotic action: still necessary and may even be sufficient. *Biol Psychiatry*, *50*(11), 873-883. https://doi.org/10.1016/s0006-3223(01)01251-3

Kapur, S., & Seeman, P. (2001). Does fast dissociation from the dopamine d(2) receptor explain the action of atypical antipsychotics?: A new hypothesis. *Am J Psychiatry*, *158*(3), 360-369. https://doi.org/10.1176/appi.ajp.158.3.360

Kapur, S., Zipursky, R., Jones, C., Remington, G., & Houle, S. (2000). Relationship between dopamine D(2) occupancy, clinical response, and side effects: a double-blind PET study of first-episode schizophrenia. *Am J Psychiatry*, *157*(4), 514-520. https://doi.org/10.1176/appi.ajp.157.4.514

Kapur, S., Zipursky, R. B., & Remington, G. (1999). Clinical and theoretical implications of 5-HT2 and D2 receptor occupancy of clozapine, risperidone, and olanzapine in schizophrenia. *Am J Psychiatry*, *156*(2), 286-293. https://doi.org/10.1176/ajp.156.2.286

Kay, S. R., Opler, L. A., & Lindenmayer, J. P. (1989). The Positive and Negative Syndrome Scale (PANSS): rationale and standardisation. *Br J Psychiatry Suppl*(7), 59-67. https://www.ncbi.nlm.nih.gov/pubmed/2619982

Keedy, S. K., Rosen, C., Khine, T., Rajarethinam, R., Janicak, P. G., & Sweeney, J. A. (2009). An fMRI study of visual attention and sensorimotor function before and after antipsychotic treatment in first-episode schizophrenia. *Psychiatry Res*, *172*(1), 16-23. https://doi.org/10.1016/j.pscychresns.2008.06.003

Kempton, M. J., Ettinger, U., Foster, R., Williams, S. C., Calvert, G. A., Hampshire, A., Zelaya, F. O., O'Gorman, R. L., McMorris, T., Owen, A. M., & Smith, M. S. (2011). Dehydration affects brain structure and function in healthy adolescents. *Hum Brain Mapp*, *32*(1), 71-79. https://doi.org/10.1002/hbm.20999

Keysers, C., Gazzola, V., & Wagenmakers, E. J. (2020). Using Bayes factor hypothesis testing in neuroscience to establish evidence of absence. *Nat Neurosci*, *23*(7), 788-799. https://doi.org/10.1038/s41593-020-0660-4

Khalili-Mahani, N., Rombouts, S. A., van Osch, M. J., Duff, E. P., Carbonell, F., Nickerson, L. D., Becerra, L., Dahan, A., Evans, A. C., Soucy, J. P., Wise, R., Zijdenbos, A. P., & van Gerven, J. M. (2017). Biomarkers, designs, and interpretations of resting-state fMRI in translational pharmacological

research: A review of state-of-the-Art, challenges, and opportunities for studying brain chemistry. *Hum Brain Mapp*, *38*(4), 2276-2325. https://doi.org/10.1002/hbm.23516
Kharkwal, G., Brami-Cherrier, K., Lizardi-Ortiz, J. E., Nelson, A. B., Ramos, M., Del Barrio, D., Sulzer, D., Kreitzer, A. C., & Borrelli, E. (2016). Parkinsonism Driven by Antipsychotics Originates from Dopaminergic Control of Striatal Cholinergic Interneurons. *Neuron*, *91*(1), 67-78. https://doi.org/10.1016/j.neuron.2016.06.014
Kindler, J., Jann, K., Homan, P., Hauf, M., Walther, S., Strik, W., Dierks, T., & Hubl, D. (2015). Static and dynamic characteristics of cerebral blood flow during the resting state in schizophrenia. *Schizophr Bull*, *41*(1), 163-170. https://doi.org/10.1093/schbul/sbt180
Kindler, J., Schultze-Lutter, F., Hauf, M., Dierks, T., Federspiel, A., Walther, S., Schimmelmann, B. G., & Hubl, D. (2018). Increased Striatal and Reduced Prefrontal Cerebral Blood Flow in Clinical High Risk for Psychosis. *Schizophr Bull*, *44*(1), 182-192. https://doi.org/10.1093/schbul/sbx070
Kirschner, M., Aleman, A., & Kaiser, S. (2017). Secondary negative symptoms - A review of mechanisms, assessment and treatment. *Schizophr Res*, *186*, 29-38. https://doi.org/10.1016/j.schres.2016.05.003
Klumpers, L. E., Cole, D. M., Khalili-Mahani, N., Soeter, R. P., Te Beek, E. T., Rombouts, S. A., & van Gerven, J. M. (2012). Manipulating brain connectivity with delta(9)-tetrahydrocannabinol: a pharmacological resting state FMRI study. *Neuroimage*, *63*(3), 1701-1711. https://doi.org/10.1016/j.neuroimage.2012.07.051
Knauss, R., Fleischer, G., Grunder, W., Karger, J., & Werner, A. (1996). Pulsed field gradient NMR and nuclear magnetic relaxation studies of water mobility in hydrated collagen II. *Magn Reson Med*, *36*(2), 241-248. https://doi.org/10.1002/mrm.1910360211
Komorowski, A., Weidenauer, A., Murgas, M., Sauerzopf, U., Wadsak, W., Mitterhauser, M., Bauer, M., Hacker, M., Praschak-Rieder, N., Kasper, S., Lanzenberger, R., & Willeit, M. (2020). Association of dopamine D(2/3) receptor binding potential measured using PET and [(11)C]-(+)-PHNO with post-mortem DRD(2/3) gene expression in the human brain. *Neuroimage*, *223*, 117270. https://doi.org/10.1016/j.neuroimage.2020.117270
Konopaske, G. T., Dorph-Petersen, K. A., Pierri, J. N., Wu, Q., Sampson, A. R., & Lewis, D. A. (2007). Effect of chronic exposure to antipsychotic medication on cell numbers in the parietal cortex of macaque monkeys. *Neuropsychopharmacology*, *32*(6), 1216-1223. https://doi.org/10.1038/sj.npp.1301233
Kornhuber, J., Wiltfang, J., Riederer, P., & Bleich, S. (2006). Neuroleptic drugs in the human brain: clinical impact of persistence and region-specific distribution. *Eur Arch Psychiatry Clin Neurosci*, *256*(5), 274-280. https://doi.org/10.1007/s00406-006-0661-7
Kovacs, A., Harsing, L. G., Jr., & Szenasi, G. (2012). Vasoconstrictor 5-HT receptors in the smooth muscle of the rat middle cerebral artery. *Eur J Pharmacol*, *689*(1-3), 160-164. https://doi.org/10.1016/j.ejphar.2012.05.031
Kraguljac, N. V., McDonald, W. M., Widge, A. S., Rodriguez, C. I., Tohen, M., & Nemeroff, C. B. (2021). Neuroimaging Biomarkers in Schizophrenia. *Am J Psychiatry*, *178*(6), 509-521. https://doi.org/10.1176/appi.ajp.2020.20030340
Kraguljac, N. V., White, D. M., Hadley, J. A., Visscher, K., Knight, D., ver Hoef, L., Falola, B., & Lahti, A. C. (2016). Abnormalities in large scale functional networks in unmedicated patients with schizophrenia and effects of risperidone. *Neuroimage Clin*, *10*, 146-158. https://doi.org/10.1016/j.nicl.2015.11.015
Kumakura, Y., & Cumming, P. (2009). PET studies of cerebral levodopa metabolism: a review of clinical findings and modeling approaches. *Neuroscientist*, *15*(6), 635-650. https://doi.org/10.1177/1073858409338217
Kundu, P., Benson, B. E., Baldwin, K. L., Rosen, D., Luh, W. M., Bandettini, P. A., Pine, D. S., & Ernst, M. (2015). Robust resting state fMRI processing for studies on typical brain development based on multi-echo EPI acquisition. *Brain Imaging Behav*, *9*(1), 56-73. https://doi.org/10.1007/s11682-014-9346-4
Kundu, P., Brenowitz, N. D., Voon, V., Worbe, Y., Vertes, P. E., Inati, S. J., Saad, Z. S., Bandettini, P. A., & Bullmore, E. T. (2013). Integrated strategy for improving functional connectivity mapping using multiecho fMRI. *Proc Natl Acad Sci U S A*, *110*(40), 16187-16192. https://doi.org/10.1073/pnas.1301725110
Kundu, P., Inati, S. J., Evans, J. W., Luh, W. M., & Bandettini, P. A. (2012). Differentiating BOLD and non-BOLD signals in fMRI time series using multi-echo EPI. *Neuroimage*, *60*(3), 1759-1770. https://doi.org/10.1016/j.neuroimage.2011.12.028
la Fougere, C., Meisenzahl, E., Schmitt, G., Stauss, J., Frodl, T., Tatsch, K., Hahn, K., Moller, H. J., & Dresel, S. (2005). D2 receptor occupancy during high- and low-dose therapy with the atypical

antipsychotic amisulpride: a 123I-iodobenzamide SPECT study. *J Nucl Med*, *46*(6), 1028-1033. https://www.ncbi.nlm.nih.gov/pubmed/15937316
Lahti, A. C., Weiler, M. A., Medoff, D. R., Tamminga, C. A., & Holcomb, H. H. (2005). Functional effects of single dose first- and second-generation antipsychotic administration in subjects with schizophrenia. *Psychiatry Res*, *139*(1), 19-30. https://doi.org/10.1016/j.pscychresns.2005.02.006
Lammertsma, A. A., & Hume, S. P. (1996). Simplified reference tissue model for PET receptor studies. *Neuroimage*, *4*(3 Pt 1), 153-158. https://doi.org/10.1006/nimg.1996.0066
Launay, J. M., Herve, P., Peoc'h, K., Tournois, C., Callebert, J., Nebigil, C. G., Etienne, N., Drouet, L., Humbert, M., Simonneau, G., & Maroteaux, L. (2002). Function of the serotonin 5-hydroxytryptamine 2B receptor in pulmonary hypertension. *Nat Med*, *8*(10), 1129-1135. https://doi.org/10.1038/nm764
Lawrie, S. M. (2022). Do antipsychotic drugs shrink the brain? Probably not. *J Psychopharmacol*, *36*(4), 425-427. https://doi.org/10.1177/02698811221092252
Legind, C. S., Broberg, B. V., Brouwer, R., Mandl, R. C. W., Ebdrup, B. H., Anhoj, S. J., Jensen, M. H., Hilker, R., Fagerlund, B., Hulshoff Pol, H. E., Glenthoj, B. Y., & Rostrup, E. (2019). Heritability of Cerebral Blood Flow and the Correlation to Schizophrenia Spectrum Disorders: A Pseudo-continuous Arterial Spin Labeling Twin Study. *Schizophr Bull*, *45*(6), 1231-1241. https://doi.org/10.1093/schbul/sbz007
Lehmann, H. E., & Hanrahan, G. E. (1954). Chlorpromazine; new inhibiting agent for psychomotor excitement and manic states. *AMA Arch Neurol Psychiatry*, *71*(2), 227-237. https://www.ncbi.nlm.nih.gov/pubmed/13123588
Leucht, S., Cipriani, A., Spineli, L., Mavridis, D., Orey, D., Richter, F., Samara, M., Barbui, C., Engel, R. R., Geddes, J. R., Kissling, W., Stapf, M. P., Lassig, B., Salanti, G., & Davis, J. M. (2013). Comparative efficacy and tolerability of 15 antipsychotic drugs in schizophrenia: a multiple-treatments meta-analysis. *Lancet*, *382*(9896), 951-962. https://doi.org/10.1016/S0140-6736(13)60733-3
Leucht, S., Corves, C., Arbter, D., Engel, R. R., Li, C., & Davis, J. M. (2009). Second-generation versus first-generation antipsychotic drugs for schizophrenia: a meta-analysis. *Lancet*, *373*(9657), 31-41. https://doi.org/10.1016/S0140-6736(08)61764-X
Leucht, S., Kane, J. M., Kissling, W., Hamann, J., Etschel, E., & Engel, R. R. (2005). What does the PANSS mean? *Schizophr Res*, *79*(2-3), 231-238. https://doi.org/10.1016/j.schres.2005.04.008
Leucht, S., Komossa, K., Rummel-Kluge, C., Corves, C., Hunger, H., Schmid, F., Asenjo Lobos, C., Schwarz, S., & Davis, J. M. (2009). A meta-analysis of head-to-head comparisons of second-generation antipsychotics in the treatment of schizophrenia. *Am J Psychiatry*, *166*(2), 152-163. https://doi.org/10.1176/appi.ajp.2008.08030368
Levine, S. Z., & Leucht, S. (2012). Early symptom response to antipsychotic medication as a marker of subsequent symptom change: an eighteen-month follow-up study of recent episode schizophrenia. *Schizophr Res*, *141*(2-3), 168-172. https://doi.org/10.1016/j.schres.2012.08.030
Lieberman, J. A. (2004). Dopamine partial agonists: a new class of antipsychotic. *CNS Drugs*, *18*(4), 251-267. https://doi.org/10.2165/00023210-200418040-00005
Lin, X., Deng, J., Dong, G., Li, S., Wu, P., Sun, H., Liu, L., Shi, J., Fan, Y., Lu, L., & Li, P. (2021). Effects of Chronic Pharmacological Treatment on Functional Brain Network Connectivity in Patients with Schizophrenia. *Psychiatry Res*, *295*, 113338. https://doi.org/10.1016/j.psychres.2020.113338
Linden, D. E., & Fallgatter, A. J. (2009). Neuroimaging in psychiatry: from bench to bedside. *Front Hum Neurosci*, *3*, 49. https://doi.org/10.3389/neuro.09.049.2009
Liu, J., Qiu, M., Constable, R. T., & Wexler, B. E. (2012). Does baseline cerebral blood flow affect task-related blood oxygenation level dependent response in schizophrenia? *Schizophr Res*, *140*(1-3), 143-148. https://doi.org/10.1016/j.schres.2012.06.028
Liu, Y., Beyer, A., & Aebersold, R. (2016). On the Dependency of Cellular Protein Levels on mRNA Abundance. *Cell*, *165*(3), 535-550. https://doi.org/10.1016/j.cell.2016.03.014
Loryan, I., Melander, E., Svensson, M., Payan, M., Konig, F., Jansson, B., & Hammarlund-Udenaes, M. (2016). In-depth neuropharmacokinetic analysis of antipsychotics based on a novel approach to estimate unbound target-site concentration in CNS regions: link to spatial receptor occupancy. *Mol Psychiatry*, *21*(11), 1527-1536. https://doi.org/10.1038/mp.2015.229
Lui, S., Li, T., Deng, W., Jiang, L., Wu, Q., Tang, H., Yue, Q., Huang, X., Chan, R. C., Collier, D. A., Meda, S. A., Pearlson, G., Mechelli, A., Sweeney, J. A., & Gong, Q. (2010). Short-term effects of antipsychotic treatment on cerebral function in drug-naive first-episode schizophrenia revealed by "resting state" functional magnetic resonance imaging. *Arch Gen Psychiatry*, *67*(8), 783-792. https://doi.org/10.1001/archgenpsychiatry.2010.84

Maia, T. V., & Frank, M. J. (2017). An Integrative Perspective on the Role of Dopamine in Schizophrenia. *Biol Psychiatry*, *81*(1), 52-66. https://doi.org/10.1016/j.biopsych.2016.05.021
Mailman, R. B., & Murthy, V. (2010). Third generation antipsychotic drugs: partial agonism or receptor functional selectivity? *Curr Pharm Des*, *16*(5), 488-501. https://doi.org/10.2174/138161210790361461
Mandeville, J. B., Choi, J. K., Jarraya, B., Rosen, B. R., Jenkins, B. G., & Vanduffel, W. (2011). fMRI of cocaine self-administration in macaques reveals functional inhibition of basal ganglia. *Neuropsychopharmacology*, *36*(6), 1187-1198. https://doi.org/10.1038/npp.2011.1
Mandeville, J. B., Sander, C. Y. M., Jenkins, B. G., Hooker, J. M., Catana, C., Vanduffel, W., Alpert, N. M., Rosen, B. R., & Normandin, M. D. (2013). A receptor-based model for dopamine-induced fMRI signal. *Neuroimage*, *75*, 46-57. https://doi.org/10.1016/j.neuroimage.2013.02.036
Marcellino, D., Kehr, J., Agnati, L. F., & Fuxe, K. (2012). Increased affinity of dopamine for D(2) -like versus D(1) -like receptors. Relevance for volume transmission in interpreting PET findings. *Synapse*, *66*(3), 196-203. https://doi.org/10.1002/syn.21501
Markello, R. D., Arnatkeviciute, A., Poline, J. B., Fulcher, B. D., Fornito, A., & Misic, B. (2021). Standardizing workflows in imaging transcriptomics with the abagen toolbox. *Elife*, *10*. https://doi.org/10.7554/eLife.72129
Marota, J. J., Mandeville, J. B., Weisskoff, R. M., Moskowitz, M. A., Rosen, B. R., & Kosofsky, B. E. (2000). Cocaine activation discriminates dopaminergic projections by temporal response: an fMRI study in Rat. *Neuroimage*, *11*(1), 13-23. https://doi.org/10.1006/nimg.1999.0520
Marques, J. P., Kober, T., Krueger, G., van der Zwaag, W., Van de Moortele, P. F., & Gruetter, R. (2010). MP2RAGE, a self bias-field corrected sequence for improved segmentation and T1-mapping at high field. *Neuroimage*, *49*(2), 1271-1281. https://doi.org/10.1016/j.neuroimage.2009.10.002
Martel, A. C., & Galvan, A. (2022). Connectivity of the corticostriatal and thalamostriatal systems in normal and parkinsonian states: An update. *Neurobiol Dis*, *174*, 105878. https://doi.org/10.1016/j.nbd.2022.105878
Martinez, D., Slifstein, M., Broft, A., Mawlawi, O., Hwang, D. R., Huang, Y., Cooper, T., Kegeles, L., Zarahn, E., Abi-Dargham, A., Haber, S. N., & Laruelle, M. (2003). Imaging human mesolimbic dopamine transmission with positron emission tomography. Part II: amphetamine-induced dopamine release in the functional subdivisions of the striatum. *J Cereb Blood Flow Metab*, *23*(3), 285-300. https://doi.org/10.1097/01.WCB.0000048520.34839.1A
Martinot, J. L., Paillere-Martinot, M. L., Poirier, M. F., Dao-Castellana, M. H., Loc'h, C., & Maziere, B. (1996). In vivo characteristics of dopamine D2 receptor occupancy by amisulpride in schizophrenia. *Psychopharmacology (Berl)*, *124*(1-2), 154-158. https://doi.org/10.1007/BF02245616
McColgan, P., Gregory, S., Seunarine, K. K., Razi, A., Papoutsi, M., Johnson, E., Durr, A., Roos, R. A. C., Leavitt, B. R., Holmans, P., Scahill, R. I., Clark, C. A., Rees, G., Tabrizi, S. J., & Track-On, H. D. I. (2018). Brain Regions Showing White Matter Loss in Huntington's Disease Are Enriched for Synaptic and Metabolic Genes. *Biol Psychiatry*, *83*(5), 456-465. https://doi.org/10.1016/j.biopsych.2017.10.019
McCutcheon, R. A., Abi-Dargham, A., & Howes, O. D. (2019). Schizophrenia, Dopamine and the Striatum: From Biology to Symptoms. *Trends Neurosci*, *42*(3), 205-220. https://doi.org/10.1016/j.tins.2018.12.004
McCutcheon, R. A., Brown, K., Nour, M. M., Smith, S. M., Veronese, M., Zelaya, F., Osugo, M., Jauhar, S., Hallett, W., Mehta, M. M., & Howes, O. D. (2021). Dopaminergic organization of striatum is linked to cortical activity and brain expression of genes associated with psychiatric illness. *Sci Adv*, *7*(24). https://doi.org/10.1126/sciadv.abg1512
McCutcheon, R. A., Reis Marques, T., & Howes, O. D. (2020). Schizophrenia-An Overview. *JAMA Psychiatry*, *77*(2), 201-210. https://doi.org/10.1001/jamapsychiatry.2019.3360
Mehta, M. A., McGowan, S. W., Lawrence, A. D., Aitken, M. R., Montgomery, A. J., & Grasby, P. M. (2003). Systemic sulpiride modulates striatal blood flow: relationships to spatial working memory and planning. *Neuroimage*, *20*(4), 1982-1994. https://doi.org/10.1016/j.neuroimage.2003.08.007
Meibohm, B., & Derendorf, H. (1997). Basic concepts of pharmacokinetic/pharmacodynamic (PK/PD) modelling. *Int J Clin Pharmacol Ther*, *35*(10), 401-413. https://www.ncbi.nlm.nih.gov/pubmed/9352388
Meisenzahl, E. M., Schmitt, G., Grunder, G., Dresel, S., Frodl, T., la Fougere, C., Scheuerecker, J., Schwarz, M., Boerner, R., Stauss, J., Hahn, K., & Moller, H. J. (2008). Striatal D2/D3 receptor occupancy, clinical response and side effects with amisulpride: an iodine-123-iodobenzamide SPET study. *Pharmacopsychiatry*, *41*(5), 169-175. https://doi.org/10.1055/s-2008-1076727
Meltzer, H. Y. (1988). New insights into schizophrenia through atypical antipsychotic drugs. *Neuropsychopharmacology*, *1*(3), 193-196. https://doi.org/10.1016/0893-133x(88)90015-2

Metzger, C. D., Wiegers, M., Walter, M., Abler, B., & Graf, H. (2015). Local and Global Resting State Activity in the Noradrenergic and Dopaminergic Pathway Modulated by Reboxetine and Amisulpride in Healthy Subjects. *Int J Neuropsychopharmacol*, *19*(2). https://doi.org/10.1093/ijnp/pyv080

Michels, L., Scherpiet, S., Stampfli, P., Herwig, U., & Bruhl, A. B. (2016). Baseline Perfusion Alterations Due to Acute Application of Quetiapine and Pramipexole in Healthy Adults. *Int J Neuropsychopharmacol*, *19*(11). https://doi.org/10.1093/ijnp/pyw067

Midha, K. K., Chakraborty, B. S., Ganes, D. A., Hawes, E. M., Hubbard, J. W., Keegan, D. L., Korchinski, E. D., & McKay, G. (1989). Intersubject variation in the pharmacokinetics of haloperidol and reduced haloperidol. *J Clin Psychopharmacol*, *9*(2), 98-104. https://doi.org/10.1097/00004714-198904000-00005

Miller, D. D., Andreasen, N. C., O'Leary, D. S., Rezai, K., Watkins, G. L., Ponto, L. L., & Hichwa, R. D. (1997). Effect of antipsychotics on regional cerebral blood flow measured with positron emission tomography. *Neuropsychopharmacology*, *17*(4), 230-240. https://doi.org/10.1016/S0893-133X(97)00042-0

Miller, D. D., Andreasen, N. C., O'Leary, D. S., Watkins, G. L., Boles Ponto, L. L., & Hichwa, R. D. (2001). Comparison of the effects of risperidone and haloperidol on regional cerebral blood flow in schizophrenia. *Biol Psychiatry*, *49*(8), 704-715. https://doi.org/10.1016/s0006-3223(00)01001-5

Modinos, G., Egerton, A., McMullen, K., McLaughlin, A., Kumari, V., Barker, G. J., Williams, S. C. R., & Zelaya, F. (2018). Increased resting perfusion of the hippocampus in high positive schizotypy: A pseudocontinuous arterial spin labeling study. *Hum Brain Mapp*, *39*(10), 4055-4064. https://doi.org/10.1002/hbm.24231

Modinos, G., Simsek, F., Azis, M., Bossong, M., Bonoldi, I., Samson, C., Quinn, B., Perez, J., Broome, M. R., Zelaya, F., Lythgoe, D. J., Howes, O. D., Stone, J. M., Grace, A. A., Allen, P., & McGuire, P. (2018). Prefrontal GABA levels, hippocampal resting perfusion and the risk of psychosis. *Neuropsychopharmacology*, *43*(13), 2652-2659. https://doi.org/10.1038/s41386-017-0004-6

Molina, V., Sanz, J., Reig, S., Martinez, R., Sarramea, F., Luque, R., Benito, C., Gispert, J. D., Pascau, J., & Desco, M. (2005). Hypofrontality in men with first-episode psychosis. *Br J Psychiatry*, *186*, 203-208. https://doi.org/10.1192/bjp.186.3.203

Moncrieff, J., & Leo, J. (2010). A systematic review of the effects of antipsychotic drugs on brain volume. *Psychol Med*, *40*(9), 1409-1422. https://doi.org/10.1017/S0033291709992297

Mouchlianitis, E., McCutcheon, R., & Howes, O. D. (2016). Brain-imaging studies of treatment-resistant schizophrenia: a systematic review. *Lancet Psychiatry*, *3*(5), 451-463. https://doi.org/10.1016/S2215-0366(15)00540-4

Mukherjee, J., Christian, B. T., Dunigan, K. A., Shi, B., Narayanan, T. K., Satter, M., & Mantil, J. (2002). Brain imaging of 18F-fallypride in normal volunteers: blood analysis, distribution, test-retest studies, and preliminary assessment of sensitivity to aging effects on dopamine D-2/D-3 receptors. *Synapse*, *46*(3), 170-188. https://doi.org/10.1002/syn.10128

Mukherjee, J., Yang, Z. Y., Brown, T., Lew, R., Wernick, M., Ouyang, X., Yasillo, N., Chen, C. T., Mintzer, R., & Cooper, M. (1999). Preliminary assessment of extrastriatal dopamine D-2 receptor binding in the rodent and nonhuman primate brains using the high affinity radioligand, 18F-fallypride. *Nucl Med Biol*, *26*(5), 519-527. https://doi.org/10.1016/s0969-8051(99)00012-8

Narendran, R., Mason, N. S., Chen, C. M., Himes, M., Keating, P., May, M. A., Rabiner, E. A., Laruelle, M., Mathis, C. A., & Frankle, W. G. (2011). Evaluation of dopamine D(2)/(3) specific binding in the cerebellum for the positron emission tomography radiotracer [(1)(1)C]FLB 457: implications for measuring cortical dopamine release. *Synapse*, *65*(10), 991-997. https://doi.org/10.1002/syn.20926

Nathan, P. J., Phan, K. L., Harmer, C. J., Mehta, M. A., & Bullmore, E. T. (2014). Increasing pharmacological knowledge about human neurological and psychiatric disorders through functional neuroimaging and its application in drug discovery. *Curr Opin Pharmacol*, *14*, 54-61. https://doi.org/10.1016/j.coph.2013.11.009

Natu, V. S., Gomez, J., Barnett, M., Jeska, B., Kirilina, E., Jaeger, C., Zhen, Z., Cox, S., Weiner, K. S., Weiskopf, N., & Grill-Spector, K. (2019). Apparent thinning of human visual cortex during childhood is associated with myelination. *Proc Natl Acad Sci U S A*, *116*(41), 20750-20759. https://doi.org/10.1073/pnas.1904931116

Navari, S., & Dazzan, P. (2009). Do antipsychotic drugs affect brain structure? A systematic and critical review of MRI findings. *Psychol Med*, *39*(11), 1763-1777. https://doi.org/10.1017/S0033291709005315

Nejad, A. B., Ebdrup, B. H., Glenthoj, B. Y., & Siebner, H. R. (2012). Brain connectivity studies in schizophrenia: unravelling the effects of antipsychotics. *Curr Neuropharmacol*, *10*(3), 219-230. https://doi.org/10.2174/157015912803217305

Nickerson, L. D., Smith, S. M., Ongur, D., & Beckmann, C. F. (2017). Using Dual Regression to Investigate Network Shape and Amplitude in Functional Connectivity Analyses. *Front Neurosci*, *11*, 115. https://doi.org/10.3389/fnins.2017.00115

Nord, M., & Farde, L. (2011). Antipsychotic occupancy of dopamine receptors in schizophrenia. *CNS Neurosci Ther*, *17*(2), 97-103. https://doi.org/10.1111/j.1755-5949.2010.00222.x

Nordquist, R. E., Risterucci, C., Moreau, J. L., von Kienlin, M., Kunnecke, B., Maco, M., Freichel, C., Riemer, C., & Spooren, W. (2008). Effects of aripiprazole/OPC-14597 on motor activity, pharmacological models of psychosis, and brain activity in rats. *Neuropharmacology*, *54*(2), 405-416. https://doi.org/10.1016/j.neuropharm.2007.10.010

O'Brien, K. R., Kober, T., Hagmann, P., Maeder, P., Marques, J., Lazeyras, F., Krueger, G., & Roche, A. (2014). Robust T1-weighted structural brain imaging and morphometry at 7T using MP2RAGE. *PLoS One*, *9*(6), e99676. https://doi.org/10.1371/journal.pone.0099676

Oliveira, I. A. F., Guimaraes, T. M., Souza, R. M., Dos Santos, A. C., Machado-de-Sousa, J. P., Hallak, J. E. C., & Leoni, R. F. (2018). Brain functional and perfusional alterations in schizophrenia: an arterial spin labeling study. *Psychiatry Res Neuroimaging*, *272*, 71-78. https://doi.org/10.1016/j.pscychresns.2017.12.001

Onwordi, E. C., Halff, E. F., Whitehurst, T., Mansur, A., Cotel, M. C., Wells, L., Creeney, H., Bonsall, D., Rogdaki, M., Shatalina, E., Reis Marques, T., Rabiner, E. A., Gunn, R. N., Natesan, S., Vernon, A. C., & Howes, O. D. (2020). Synaptic density marker SV2A is reduced in schizophrenia patients and unaffected by antipsychotics in rats. *Nat Commun*, *11*(1), 246. https://doi.org/10.1038/s41467-019-14122-0

Osimo, E. F., Beck, K., Reis Marques, T., & Howes, O. D. (2019). Synaptic loss in schizophrenia: a meta-analysis and systematic review of synaptic protein and mRNA measures. *Mol Psychiatry*, *24*(4), 549-561. https://doi.org/10.1038/s41380-018-0041-5

Ota, M., Sato, N., Sakai, K., Okazaki, M., Maikusa, N., Hattori, K., Hori, H., Teraishi, T., Shimoji, K., Yamada, K., & Kunugi, H. (2014). Altered coupling of regional cerebral blood flow and brain temperature in schizophrenia compared with bipolar disorder and healthy subjects. *J Cereb Blood Flow Metab*, *34*(12), 1868-1872. https://doi.org/10.1038/jcbfm.2014.151

Overton, D. J., Bhagwat, N., Viviano, J. D., Jacobs, G. R., & Voineskos, A. N. (2020). Identifying psychosis spectrum youth using support vector machines and cerebral blood perfusion as measured by arterial spin labeled fMRI. *Neuroimage Clin*, *27*, 102304. https://doi.org/10.1016/j.nicl.2020.102304

Ozbilen, M., & Adams, C. E. (2009). Systematic overview of Cochrane reviews for anticholinergic effects of antipsychotic drugs. *J Clin Psychopharmacol*, *29*(2), 141-146. https://doi.org/10.1097/JCP.0b013e31819a91f1

Pani, L., & Gessa, G. L. (2002). The substituted benzamides and their clinical potential on dysthymia and on the negative symptoms of schizophrenia. *Mol Psychiatry*, *7*(3), 247-253. https://doi.org/10.1038/sj.mp.4001040

Parkes, L. M., Rashid, W., Chard, D. T., & Tofts, P. S. (2004). Normal cerebral perfusion measurements using arterial spin labeling: reproducibility, stability, and age and gender effects. *Magn Reson Med*, *51*(4), 736-743. https://doi.org/10.1002/mrm.20023

Peralta, V., Cuesta, M. J., Martinez-Larrea, A., & Serrano, J. F. (2000). Differentiating primary from secondary negative symptoms in schizophrenia: a study of neuroleptic-naive patients before and after treatment. *Am J Psychiatry*, *157*(9), 1461-1466. https://doi.org/10.1176/appi.ajp.157.9.1461

Pillinger, T., McCutcheon, R. A., Vano, L., Mizuno, Y., Arumuham, A., Hindley, G., Beck, K., Natesan, S., Efthimiou, O., Cipriani, A., & Howes, O. D. (2020). Comparative effects of 18 antipsychotics on metabolic function in patients with schizophrenia, predictors of metabolic dysregulation, and association with psychopathology: a systematic review and network meta-analysis. *Lancet Psychiatry*, *7*(1), 64-77. https://doi.org/10.1016/S2215-0366(19)30416-X

Pinkham, A., Loughead, J., Ruparel, K., Wu, W. C., Overton, E., Gur, R., & Gur, R. (2011). Resting quantitative cerebral blood flow in schizophrenia measured by pulsed arterial spin labeling perfusion MRI. *Psychiatry Res*, *194*(1), 64-72. https://doi.org/10.1016/j.pscychresns.2011.06.013

Pinkham, A. E., Liu, P., Lu, H., Kriegsman, M., Simpson, C., & Tamminga, C. (2015). Amygdala Hyperactivity at Rest in Paranoid Individuals With Schizophrenia. *Am J Psychiatry*, *172*(8), 784-792. https://doi.org/10.1176/appi.ajp.2014.14081000

Ploeger, B. A., van der Graaf, P. H., & Danhof, M. (2009). Incorporating receptor theory in mechanism-based pharmacokinetic-pharmacodynamic (PK-PD) modeling. *Drug Metab Pharmacokinet*, *24*(1), 3-15. https://doi.org/10.2133/dmpk.24.3

Porras, G., Di Matteo, V., Fracasso, C., Lucas, G., De Deurwaerdere, P., Caccia, S., Esposito, E., & Spampinato, U. (2002). 5-HT2A and 5-HT2C/2B receptor subtypes modulate dopamine release induced in vivo by amphetamine and morphine in both the rat nucleus accumbens and striatum. *Neuropsychopharmacology*, *26*(3), 311-324. https://doi.org/10.1016/S0893-133X(01)00333-5

Potkin, S. G., Kane, J. M., Correll, C. U., Lindenmayer, J. P., Agid, O., Marder, S. R., Olfson, M., & Howes, O. D. (2020). The neurobiology of treatment-resistant schizophrenia: paths to antipsychotic resistance and a roadmap for future research. *NPJ Schizophr*, *6*(1), 1. https://doi.org/10.1038/s41537-019-0090-z

Power, J. D., Mitra, A., Laumann, T. O., Snyder, A. Z., Schlaggar, B. L., & Petersen, S. E. (2014). Methods to detect, characterize, and remove motion artifact in resting state fMRI. *Neuroimage*, *84*, 320-341. https://doi.org/10.1016/j.neuroimage.2013.08.048

Preller, K. H., Duerler, P., Burt, J. B., Ji, J. L., Adkinson, B., Stampfli, P., Seifritz, E., Repovs, G., Krystal, J. H., Murray, J. D., Anticevic, A., & Vollenweider, F. X. (2020). Psilocybin Induces Time-Dependent Changes in Global Functional Connectivity. *Biol Psychiatry*, *88*(2), 197-207. https://doi.org/10.1016/j.biopsych.2019.12.027

Prince, J. A., Blennow, K., Gottfries, C. G., Karlsson, I., & Oreland, L. (1999). Mitochondrial function is differentially altered in the basal ganglia of chronic schizophrenics. *Neuropsychopharmacology*, *21*(3), 372-379. https://doi.org/10.1016/S0893-133X(99)00016-0

Puech, A., Fleurot, O., & Rein, W. (1998). Amisulpride, and atypical antipsychotic, in the treatment of acute episodes of schizophrenia: a dose-ranging study vs. haloperidol. The Amisulpride Study Group. *Acta Psychiatr Scand*, *98*(1), 65-72. https://doi.org/10.1111/j.1600-0447.1998.tb10044.x

Rajasekaran, A., Venkatasubramanian, G., Berk, M., & Debnath, M. (2015). Mitochondrial dysfunction in schizophrenia: pathways, mechanisms and implications. *Neurosci Biobehav Rev*, *48*, 10-21. https://doi.org/10.1016/j.neubiorev.2014.11.005

Richiardi, J., Altmann, A., Milazzo, A. C., Chang, C., Chakravarty, M. M., Banaschewski, T., Barker, G. J., Bokde, A. L., Bromberg, U., Buchel, C., Conrod, P., Fauth-Buhler, M., Flor, H., Frouin, V., Gallinat, J., Garavan, H., Gowland, P., Heinz, A., Lemaitre, H., . . . consortium, I. (2015). BRAIN NETWORKS. Correlated gene expression supports synchronous activity in brain networks. *Science*, *348*(6240), 1241-1244. https://doi.org/10.1126/science.1255905

Riederer, I., Bohn, K. P., Preibisch, C., Wiedemann, E., Zimmer, C., Alexopoulos, P., & Forster, S. (2018). Alzheimer Disease and Mild Cognitive Impairment: Integrated Pulsed Arterial Spin-Labeling MRI and (18)F-FDG PET. *Radiology*, *288*(1), 198-206. https://doi.org/10.1148/radiol.2018170575

Ritchie, J., Pantazatos, S. P., & French, L. (2018). Transcriptomic characterization of MRI contrast with focus on the T1-w/T2-w ratio in the cerebral cortex. *Neuroimage*, *174*, 504-517. https://doi.org/10.1016/j.neuroimage.2018.03.027

Rizzo, G., Veronese, M., Expert, P., Turkheimer, F. E., & Bertoldo, A. (2016). MENGA: A New Comprehensive Tool for the Integration of Neuroimaging Data and the Allen Human Brain Transcriptome Atlas. *PLoS One*, *11*(2), e0148744. https://doi.org/10.1371/journal.pone.0148744

Rizzo, G., Veronese, M., Heckemann, R. A., Selvaraj, S., Howes, O. D., Hammers, A., Turkheimer, F. E., & Bertoldo, A. (2014). The predictive power of brain mRNA mappings for in vivo protein density: a positron emission tomography correlation study. *J Cereb Blood Flow Metab*, *34*(5), 827-835. https://doi.org/10.1038/jcbfm.2014.21

Rizzo, G., Veronese, M., Tonietto, M., Zanotti-Fregonara, P., Turkheimer, F. E., & Bertoldo, A. (2014). Kinetic modeling without accounting for the vascular component impairs the quantification of [(11)C]PBR28 brain PET data. *J Cereb Blood Flow Metab*, *34*(6), 1060-1069. https://doi.org/10.1038/jcbfm.2014.55

Rodda, K. E., Dean, B., McIntyre, I. M., & Drummer, O. H. (2006). Brain distribution of selected antipsychotics in schizophrenia. *Forensic Sci Int*, *157*(2-3), 121-130. https://doi.org/10.1016/j.forsciint.2005.03.017

Rogeau, A., Nordio, G., Veronese, M., Brown, K., Nour, M. M., Osugo, M., Jauhar, S., Howes, O. D., & McCutcheon, R. A. (2022). The relationship between glutamate, dopamine, and cortical gray matter: A simultaneous PET-MR study. *Mol Psychiatry*, *27*(8), 3493-3500. https://doi.org/10.1038/s41380-022-01596-6

Romero-Garcia, R., Whitaker, K. J., Vasa, F., Seidlitz, J., Shinn, M., Fonagy, P., Dolan, R. J., Jones, P. B., Goodyer, I. M., Consortium, N., Bullmore, E. T., & Vertes, P. E. (2018). Structural covariance

networks are coupled to expression of genes enriched in supragranular layers of the human cortex. *Neuroimage*, *171*, 256-267. https://doi.org/10.1016/j.neuroimage.2017.12.060

Romme, I. A., de Reus, M. A., Ophoff, R. A., Kahn, R. S., & van den Heuvel, M. P. (2017). Connectome Disconnectivity and Cortical Gene Expression in Patients With Schizophrenia. *Biol Psychiatry*, *81*(6), 495-502. https://doi.org/10.1016/j.biopsych.2016.07.012

Rubio, J. M., Malhotra, A. K., & Kane, J. M. (2021). Towards a framework to develop neuroimaging biomarkers of relapse in schizophrenia. *Behav Brain Res*, *402*, 113099. https://doi.org/10.1016/j.bbr.2020.113099

Sabaroedin, K., Tiego, J., & Fornito, A. (2023). Circuit-Based Approaches to Understanding Corticostriatothalamic Dysfunction Across the Psychosis Continuum. *Biol Psychiatry*, *93*(2), 113-124. https://doi.org/10.1016/j.biopsych.2022.07.017

Sagi, Y., Tavor, I., Hofstetter, S., Tzur-Moryosef, S., Blumenfeld-Katzir, T., & Assaf, Y. (2012). Learning in the fast lane: new insights into neuroplasticity. *Neuron*, *73*(6), 1195-1203. https://doi.org/10.1016/j.neuron.2012.01.025

Salgado-Pineda, P., Delaveau, P., Falcon, C., & Blin, O. (2006). Brain T1 intensity changes after levodopa administration in healthy subjects: a voxel-based morphometry study. *Br J Clin Pharmacol*, *62*(5), 546-551. https://doi.org/10.1111/j.1365-2125.2006.02695.x

Sambataro, F., Blasi, G., Fazio, L., Caforio, G., Taurisano, P., Romano, R., Di Giorgio, A., Gelao, B., Lo Bianco, L., Papazacharias, A., Popolizio, T., Nardini, M., & Bertolino, A. (2010). Treatment with olanzapine is associated with modulation of the default mode network in patients with Schizophrenia. *Neuropsychopharmacology*, *35*(4), 904-912. https://doi.org/10.1038/npp.2009.192

Sander, C. Y., Hooker, J. M., Catana, C., Normandin, M. D., Alpert, N. M., Knudsen, G. M., Vanduffel, W., Rosen, B. R., & Mandeville, J. B. (2013). Neurovascular coupling to D2/D3 dopamine receptor occupancy using simultaneous PET/functional MRI. *Proc Natl Acad Sci U S A*, *110*(27), 11169-11174. https://doi.org/10.1073/pnas.1220512110

Sander, C. Y., Hooker, J. M., Catana, C., Rosen, B. R., & Mandeville, J. B. (2016). Imaging Agonist-Induced D2/D3 Receptor Desensitization and Internalization In Vivo with PET/fMRI. *Neuropsychopharmacology*, *41*(5), 1427-1436. https://doi.org/10.1038/npp.2015.296

Sarpal, D. K., Argyelan, M., Robinson, D. G., Szeszko, P. R., Karlsgodt, K. H., John, M., Weissman, N., Gallego, J. A., Kane, J. M., Lencz, T., & Malhotra, A. K. (2016). Baseline Striatal Functional Connectivity as a Predictor of Response to Antipsychotic Drug Treatment. *Am J Psychiatry*, *173*(1), 69-77. https://doi.org/10.1176/appi.ajp.2015.14121571

Sarpal, D. K., Lencz, T., & Malhotra, A. K. (2016). In Support of Neuroimaging Biomarkers of Treatment Response in First-Episode Schizophrenia. *Am J Psychiatry*, *173*(7), 732-733. https://doi.org/10.1176/appi.ajp.2016.16030320

Sarpal, D. K., Robinson, D. G., Lencz, T., Argyelan, M., Ikuta, T., Karlsgodt, K., Gallego, J. A., Kane, J. M., Szeszko, P. R., & Malhotra, A. K. (2015). Antipsychotic treatment and functional connectivity of the striatum in first-episode schizophrenia. *JAMA Psychiatry*, *72*(1), 5-13. https://doi.org/10.1001/jamapsychiatry.2014.1734

Schobel, S. A., Chaudhury, N. H., Khan, U. A., Paniagua, B., Styner, M. A., Asllani, I., Inbar, B. P., Corcoran, C. M., Lieberman, J. A., Moore, H., & Small, S. A. (2013). Imaging patients with psychosis and a mouse model establishes a spreading pattern of hippocampal dysfunction and implicates glutamate as a driver. *Neuron*, *78*(1), 81-93. https://doi.org/10.1016/j.neuron.2013.02.011

Schoemaker, H., Claustre, Y., Fage, D., Rouquier, L., Chergui, K., Curet, O., Oblin, A., Gonon, F., Carter, C., Benavides, J., & Scatton, B. (1997). Neurochemical characteristics of amisulpride, an atypical dopamine D2/D3 receptor antagonist with both presynaptic and limbic selectivity. *J Pharmacol Exp Ther*, *280*(1), 83-97. https://www.ncbi.nlm.nih.gov/pubmed/8996185

Schwarz, A. J., Becerra, L., Upadhyay, J., Anderson, J., Baumgartner, R., Coimbra, A., Evelhoch, J., Hargreaves, R., Robertson, B., Iyengar, S., Tauscher, J., Bleakman, D., & Borsook, D. (2011). A procedural framework for good imaging practice in pharmacological fMRI studies applied to drug development #1: processes and requirements. *Drug Discov Today*, *16*(13-14), 583-593. https://doi.org/10.1016/j.drudis.2011.05.006

Schwarz, A. J., Zocchi, A., Reese, T., Gozzi, A., Garzotti, M., Varnier, G., Curcuruto, O., Sartori, I., Girlanda, E., Biscaro, B., Crestan, V., Bertani, S., Heidbreder, C., & Bifone, A. (2004). Concurrent pharmacological MRI and in situ microdialysis of cocaine reveal a complex relationship between the central hemodynamic response and local dopamine concentration. *Neuroimage*, *23*(1), 296-304. https://doi.org/10.1016/j.neuroimage.2004.05.001

Sekhar, G. N., Fleckney, A. L., Boyanova, S. T., Rupawala, H., Lo, R., Wang, H., Farag, D. B., Rahman, K. M., Broadstock, M., Reeves, S., & Thomas, S. A. (2019). Region-specific blood-brain barrier transporter changes leads to increased sensitivity to amisulpride in Alzheimer's disease. *Fluids Barriers CNS*, *16*(1), 38. https://doi.org/10.1186/s12987-019-0158-1

Selvaggi, P., Hawkins, P. C. T., Dipasquale, O., Rizzo, G., Bertolino, A., Dukart, J., Sambataro, F., Pergola, G., Williams, S. C. R., Turkheimer, F., Zelaya, F., Veronese, M., & Mehta, M. A. (2019). Increased cerebral blood flow after single dose of antipsychotics in healthy volunteers depends on dopamine D2 receptor density profiles. *Neuroimage*, *188*, 774-784. https://doi.org/10.1016/j.neuroimage.2018.12.028

Selvaggi, P., Jauhar, S., Kotoula, V., Pepper, F., Veronese, M., Santangelo, B., Zelaya, F., Turkheimer, F. E., Mehta, M. A., & Howes, O. D. (2022). Reduced cortical cerebral blood flow in antipsychotic-free first-episode psychosis and relationship to treatment response. *Psychol Med*, 1-11. https://doi.org/10.1017/S0033291722002288

Selvaggi, P., Rizzo, G., Mehta, M. A., Turkheimer, F. E., & Veronese, M. (2021). Integration of human whole-brain transcriptome and neuroimaging data: Practical considerations of current available methods. *J Neurosci Methods*, *355*, 109128. https://doi.org/10.1016/j.jneumeth.2021.109128

Shcherbinin, S., Doyle, O., Zelaya, F. O., de Simoni, S., Mehta, M. A., & Schwarz, A. J. (2015). Modulatory effects of ketamine, risperidone and lamotrigine on resting brain perfusion in healthy human subjects. *Psychopharmacology (Berl)*, *232*(21-22), 4191-4204. https://doi.org/10.1007/s00213-015-4021-z

Shen, E. H., Overly, C. C., & Jones, A. R. (2012). The Allen Human Brain Atlas: comprehensive gene expression mapping of the human brain. *Trends Neurosci*, *35*(12), 711-714. https://doi.org/10.1016/j.tins.2012.09.005

Shin, J., French, L., Xu, T., Leonard, G., Perron, M., Pike, G. B., Richer, L., Veillette, S., Pausova, Z., & Paus, T. (2018). Cell-Specific Gene-Expression Profiles and Cortical Thickness in the Human Brain. *Cereb Cortex*, *28*(9), 3267-3277. https://doi.org/10.1093/cercor/bhx197

Slifstein, M., Kegeles, L. S., Xu, X., Thompson, J. L., Urban, N., Castrillon, J., Hackett, E., Bae, S. A., Laruelle, M., & Abi-Dargham, A. (2010). Striatal and extrastriatal dopamine release measured with PET and [(18)F] fallypride. *Synapse*, *64*(5), 350-362. https://doi.org/10.1002/syn.20734

Smart, K., Gallezot, J. D., Nabulsi, N., Labaree, D., Zheng, M. Q., Huang, Y., Carson, R. E., Hillmer, A. T., & Worhunsky, P. D. (2020). Separating dopamine D(2) and D(3) receptor sources of [(11)C]-(+)-PHNO binding potential: Independent component analysis of competitive binding. *Neuroimage*, *214*, 116762. https://doi.org/10.1016/j.neuroimage.2020.116762

Smieskova, R., Fusar-Poli, P., Allen, P., Bendfeldt, K., Stieglitz, R. D., Drewe, J., Radue, E. W., McGuire, P. K., Riecher-Rossler, A., & Borgwardt, S. J. (2009). The effects of antipsychotics on the brain: what have we learnt from structural imaging of schizophrenia?--a systematic review. *Curr Pharm Des*, *15*(22), 2535-2549. https://doi.org/10.2174/138161209788957456

Smith, D. V., Utevsky, A. V., Bland, A. R., Clement, N., Clithero, J. A., Harsch, A. E., McKell Carter, R., & Huettel, S. A. (2014). Characterizing individual differences in functional connectivity using dual-regression and seed-based approaches. *Neuroimage*, *95*, 1-12. https://doi.org/10.1016/j.neuroimage.2014.03.042

Smith, S. M. (2002). Fast robust automated brain extraction. *Hum Brain Mapp*, *17*(3), 143-155. https://doi.org/10.1002/hbm.10062

Smith, S. M., & Nichols, T. E. (2009). Threshold-free cluster enhancement: addressing problems of smoothing, threshold dependence and localisation in cluster inference. *Neuroimage*, *44*(1), 83-98. https://doi.org/10.1016/j.neuroimage.2008.03.061

Snitz, B. E., MacDonald, A., 3rd, Cohen, J. D., Cho, R. Y., Becker, T., & Carter, C. S. (2005). Lateral and medial hypofrontality in first-episode schizophrenia: functional activity in a medication-naive state and effects of short-term atypical antipsychotic treatment. *Am J Psychiatry*, *162*(12), 2322-2329. https://doi.org/10.1176/appi.ajp.162.12.2322

Snyder, S. H. (1976). The dopamine hypothesis of schizophrenia: focus on the dopamine receptor. *Am J Psychiatry*, *133*(2), 197-202. https://doi.org/10.1176/ajp.133.2.197

Sparshatt, A., Taylor, D., Patel, M. X., & Kapur, S. (2009). Amisulpride - dose, plasma concentration, occupancy and response: implications for therapeutic drug monitoring. *Acta Psychiatr Scand*, *120*(6), 416-428. https://doi.org/10.1111/j.1600-0447.2009.01429.x

Stamford, J. A., Kruk, Z. L., & Millar, J. (1988). Actions of dopamine antagonists on stimulated striatal and limbic dopamine release: an in vivo voltammetric study. *Br J Pharmacol*, *94*(3), 924-932. https://doi.org/10.1111/j.1476-5381.1988.tb11605.x

Stone, J. M., Davis, J. M., Leucht, S., & Pilowsky, L. S. (2009). Cortical dopamine D2/D3 receptors are a common site of action for antipsychotic drugs--an original patient data meta-analysis of the SPECT and PET in vivo receptor imaging literature. *Schizophr Bull*, *35*(4), 789-797. https://doi.org/10.1093/schbul/sbn009

Sukumar, N., Sabesan, P., Anazodo, U., & Palaniyappan, L. (2020). Neurovascular Uncoupling in Schizophrenia: A Bimodal Meta-Analysis of Brain Perfusion and Glucose Metabolism. *Front Psychiatry*, *11*, 754. https://doi.org/10.3389/fpsyt.2020.00754

Tauscher, J., Hussain, T., Agid, O., Verhoeff, N. P., Wilson, A. A., Houle, S., Remington, G., Zipursky, R. B., & Kapur, S. (2004). Equivalent occupancy of dopamine D1 and D2 receptors with clozapine: differentiation from other atypical antipsychotics. *Am J Psychiatry*, *161*(9), 1620-1625. https://doi.org/10.1176/appi.ajp.161.9.1620

Taylor, D., Barnes, T. R. E., & Young, A. (2021). *The Maudsley prescribing guidelines in psychiatry* (Fourteenth edition. ed.). Wiley Blackwell.

Tost, H., Braus, D. F., Hakimi, S., Ruf, M., Vollmert, C., Hohn, F., & Meyer-Lindenberg, A. (2010). Acute D2 receptor blockade induces rapid, reversible remodeling in human cortical-striatal circuits. *Nat Neurosci*, *13*(8), 920-922. https://doi.org/10.1038/nn.2572

Tregellas, J. R. (2014). Neuroimaging biomarkers for early drug development in schizophrenia. *Biol Psychiatry*, *76*(2), 111-119. https://doi.org/10.1016/j.biopsych.2013.08.025

Turkheimer, F. E., Selvaggi, P., Mehta, M. A., Veronese, M., Zelaya, F., Dazzan, P., & Vernon, A. C. (2020). Normalizing the Abnormal: Do Antipsychotic Drugs Push the Cortex Into an Unsustainable Metabolic Envelope? *Schizophr Bull*, *46*(3), 484-495. https://doi.org/10.1093/schbul/sbz119

Tziortzi, A. C., Haber, S. N., Searle, G. E., Tsoumpas, C., Long, C. J., Shotbolt, P., Douaud, G., Jbabdi, S., Behrens, T. E., Rabiner, E. A., Jenkinson, M., & Gunn, R. N. (2014). Connectivity-based functional analysis of dopamine release in the striatum using diffusion-weighted MRI and positron emission tomography. *Cereb Cortex*, *24*(5), 1165-1177. https://doi.org/10.1093/cercor/bhs397

Tziortzi, A. C., Searle, G. E., Tzimopoulou, S., Salinas, C., Beaver, J. D., Jenkinson, M., Laruelle, M., Rabiner, E. A., & Gunn, R. N. (2011). Imaging dopamine receptors in humans with [11C]-(+)-PHNO: dissection of D3 signal and anatomy. *Neuroimage*, *54*(1), 264-277. https://doi.org/10.1016/j.neuroimage.2010.06.044

Uchida, H., Takeuchi, H., Graff-Guerrero, A., Suzuki, T., Watanabe, K., & Mamo, D. C. (2011). Dopamine D2 receptor occupancy and clinical effects: a systematic review and pooled analysis. *J Clin Psychopharmacol*, *31*(4), 497-502. https://doi.org/10.1097/JCP.0b013e3182214aad

Ullmer, C., Schmuck, K., Kalkman, H. O., & Lubbert, H. (1995). Expression of serotonin receptor mRNAs in blood vessels. *FEBS Lett*, *370*(3), 215-221. https://doi.org/10.1016/0014-5793(95)00828-w

van Erp, T. G. M., Walton, E., Hibar, D. P., Schmaal, L., Jiang, W., Glahn, D. C., Pearlson, G. D., Yao, N., Fukunaga, M., Hashimoto, R., Okada, N., Yamamori, H., Bustillo, J. R., Clark, V. P., Agartz, I., Mueller, B. A., Cahn, W., de Zwarte, S. M. C., Hulshoff Pol, H. E., . . . Turner, J. A. (2018). Cortical Brain Abnormalities in 4474 Individuals With Schizophrenia and 5098 Control Subjects via the Enhancing Neuro Imaging Genetics Through Meta Analysis (ENIGMA) Consortium. *Biol Psychiatry*, *84*(9), 644-654. https://doi.org/10.1016/j.biopsych.2018.04.023

van Veelen, N. M., Vink, M., Ramsey, N. F., van Buuren, M., Hoogendam, J. M., & Kahn, R. S. (2011). Prefrontal lobe dysfunction predicts treatment response in medication-naive first-episode schizophrenia. *Schizophr Res*, *129*(2-3), 156-162. https://doi.org/10.1016/j.schres.2011.03.026

Vasa, F., Seidlitz, J., Romero-Garcia, R., Whitaker, K. J., Rosenthal, G., Vertes, P. E., Shinn, M., Alexander-Bloch, A., Fonagy, P., Dolan, R. J., Jones, P. B., Goodyer, I. M., consortium, N., Sporns, O., & Bullmore, E. T. (2018). Adolescent Tuning of Association Cortex in Human Structural Brain Networks. *Cereb Cortex*, *28*(1), 281-294. https://doi.org/10.1093/cercor/bhx249

Vernaleken, I., Peters, L., Raptis, M., Lin, R., Buchholz, H. G., Zhou, Y., Winz, O., Rosch, F., Bartenstein, P., Wong, D. F., Schafer, W. M., & Grunder, G. (2011). The applicability of SRTM in [(18)F]fallypride PET investigations: impact of scan durations. *J Cereb Blood Flow Metab*, *31*(9), 1958-1966. https://doi.org/10.1038/jcbfm.2011.73

Vernaleken, I., Siessmeier, T., Buchholz, H. G., Hartter, S., Hiemke, C., Stoeter, P., Rosch, F., Bartenstein, P., & Grunder, G. (2004). High striatal occupancy of D2-like dopamine receptors by amisulpride in the brain of patients with schizophrenia. *Int J Neuropsychopharmacol*, *7*(4), 421-430. https://doi.org/10.1017/S1461145704004353

Vernon, A. C., Crum, W. R., Lerch, J. P., Chege, W., Natesan, S., Modo, M., Cooper, J. D., Williams, S. C., & Kapur, S. (2014). Reduced cortical volume and elevated astrocyte density in rats chronically

treated with antipsychotic drugs-linking magnetic resonance imaging findings to cellular pathology. *Biol Psychiatry*, *75*(12), 982-990. https://doi.org/10.1016/j.biopsych.2013.09.012

Vernon, A. C., Natesan, S., Crum, W. R., Cooper, J. D., Modo, M., Williams, S. C., & Kapur, S. (2012). Contrasting effects of haloperidol and lithium on rodent brain structure: a magnetic resonance imaging study with postmortem confirmation. *Biol Psychiatry*, *71*(10), 855-863. https://doi.org/10.1016/j.biopsych.2011.12.004

Vernon, A. C., Natesan, S., Modo, M., & Kapur, S. (2011). Effect of chronic antipsychotic treatment on brain structure: a serial magnetic resonance imaging study with ex vivo and postmortem confirmation. *Biol Psychiatry*, *69*(10), 936-944. https://doi.org/10.1016/j.biopsych.2010.11.010

Veronese, M., Santangelo, B., Jauhar, S., D'Ambrosio, E., Demjaha, A., Salimbeni, H., Huajie, J., McCrone, P., Turkheimer, F., & Howes, O. (2021). A potential biomarker for treatment stratification in psychosis: evaluation of an [(18)F] FDOPA PET imaging approach. *Neuropsychopharmacology*, *46*(6), 1122-1132. https://doi.org/10.1038/s41386-020-00866-7

Veronese, M., Zanotti-Fregonara, P., Rizzo, G., Bertoldo, A., Innis, R. B., & Turkheimer, F. E. (2016). Measuring specific receptor binding of a PET radioligand in human brain without pharmacological blockade: The genomic plot. *Neuroimage*, *130*, 1-12. https://doi.org/10.1016/j.neuroimage.2016.01.058

Vertes, P. E., Rittman, T., Whitaker, K. J., Romero-Garcia, R., Vasa, F., Kitzbichler, M. G., Wagstyl, K., Fonagy, P., Dolan, R. J., Jones, P. B., Goodyer, I. M., Consortium, N., & Bullmore, E. T. (2016). Gene transcription profiles associated with inter-modular hubs and connection distance in human functional magnetic resonance imaging networks. *Philos Trans R Soc Lond B Biol Sci*, *371*(1705). https://doi.org/10.1098/rstb.2015.0362

Viviani, R., Abler, B., Seeringer, A., & Stingl, J. C. (2012). Effect of paroxetine and bupropion on human resting brain perfusion: an arterial spin labeling study. *Neuroimage*, *61*(4), 773-779. https://doi.org/10.1016/j.neuroimage.2012.03.014

Viviani, R., Graf, H., Wiegers, M., & Abler, B. (2013). Effects of amisulpride on human resting cerebral perfusion. *Psychopharmacology (Berl)*, *229*(1), 95-103. https://doi.org/10.1007/s00213-013-3091-z

Viviani, R., Sim, E. J., Lo, H., Richter, S., Haffer, S., Osterfeld, N., Thone, J., & Beschoner, P. (2009). Components of variance in brain perfusion and the design of studies of individual differences: the baseline study. *Neuroimage*, *46*(1), 12-22. https://doi.org/10.1016/j.neuroimage.2009.01.041

Voineskos, A. N., Mulsant, B. H., Dickie, E. W., Neufeld, N. H., Rothschild, A. J., Whyte, E. M., Meyers, B. S., Alexopoulos, G. S., Hoptman, M. J., Lerch, J. P., & Flint, A. J. (2020). Effects of Antipsychotic Medication on Brain Structure in Patients With Major Depressive Disorder and Psychotic Features: Neuroimaging Findings in the Context of a Randomized Placebo-Controlled Clinical Trial. *JAMA Psychiatry*, *77*(7), 674-683. https://doi.org/10.1001/jamapsychiatry.2020.0036

Vollenweider, F. X., Vollenweider-Scherpenhuyzen, M. F., Babler, A., Vogel, H., & Hell, D. (1998). Psilocybin induces schizophrenia-like psychosis in humans via a serotonin-2 agonist action. *Neuroreport*, *9*(17), 3897-3902. https://doi.org/10.1097/00001756-199812010-00024

Wall, N. R., De La Parra, M., Callaway, E. M., & Kreitzer, A. C. (2013). Differential innervation of direct- and indirect-pathway striatal projection neurons. *Neuron*, *79*(2), 347-360. https://doi.org/10.1016/j.neuron.2013.05.014

Wang, Z., Wang, J., Connick, T. J., Wetmore, G. S., & Detre, J. A. (2005). Continuous ASL (CASL) perfusion MRI with an array coil and parallel imaging at 3T. *Magn Reson Med*, *54*(3), 732-737. https://doi.org/10.1002/mrm.20574

Weinberger, D. R., & Berman, K. F. (1988). Speculation on the meaning of cerebral metabolic hypofrontality in schizophrenia. *Schizophr Bull*, *14*(2), 157-168. https://doi.org/10.1093/schbul/14.2.157

Weinberger, D. R., & Radulescu, E. (2016). Finding the Elusive Psychiatric "Lesion" With 21st-Century Neuroanatomy: A Note of Caution. *Am J Psychiatry*, *173*(1), 27-33. https://doi.org/10.1176/appi.ajp.2015.15060753

Weinberger, D. R., & Radulescu, E. (2021). Structural Magnetic Resonance Imaging All Over Again. *JAMA Psychiatry*, *78*(1), 11-12. https://doi.org/10.1001/jamapsychiatry.2020.1941

Winkler, A. M., Ridgway, G. R., Webster, M. A., Smith, S. M., & Nichols, T. E. (2014). Permutation inference for the general linear model. *Neuroimage*, *92*(100), 381-397. https://doi.org/10.1016/j.neuroimage.2014.01.060

Wong, N. M., Dipasquale, O., Turkheimer, F., Findon, J. L., Wichers, R. H., Dimitrov, M., Murphy, C. M., Stoencheva, V., Robertson, D. M., Murphy, D. G., Daly, E., & McAlonan, G. M. (2022). Differences in social brain function in autism spectrum disorder are linked to the serotonin transporter: A randomised placebo-controlled single-dose crossover trial. *J Psychopharmacol*, *36*(6), 723-731. https://doi.org/10.1177/02698811221092509

World Health Organization, S., World Health, O., World Health, O., World Health, O., & ProQuest. (1992). *The ICD-10 classification of mental and behavioural disorders : clinical descriptions and diagnostic guidelines*. World Health Organization. http://catalogue.londonmet.ac.uk/record=b1683372~S1

Wulff, S., Pinborg, L. H., Svarer, C., Jensen, L. T., Nielsen, M. O., Allerup, P., Bak, N., Rasmussen, H., Frandsen, E., Rostrup, E., & Glenthoj, B. Y. (2015). Striatal D(2/3) Binding Potential Values in Drug-Naive First-Episode Schizophrenia Patients Correlate With Treatment Outcome. *Schizophr Bull*, *41*(5), 1143-1152. https://doi.org/10.1093/schbul/sbu220

Wylie, K. P., Smucny, J., Legget, K. T., & Tregellas, J. R. (2016). Targeting Functional Biomarkers in Schizophrenia with Neuroimaging. *Curr Pharm Des*, *22*(14), 2117-2123. https://doi.org/10.2174/1381612822666160127113912

Zhu, J., Zhuo, C., Xu, L., Liu, F., Qin, W., & Yu, C. (2017). Altered Coupling Between Resting-State Cerebral Blood Flow and Functional Connectivity in Schizophrenia. *Schizophr Bull*, *43*(6), 1363-1374. https://doi.org/10.1093/schbul/sbx051

Appendix A (Selvaggi et al., Neuroimage, 2019)

NeuroImage 188 (2019) 774–784

Contents lists available at ScienceDirect

NeuroImage

journal homepage: www.elsevier.com/locate/neuroimage

Increased cerebral blood flow after single dose of antipsychotics in healthy volunteers depends on dopamine D2 receptor density profiles

Pierluigi Selvaggi [a,*], Peter C.T. Hawkins [a], Ottavia Dipasquale [a], Gaia Rizzo [b,c], Alessandro Bertolino [d], Juergen Dukart [e], Fabio Sambataro [f], Giulio Pergola [d], Steven C.R. Williams [a], Federico Turkheimer [a], Fernando Zelaya [a], Mattia Veronese [a,1], Mitul A. Mehta [a,1]

[a] Department of Neuroimaging, Institute of Psychiatry, Psychology and Neuroscience, King's College London, SE5 8AF, London, United Kingdom
[b] Invicro, W12 0NN, London, UK
[c] Division of Brain Sciences, Department of Medicine, Imperial College London, SW72AZ, London, UK
[d] Department of Basic Medical Science, Neuroscience and Sense Organs, University of Bari Aldo Moro, IT-70124, Bari, BA, Italy
[e] F. Hoffmann-La Roche, Pharma Research Early Development, Roche Innovation Centre Basel, CH-4070, Basel, Switzerland
[f] Department of Experimental and Clinical Medical Sciences, University of Udine, IT-33100, Udine, Italy

ARTICLE INFO

Keywords:
CBF
Antipsychotics
ASL
PET
D_2R
mRNA expression
DRD2

ABSTRACT

As a result of neuro-vascular coupling, the functional effects of antipsychotics in human brain have been investigated in both healthy and clinical populations using haemodynamic markers such as regional Cerebral Blood Flow (rCBF). However, the relationship between observed haemodynamic effects and the pharmacological action of these drugs has not been fully established. Here, we analysed Arterial Spin Labelling (ASL) rCBF data from a placebo-controlled study in healthy volunteers, who received a single dose of three different D2 receptor (D_2R) antagonists and tested the association of the main effects of the drugs on rCBF against normative population maps of D_2R protein density and gene-expression data. In particular, we correlated CBF changes after antipsychotic administration with non-displaceable binding potential (BP_{ND}) template maps of the high affinity D_2-antagonist Positron Emission Tomography (PET) ligand [^{18}F]Fallypride and with brain post-mortem microarray mRNA expression data for the *DRD2* gene from the Allen Human Brain Atlas (ABA). For all antipsychotics, rCBF changes were directly proportional to brain D_2R densities and *DRD2* mRNA expression measures, although PET BP_{ND} spatial profiles explained more variance as compared with mRNA profiles (PET R^2 range = 0.20–0.60, mRNA PET R^2 range 0.04–0.20, pairwise-comparisons all $p_{corrected}<0.05$). In addition, the spatial coupling between ΔCBF and D_2R profiles varied between the different antipsychotics tested, possibly reflecting differential affinities. Overall, these results indicate that the functional effects of antipsychotics as measured with rCBF are tightly correlated with the distribution of their target receptors in striatal and extra-striatal regions. Our results further demonstrate the link between neurotransmitter targets and haemodynamic changes reinforcing rCBF as a robust in-vivo marker of drug effects. This work is important in bridging the gap between pharmacokinetic and pharmacodynamics of novel and existing compounds.

1. Introduction

Antipsychotics are still the preferred choice for the treatment of conditions such as schizophrenia and other mental health disorders with psychotic features (Stroup et al., 2009). The main target of most of these compounds is the dopamine D_2 receptor (D_2R) (Burt et al., 1977; Farde et al., 1986) where they act as antagonists or partial agonists. D_2R occupancy of antipsychotics has been assessed *in vivo* with emission tomography in healthy controls and clinical populations (Agid et al., 2007; Kapur et al., 1995; Nyberg et al., 1995) and it has also been linked with

* Corresponding author. Centre for Neuroimaging Sciences, Institute of Psychiatry, Psychology & Neuroscience, King's College London, De Crespigny Park, SE5 8AF, London, UK.
E-mail address: pierluigi.selvaggi@kcl.ac.uk (P. Selvaggi).
[1] Designated equal contribution as senior author.

https://doi.org/10.1016/j.neuroimage.2018.12.028
Received 8 June 2018; Received in revised form 5 December 2018; Accepted 12 December 2018
Available online 13 December 2018

treatment response (Kapur et al., 2000). While antipsychotics have been well characterized in terms of their pharmacokinetics (PK) and clinical response, their impact on brain physiology and function is still not well understood. A deeper understanding of these effects is crucial to uncover biological mechanisms driving their clinical efficacy as well as their side effects.

Functional effects of antipsychotics in the brain have been investigated using different neuroimaging tools. Seminal work using Positron Emission Tomography (PET) [^{18}F]fluorodeoxyglucose and [^{15}O]H_2O showed that drug naïve first episode psychosis patients, had increased glucose utilization after treatment with antipsychotics (DeLisi et al., 1985; Holcomb et al., 1996) and greater perfusion (Goozee et al., 2014; Miller et al., 2001, 1997) in the basal ganglia. Similar results were also obtained in healthy volunteers using a single dose of antipsychotics (Kim et al., 2013; Mehta, 2003). Studies using Arterial Spin Labelling (ASL), a Magnetic Resonance Imaging (MRI) sequence designed to quantitatively measure regional cerebral blood flow (rCBF), found results in line with the earlier PET studies. In particular (Fernández-Seara et al., 2011), reported increased rCBF in the striatum and thalamus in healthy volunteers after a single oral dose of 10 mg of metoclopramide (a D_2R antagonist) and (Handley et al., 2013) showed that both haloperidol 3 mg (a D_2R antagonist) and aripiprazole 10 mg (a D_2R partial agonist with 5-HT2a antagonism properties) increased rCBF in the striatum in healthy volunteers with a larger effect size for haloperidol. Recently, we tested the effects of a single clinical effective dose of different antipsychotics (Hawkins et al., 2018). Consistent with the existing literature, 3 mg haloperidol, 2 mg risperidone and 0.5 mg risperidone increased striatal rCBF as compared with placebo.

One of the major limitations of pharmacological MRI studies stands on the haemodynamic nature of the main functional measures (e.g. BOLD and rCBF). According to the neurovascular coupling model (Attwell and Iadecola, 2002; Logothetis et al., 2001) changes in haemodynamic MRI measures reflect a complex cascade of cellular, metabolic and vascular events associated with changes in neuronal activity (Heeger and Ress, 2002; Hoge et al., 1999; Singh, 2012). In line with this model, the main effects of drug may be interpreted as the result of dose-dependent enhanced or reduced pre- or post-synaptic activity due to the action of the drug on its targets (Khalili-Mahani et al., 2017). Although many antipsychotics bind to numerous receptors, the effects on rCBF have been tacitly attributed to D_2R blockade. In particular, D_2R antagonism would lead to enhanced neurotransmitter turnover in the dopaminergic synapses inducing metabolic activity and therefore perfusion demands (Goozee et al., 2014; Handley et al., 2013). The findings of altered dopamine synthesis capacity after acute antipsychotics administration in human volunteers and rats support this hypothesis (Hertel et al., 1996; Ito et al., 2009; Vernaleken et al., 2008). However, since MRI does not measure neuronal activity directly, making a link between neuro-receptor binding and haemodynamic effects of these compounds requires a degree of conjecture. In addition, in the case of dopaminergic drugs, MRI hemodynamic changes have also been related to non-neuronal mechanisms including the action of D_1-like receptors on vessels and D_2-like receptors (mainly D_3R) on perivascular astrocytes and endothelial cells (Choi et al., 2006; Krimer et al., 1998). For these reasons, despite the body of evidence, the neurochemical mechanisms underlying CBF changes after antipsychotics administration remain unclear. The use of multimodal approaches, e.g. combining MR measures with *ex-vivo* autoradiography (Dukart et al., 2018), have started to fill this gap of knowledge.

Receptor occupancy theory posits that the magnitude of the drug response is a function of receptor availability (Clark, 1970; Ploeger et al., 2009). In other words, incremental changes in functional response correspond to increments of the fraction of receptors bound. This relationship also depends on specific characteristics of each compound, such as receptor affinity (i.e. K_i). This basic pharmacology principle has been used to characterize the spatial profile of drug effects in the brain (also called "drug fingerprinting") assuming that brain regions with high density of the target receptor will show higher magnitude of drug effects (Khalili-Mahani et al., 2017). This approach has been proposed to describe MRI changes to dopaminergic drugs in preclinical data (Mandeville et al., 2013). Indeed, a monotonic increase in regional Cerebral Blood Volume (rCBV) has been observed following injection of an increasing dose of the D_2/D_3 antagonist radiotracer [^{11}C]raclopride in the striatum of two male rhesus macaques (Sander et al., 2013). Interestingly, [^{11}C]raclopride non-displaceable binding potential changes (BP_{ND}) reflecting changes in D_2/D_3 receptor occupancy, correlated with the amplitude of hemodynamic changes (i.e. rCBV): the higher the dose the larger rCBV increase; and in time: BP_{ND} variation and changes in rCBV showed similar temporal profiles. The same group also found an inverse relationship between receptor occupancy and rCBV with the selective D_2/D_3 agonist quinpirole in male rhesus macaques (i.e. rCBV decrease in face of dose-dependent increase of receptor occupancy) (Sander et al., 2016). Both studies provide evidence for a neurovascular coupling mechanism linking MR haemodynamic changes and D_2/D_3 receptors pharmacological modulation in non-human primates although they are limited to the striatal region.

The aim of the present work is to test in humans whether rCBF changes induced by a single dose of different antipsychotics co-varies with *in vivo* measures of D_2R distribution. In particular, we employed two datasets from healthy volunteers (Hawkins et al., 2018) to evaluate the spatial correlation between rCBF variation in the placebo vs antipsychotic comparison against the population-based receptor density profiles derived from human PET scans using the high affinity D_2/D_3 antagonist [^{18}F]Fallypride (Mukherjee et al., 1995). We also investigated the same relationship at the gene expression level using *post-mortem* mRNA expression measures of the *DRD2* gene (the gene coding for D_2R) extracted from the Human Allen Brain Atlas (ABA) (Hawrylycz et al., 2012). Brain mRNA expression variation across brain regions has been shown to be associated with resting state fMRI networks suggesting that brain hemodynamic response may be linked to the architecture of the human brain transcriptome (Hawrylycz et al., 2015; Richiardi et al., 2015). Here, brain microarray mRNA expression data was chosen as a proxy to protein-level receptor density in the human brain. In fact, while post-transcriptional events may alter the relationship between gene expression and protein synthesis (Liu et al., 2016), brain mRNA expression maps have been shown to predict *in vivo* proteins level as measured with PET (Beliveau et al., 2017; Rizzo et al., 2014).

Following the receptor occupancy theory and the neurovascular coupling model proposed by (Sander et al., 2013) we hypothesized that there will be a detectable linear relationship between main effects of antipsychotics on CBF measures and D_2R receptor density profiles evaluated at the protein and gene expression level. Even though brain microarray mRNA expression data from the ABA is noisier and more discrete (i.e. limited number of samples) than the PET BP_{ND} maps, we expect CBF increases after antipsychotics to be linearly associated also with *DRD2* mRNA expression spatial profiles. However, given the fact that mRNA expression only approximates cellular protein levels due to post-transcriptional regulatory mechanisms we predict microarray data to explain less variance in CBF changes than PET derived maps.

2. Materials and methods

2.1. Participants and study design

Data were collected as part of a project approved by the National Research Ethics Service Committee London – Brent (REC reference: 13/LO/1183). Details about participants, protocol and study design have been described in detail in (Hawkins et al., 2018). Briefly, forty-two healthy male subjects were enrolled in a double-blind, placebo-controlled, randomised, fully counterbalanced, three-session crossover design. Participants were randomised into two equal parallel study groups (Group 1 age mean/SD 27.6/6.9; Group 2 age mean/SD 28.3/6.3). In the first group participants received placebo, 7.5 mg of

olanzapine (OLA), or 3 mg of haloperidol (HAL) on each study day. In the second group, participants received placebo, 0.5 or 2 mg risperidone (lowRIS and highRIS respectively). All but lowRIS dosage were chosen in order to achieve on average at least 60% of D2 receptor occupancy (Kapur et al., 2000; Tauscher et al., 2004). On dosing day, participants followed a standardised regime. The MRI scan was performed at the time of predicted peak level of plasma concentration of the drug after oral administration (T_{max}): approximately 5 h after drug administration for Group 1 and 2 h for Group 2 (de Greef et al., 2011; Midha et al., 1989; Nyberg et al., 1995; Tauscher et al., 2004). Study days were seven days apart to allow washout between sessions. After the final visit, a follow-up phone call was made to monitor potential adverse events related to the study drugs.

2.2. MRI acquisition and pre-processing

All scans were conducted on a GE MR750 3 Tesla scanner using a 12-channel head coil. ASL image data were acquired using a 3D pseudo-continuous ASL sequence (3DpCASL) with a multi-shot, segmented 3D stack of axial spirals (8-arms) readout with a resultant spatial resolution (after re-gridding and Fourier Transformation) of $2 \times 2 \times 3$mm. Four control-label pairs were used to derive a perfusion weighted difference image. The labelling RF pulse had a duration of 1.5s and a post-labelling delay of 1.5s. The sequence included background suppression for optimum reduction of the static tissue signal. A proton density image was acquired in 48s using the same acquisition parameters in order to compute the CBF map in standard physiological units (ml blood/100 g tissue/min). Pre-processing of all CBF data was performed exactly as described in (Hawkins et al., 2018) (for further details please see Supplementary Materials).

2.3. Receptor density profiles

Fig. 1 shows the general framework of the analysis. D_2R profiles where extracted from an independent [^{18}F]Fallypride PET template obtained by averaging six binding potential (BP_{ND}) whole brain maps acquired in healthy young volunteers (age range: 18–30 years) who did not participate in the drug study (Dunn et al., 2009). [^{18}F]Fallypride is a D_2/D_3 receptor antagonist and it is a well-established PET radiotracer in the study of D_2-like receptor distribution in the brain (Mukherjee et al., 1995). Compared with other D_2-like antagonist radiotracers (e.g. [^{11}C] raclopride), [^{18}F]Fallypride has higher affinity and higher signal-to-noise ratios *in vivo* and therefore provides reliable quantitative measures of D_2R concentration including extra-striatal brain regions (Mukherjee et al., 2002; Stark et al., 2018). The [^{18}F]Fallypride template was segmented with the Desikan-Killiany Atlas (Desikan et al., 2006) and for each of the 85 Regions of Interest (ROIs) of the template, the voxel-wise mean BP_{ND} value was extracted with the *fslsmeants* function implemented in the Functional Software Library suite (FSL, FMRIB, Oxford, UK). Conventional parametric modelling of regional BP_{ND} was performed by using the cerebellum as reference region (Ichise et al., 2003). Therefore, both left and right cerebellar ROIs (namely "rh_cerebellum_cortex" and "lh_cerebellum_cortex") were excluded from correlation analyses with CBF profiles. To compare the contribution of striatal vs extra-striatal regions to this association, we also extracted BP_{ND} profiles from a [^{11}C]raclopride template obtained from a matchted group of healthy controls (Grecchi et al., 2014) (see Supplementary Material).

2.4. CBF profiles

CBF profiles were obtained from maps of CBF changes at the group level. In particular, for each antipsychotic, a group-wide paired T-test was performed in SPM12 for each drug vs placebo. Whole brain total blood flow was added as a covariate of no interest in the model to account for peripheral (global) drug effects and between-subjects variability in global brain perfusion (Handley et al., 2013; Viviani et al., 2013, 2009). For each antipsychotic the main effect of the drug was tested using group voxel-wise paired t-tests with cluster-level FWE correction (alpha = 0.05, cluster defining threshold = 0.001) as implemented in SPM12. In agreement with previous studies (Handley et al., 2013; Hawkins et al., 2018), we identified statistically significant increases in CBF after drug administration (against placebo) and have thus focussed on this contrast in the remainder of this work. Therefore, DRUG>PLACEBO contrast maps for each antipsychotic where segmented by using the Desikan-Killiany Atlas (Desikan et al., 2006) using the same approach used for the extraction of receptor profiles. This resulted in 85 ΔCBF profiles measuring the antipsychotic induced increase of CBF in each ROI. For consistency with the receptor profile data, we carried out correlation analyses excluding the two cerebellum ROIs.

2.5. Statistical analysis for the ΔCBF/receptor density profiles correlations

To test the associations between ΔCBF profiles (derived for each antipsychotic) and D_2/D_3 receptor density profiles, linear regression models as implemented in SPSS were used (IBM, SPSS Statistics, Version 23). Normal distribution of the residuals of the regression models were tested by Shapiro-Wilk test. BP_{ND} data were transformed using a natural logarithmic function (ln) so that the residuals conformed to a normal distribution. For all linear regression models Mahalanobis distance and Cook's distance were computed in order to explore the presence of multivariate outliers and estimate the presence of highly influential data points. To identify multivariate outliers, Mahalanobis distance values were compared to a chi-square distribution with degrees of freedom equal to the number of variables (two in this case) with $p = 0.001$ (Finch, 2012; Tabachnick and Fidell, 2013). Any data point with Cook's distance higher than 1 was considered as highly influential outlier and excluded from the analysis (Cook and Weisberg, 1982). To further control for the effect of extreme observation we also used the bias-corrected accelerated bootstrap technique as implemented in SPSS (Efron and Tibshirani, 1986) with 10,000 resamples. Non-parametric Spearman's correlations between ΔCBF profiles and receptor BP_{ND} profiles were also performed as a countercheck. In addition, Fisher's r-to-z transformation was performed to test pairwise significance of the difference between correlation coefficients of ΔCBF profiles between different antipsychotics. Asymptotic covariance method was adopted to account for the fact that correlations had one variable in common (Lee and Preacher, 2013).

2.6. mRNA profiles and genetic correlations

DRD2 gene brain microarray mRNA expression values were extracted from ABA data (http://human.brain-map.org) by using the Multimodal Environment for Neuroimaging and Genomic Analysis (MENGA) toolbox (http://www.nitrc.org/projects/menga/) (Rizzo et al., 2016). The same toolbox was used to carry out correlations with ΔCBF profiles of each antipsychotic. First, antipsychotics' contrast images (DRUG>PLACEBO) were resampled in the ABA space. Then, each CBF image sample was spatially matched with the corresponding genomic ABA sample within a search window of a sphere of 5 mm radius centred on the MNI coordinates of the ABA sample. Both CBF contrast image and ABA data were then segmented using the list of structures (N = 169) provided by the ABA (Hawrylycz et al., 2012). A subset of 89 structures (ROIs), each containing at least one genomic sample for all the six ABA brains (donors), was selected to perform correlations between ΔCBF profiles and gene expression. For each donor, samples data were converted from their original log2 intensity in z-scores using mean and standard deviation as normalization factor for a given subject. This was done to minimize bias related to inter-donor variability in the ABA dataset. For the *DRD2* gene a unique profile was obtained by selecting the probe which expression values were highly consistent across donors. In particular, distributions of expression values for all the probes were evaluated across donors, retaining the probe with the most symmetric and least skewed distribution. In the case of multiple samples within the same ROI, the average

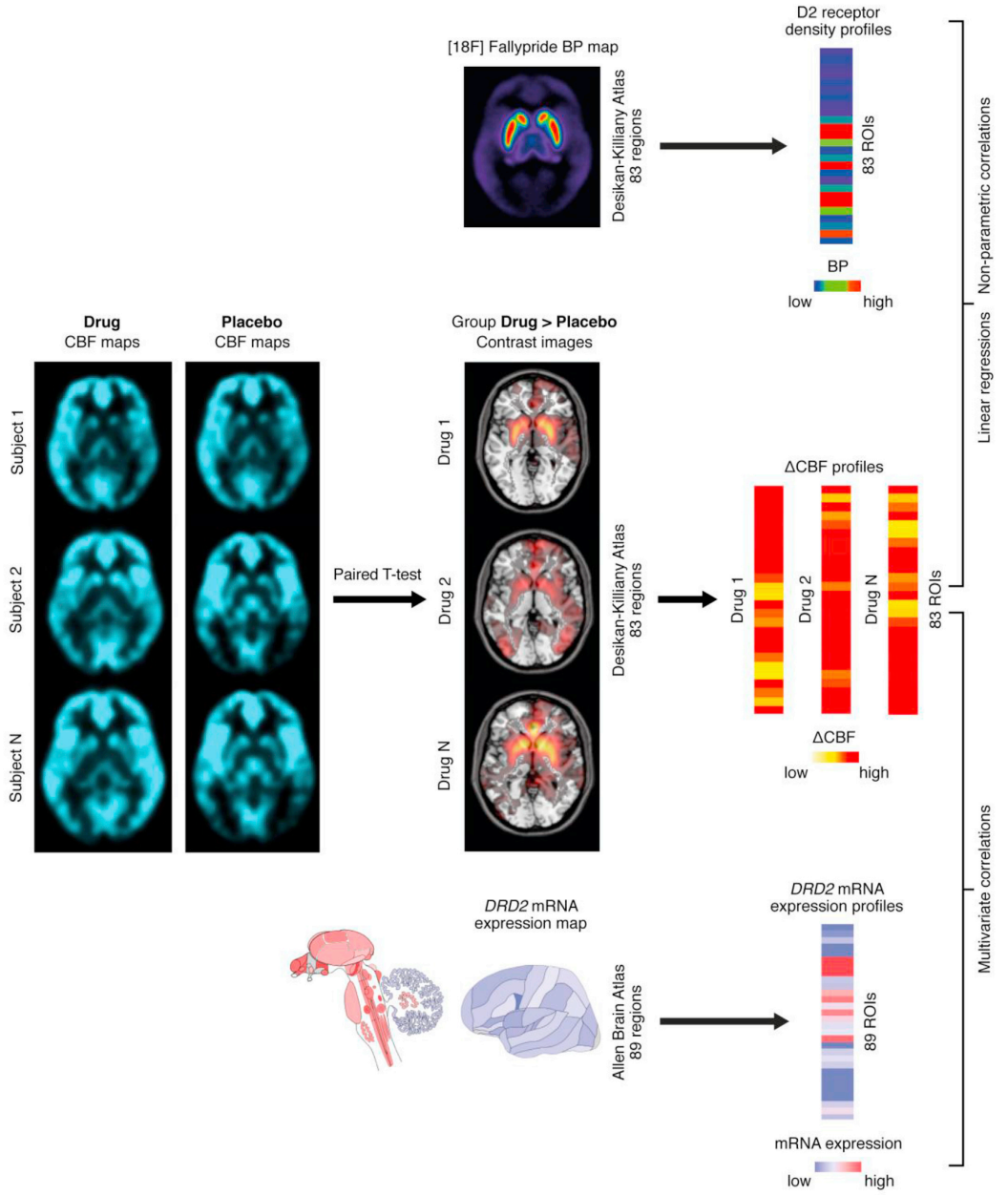

Fig. 1. General framework of the analysis. Group-level map showing main effect of drug was computed for each antipsychotic. The resulting maps and the [18F] Fallypride PET template were segmented into 83 ROIs by using the Desikan-Killiany Atlas (Desikan et al., 2006). For each ROI ΔCBF profiles and [18F]Fallypride BP_{ND} template values were extracted and then correlated. *DRD2* gene brain microarray mRNA expression values were extracted from ABA data (http://human.brain-map.org) (Hawrylycz et al., 2012). MENGA software (http://www.nitrc.org/projects/menga/) (Rizzo et al., 2016) was used to extract DRD2 mRNA expression profiles which then entered multivariate correlation analysis against ΔCBF profiles (please refer to Material and methods and Supplementary Material for a more detailed description).

between samples within the ROI was calculated (Rizzo et al., 2016).

After completing the matching and the extraction of ΔCBF and gene expression profiles, two different correlations were performed: 1) between-donors correlation or gene auto-correlation returning the biological variability of the spatial profile of mRNA expression between donors (the higher the gene autocorrelation the lower the heterogeneity in mRNA expression spatial profile between donors); 2) correlation between each gene expression and the ΔCBF by ROIs also called cross-correlation. A Principal Component Analysis (PCA) on mRNA expression measures of the 6 ABA donors was performed beforehand in order to extract the component that accounted at least for the 95% of the total variance in the mRNA expression data. In particular, the PCA was performed on an 89×6 matrix (89 ROIs by 6 donors) and represented a consistent spatial mRNA expression profile across all donors. This component was then used in the regression model against CBF profiles. Significance was assessed with a bootstrapping approach resulting in a chance likelihood of the correlation coefficient expressed as a %. More specifically, ROIs were permuted within donors repeating the correlation between PCA component and CBF profiles 1000 times, in order to obtain a measure of the likelihood that the correlation found was different from chance level. For further details on ABA mRNA processing and analysis see Supplementary Material and (Rizzo et al., 2016). A multivariate spatial correlation using MENGA was also performed between *DRD2* gene expression profiles and [^{18}F]Fallypride BP_{ND} maps (see Supplementary Material). As for protein density profile analysis, Fisher's r-to-z transformation was performed to test pairwise significance of the difference between correlation coefficients of ΔCBF profiles between different antipsychotics and also between PET and mRNA profiles.

3. Results

3.1. Main effect of antipsychotic on CBF

Group paired T-tests revealed that all antipsychotics but olanzapine, produced a statistically significant increase of CBF in basal ganglia, in particular in the striatum with haloperidol causing the largest increase as compared with lowRIS and highRIS. In particular HAL>PLA t-contrast revealed a significant cluster in the left Putamen; OLA>PLA t-contrast revealed a significant cluster in the righ parietal cortex and in the right parahippocampus; lowRIS>PLA t-contrast revealed a significant cluster in the left caudate; highRIS>PLA t-contrast revealed a significant cluster in the left caudate. None of the DRUG<PLA t-contrast revealed statistically significant clusters. Full statistics and voxel-wise t-maps are in Supplementary Material.

3.2. CBF changes with D_2 receptor profiles correlations

All antipsychotic ΔCBF profiles significantly correlated with [^{18}F]Fallypride BP_{ND} template values (Table 1 and Fig. 2). HAL ΔCBF had the strongest correlation with [^{18}F]Fallypride BP_{ND} template ($R_{linear} = 0.78$) followed by RIS ($R_{linear} = 0.73$ and $R_{linear} = 0.72$ for lowRIS and highRIS respectively) and OLA ($R_{linear} = 0.48$). Results from linear models and non-parametric Spearman correlations were consistent. In all linear regressions, none of the data points were identified as a highly influential outlier (all Cook's distances> 1) or multivariate outliers (all Mahalanobis distances $p > 0.01$). Results were retained after 10,000 resamples (all bootstrapped $p < 0.01$). The rank of order and R_{linear} values matched the variation in affinity with D_2 receptor (McCormick et al., 2010), with the stronger the association between ΔCBF profiles and D_2 receptor densities the lower the Ki (Table 1 and Fig. 4). In the pairwise correlation comparisons we found significant difference for HAL vs OLA ($z = 5.46$), lowRIS vs OLA ($z = 4.19$) and vs highRIS vs OLA ($z = 3.90$) (all $p_{two-tailed} < 0.01$, Bonferroni corrected, Fig. 4). All the other comparisons were not significant. To compare striatal vs extra-striatal contributions to this association we also performed correlations between ΔCBF and receptor density profiles by extracting BP_{ND} values from a [^{11}C]raclopride PET template. We found weaker correlation with [^{11}C]raclopride BP_{ND} template as compared with [^{18}F]Fallypride BP_{ND} template (see Supplementary material).

3.3. mRNA expression correlations

The average correlation coefficient (R^2) of the genomic autocorrelation analysis for the *DRD2* gene was 0.575 (standard deviation = 0.058) for the six donors. This result indicated good stability between donors of *DRD2* mRNA expression spatial profile (Rizzo et al., 2016).

For the different antipsychotic drugs, the correlation coefficients were all positive and statistically significant (Fig. 3 and Table 1) and also significantly lower than those obtained for the PET template (PET R^2 range = 0.20–0.60; mRNA PET R^2 range 0.04–0.20; pairwise-comparisons all $p < 0.05$). As for the correlation with [^{18}F]Fallypride values, genomic mRNA expression correlations qualitatively mirrored Ki differences (McCormick et al., 2010) between antipsychotics at D_2R (Fig. 4). However, none of the pairwise comparisons between correlation coefficients between antipsychotics were statistically significant after correction for multiple comparisons.

4. Discussion

The aim of the present study was to investigate the relationship between the effects of single clinical effective doses of antipsychotics on rCBF and receptor distribution profiles in the brain as indexed by [^{18}F]Fallypride BP_{ND} values extracted from a template map and brain *DRD2* mRNA expression profiles. Consistently with our hypothesis, we found that for all compounds there was a spatial coupling between drug-induced CBF changes and D_2 receptor density profiles (at both protein and gene expression level). In addition, we found that mRNA data explained less variance in CBF changes than PET derived map.

4.1. Receptor density profiles

The association between CBF changes induced by all antipsychotics and receptor brain spatial distribution of D_2R matches earlier evidence in non-human primates showing large CBF increases after injection of the D_2 antagonist PET tracer [^{11}C]raclopride in brain regions with high D_2R density (Sander et al., 2013). This suggests that the relationship between the physiological response to D_2R antagonist and D_2R availability described by (Sander et al., 2013) in preclinical models also exists *in vivo* in humans. Furthermore, we have shown that the relationship between ASL-CBF increases after antipsychotic administration also matched [^{18}F]

Table 1
Summary of the correlations of ΔCBF profiles D_2 receptor profiles ([^{18}F]Fallypride BP_{ND} template) and of genomic multivariate cross-correlations of antipsychotics' ΔCBF profiles with *DRD2* mRNA expression profiles.

DRUG>PLA contrast	[^{18}F]Fallypride BP_{ND} template				*DRD2* mRNA expression	
	R_{linear}	p_{linear}	Spearman rho	$p_{Spearman}$	R	Chance likelihood
HAL	+0.78	$p < 0.001$	0.61	$p < 0.001$	+0.34	0%
OLA	+0.48	$p < 0.001$	0.51	$p < 0.001$	+0.21	0%
lowRIS	+0.73	$p < 0.001$	0.76	$p < 0.001$	+0.43	0%
highRIS	+0.72	$p < 0.001$	0.61	$p < 0.001$	+0.45	2%

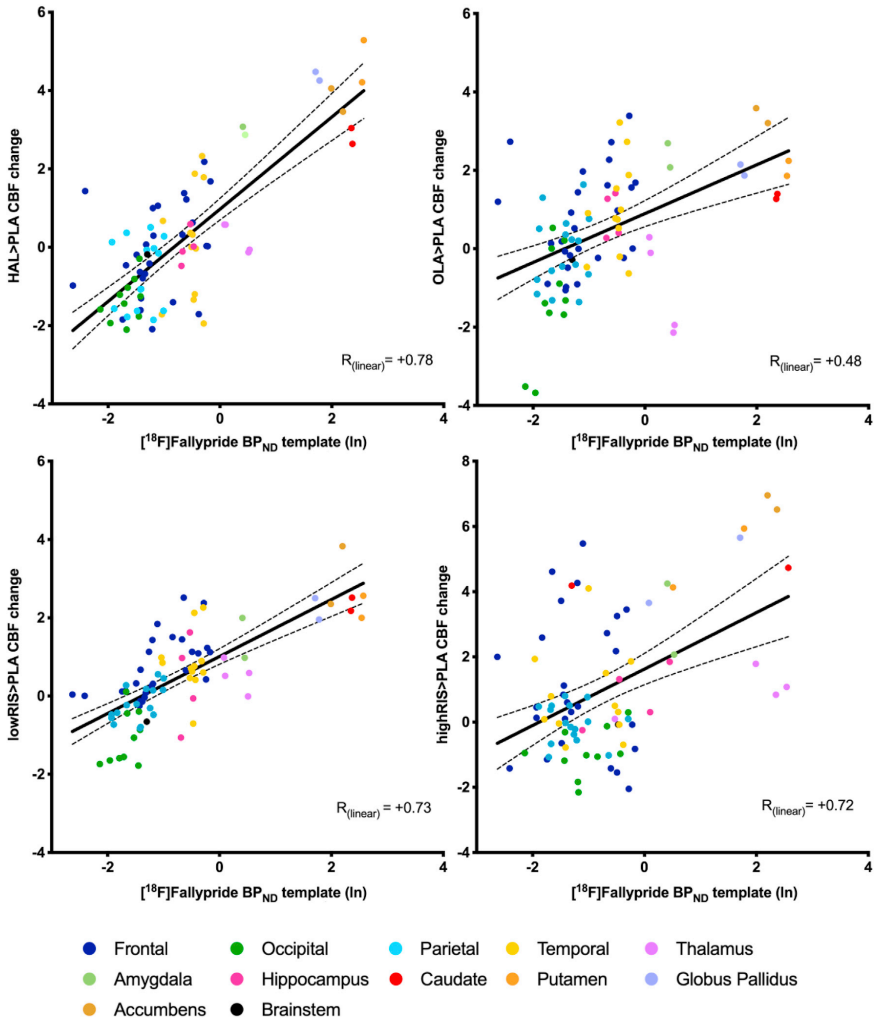

Fig. 2. Scatterplots of ΔCBF/receptor density profiles correlations. Top row: scatterplot of the correlation between HAL ΔCBF profiles and [18F]Fallypride BP_{ND} template (left) and of the correlation between OLA ΔCBF profiles and [18F]Fallypride BP_{ND} template (right). Bottom row: scatterplot of the correlation between lowRIS ΔCBF profiles and [18F]Fallypride BP_{ND} template (left) and of the correlation between highRIS ΔCBF profiles and [18F]Fallypride BP_{ND} template (right). Dashed lines indicate 95% confidence bands.

Fallypride BP_{ND} template values in extra-striatal ROIs significantly populated by D_2R such as the thalamus and the amygdala, even though they show lower BP_{ND} template values as compared with striatal ROIs. These results extend earlier evidence (Sander et al., 2016) and suggest that the linear coupling between CBF response to dopaminergic drugs and D_2R concentration might also be a valid model outside the striatum. This interpretation is also supported by the weaker correlation of ΔCBF with [^{11}C]raclopride BP_{ND} template as compared with [^{18}F]Fallypride BP_{ND} template (Supplementary Material). Of note, in Sander et al. (2016; 2013) the functional measure was rCBV instead of rCBF. However, given the tight association between rCBV changes and rCBF changes (Ito et al., 2005), we believe this difference will not affect the interpretation of our findings.

4.2. Microarray mRNA expression data

We found that for all antipsychotics, the ΔCBF profiles also correlated with microarray mRNA expression data extracted from the ABA. All genomic correlations were positive and therefore in the same direction of [^{18}F]Fallypride BP_{ND} template linear models. Notably, microarray mRNA expression measures explained less variance in ΔCBF than [^{18}F]Fallypride BP_{ND} template values. This is consistent with our hypothesis motivated by the existence of a large variability between mRNA expression and protein synthesis due to post-transcriptional regulation

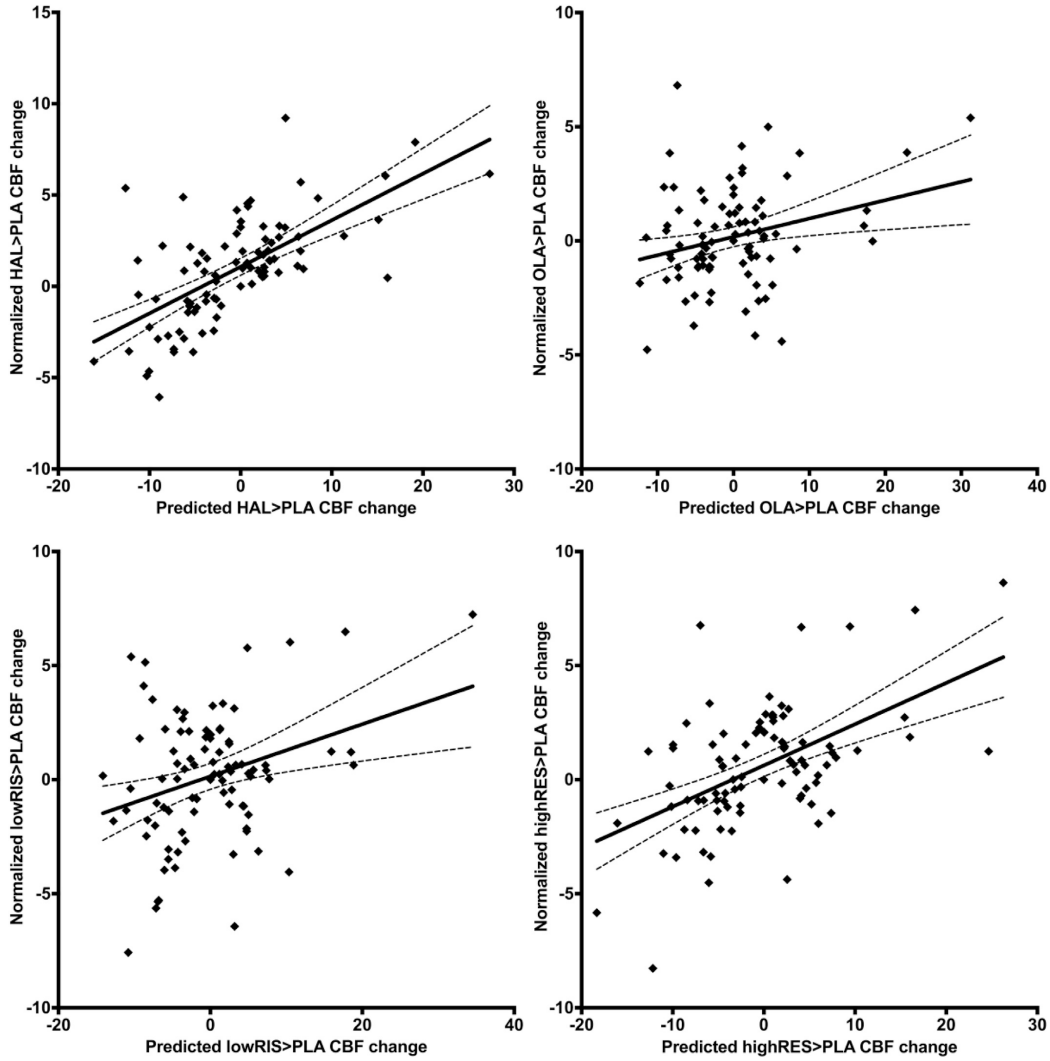

Fig. 3. Scatterplots of the genomic correlation. For all scatterplots on the y axis normalized DRUG>PLACEBO CBF changes and on the x axis DRUG>PLACEBO CBF changes predicted by the first Principal Component of the mRNA expression measures of the 6 ABA donors. Top right: HAL; Top left: OLA; Bottom right: lowRIS; Bottom left: highRIS. Dashed lines indicate 95% confidence bands.

mechanisms (Liu et al., 2016). Our findings are consistent with previous works that have linked the spatial architecture of the brain transcriptome to brain structure (Grecchi et al., 2017; Veronese et al., 2015), function (Hawrylycz et al., 2015; Richiardi et al., 2015) and *in vivo* measures of brain proteins (Gryglewski et al., 2018; Rizzo et al., 2016, 2014; Veronese et al., 2016). Here we could show that *post mortem* brain mRNA expression data may potentially be used to map also variations in MRI functional response to drug stimulation. However, such mapping has still many limitations to be addressed in order to adopt it extensively in the context of pharmacological-MRI studies. For instance, it might be difficult to use mRNA expression mapping in neurotransmitter systems where protein synthesis is highly dependent on post-transcriptional regulation mechanisms (e.g. serotonin system) (Beliveau et al., 2017; Rizzo et al., 2014). While further studies are needed to fully validate this mRNA expression-MRI approach, it might be especially valuable for profiling the functional effects of drugs with poorly characterized or unknown targets. Interestingly, as for the correlation with receptor density profiles, the rank order of correlations between ΔCBF and *DRD2* mRNA expression measures mirrored affinity profiles of the compounds, although these differences were only numerical. It is worth noting that

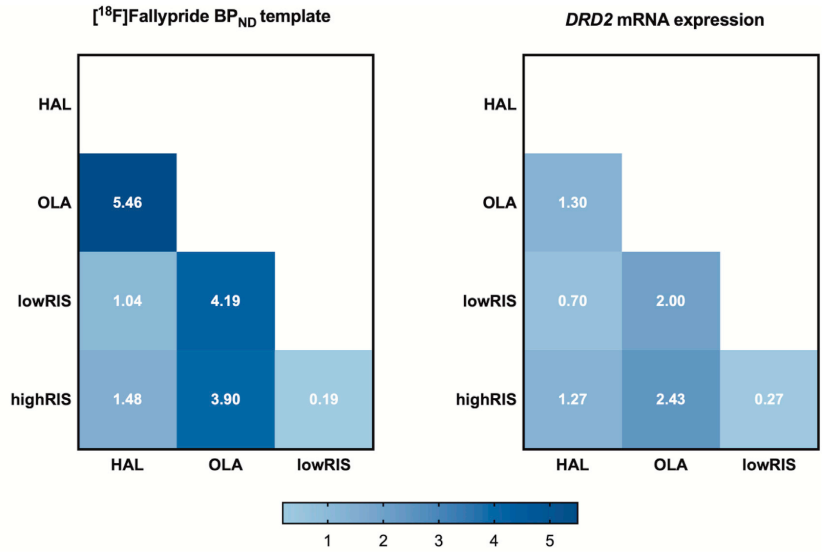

Fig. 4. Differential strength of association between ΔCBF and D_2R profiles. Heat maps showing z-values for the pairwise comparison of correlations. Colour bar indicates z-scores. On the left correlations with [^{18}F]Fallypride BP_{ND} template values, on the right correlations with mRNA microarray data from the ABA. HAL = haloperidol, OLA = olanzapine, lowRIS = low dose of risperidone, highRIS = high dose of risperidone. The following tests were performed HAL vs OLA, HAL vs lowRIS, HAL vs highRIS, lowRIS vs OLA, highRIS vs OLA, highRIS vs lowRIS.

the variance explained by genomic correlation was lower than the PET correlations (Table 1), which might have reduced the chance of detecting any significant difference on the pairwise comparison between the correlation coefficients.

These findings represent a further evidence supporting the hypothesized PK/PD model of antipsychotic effect of CBF measures (Mandeville et al., 2013). Indeed, we were able to show that quantitative measures of brain functional effect of antipsychotics (i.e. CBF changes) are directly associated with receptor density measures. However, intrinsic limitations of the ABA dataset should be considered when evaluating mRNA/ΔCBF relationships. First the number of available ABA donors is limited (N = 6) and therefore only approximates population-level brain mRNA expression templates. However, despite this limitation, ABA data has been showed to be able to predict brain protein densities (Beliveau et al., 2017; Gryglewski et al., 2018; Rizzo et al., 2016, 2014; Veronese et al., 2016) and other neuroimaging measures (Hawrylycz et al., 2015; Richiardi et al., 2015; Ritchie et al., 2018). Another limitation is that different approaches have been proposed to analyse this dataset (French and Paus, 2015; Gryglewski et al., 2018). The fact that different strategies in ABA dataset processing could affect reproducibility of the findings is under debate (Arnatkeviciute et al., 2018). We have also analysed the mRNA/ΔCBF correlations using a different methods that employs whole-brain voxel-wise mRNA expression maps obtained from variograms (Gryglewski et al., 2018). The results of this analysis were comparable with the analysis performed in MENGA (Supplementary Materials). Therefore we believe that it is unlikely that this methological issue could have biased our results.

4.3. *Differential strength of association between ΔCBF and receptor density profiles*

The correlation strength between ΔCBF and receptor density measured with PET varied between the different antipsychotics tested (Fig. 4). One possible interpretation of this difference might be related to the differential affinities for these compounds to D_2R (Dukart et al., 2018). Our data seems to be in line with this hypothesis. In fact, the strengths of the association were higher for antipsychotics with higher affinity for D_2R (Table 1 and Fig. S1). In particular, HAL was the drug with the highest correlation coefficient and the lowest Ki, whereas OLA showed the lowest correlation coefficient and the highest Ki. Both lowRIS and highRIS were in the middle between HAL and OLA. Another possible interpretation might be that related with the different secondary affinities between the drugs. For instance, for compounds with an high affinity with 5HT2a receptors like risperidone and olanzapine, part of the effect on CBF might also be linked with a mechanism different from D_2R blockade (Goozee et al., 2014). In fact, both OLA and RIS as well as other second-generation antipsychotics (e.g. aripiprazole) showed decreases in CBF especially in cortical areas with a mechanism that is possibly mediated by 5HT2a receptors (Handley et al., 2013; Lahti et al., 2005). We did not find differences in correlations between the two different doses of risperidone, despite the fact that they do show different effect size in CBF increase (as shown in Fig. 2 bottom row). This might indicate that the coupling between the measurable physiological effects and target receptor distribution can be detected regardless the dose of the compound if that dose is able to produce detectable functional effects. Nonetheless, differences in brain disposition of antipsychotics have been reported in previous studies (Kornhuber et al., 2006; Rodda et al., 2006). In particular, animal data suggested that antipsychotics (including the ones considered in the present work) show different blood-brain barrier penetration and brain clearance leading to dissimilar spatial distribution in the brain (Loryan et al., 2016). Even though these dissimilarities have been reported to be only moderate (Loryan et al., 2016), brain disposition is a factor to be considered in addition to receptor affinity when linking the pharmacodynamics of each antipsychotic with receptor occupancy. Therefore, without maps of brain deposition variation, conclusions regarding the D_2R affinities and strength of associations between receptors and CBF are necessarily incomplete.

4.4. Limitations

A number of limitations need to be considered for the present study. First, we used population-based profiles of D_2R density as the spatial architecture of D_2R is typically consistent across individuals (Rizzo et al., 2014; Veronese et al., 2016). For example, the striatum always has higher D_2R density than the thalamus which in turn has higher D_2R density than the cortex. However, variance in density between individuals within the same brain region (Farde et al., 1995) may drive inter-individual differences in the drug functional response. Individualized receptor profiles mapping is therefore necessary to bring more precision to the method and to further validate the present findings. Nevertheless, normative atlases for protein and mRNA expressions have proven useful in many different applications, suggesting that the core *spatial* architecture of the brain receptor systems is consistent across individuals (Beliveau et al., 2017; Rizzo et al., 2016, 2014; Veronese et al., 2016).

In addition, we considered only local effects by matching CBF changes and D_2R receptor density measures with the same ROIs. However, studies in patients and healthy volunteers showed that antipsychotics also produce changes in functional connectivity in rs-fMRI suggesting the existence of downstream effects (Cole et al., 2013; Sarpal et al., 2015) that were not included in our analyses.

As discussed above, increases in CBF after acute antipsychotic challenge have been usually interpreted as the result of a neuronal metabolic changes due to D_2R blockade. D_2-like receptors are also present in perivascular astrocytes and endothelial cells modulating brain hemodynamic changes. However these receptors are mainly D_3R and not D_2R (Choi et al., 2006). Together with the knowledge that the affinity of these compounds for D_2R is higher than for D_3R we expect the change in CBF is mainly neuronal in origin. In addition, both risperidone and olanzapine, but not haloperidol, act as antagonists at the serotonin-2a receptors (5HT2a) (Meltzer, 1999). Blockade of 5HT2a receptors on smooth-muscle cells of brain arteries has been shown to induce relative vasodilation in animal models (i.e. blocking vasoconstriction caused by the endogenous ligand serotonin) (Kovács et al., 2012). Therefore, the degree to which these non-neuronal effects contribute to the associations described here is not known. Finally, we believe that the limited sample size offered by the ABA ($N = 6$) could have undermined power in detecting a linear relationship between mRNA data and rCBF changes. This factor could also be an alternative explanation of the difference we found between mRNA and PET correlations with rCBF.

5. Conclusion

Understanding the link between neurochemical changes and brain function is crucial to uncover mechanisms underlining the effects of psychopharmacological treatment and between-subjects variability in response. In this work we investigated the case of antipsychotics whose functional effect, evaluated as changes in CBF measures, mirror the well-known spatial distributions of their main target (i.e. D_2R). The characterisation of the haemodynamic response using this multimodal approach might be applicable also for other classes of drugs and it becomes particularly valuable for profiling compounds known to bind to multiple targets or with unknown or poorly characterised targets. Finally, our work demonstrates that the use of MRI 3D pCASL as a measure of regional CBF offers an efficient, non-invasive tool to investigate CNS penetration in the process of psychotropic drug development that is also linked with brain chemistry.

Funding

Contract grant sponsor: Hoffmann – LaRoche Pharmaceuticals.

This paper represents independent research part funded by the National Institute for Health Research Biomedical Research Centre at South London and Maudsley NHS Foundation Trust and King's College London that support PS, OD, SCRW, FZ, MV and MAM. The views expressed are those of the authors and not necessarily those of the NHS, the NIHR or the Department of Health and Social Care. PS is supported by a PhD studentship jointly funded by the NIHR-BRC at SLaM and the Department of Neuroimaging, King's College London.

Conflicts of interest

AB is a stockholder of Hoffmann-La Roche Ltd. He has also received consulting fees from Biogen and lecture fees from Otsuka, Janssen, Lundbeck. FS is a former employee of F. Hoffmann-La Roche Ltd. GP has been the academic supervisor of a Roche collaboration grant (years 2015–16) that funds his salary. JD is current employees of F. Hoffmann-La Roche Ltd. and received support in form of salaries. SCRW has received grant funding from the Medical Research Council (UK), Wellcome Trust (UK), National Institute for Health Research (UK) and support for investigator led studies from Takeda, Pfizer, Lundbeck, P1Vital, Roche and Eli Lilly. In the past 3 years MAM has acted as an advisory board member for Lundbeck and Forum Pharmaceuticals. He also holds research funding from Lundbeck, Takeda and Johnson & Johnson. No other conflict of interested are disclosed.

Acknowledgments

MRI data were collected at the NIHR/Wellcome Trust King's Clinical Research Facility (CRF). Authors are grateful to the CRF team and to Dr Ndabezinhle Mazibuko and Stephanie Stephenson (Department of Neuroimaging, Institute of Psychiatry, Psychology and Neuroscience, King's College London, London, United Kingdom) for their help on data acquisition. We also gratefully acknowledge the work of Dr Joel Dunn (Kings College London and Guy's and St Thomas' PET Centre, School of Biomedical Engineering and Imaging Sciences, King's College London, London, UK) who contributed to the creation of PET templates. We also thank Gill Brown (London College of Communication, UAL, London, UK) for her help on illustrations. Finally, we thank all the volunteers who took part in the study.

Appendix A. Supplementary data

Supplementary data to this article can be found online at https://doi.org/10.1016/j.neuroimage.2018.12.028.

References

Agid, O., Mamo, D., Ginovart, N., Vitcu, I., Wilson, A.A., Zipursky, R.B., Kapur, S., 2007. Striatal vs extrastriatal dopamine D2 receptors in antipsychotic response|[mdash]|A double-blind PET study in schizophrenia. Neuropsychopharmacology 32, 1209–1215. https://doi.org/10.1038/sj.npp.1301242.

Arnatkeviciute, A., Fulcher, Ben D., Fornito, A., 2018. A practical guide to linking brain-wide gene expression and neuroimaging data. bioRxiv 380089. https://doi.org/10.1101/380089.

Attwell, D., Iadecola, C., 2002. The neural basis of functional brain imaging signals. Trends Neurosci. 25, 621–625. https://doi.org/10.1016/S0166-2236(02)02264-6.

Beliveau, V., Ganz, M., Feng, L., Ozenne, B., Højgaard, L., Fisher, P.M., Svarer, C., Greve, D.N., Knudsen, G.M., 2017. A high-resolution in vivo atlas of the human brain's serotonin system. J. Neurosci. 37, 120–128. https://doi.org/10.1523/JNEUROSCI.2830-16.2017.

Burt, D.R., Creese, I., Snyder, S.H., 1977. Antischizophrenic drugs: chronic treatment elevates dopamine receptor binding in brain. Science 196 (4287), 326–328. http://doi.org/10.1126/science.847477.

Choi, J.-K., Chen, Y.I., Hamel, E., Jenkins, B.G., 2006. Brain hemodynamic changes mediated by dopamine receptors: role of the cerebral microvasculature in dopamine-mediated neurovascular coupling. Neuroimage 30, 700–712. https://doi.org/10.1016/j.neuroimage.2005.10.029.

Clark, A.J., 1970. Methods of General Pharmacology, General Pharmacology. Springer Berlin Heidelberg, Berlin, Heidelberg. https://doi.org/10.1007/978-3-662-28641-8_2.

Cole, D.M., Oei, N.Y.L., Soeter, R.P., Both, S., van Gerven, J.M.A., Rombouts, S.A.R.B., Beckmann, C.F., 2013. Dopamine-dependent architecture of cortico-subcortical network connectivity. Cerebr. Cortex 23, 1509–1516. https://doi.org/10.1093/cercor/bhs136.

Cook, R.D., Weisberg, S., 1982. Residuals and Influence in Regression.

de Greef, Rik, Maloney, Alan, Olsson-Gisleskog, Per, Schoemaker, Joep, Panagides, John, 2011. Dopamine D2 occupancy as a biomarker for antipsychotics: quantifying the relationship with efficacy and extrapyramidal symptoms. AAPS J.

DeLisi, L.E., Holcomb, H.H., Cohen, R.M., Pickar, D., Carpenter, W., Morihisa, J.M., King, A.C., Kessler, R., Buchsbaum, M.S., 1985. Positron emission tomography in schizophrenic patients with and without neuroleptic medication. J. Cerebr. Blood Flow Metabol. 5, 201–206. https://doi.org/10.1038/jcbfm.1985.26.

Desikan, R.S., Ségonne, F., Fischl, B., Quinn, B.T., Dickerson, B.C., Blacker, D., Buckner, R.L., Dale, A.M., Maguire, R.P., Hyman, B.T., Albert, M.S., Killiany, R.J., 2006. An automated labeling system for subdividing the human cerebral cortex on MRI scans into gyral based regions of interest. Neuroimage 31, 968–980. https://doi.org/10.1016/j.neuroimage.2006.01.021.

Dukart, J., Holiga, Š., Chatham, C., Hawkins, P., Forsyth, A., McMillan, R., Myers, J., Lingford-Hughes, A.R., Nutt, D.J., Merlo-Pich, E., Risterucci, C., Boak, L., Umbricht, D., Schobel, S., Liu, T., Mehta, M.A., Zelaya, F.O., Williams, S.C., Brown, G., Paulus, M., Honey, G.D., Muthukumaraswamy, S., Hipp, J., Bertolino, A., Sambataro, F., 2018. Cerebral blood flow predicts differential neurotransmitter activity. Sci. Rep. 8, 4074. https://doi.org/10.1038/s41598-018-22444-0.

Dunn, J.T., Stone, J., Cleij, M., Marsden, P.K., O'Doherty, M., Reed, L.J., 2009. Differential occupancy of striatal versus extrastriatal dopamine D2/D3 receptors by the typical antipsychotic Haloperidol in man measured using [18F]-Fallypride PET. Neuroimage 47, S176. https://doi.org/10.1016/S1053-8119(09)71925-1.

Efron, B., Tibshirani, R., 1986. Bootstrap methods for standard errors, confidence intervals, and other measures of statistical accuracy. Stat. Sci. 1, 54–75. https://doi.org/10.1214/ss/1177013815.

Farde, L., Hall, H., Ehrin, E., Sedvall, G., 1986. Quantitative analysis of D2 dopamine receptor binding in the living human brain by PET. Science 231, 258–261.

Farde, L., Hall, H., Pauli, S., Halldin, C., 1995. Variability in D_2-dopamine receptor density and affinity: a PET study with [^{11}C]raclopride in man. Synapse 20, 200–208. https://doi.org/10.1002/syn.890200303.

Fernández-Seara, M.A., Aznárez Sanado, M., Mengual, E., Irigoyen, J., Heukamp, F., Pastor, M.A., 2011. Effects on resting cerebral blood flow and functional connectivity induced by metoclopramide: a perfusion MRI study in healthy volunteers. Br. J. Pharmacol. 163, 1639–1652. https://doi.org/10.1111/j.1476-5381.2010.01161.x.

Finch, W.H., 2012. Distribution of variables by method of outlier detection. Front. Psychol. 3, 211. https://doi.org/10.3389/fpsyg.2012.00211.

French, L., Paus, T., 2015. A FreeSurfer view of the cortical transcriptome generated from the allen human brain atlas. Front. Neurosci. 9, 323. https://doi.org/10.3389/fnins.2015.00323.

Goozee, R., Handley, R., Kempton, M.J., Dazzan, P., 2014. A systematic review and meta-analysis of the effects of antipsychotic medications on regional cerebral blood flow (rCBF) in schizophrenia: association with response to treatment. Neurosci. Biobehav. Rev. 43, 118–136.

Grecchi, E., Doyle, O.M., Bertoldo, A., Pavese, N., Turkheimer, F.E., 2014. Brain shaving: adaptive detection for brain PET data. Phys. Med. Biol. 59, 2517–2534. https://doi.org/10.1088/0031-9155/59/10/2517.

Grecchi, E., Veronese, M., Bodini, B., García-Lorenzo, D., Battaglini, M., Stankoff, B., Turkheimer, F.E., 2017. Multimodal partial volume correction: application to [11C] PIB PET/MRI myelin imaging in multiple sclerosis. J. Cerebr. Blood Flow Metabol. 37, 3803–3817. https://doi.org/10.1177/0271678X17712183.

Gryglewski, G., Seiger, R., James, G.M., Godbersen, G.M., Komorowski, A., Unterholzner, J., Michenthaler, P., Hahn, A., Wadsak, W., Mitterhauser, M., Kasper, S., Lanzenberger, R., 2018. Spatial analysis and high resolution mapping of the human whole-brain transcriptome for integrative analysis in neuroimaging. Neuroimage 176, 259–267. https://doi.org/10.1016/j.neuroimage.2018.04.068.

Handley, R., Zelaya, F.O., Reinders, A.A.T.S., Marques, T.R., Mehta, M.A., O'Gorman, R., Alsop, D.C., Taylor, H., Johnston, A., Williams, S., McGuire, P., Pariante, C.M., Kapur, S., Dazzan, P., 2013. Acute effects of single-dose aripiprazole and haloperidol on resting cerebral blood flow (rCBF) in the human brain. Hum. Brain Mapp. 34, 272–282. https://doi.org/10.1002/hbm.21436.

Hawkins, P.C.T., Wood, T.C., Vernon, A.C., Bertolino, A., Sambataro, F., Dukart, J., Merlo-Pich, E., Risterucci, C., Silber-Baumann, H., Walsh, E., Mazibuko, N., Zelaya, F.O., Mehta, M.A., 2018. An investigation of regional cerebral blood flow and tissue structure changes after acute administration of antipsychotics in healthy male volunteers. Hum. Brain Mapp. 39, 319–331. https://doi.org/10.1002/hbm.23844.

Hawrylycz, M., Miller, J.A., Menon, V., Feng, D., Dolbeare, T., Guillozet-Bongaarts, A.L., Jegga, A.G., Aronow, B.J., Lee, C.-K., Bernard, A., Glasser, M.F., Dierker, D.L., Menche, J., Szafer, A., Collman, F., Grange, P., Berman, K.A., Mihalas, S., Yao, Z., Stewart, L., Barabási, A.-L., Schulkin, J., Phillips, J., Ng, L., Dang, C., Haynor, D.R., Jones, A., Van Essen, D.C., Koch, C., Lein, E., 2015. Canonical genetic signatures of the adult human brain. Nat. Neurosci. 18, 1832–1844. https://doi.org/10.1038/nn.4171.

Hawrylycz, M.J., Lein, E.S., Guillozet-Bongaarts, A.L., Shen, E.H., Ng, L., Miller, J.A., van de Lagemaat, L.N., Smith, K.A., Ebbert, A., Riley, Z.L., Abajian, C., Beckmann, C.F., Bernard, A., Bertagnolli, D., Boe, A.F., Cartagena, P.M., Chakravarty, M.M., Chapin, M., Chong, J., Dalley, R.A., Daly, B.D., Dang, C., Datta, S., Dee, N., Dolbeare, T.A., Faber, V., Feng, D., Fowler, D.R., Goldy, J., Gregor, B.W., Haradon, Z., Haynor, D.R., Hohmann, J.G., Horvath, S., Howard, R.E., Jeromin, A., Jochim, J.M., Kinnunen, M., Lau, C., Lazarz, E.T., Lee, C., Lemon, T.A., Li, L., Li, Y., Morris, J.A., Overly, C.C., Parker, P.D., Parry, S.E., Reding, M., Royall, J.J., Schulkin, J., Sequeira, P.A., Slaughterbeck, C.R., Smith, S.C., Sodt, A.J., Sunkin, S.M., Swanson, B.E., Vawter, M.P., Williams, D., Wohnoutka, P., Zielke, H.R., Geschwind, D.H., Hof, P.R., Smith, S.M., Koch, C., Grant, S.G.N., Jones, A.R., 2012. An anatomically comprehensive atlas of the adult human brain transcriptome. Nature 489, 391–399. https://doi.org/10.1038/nature11405.

Heeger, D.J., Ress, D., 2002. What does fMRI tell us about neuronal activity? Nat. Rev. Neurosci. 3, 142–151. https://doi.org/10.1038/nrn730.

Hertel, P., Nomikos, G.G., Iurlo, M., Svensson, T.H., 1996. Risperidone: regional effects in vivo on release and metabolism of dopamine and serotonin in the rat brain. Psychopharmacology 124, 74–86. https://doi.org/10.1007/BF02245607.

Hoge, R.D., Atkinson, J., Gill, B., Crelier, G.R., Marrett, S., Pike, G.B., 1999. Linear coupling between cerebral blood flow and oxygen consumption in activated human cortex. Proc. Natl. Acad. Sci. U.S.A. 96, 9403–9408. https://doi.org/10.1073/pnas.96.16.9403.

Holcomb, H.H., Cascella, N.G., Thaker, G.K., Medoff, D.R., Dannals, R.F., Tamminga, C.A., 1996. Functional sites of neuroleptic drug action in the human brain: PET/FDG studies with and without haloperidol. Am. J. Psychiatry 153, 41–49. https://doi.org/10.1176/ajp.153.1.41.

Ichise, M., Liow, J.-S., Lu, J.-Q., Takano, A., Model, K., Toyama, H., Suhara, T., Suzuki, K., Innis, R.B., Carson, R.E., 2003. Linearized reference tissue parametric imaging methods: application to [11C]DASB positron emission tomography studies of the serotonin transporter in human brain. J. Cerebr. Blood Flow Metabol. 23, 1096–1112. https://doi.org/10.1097/01.WCB.0000085441.37552.CA.

Ito, H., Kanno, I., Fukuda, H., 2005. Human cerebral circulation: positron emission tomography studies. Ann. Nucl. Med. 19, 65–74. https://doi.org/10.1007/BF03027383.

Ito, H., Takano, H., Takahashi, H., Arakawa, R., Miyoshi, M., Kodaka, F., Okumura, M., Otsuka, T., Suhara, T., 2009. Effects of the antipsychotic risperidone on dopamine synthesis in human brain measured by positron emission tomography with L-[-11C] DOPA: a stabilizing effect for dopaminergic neurotransmission? J. Neurosci. 29, 13730–13734. https://doi.org/10.1523/JNEUROSCI.4172-09.2009.

Kapur, S., Remington, G., Zipursky, R.B., Wilson, A.A., Houle, S., 1995. The D2 dopamine receptor occupancy of risperidone and its relationship to extrapyramidal symptoms: a pet study. Life Sci. 57, PL103–PL107.

Kapur, S., Zipursky, R., Jones, C., Remington, G., Houle, S., 2000. Relationship between dopamine D2 occupancy, clinical response, and side effects: a double-blind PET study of first-episode schizophrenia. Am. J. Psychiatry 157, 514–520.

Khalili-Mahani, N., Rombouts, S.A.R.B., van Osch, M.J.P., Duff, E.P., Carbonell, F., Nickerson, L.D., Becerra, L., Dahan, A., Evans, A.C., Soucy, J.-P., Wise, R., Zijdenbos, A.P., van Gerven, J.M., 2017. Biomarkers, designs, and interpretations of resting-state fMRI in translational pharmacological research: a review of state-of-the-Art, challenges, and opportunities for studying brain chemistry. Hum. Brain Mapp. 38, 2276–2325. https://doi.org/10.1002/hbm.23516.

Kim, E., Howes, O.D., Turkheimer, F.E., Kim, B.H., Jeong, J.M., Kim, J.W., Lee, J.S., Jang, I.J., Shin, S.G., Kapur, S., Kwon, J.S., 2013. The relationship between antipsychotic D2 occupancy and change in frontal metabolism and working memory : a dual [(11)C]raclopride and [(18)F]FDG imaging study with aripiprazole. Psychopharmacology 227, 221–229.

Kornhuber, J., Wiltfang, J., Riederer, P., Bleich, S., 2006. Neuroleptic drugs in the human brain: clinical impact of persistence and region-specific distribution. Eur. Arch. Psychiatry Clin. Neurosci. 256, 274–280. https://doi.org/10.1007/s00406-006-0661-7.

Kovács, A., Hársing, L.G., Szénási, G., 2012. Vasoconstrictor 5-HT receptors in the smooth muscle of the rat middle cerebral artery. Eur. J. Pharmacol. 689, 160–164. https://doi.org/10.1016/j.ejphar.2012.05.031.

Krimer, L.S., Muly, E.C., Williams, G.V., Goldman-Rakic, P.S., 1998. Dopaminergic regulation of cerebral cortical microcirculation. Nat. Neurosci. 1, 286–289. https://doi.org/10.1038/1099.

Lahti, A.C., Weiler, M.A., Medoff, D.R., Tamminga, C.A., Holcomb, H.H., 2005. Functional effects of single dose first- and second-generation antipsychotic administration in subjects with schizophrenia. Psychiatr. Res. Neuroimaging 139, 19–30. https://doi.org/10.1016/j.pscychresns.2005.02.006.

Lee, I.A., Preacher, K.J., 2013. Calculation for the Test of the Difference between Two Dependent Correlations with One Variable in Common [Computer Software]. Retrieved July 18 2016.

Liu, Y., Beyer, A., Aebersold, R., 2016. On the dependency of cellular protein levels on mRNA abundance. Cell 165, 535–550. https://doi.org/10.1016/j.cell.2016.03.014.

Logothetis, N.K., Pauls, J., Augath, M., Trinath, T., Oeltermann, A., 2001. Neurophysiological investigation of the basis of the fMRI signal. Nature 412, 150–157. https://doi.org/10.1038/35084005.

Loryan, I., Melander, E., Svensson, M., Payan, M., König, F., Jansson, B., Hammarlund-Udenaes, M., 2016. In-depth neuropharmacokinetic analysis of antipsychotics based on a novel approach to estimate unbound target-site concentration in CNS regions: link to spatial receptor occupancy. Nature Publishing Group 21, 1527–1536. https://doi.org/10.1038/mp.2015.229.

Mandeville, J.B., Sander, C.Y.M., Jenkins, B.G., Hooker, J.M., Catana, C., Vanduffel, W., Alpert, N.M., Rosen, B.R., Normandin, M.D., 2013. A receptor-based model for dopamine-induced fMRI signal. Neuroimage 75, 46–57. https://doi.org/10.1016/j.neuroimage.2013.02.036.

McCormick, P.N., Kapur, S., Graff-Guerrero, A., Raymond, R., Nobrega, J.N., Wilson, A.A., 2010. The antipsychotics olanzapine, risperidone, clozapine, and haloperidol are D2-selective ex vivo but not in vitro. Neuropsychopharmacology 35, 1826–1835. https://doi.org/10.1038/npp.2010.50.

Mehta, M., 2003. Systemic sulpiride modulates striatal blood flow: relationships to spatial working memory and planning. Neuroimage 20, 1982–1994. https://doi.org/10.1016/j.neuroimage.2003.08.007.

Meltzer, H.Y., 1999. The role of serotonin in antipsychotic drug action. Neuropsychopharmacology 21. https://doi.org/10.1016/S0893-133X(99)00046-9, 106S–115S.

Midha, K.K., Chakraborty, B.S., Ganes, D.A., Hawes, E.M., Hubbard, J.W., Keegan, D.L., Korchinski, E.D., McKay, G., 1989. Intersubject variation in the pharmacokinetics of haloperidol and reduced haloperidol. J. Clin. Psychopharmacol.

Miller, D.D., Andreasen, N.C., O'Leary, D.S., Watkins, G.L., Boles Ponto, L.L., Hichwa, R.D., 2001. Comparison of the effects of risperidone and haloperidol on regional cerebral blood flow in schizophrenia. BPS 49, 704–715. https://doi.org/10.1016/S0006-3223(00)01001-5.

Miller, D.D., Andreasen, N.C., O'Leary, D.S., Rezai, K., Watkins, L., Boles Ponto, L.L., Hichwa, R.D., 1997. Effect of antipsychotics on regional cerebral blood flow measured with positron emission tomography. Neuropsychopharmacology 17, 230–240.

Mukherjee, J., Christian, B.T., Dunigan, K.A., Shi, B., Narayanan, T.K., Satter, M., Mantil, J., 2002. Brain imaging of 18F-fallypride in normal volunteers: blood analysis, distribution, test-retest studies, and preliminary assessment of sensitivity to aging effects on dopamine D-2/D-3 receptors. Synapse 46, 170–188. https://doi.org/10.1002/syn.10128.

Mukherjee, J., Yang, Z.-Y., Das, M.K., Brown, T., 1995. Fluorinated benzamide neuroleptics—III. Development of (S)-N-[(1-allyl-2-pyrrolidinyl)methyl]-5-(3-[18F] fluoropropyl)-2,3-dimethoxybenzamide as an improved dopamine D-2 receptor tracer. Nucl. Med. Biol. 22, 283–296.

Nyberg, S., Farde, L., Halldin, C., Dahl, M.L., 1995. D2 dopamine receptor occupancy during low-dose treatment with haloperidol decanoate. Am. J. 152 (2), 173–178. http://doi.org/10.1176/ajp.152.2.173.

Ploeger, B.A., van der GRAAF, P.H., M.D, D.M., 2009. Incorporating Receptor Theory in Mechanism-based Pharmacokinetic-pharmacodynamic (PK-PD) Modeling, vol. 24. Elsevier, pp. 3–15. https://doi.org/10.2133/dmpk.24.3, 2009.

Richiardi, J., Altmann, A., Milazzo, A.C., Chang, C., 2015. Correlated gene expression supports synchronous activity in brain networks. Science 348, 1241–1244. https://doi.org/10.1126/science.1255905.

Ritchie, J., Pantazatos, S.P., French, L., 2018. Transcriptomic characterization of MRI contrast with focus on the T1-w/T2-w ratio in the cerebral cortex. Neuroimage 174, 504–517. https://doi.org/10.1016/j.neuroimage.2018.03.027.

Rizzo, G., Veronese, M., Expert, P., Turkheimer, F.E., Bertoldo, A., 2016. MENGA: a new comprehensive tool for the integration of neuroimaging data and the allen human brain transcriptome atlas. PLoS One 11. https://doi.org/10.1371/journal.pone.0148744 e0148744–20.

Rizzo, G., Veronese, M., Heckemann, R.A., Selvaraj, S., Howes, O.D., Hammers, A., Turkheimer, F.E., Bertoldo, A., 2014. The predictive power of brain mRNA mappings for in vivo protein density: a positron emission tomography correlation study. J. Cerebr. Blood Flow Metabol. 34, 827–835. https://doi.org/10.1038/jcbfm.2014.21.

Rodda, K.E., Dean, B., McIntyre, I.M., Drummer, O.H., 2006. Brain distribution of selected antipsychotics in schizophrenia. Forensic Sci. Int. 157, 121–130. https://doi.org/10.1016/j.forsciint.2005.03.017.

Sander, C.Y., Hooker, J.M., Catana, C., Normandin, M.D., Alpert, N.M., Knudsen, G.M., Vanduffel, W., Rosen, B.R., Mandeville, J.B., 2013. Neurovascular coupling to D2/D3 dopamine receptor occupancy using simultaneous PET/functional MRI. Proc. Natl. Acad. Sci. U.S.A. 110, 11169–11174. https://doi.org/10.1073/pnas.1220512110.

Sander, C.Y., Hooker, J.M., Catana, C., Rosen, B.R., Mandeville, J.B., 2016. Imaging agonist-induced D2/D3 receptor desensitization and internalization in vivo with PET/fMRI. Neuropsychopharmacology 41, 1427–1436. https://doi.org/10.1038/npp.2015.296.

Sarpal, D.K., Robinson, D.G., Lencz, T., Argyelan, M., Ikuta, T., Karlsgodt, K., Gallego, J.A., Kane, J.M., Szeszko, P.R., Malhotra, A.K., 2015. Antipsychotic treatment and functional connectivity of the striatum in first-episode schizophrenia. JAMA Psychiatry 72, 5–13. https://doi.org/10.1001/jamapsychiatry.2014.1734.

Singh, K.D., 2012. Which "neural activity" do you mean? fMRI, MEG, oscillations and neurotransmitters. Neuroimage 62, 1121–1130. https://doi.org/10.1016/j.neuroimage.2012.01.028.

Stark, A.J., Smith, C.T., Petersen, K.J., Trujillo, P., van Wouwe, N.C., Donahue, M.J., Kessler, R.M., Deutch, A.Y., Zald, D.H., Claassen, D.O., 2018. [18F]fallypride characterization of striatal and extrastriatal D2/3 receptors in Parkinson's disease. YNICL 18, 1–42. https://doi.org/10.1016/j.nicl.2018.02.010.

Stroup, T.S., Lieberman, J.A., McEvoy, J.P., Davis, S.M., Swartz, M.S., Keefe, R.S.E., Miller, A.L., Rosenheck, R.A., Hsiao, J.K., 2009. Results of phase 3 of the CATIE schizophrenia trial. Schizophr. Res. 107, 1–12. https://doi.org/10.1016/j.schres.2008.10.011.

Tabachnick, B.G., Fidell, L.S., 2013. Using Multivariate Statistics.

Tauscher, J., Hussain, T., Agid, O., Verhoeff, N.P.L.G., Wilson, A.A., Houle, S., Remington, G., Zipursky, R.B., Kapur, S., 2004. Equivalent occupancy of dopamine D1 and D2 receptors with clozapine: differentiation from other atypical antipsychotics. Am. J. Psychiatry 161, 1620–1625. https://doi.org/10.1176/appi.ajp.161.9.1620.

Vernaleken, I., Kumakura, Y., Buchholz, H.-G., Siessmeier, T., Hilgers, R.-D., Bartenstein, P., Cumming, P., Gründer, G., 2008. Baseline [^{18}F]-FDOPA kinetics are predictive of haloperidol-induced changes in dopamine turnover and cognitive performance: a positron emission tomography study in healthy subjects. Neuroimage 40, 1222–1231. https://doi.org/10.1016/j.neuroimage.2007.12.045.

Veronese, M., Bodini, B., García-Lorenzo, D., Battaglini, M., Bongarzone, S., Comtat, C., Bottlaender, M., Stankoff, B., Turkheimer, F.E., 2015. Quantification of [(11)C]PIB PET for imaging myelin in the human brain: a test-retest reproducibility study in high-resolution research tomography. J. Cerebr. Blood Flow Metabol. 35, 1771–1782. https://doi.org/10.1038/jcbfm.2015.120.

Veronese, M., Zanotti-Fregonara, P., Rizzo, G., Bertoldo, A., Innis, R.B., Turkheimer, F.E., 2016. Measuring specific receptor binding of a PET radioligand in human brain without pharmacological blockade: the genomic plot. Neuroimage 130, 1–12. https://doi.org/10.1016/j.neuroimage.2016.01.058.

Viviani, R., Graf, H., Wiegers, M., Abler, B., 2013. Effects of amisulpride on human resting cerebral perfusion. Psychopharmacology 229, 95–103. https://doi.org/10.1007/s00213-013-3091-z.

Viviani, R., Sim, E.-J., Lo, H., Richter, S., Haffer, S., Osterfeld, N., Thöne, J., Beschoner, P., 2009. Components of variance in brain perfusion and the design of studies of individual differences: the baseline study. Neuroimage 46, 12–22. https://doi.org/10.1016/j.neuroimage.2009.01.041.

Appendix B (Selvaggi et al., J Neurosci Methods, 2021)

Journal of Neuroscience Methods 355 (2021) 109128

Contents lists available at ScienceDirect

Journal of Neuroscience Methods

journal homepage: www.elsevier.com/locate/jneumeth

Integration of human whole-brain transcriptome and neuroimaging data: Practical considerations of current available methods

Pierluigi Selvaggi [a,*], Gaia Rizzo [b,c], Mitul A. Mehta [a], Federico E. Turkheimer [a], Mattia Veronese [a]

[a] Department of Neuroimaging, Institute of Psychiatry, Psychology and Neuroscience, King's College London, London, UK
[b] Invicro, W12 0NN, London, UK
[c] Division of Brain Sciences, Department of Medicine, Imperial College London, SW72AZ, London, UK

ARTICLE INFO

Keywords:
Allen brain atlas
Neuroimaging
Transcriptomics
mRNA
Gene expression
Review
Methods

ABSTRACT

The Allen Human Brain Atlas (AHBA) is the first example of human brain transcriptomic mappings and detailed anatomical annotations which, for the first time, has allowed the integration of human brain transcriptomics with neuroimaging. This has been made possible because the AHBA offered an original dataset that contains mRNA expression measures for >20,000 genes covering the whole brain and, critically, in a standard stereotaxic space. In recent years many different methods have been used to integrate this data set with brain imaging data, although this endeavour has lacked harmony in terms of the workflow of data processing and subsequent analyses. In this work we discuss five main issues that experience has highlighted as in need of thorough consideration when integrating the AHBA with neuroimaging. These concerns are corroborated by comparing the performance of three different publicly available methods in correlating the same measures of serotonin receptors density with the correspondent AHBA mRNA maps. In this representative case, we were able to show how these methods can lead to discrepant results, suggesting that processing options are not neutral. We believe that the field should take into serious consideration these issues as they could undermine reproducibility and, in the end, the intrinsic value of the AHBA. We also advise on possible strategies to overcome these discrepancies. Finally, we encourage authors towards practices that will improve reproducibility such as transparency in reporting, algorithm and data sharing, collaboration.

1. Introduction

The release of the Allen Human Brain Atlas (AHBA) (Hawrylycz et al., 2012) offered a unique opportunity to integrate brain transcriptomics with neuroimaging data. The AHBA is a free access multimodal dataset (Shen et al., 2012) containing comprehensive genome-wide whole-brain microarray transcriptomic, structural Magnetic Resonance Imaging (MRI) and histological information obtained from six healthy adult human donors. At the time of writing Scopus counts a total of 987 citations for the original paper from the Allen Institute for Brain Science (Hawrylycz et al., 2012). This highlights the growing interest on whole-brain transcriptomics. One popular application of this dataset has been to combine mRNA expression data from the AHBA with brain imaging measures and to explore possible associations by running spatial correlations between the two (Rizzo et al., 2014a; Veronese et al., 2015; Rizzo et al., 2016; Beliveau et al., 2017; Komorowski et al., 2017; Gryglewski et al., 2018; Ritchie et al., 2018; Shin et al., 2018; Liu et al., 2019; Patania et al., 2019; Komorowski et al., 2020; Norgaard et al., 2020; Patel et al., 2020).

The atlas features the expression levels of >20,000 genes profiled by ~60,000 microarray probes in different brain regions that are spatially-resolved in the standard Montreal Neurological Institute (MNI) coordinates system. This allows a one-to-one spatial matching with neuroimaging data (Shen et al., 2012), and mRNA data from the AHBA has been found to be associated with T1-weighted (McColgan et al., 2018), T1-weighted/T2-weighted ratio images (Ritchie et al., 2018), cortical thickness (French and Paus, 2015; McColgan et al., 2018; Shin et al., 2018), diffusion-weighted MRI images (Forest et al., 2017; Romme et al., 2017), Positron Emission Tomography data (PET) (Rizzo et al., 2014a 2014b; Veronese et al., 2016; Beliveau et al., 2017; Gryglewski

* Corresponding author at: Centre for Neuroimaging Sciences, Institute of Psychiatry, Psychology & Neuroscience, King's College London, De Crespigny Park; SE5 8AF, London, UK.
E-mail address: pierluigi.selvaggi@kcl.ac.uk (P. Selvaggi).

https://doi.org/10.1016/j.jneumeth.2021.109128
Received 12 November 2020; Received in revised form 12 February 2021; Accepted 1 March 2021
Available online 17 March 2021

et al., 2018; Komorowski et al., 2020; Nørgaard et al., 2020), functional MRI networks and functional connectivity measures (Cioli et al., 2014; Hawrylycz et al., 2015; Richiardi et al., 2015; Vértes et al., 2016). Since AHBA publication in 2012, a number of authors developed distinct pipelines to process AHBA data and match them with brain images. Notably, AHBA data analysis is a non-trivial task because different choices could be made in the various analysis steps required to integrate mRNA expression measures with imaging data. Analysis of complex data are at higher risk of poor reproducibility without standardization of methods (Lindquist, 2020). We identified five main issues that could potentially impact the results: i) probe selection, ii) spatial mapping of samples, iii) data normalization and between-donors variability, iv) region selection, and v) statistics. In this paper we evaluate their possible impact on the final quantitative result, e.g. the degree of association between mRNA and neuroimaging data. In addition, we compared correlations of AHBA data with *in vivo* protein density measures from the same PET neuroimaging dataset (Beliveau et al., 2017) performed with three different publicly available tools (French and Paus, 2015; Rizzo et al., 2016; Gryglewski et al., 2018). While the comparisons used are not necessarily generalizable to all possible applications of the AHBA they clearly illustrate the impact of these issues on results. Therefore, it represents an ideal test-case that shows how the magnitude of mRNA-to-protein correlations could differ between methods.

2. Source of variability in AHBA data analysis

2.1. Probe selection

In the AHBA, mRNA expression for each gene is measured with multiple probes (on average 2.0 ± 1.4 probes per gene). Therefore, it becomes important to define a unique mRNA profile that is representative of each gene. Even though the AHBA documentation suggests data filtering strategies based on intensity of the signal compared with background noise, (http://human.brain-map.org/static/docs) to date there is no consensus on which is the best method for probe selection when 2 or more probes pass this threshold for the same gene. Filtering against the background noise or comparison against expression of house-keeping genes (French and Paus, 2015) could also be useful to assess whether or not a gene is significantly expressed in certain brain regions. Many other different strategies have been proposed for probe selection including consistency measures (e.g. correlations between probes) (Hawrylycz et al., 2015; Myers et al., 2015; Burt et al., 2018), distribution-based measures (e.g. by discarding probes showing the highest variance (Richiardi et al., 2015; Negi and Guda, 2017) or the least skewed distribution (Rizzo et al., 2016) or spatial variability measures (Gryglewski et al., 2018). Other authors did not select any probe and instead utilized all available probes (Rizzo et al., 2014a b) or created a unique profile by simply averaging their expression (French and Paus, 2015; Ritchie et al., 2018). Each method has its own advantages and disadvantages. For instance, correlation-based methods cannot be used for genes with less than 3 probes available. Distribution methods might be driven by between-donors variance (see below) instead of between probes variability. In addition, averaging may introduce bias while single probe analysis will increase variability. Moreover, works that analysed all available probes revealed that different probes showed different results in cross-correlation with protein density measures derived from PET (Rizzo et al., 2014a) which further suggest how critical is the probe selection step. Cross-correlation with protein density measures could be an additional strategy to be explored. Another method that has been proposed for probe selection is to compare microarray data with RNA sequencing (RNAseq) data (Myers et al., 2015). RNAseq offers higher sensitivity and specificity as compared with microarray technique. However, the implementation of this method is limited by the fact that RNAseq data in AHBA is available only for two donors (and for a limited number of samples). Furthermore, it is important to note that some genes have different transcript isoforms (e.g the *DRD2* gene has two different transcripts which code for the short and long isoform of the dopamine D2 receptor). It might be possible that some probes used in the AHBA are specific to some transcript isoforms. Therefore, in this case not all the probes are biologically interchangeable which further complicates the probe selection task. Finally, another relevant issue that relates with probe selection is the annotation of the probes to a specific gene. In particular, the AHBA contains not-annotated probes and, in addition, there is a risk that probes currently assigned to a specific gene in the AHBA could need re-annotation given the continuous updates of the public sequencing databases (Richiardi et al., 2015; Romero-Garcia et al., 2018)

2.2. Spatial mapping of samples

The Allen Institute, prior to dissection, acquired whole brain T1-weighted MRI images from each donor which were subsequently registered in standard MNI-152 space, such that mRNA samples across brain regions could be identified using native and MNI coordinates. In addition, each sample is associated with an anatomical ID. Even though a common standard space allows a one-to-one matching between mRNA expression and imaging signals, the distribution of AHBA sampling is sparser and more discrete than voxel-wise images that are commonly used in neuroimaging. One possible solution that has been proposed to overcome this issue is to implement a region-based segmentation approach where the whole AHBA dataset is resolved into discrete brain regions using a reference atlas (Rizzo et al., 2014a; French and Paus, 2015; Beliveau et al., 2017; Komorowski et al., 2017; Burt et al., 2018). This approach has two main drawbacks: i) the transcriptomic-imaging integration is highly dependent on the atlas adopted, ii) it might be possible that samples are inaccurately assigned to a different brain region that is close to the one where the sample was taken originally. To mitigate these problems, other authors took advantage of the detailed anatomical annotations of the AHBA instead of using external atlases (Cioli et al., 2014; Rizzo et al., 2016; Ritchie et al., 2018). The AHBA in fact provides, along with each tissue sample, anatomical annotations (called anatomical IDs). These annotations are offered at two different resolutions: coarse level (26 regions) and structure level (169 regions). Brain images can then be resampled in the AHBA space identifying for each transcriptomic sample its corresponding imaging sample. All the data points can be then analysed separately (Cioli et al., 2014; Ritchie et al., 2018) or combined into groups of samples defined using the different levels of resolution offered by the AHBA (Rizzo et al., 2016). Works that used the AHBA anatomical annotations have the advantage that they work on a common parcellation framework that is provided by the AHBA and that is closer to the raw data, even though it does not always match segmentations typically used in imaging analysis. Regardless the strategy used for segmentation, studies often do not consider the fact that, even if all the six donors have been sampled within the same anatomical regions, donors differ in each region with regard to both number and position of the samples.

Gryglewski et al. (2018) proposed a spatial analysis method that employs variogram models and Gaussian Process Regression to predict gene expression measures in locations that were not originally sampled in the AHBA. In particular, the authors computed variograms models to relate the distance and the variance in mRNA expression between AHBA samples. These models were then used to predict missing expression measures having as output whole-brain voxel-wise mRNA expression measures for each gene. The clear advantage of this approach is that overcomes the lack of samples homogeneity between brain regions without requiring any kind of pre-defined brain parcellation. However, it relies on the assumption that neighbouring samples have similar mRNA expression which might not be necessarily and consistently met for all brain regions (i.e. cortical vs subcortical regions) (Arnatkeviciute et al., 2019). In addition many different spatial gradients of co-expression might be present in the brain that reflects hierarchical segregation of brain structures (Burt et al., 2018; Vogel et al., 2020)

rather than distance measures.

Finally, another important source of variability is the spatial normalization and registration. The vast majority of the AHBA brain parcellation is performed at the group level (all the donors together). However, the normalization performed by the Allen Institute was not consistent between donors (e.g. linear and non-linear transformation were used for different donors (Hawrylycz et al., 2012). Normalization and segmentation strategies applied to each individual brain have been also proposed and they show better accuracy in assigning samples to brain regions as compared with conventional normalization procedures (Burt et al., 2018; Romero-Garcia et al., 2018). However, because brain data could be registered using many different tools that will have different outputs (Dadar et al., 2018), we anticipate that using different registration strategies from the one provided by the AHBA will further increase variability and possibly inconsistency between studies.

2.3. Region selection

Related to the previous point, a number of different strategies have also been used to select brain regions used to carry out correlation analysis of AHBA data with imaging datasets. For instance some authors limited the analyses to cortical regions (French and Paus, 2015; Richiardi et al., 2015; Burt et al., 2018; Ritchie et al., 2018) whereas other authors performed cross-correlations in the whole brain, including both cortical and subcortical areas (Rizzo et al., 2014a; Beliveau et al., 2017; Komorowski et al., 2017; Gryglewski et al., 2018). While in some cases the choice of excluding subcortical brain areas is due to the specific research question addressed (Richiardi et al., 2015; Ritchie et al., 2018) in other cases careful considerations have to be made when including both cortical and subcortical regions. In fact variance in gene expression has been reported to be different between cortical and subcortical regions (Hawrylycz et al., 2015) and therefore the inclusion or the exclusion of subcortical areas from the analysis could potentially lead to different degrees of inconsistency in the results depending on the homogeneity of mRNA expression across the whole brain of the specific gene(s) considered (Beliveau et al., 2017; Komorowski et al., 2017; Gryglewski et al., 2018). In addition, AHBA sampling covered only the left hemisphere for four donors whereas for two donors both hemispheres were covered. Even though lateralization effects on brain gene expression have been reported to be modest to negligible (Hawrylycz et al., 2012; Pletikos et al., 2014), this issue is still a matter of debate (Francks, 2015; Karlebach and Francks, 2015). To avoid potential lateralization biases some authors selected samples only from the left hemisphere (discarding the data on the right hemisphere available from two donors, (French and Paus, 2015; Rizzo et al., 2016) while other author analysed the whole dataset as it is pooling the data from left and right hemispheres together (Richiardi et al., 2015; Burt et al., 2018) or mirrored the left samples to synthetically create the corresponding missing samples on the right hemisphere (Gryglewski et al., 2018). Given the fact that the impact of lateralization on specific gene sets and specific brain regions is still unknown this issue must be considered when performing region selection. Finally, as discussed before, brain regions can have quite a substantial different number of samples, questioning whether there should be a minimum number of samples defining the mRNA expression of a particular regions to be chosen for the analysis. Irrespective of the number of the samples, brain regions also differ in terms of spatial extension. Large regions are expected to show higher variability in gene expression, as they are more likely to encompass sub-regions characterized by different gene expression patterns (Hawrylycz et al., 2012; Vértes et al., 2016).

2.4. Data normalization and between-donor variability

AHBA data comes from post-mortem brains of 6 different donors. The donors are 5 males and 1 female, the age range is 24–57 years and they have different ethnic background (3 Caucasians, 2 African Americans, 1 Latin). We have already mentioned in the previous section the fact that only two out of the six donors were sampled in both hemispheres. Moreover, donors also differ with regard to many other characteristics: cause of death, post-mortem intervals, brain pH, tissue cytoarchitectural integrity, RNA quality, number of sampling, sampling sites, number and type of probes used for each gene (http://human.brain-map.org/static/docs). It is also important to consider that in a large study like the one performed by the Allen Institute for Brain Science, that spans over a number of years, systematic biases are very likely to be introduced. The AHBA provides normalized data as well as raw data expressed in log2 intensity. The Allen Institute used two separate normalizations: within-donors normalization to account for array-related and dissection-related biases and differences in RNA integrity number (RIN); and between-donor normalization to allow comparison across brains (http://help.brain-map.org/download/attachments/2818165/Normalization_WhitePaper.pdf). However, the aim of the normalization provided by the AHBA was to minimize the effects of technical and systematic biases preserving the intrinsic biological variability thus allowing biologically meaningful within- and between-brain comparisons. While preserving this information might be valuable for analysis within the AHBA data (Forest et al., 2017; Negi and Guda, 2017), between-donor variability must be minimized when AHBA data is aggregated for cross-comparison with external imaging datasets. Different normalization approaches have been used like z-score transformation (Rizzo et al., 2016; Burt et al., 2018; Romero-Garcia et al., 2018) and scaling to average (Gryglewski et al., 2018). Normalization strategies could also introduce bias when data from mRNA data is used to predict missing data in the opposite hemisphere or in brain areas not originally sampled in the AHBA (Gryglewski et al., 2018) by reducing the estimated variance. In addition, the order with which the mRNA samples are pre-processed to match with neuroimaging-derived measures (including z-normalization, sample averaging, log transformation) might lead to different results. It is still unknown what normalization strategy should be and no consensus or recommendations in this regard have been proposed.

2.5. Statistics

Another relevant point of disagreement between studies is which statistical test use to correlate AHBA mRNA expression measures with imaging data. Most authors employed Spearman rank correlation analysis given the fact that AHBA data pooled from all the donors and all the regions does not follow a normal distribution for most of the genes (Rizzo et al., 2014a; French and Paus, 2015; Komorowski et al., 2017; Burt et al., 2018; Gryglewski et al., 2018; Ritchie et al., 2018). However, other authors employed the General Lineal Model and Pearson correlation (Rizzo et al., 2016; Veronese et al., 2016; Beliveau et al., 2017). As a general rule normality should be always checked beforehand or non-parametric testing should be used as a countercheck. Moreover, before performing any kind of correlational analysis consistency of tests across donors should be always considered. That is because the spatial pattern of mRNA expression could be heavily affected by inter-subject and intra-subject variability. While this issue might be less relevant in the future when data for more donors would be added to the AHBA, at the moment, with data coming from only six donors, this variability has to be seriously taken into account. Genes with highly variable spatial patterns between donors are more likely to produce spurious results in correlation analysis. This preliminarily check has been shown to improve stability and interpretability of the results (Rizzo et al., 2014a). Another way to control for inter-subject heterogeneity in correlation analysis that has been proposed is the use of multivariate correlations where mRNA data from different donors is weighted to reflect biological variability (Rizzo et al., 2016).

3. Comparison of publicly available methods

3.1. Rationale

Among all the different applications of AHBA data in neuroimaging, three different tools have been publicly released to process and analyse this dataset (French and Paus, 2015; Rizzo et al., 2016; Gryglewski et al., 2018). All offer a simplified and relatively easy-to-use analysis framework and they are also free and publicly available. Here we present a representative test in which we used these tools to investigate the degree of correlation between brain transcripts (as reported by AHBA) and the corresponding *in vivo* protein measures (as returned by PET). Correlation of PET *in vivo* measures of protein levels in the brain with the genetic data of the AHBA has been a popular task in recent years (Veronese et al., 2016; Beliveau et al., 2017; Komorowski et al., 2017; Gryglewski et al., 2018). This application is based on the core function of mRNA that is to carry genetic information taken from the DNA to produce the correct linear sequence of amino-acids for protein synthesis. Therefore, we should expect a direct relationship between mRNA levels and protein density measures that could vary depending on the presence of transcriptional and post-transcriptional regulatory mechanisms. We are aware that many other applications of the AHBA dataset exist other than correlation with PET data, such as correlation with functional and structural MRI measures. However, this application relies on the biologically plausible assumption of correspondence between mRNA expression and protein synthesis (Liu et al., 2016) and therefore in our view constitutes an ideal case to test reproducibility of methods.

3.2. Methods

3.2.1. Comparison of tools

In our example we focused on the serotonin system and used the NRU Serotonin Atlas (https://xtra.nru.dk/FS5ht-atlas/) (Beliveau et al., 2017) for the four main serotonin receptors (5-HT_{1a}R, 5-HT_{1b}R, 5-HT_{2a}R and 5-HT_4R) and for the serotonin transporter (5-HTT) as the imaging reference. This NRU atlas represented an optimal testing case for this analysis: i) it uses high sensitivity/specificity PET ligands that can reliably and robustly map brain concentrations of these protein in the brain; ii) it is an high-resolution, population-based atlas that is also calibrated with post-mortem human brain autoradiography; iii) the relationship between protein levels within the serotonin system as assessed by PET and mRNA expression has been well established and independently replicated (Beliveau et al., 2017; Komorowski et al., 2017; Gryglewski et al., 2018).

All the images are registered in MNI space and represents average distribution of serotonin proteins generated from 210 healthy volunteers (age range: 18–45 years) scanned with different PET radioligands selective for each of the targets. Each image entered correlation analyses against mRNA expression values of the corresponding gene (namely *HTR1A*, *HTR1B*, *HTR2A*, *HTR4* and *SCL6A4*) extracted from the AHBA. In the original publication of the NRU Serotonin Atlas (Beliveau et al., 2017) the authors already assessed the spatial association between protein concentrations and mRNA expression from the AHBA by using the tool by (French and Paus, 2015). Briefly this tool maps gene expression data from the AHBA into cortical and subcortical regions defined by the Desikan-Killiany atlas (Desikan et al., 2006) using the FreeSurfer software. In this method expression values are averaged across probes and median values are extracted for each region and across donors. For this tool we report the results as they are presented in the NRU Serotonin Atlas paper (Beliveau et al., 2017) where mRNA values are averaged between left and right hemispheres and no normalization is performed. The second tool used for the comparison is MENGA (Rizzo et al., 2016). MENGA takes advantage of the brain parcellation provided by the AHBA. In addition, gene expression data is normalized using z-score transformation and probe selection is performed by selecting the probes with the less skewed distribution. In this comparison we correlated density measures of the major serotonin proteins using mRNA expression data using the default settings of the MENGA software exactly as they are reported in the original publication (Rizzo et al., 2016). In particular we used the simplified coarse level to define the regions (15 regions), a 5 mm radius search window and univariate correlations. The third method used in this comparison is the one proposed by (Gryglewski et al., 2018). This tool offers voxel-wise brain mRNA expression maps that are obtained by predicting expression measures for each voxel from AHBA samples using variogram models. Probes selection excluded the ones that showed high spatial variability and low correlation with other probes. Moreover between-donors variability is minimized by mean-centering expression measures for each sample. We downloaded whole-brain voxel-wise expression maps for *HTR1A*, *HTR1B*, *HTR2A*, *HTR4* and *SCL6A4* genes (http://www.meduniwien.ac.at/neuroimaging/mRNA.html). Each image derived from (Gryglewski et al., 2018) was then segmented into 84 cortical and subcortical regions by using the Desikan-Killiany atlas and for each region mRNA expression data for all the genes were extracted. The same segmentation was applied to the NRU Serotonin Atlas to extract protein density measures. Then, Pearson's product moment and the Spearman rank correlation analyses were used to correlate mRNA expression data and protein density measures for all the methods considered. The threshold for significance was $p = 0.05$ with within-gene Bonferroni correction for multiple comparison. Of note, one important difference between methods is the number of regions selected. Both French and Paus and Gryglewski et al. methods are based on the segmentation provided by the Desikan-Killiany atlas which contains 84 regions, whereas in the default settings used in MENGA only 15 regions are included. This setting is included as default in the MENGA software to guarantee that all regions in all donors contain at least 10 AHBA sample. Due to the different number of regions, the correlations will therefore have different degrees of freedom depending on the method used (82 for French and Paus and Gryglewski et al. methods and 13 for MENGA, see below). Results are reported in $R_{(df)}$.

Table 1 summarizes the key differences between the three methods considered here.

3.2.2. Impact of data processing

Even though an extensive quantitative analysis on the impact of different choices in AHBA processing is beyond the scope of this manuscript and partially covered elsewhere (Rizzo et al., 2016, Veronese et al., 2016; Arnatkeviciute et al., 2019) we have also performed additional analysis to provide an example of how specific analysis steps had an impact on the results obtained by the methods chosen in our comparison. In particular, we assessed i) the role of genetic auto-correlation (i.e. between-donors variability), ii) differences in correlation strength when different atlas resolutions are used, iii) differences in mRNA/protein correlations when different probes are selected for each gene.

To address the point of between-donors variability (i) we have performed consistency analysis to verify the stability of the spatial pattern of mRNA expression for the selected genes across the AHBA donors (Rizzo et al., 2016). Briefly, this analysis consists in between-donors auto-correlation of mRNA samples returning Pearson's correlation coefficients (mean and standard deviation of all couplings) for each pairs of donors for each gene considered. This method flags genes with highly variable spatial patterns between donors and indirectly inform on the level of noise/heterogeneity in the data. We also tested performance of each of the methods used in this comparison after varying the number of brain regions used (ii). In particular for both French and Paus (2015) and Gryglewski et al. (2018) methods we tested the correlation between protein levels and mRNA data using three subsets of 20, 40 and 60 brain regions randomly selected from the Desikan-Killiany atlas which is the standard space adopted by these methods. The MENGA toolbox does not adopt the Desikan-Killiany atlas, but provides different segmentations derived from the AHBA data structure: the structure level (169 regions),

Table 1
Main differences in processing default options between the methods selected for the comparison.

Settings	French and Paus (2015)	Gryglewski et al. (2018)	Rizzo et al. (2016)
Probe selection	Average of all available probes for a gene	Exclusion of probes with low correlation with other probes and high spatial variability between donors	Exclusion of probes with high skewed distribution across donors
Flag of transcripts isoforms	no	no	no
Re-annotation of probes	no	no	no
RNAseq check	no	no	no
Spatial mapping	Freesurfer segmentation using the Desikan-Killiany atlas and average within ROIs	Voxel-wise maps in MNI space obtained through variogram analysis. Freedom of choice on how segment voxel-wise maps	Anatomical annotations provided by the AHBA
Region selection	Free choice Data from the left hemisphere only	Free choice Data from both hemispheres (missing data predicted if right hemisphere not present)	Free choice Data from the left hemisphere only
Data normalization	No normalization	mean-centering	z-score transformation
Statistics	Free choice	Free choice	Linear correlation Multivariate correlation
Major findings	• Association between serotonin receptor densities profiles and mRNA expression (Beliveau et al., 2017); • Association of structural MRI signal with mRNA expression profile specific to CA1 pyramidal cells and oligodendrocyte-specific gene-expression profiles (Patel et al., 2020); • Association between mRNA expression profiles and structural MRI anomalies in psychiatric disorders (Writing Committee for the Attention-Deficit/Hyperactivity Disorder et al., 2020) • Association between risk factor genes for diabetes and regional glucose metabolism during both normal aging and Alzheimer disease (Nugent et al., 2020) • Association between *TBR1*, *SCN1A*, *MAGEL2*, and *CACNB* gene expression spatial profile and fMRI signal in visual and motor cortices (Bueichekú et al., 2020) • Association between dynamic connectivity patterns (fMRI) and gene expression (Diez and Sepulcre, 2018) • Brain co-localization of in vivo of tau and Aβ propagation and gene expression (Sepulcre et al., 2018)	• Dopamine $D_{2/3}$ receptors binding potential and mRNA expression of *DRD2* and *DRD3* genes (Komorowski et al., 2020) • Association between thalamo-cortical connectivity and *CALB1* and *PVALB* gene expression (Müller et al., 2020) • Association between neuronal timescales and brain mRNA expression profiles (Gao et al., 2020) • Correlation between 5-HT_{1A} receptor density and mRNA coexpression gene sets (Unterholzner et al., 2020)	• Association between changes in cerebral blood flow after antipsychotic administration and DRD2 gene expression data (Selvaggi et al., 2019) • Association between PET 18 kDa translocator protein (TSPO) and gene expression (Veronese et al., 2017) • Use of mRNA data to estimate nondisplaceable fraction in PET studies (Veronese et al., 2016) • Translocator protein (TSPO) brain quantification (Zanotti-Fregonara et al., 2019) • Comparison of radioligand performance for quantification of metabotropic glutamate receptor 5 in human brain (Lohith et al., 2016)

the coarse level (26 regions) and the simplified coarse level (15 regions). For the structure level the MENGA toolbox automatically selected 90 regions discarding brain regions that contained less than 2 samples per gene. Finally, we used the MENGA toolbox to test whether different probes lead to different mRNA/protein correlations (iii). For this scope we used the simplified coarse level to extract mRNA data from 10 of all the available probes for each gene. AHBA contains only 3 probes for both *HTR1A* and *HTR1B* genes, thus all available probes were selected for these genes.

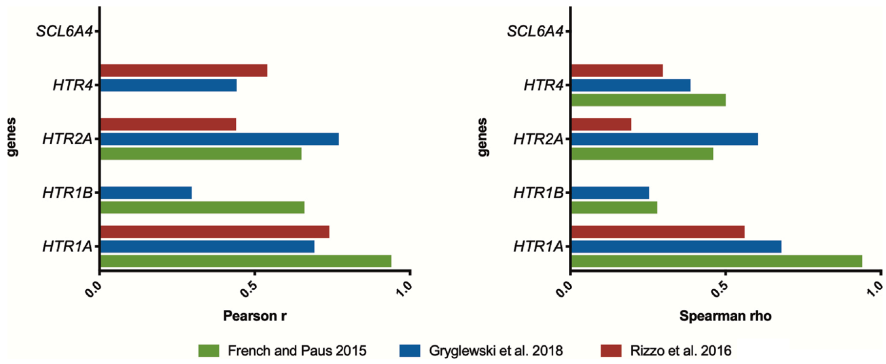

Fig. 1. Correlations of *in vivo* serotonin protein densities with AHBA data using three different publicly available tools. SCL6A4 correlations with all methods and HTR1B correlation with MENGA were not significant ($p < 0.05$), hence no bar is visible. HTR4 mRNA expression data did not pass normality test (Shapiro-Wilk test) using the French and Paus (2015) method, hence no bar is visible. Note: in the correlation analysis for the HTR2A gene, for the French and Paus (2015) method only cortical samples were selected.

3.3. Results

3.3.1. Comparison of tools

Fig. 1 shows results of correlations (expressed as correlation coefficient) for each method and each gene.

For both the serotonin transporter 5-HTT (correspondent gene *SCL6A4*) and serotonin receptor 5-HT_4 (correspondent gene *HTR4*) the three tools showed consistent results. All the methods returned very low and not significant ($p > 0.05$) correlations with 5-HTT density measures. Correlations with 5-HT_4R protein levels were comparable between methods that all returned moderate correlations (R range: 0.44 – 0.54). On the other hand, results were inconsistent between the tools for *HTR1A*, *HTR1B* and *HTR2A* genes. We found the most remarkable differences for the *HTR1B* gene. In fact, with MENGA the correlation with 5-HT_{1b}R levels was not significant ($p > 0.05$), French and Paus method showed a strong correlation ($R_{(82)} = 0.66$) and (Gryglewski et al., 2018) method showed only a modest association ($R_{(82)} = 0.29$). We found remarkable differences between methods also for the *HTR2A* gene: while using Beliveau et al. and Gryglewsky et al. methods we obtained strong associations between mRNA data and protein density levels ($R_{(82)} = 0.65$ and $R_{(82)} = 0.77$ respectively), using the Rizzo et al. method the correlation was modest ($R_{(13)} = 0.44$). Finally, for the *HTR1A* gene French and Paus method returned the highest correlation ($R_{(82)} = 0.94$) with similar correlations between the Rizzo et al. and Gryglewski et al. methods ($R_{(13)} = 0.74$ and $R = 0.69_{(82)}$ respectively).

3.3.2. Impact of data processing

Gene auto-correlation analysis revealed that the gene with the highest between-donors correlation was *HTR1A* ($R_{(13)} = 0.90$) followed by *SCL6A4* ($R_{(13)} = 0.74$) and *HTR4* ($R_{(13)} = 0.73$). By contrast both *HTR1b* and *HTR2a* showed highly variable mRNA expression spatial pattern across donors ($R_{(13)} = 0.169$ and $R_{(13)} = 0.078$ respectively).

Fig. 2 shows results of differences in mRNA/protein correlations when varying the number of brain regions considered. The MENGA

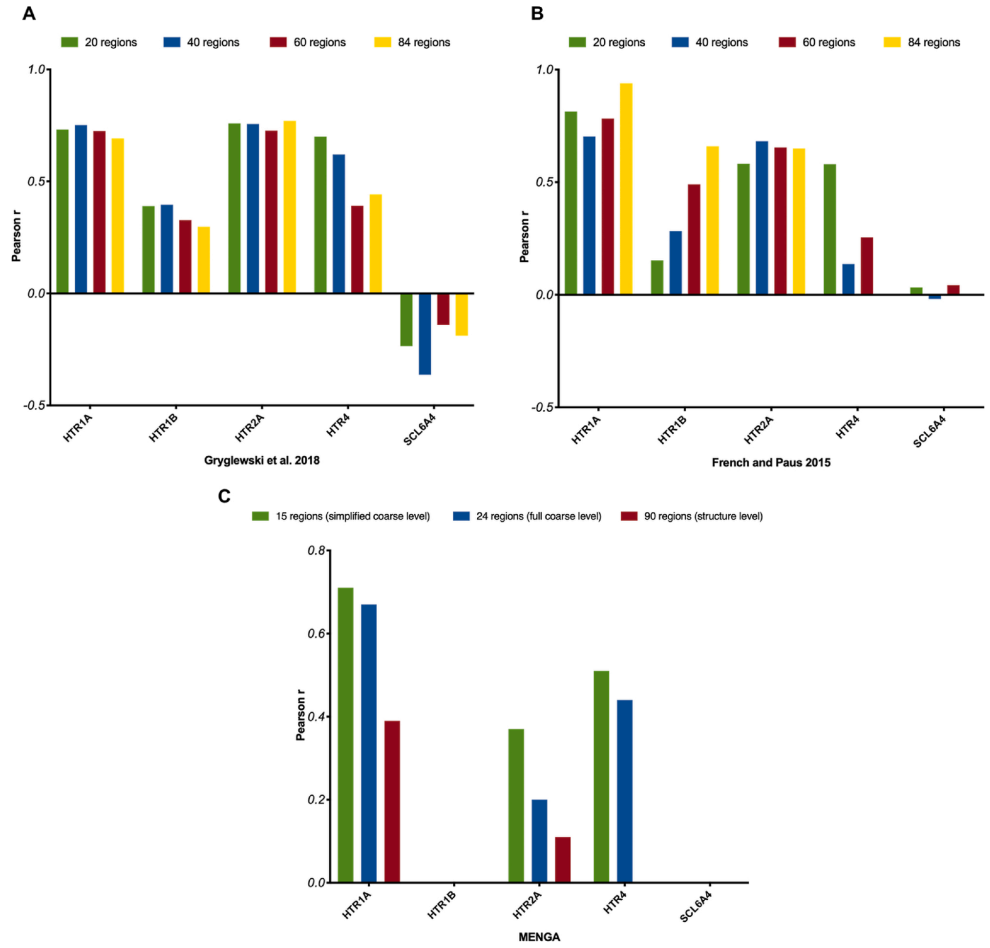

Fig. 2. Correlations of *in vivo* serotonin protein densities with AHBA data using three different publicly available tools when varying the number of regions considered. 2A Gryglewski et al., 2018, 2B French and Paus, 2015, 2C MENGA. For *HTR1B* and *SCL6A4* genes the MENGA toolbox returned R = 0, hence no bar is visible.

toolbox returned the highest variability in correlations when comparing correlations with a different number of brain regions. This effect was particularly evident in the case of *HTR2A* (R range: 0.11 – 0.37) and *HTR4* (R range: 0 – 0.51) genes. The effect of segmentation was less pronounced in Gryglewski et al. and French and Paus methods as compared with MENGA, however high variability in correlations were evident for *HTR4* (R range: 0 – 0.58) and *HTR1B* (R range: 0.15 – 0.66) genes in French and Paus method and for *HTR4* gene (R range: 0.44 – 0.7) in Gryglewski et al. method.

Fig. 3 shows mRNA/protein levels correlation for each gene using different probes available in the AHBA. Correlations between *SCL6A4* and *HTR4* mRNA expression with their respective protein levels where highly variable depending on the probe considered, whereas more consistent results between probes were observed in the case of *HTR1A* and *HTR2A* genes.

3.4. Discussion

3.4.1. Comparison of tools

In our comparison we obtained consistent results between the three methods considered only for 5-HTT and 5-HT_4R density profiles. Results were inconsistent between the tools for *HTR1A*, *HTR1B* and *HTR2A* genes. As regard 5-HTT the analysis performed with all tools suggest that there is a poor spatial correspondence between 5-HTT density measures and the expression map of its corresponding gene. One possible explanation for the lack of association in this case might be related to the fact 5-HTT is often located on the terminal projections of serotonin neurons and therefore distant from the soma where most of corresponding mRNA is present (Tao-Cheng and Zhou, 1999; Beliveau et al., 2017). The *HTR1B* gene showed also high variability between tools. The inconsistency found for the case of the HTR1B gene might be explained by differential mRNA/protein association between cortical and subcortical regions due to different expression of 5-HT_{1b}R auto-receptor (presynaptic) and 5-HT_{1b}R hetero-receptors (postsynaptic) in different brain regions (Beliveau et al., 2017). This difference might explain why the correlation with 5-HT_{1b}R using the MENGA software was not significant. In fact, among the 15 regions provided in MENGA only 6 regions refer to the neocortex. The difference in performance between French and Paus (2015) and (Gryglewski et al., 2018) methods is more difficult to interpret. The ratio between cortical and subcortical regions is the same between the two methods as the same atlas has been applied. However, Spearman correlation returned very similar results between French and Paus (2015) and (Gryglewski et al., 2018) methods. One possible interpretation of these results might stand on different skewness in the data extracted using the two methods. For instance high skewed distribution of data points might have inflated the linear correlation in the French and Paus (2015) method. We found less pronounced but still relevant differences for the *HTR1A* and *HTR2A* genes. Interestingly, for the *HTR2A* gene, the correlation with the French and Paus (2015) method was performed only using cortical samples and no correlation in subcortical regions was found (Beliveau et al., 2017). However, we found significant correlation in both cortical and subcortical samples using MENGA (R = 0.44) and (Gryglewski et al., 2018) method (R = 0.77), with the latter method showing a stronger association. However,

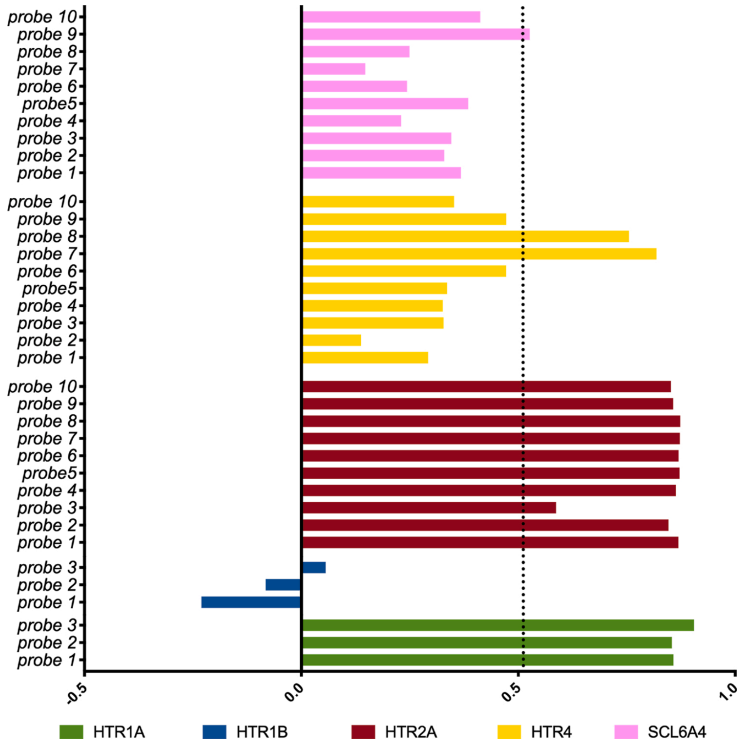

Fig. 3. Correlations of *in vivo* serotonin protein densities with AHBA data using for each gene different available probes in AHBA. Dot line indicates statistical significance threshold for N = 15, alpha = 0.05 ($R_{(13)}$ = 0.51).

after excluding subcortical samples in both MENGA and (Gryglewski et al., 2018) methods correlation coefficients dropped ($R_{MENGA} = 0.39$; $R_{Gryglewski} = 0.18$). This analysis clearly shows how heavily the results could be affected using a different selection of brain regions. Finally, all the methods showed high correlations for the *HTR1A* gene (R range = 0.69 – 0.94), with the highest correlation achieved by French and Paus (2015) tool. This is consistent with previous findings (Rizzo et al., 2014a) which also show that correlation for 5-HT_{1a}R tend to vary depending on the specific *HTR1A* probe that is selected. Therefore, we can hypothesize that different strategies in probe selection between the three methods could explain the differences we found here. Finally, despite the skewed distribution of some of the data, the Pearson's and Spearman correlation methods produced broadly similar results, but with some notable exceptions. The French and Paus method described a relationship between the HRT1B mRNA and PET data that was more than double for the Pearson's method. This indicates that data distribution should not be ignored when evaluating the associations between mRNA expression spatial patterns with imaging data.

Some limitations of this comparison should be acknowledged. The limited number of donors in the AHBA, the limited number of methods and genes tested, and the type of comparison performed here do not allow to draw any kind of definitive conclusions about the correct data analysis workflow for correlating mRNA levels with protein densities. For instance, we cannot exclude that the differences shown here could be related to any other factor other than methodological issues or that could be more or less pronounced when using different gene-sets. However, despite these limitations we were able to show that even in the ideal case where the same data (both imaging and mRNA) are used, different methods return inconsistent results. These findings suggest that methodological options in AHBA data processing are not neutral and could heavily affect reproducibility of the findings.

3.4.2. Impact of data processing

Gene autocorrelation analysis showed that *HTR1b* and *HTR2a* showed highly variable mRNA expression spatial pattern across donors. This high biological variability suggests that any results reported for these two genes should be interpreted with caution. These results are in line with previous reports (Rizzo et al., 2016; Arnatkeviciute et al., 2019) suggesting that high between-donors variability in AHBA mRNA expression data is an important source of noise in this dataset. We also found an effect of segmentation on mRNA/protein correlation strength. This effect was higher for the MENGA toolbox as compared with the other two methods. This difference might be explained by the fact that the segmentation adopted by Gryglewski et al. and French and Paus methods (i.e. Desikan-Killiany atlas) was able to include in each ROI an higher number of data points (i.e. samples) than the AHBA structure and coarse level used in MENGA. In addition, *HTR1A* and *HTR2A* genes showed more stable correlation strength than other serotonin genes across tools. This is not surprising given the homogenous distribution of these genes across cortical regions (Beliveau et al., 2017), however results obtained with other serotonin genes corroborate our concerns regarding the impact of different segmentation strategies. Finally, we found that in 2 out of 5 genes of our case example different correlations strength were obtained when using different probes. Our case example highlights that at least for some genes in the AHBA datasets mRNA expression data from different probes are not interchangeable.

It is important to highlight that our findings are limited to the specific case tested and therefore cannot immediately be generalizable to all genes and all the possible applications of the AHBA. Other authors have started to systematically assess the impact of pre-processing choices in AHBA analysis to derive guidelines (Arnatkeviciute et al., 2019).

4. General considerations

In addition to the five issues described above another important factor that limits generalizability of AHBA data analysis has to be acknowledged. The number of available ABA donors is limited (N = 6) and therefore only approximates population-level brain mRNA expression templates. Nonetheless, AHBA data has been already used as a population-based atlas and associated with a variety of neuroimaging measures. However, in our view, as discussed above the limited number of donors opens serious concerns about how between-donor variability is handled and therefore represents an important limitation. Future works should account for it.

Given the number of different applications of the AHBA dataset we anticipated that some of the issues might be more or less relevant depending on specific scenarios. Therefore, it is difficult at this stage to provide specific recommendations or guidelines that could work in all the cases. Nevertheless, we would like to propose some strategies that could improve reproducibility of the results for AHBA-imaging association studies: i) to test and externally-validate each method using normative datasets for which the relationship with brain mRNA expression measures is well-established; ii) to clean the AHBA dataset from high insensitive probes and evaluate probes annotations and their specificity in the case of transcript isoforms; iii) to validate the statistics of the methods used for each analysis step (i.e. probe selection, normalization, region selection, etc. (Arnatkeviciute et al., 2019), iv) to report the methods in a more systematic and uniform manner (similar to what is currently used for systematic reviews and meta-analysis.

5. Conclusion

The integration of brain transcriptomics with brain imaging has a great potential to help answer old and new neuroscience questions. However, there is still a lack of harmony in the methods used. Here, we have provided an overview of the most prominent methodologies and identify five main issues that might heavily affect the results. We also show that different available tools lead to different results when mRNA data is used to correlate with brain protein densities. Given this discrepancy we strongly encourage further discussion in the community to avoid reproducibility issues that could seriously jeopardize the value of this tool. Even though in our comparison we consider only mRNA/protein density correlation it is likely that the issues reviewed here might apply in many other cases. While some authors are beginning to formally address the issue (Arnatkeviciute et al., 2019), further work is necessary to achieve a consensus regarding the best approach for each scenario to make these tools reproducible and thus enhance their utility for the scientific community. We anticipate that a consensus cannot be easily reached for all the issues. As a result, we strongly advice future authors to be at least fully transparent in the description of their methods and reviewers to take into serious consideration reproducibility issues. In addition, given the concerns about reproducibility we encourage the field to discuss and define best practices, to share algorithms and data in order to boost transparency and collaborative efforts (Nichols et al., 2017). We also suggest that the impact of different options in the AHBA workflow on the results should be carefully evaluated case-by-case. Finally, we believe that it is extremely important that researchers in this fast-growing field are aware of the high risk of inconsistent results and therefore take the right steps to avoid serious controversies that emerged in other fields of neuroimaging (Eklund et al., 2016).

Author contributions

PS: Conceptualization, Methodology, writing-original draft preparation, writing-review & editing; GR: Methodology, writing-review & editing; MAM: Methodology, writing-review & editing, FET: Methodology, writing-review & editing; MV: Conceptualization, Methodology, writing-review & editing.

Declaration of Competing Interest

GR is a current employee of Invicro. In the past 3 years MAM has acted as an advisory board member for Lundbeck and Forum Pharmaceuticals. He also holds research funding from Lundbeck, Takeda and Johnson & Johnson. MV has received consulting honoraria from GSK. No other conflict of interested are disclosed.

Acknowledgments

This paper represents independent research part funded by the National Institute for Health Research (NIHR) Biomedical Research Centre at South London and Maudsley NHS Foundation Trust and King's College London, UK that support PS, MV and MAM. The views expressed are those of the authors and not necessarily those of the NHS, the NIHR or the Department of Health and Social Care. PS is supported by a PhD studentship jointly funded by the NIHR-BRC at SLaM and the Department of Neuroimaging, King's College London.

References

Arnatkeviciute, A., Fulcher, B.D., Fornito, A., 2019. A practical guide to linking brain-wide gene expression and neuroimaging data. Neuroimage (April 189), 353–367.
Beliveau, V., Ganz, M., Feng, L., Ozenne, B., Højgaard, L., Fisher, P.M., et al., 2017. A high-resolution in vivo atlas of the human brain's serotonin system. J. Neurosci. 37 (January (1)), 120–128.
Bueichekú, E., Aznárez-Sanado, M., Diez, I., d'Oleire Uquillas, F., Ortiz-Terán, L., Qureshi, A.Y., et al., 2020. Central neurogenetic signatures of the visuomotor integration system. Proc. Natl. Acad. Sci. U.S.A. (March), 6.
Burt, J.B., Demirtaş, M., Eckner, W.J., Navejar, N.M., Ji, J.L., Martin, W.J., et al., 2018. Hierarchy of transcriptomic specialization across human cortex captured by structural neuroimaging topography. Nat. Neurosci. 21 (August (9)), 1251–1259.
Cioli, C., Abdi, H., Beaton, D., Burnod, Y., Mesmoudi, S., 2014. Differences in human cortical gene expression match the temporal properties of large-scale functional networks. PLoS One 9 (December (12)) e115913.
Dadar, M., Fonov, V.S., Collins, D.L., 2018. Alzheimer's Disease neuroimaging Initiative. A comparison of publicly available linear MRI stereotaxic registration techniques. Neuroimage 1 (July (174)), 191–200.
Desikan, R.S., Ségonne, F., Fischl, B., Quinn, B.T., Dickerson, B.C., Blacker, D., et al., 2006. An automated labeling system for subdividing the human cerebral cortex on MRI scans into gyral based regions of interest. Neuroimage 31 (July (3)), 968–980.
Diez, I., Sepulcre, J., 2018. Neurogenetic profiles delineate large-scale connectivity dynamics of the human brain. Nat. Commun. 9 (September (1)), 3876.
Eklund, A., Nichols, T.E., Knutsson, H., 2016. Cluster failure: why fMRI inferences for spatial extent have inflated false-positive rates. Proc. Natl. Acad. Sci. U.S.A. 113 (July (28)), 7900–7905.
Forest, M., Iturria-Medina, Y., Goldman, J.S., Kleinman, C.L., Lovato, A., Oros Klein, K., et al., 2017. Gene networks show associations with seed region connectivity. Hum. Brain Mapp. 38 (March (6)), 3126–3140.
Francks, C., 2015. Exploring human brain lateralization with molecular genetics and genomics. Ann. N. Y. Acad. Sci. 1359 (November), 1–13.
French, L., Paus, T., 2015. A FreeSurfer view of the cortical transcriptome generated from the Allen Human Brain Atlas. Front. Neurosci. 16 (September (9)), 323.
Gao, R., van den Brink, R.L., Pfeffer, T., Voytek, B., 2020. Neuronal timescales are functionally dynamic and shaped by cortical microarchitecture. Elife 23 (November), 9.
Gryglewski, G., Seiger, R., James, G.M., Godbersen, G.M., Komorowski, A., Unterholzner, J., et al., 2018. Spatial analysis and high resolution mapping of the human whole-brain transcriptome for integrative analysis in neuroimaging. Neuroimage 1 (August 176), 259–267.
Hawrylycz, M.J., Lein, E.S., Guillozet-Bongaarts, A.L., Shen, E.H., Ng, L., Miller, J.A., et al., 2012. An anatomically comprehensive atlas of the adult human brain transcriptome. Nature 489 (September (7416)), 391–399.
Hawrylycz, M., Miller, J.A., Menon, V., Feng, D., Dolbeare, T., Guillozet-Bongaarts, A.L., et al., 2015. Canonical genetic signatures of the adult human brain. Nat. Neurosci. 18 (December (12)), 1832–1844.
Karlebach, G., Francks, C., 2015. Lateralization of gene expression in human language cortex. Cortex. 67 (June), 30–36.
Komorowski, A., James, G.M., Philippe, C., Gryglewski, G., Bauer, A., Hienert, M., et al., 2017. Association of protein distribution and gene expression revealed by PET and post-mortem quantification in the serotonergic system of the human brain. Cereb. Cortex 27 (January (1)), 117–130.
Komorowski, A., Weidenauer, A., Murgaš, M., Sauerzopf, U., Wadsak, W., Mitterhauser, M., et al., 2020. Association of dopamine D2/3 receptor binding potential measured using PET and [11C]-(+)-PHNO with post-mortem DR2/3 gene expression in the human brain. Neuroimage 17 (August), 117270.
Lindquist, M., 2020. Neuroimaging results altered by varying analysis pipelines. Nature. 582 (7810), 36–37.
Liu, Y., Beyer, A., Aebersold, R., 2016. On the dependency of cellular protein levels on mRNA abundance. Cell. 165 (April (3)), 535–550.
Liu, F., Tian, H., Li, J., Li, S., Zhuo, C., 2019. Altered voxel-wise gray matter structural brain networks in schizophrenia: association with brain genetic expression pattern. Brain Imaging Behav. 13 (April (2)), 493–502.
Lohith, T.G., Tsujikawa, T., Siméon, F.G., Veronese, M., Zoghbi, S.S., Lyoo, C.H., et al., 2016. Comparison of two PET radioligands, [11C]FPEB and [11C]SP203, for quantification of metabotropic glutamate receptor 5 in human brain. J. Cereb. Blood Flow Metab. (September), 14.
McColgan, P., Gregory, S., Seunarine, K.K., Razi, A., Papoutsi, M., Johnson, E., et al., 2018. Brain regions showing white matter loss in Huntington's disease are enriched for synaptic and metabolic genes. Biol. Psychiatry 83 (March (5)), 456–465.
Müller, E., Munn, B., Hearne, L.J., Smith, J.B., Fulcher, B., Arnatkeviciute, A., et al., 2020. Core and matrix thalamic sub-populations relate to spatio-temporal cortical connectivity gradients. Neuroimage. 11 (August), 117224.
Myers, E.M., Bartlett, C.W., Machiraju, R., Bohland, J.W., 2015. An integrative analysis of regional gene expression profiles in the human brain. Methods 73 (February), 54–70.
Negi, S.K., Guda, C., 2017. Global gene expression profiling of healthy human brain and its application in studying neurological disorders. Sci. Rep. 7 (April (1)), 897.
Nichols, T.E., Das, S., Eickhoff, S.B., Evans, A.C., Glatard, T., Hanke, M., et al., 2017. Best practices in data analysis and sharing in neuroimaging using MRI. Nat. Neurosci. 20 (February (3)), 299–303.
Nørgaard, M., Beliveau, V., Ganz, M., Svarer, C., Pinborg, L.H., Keller, S.H., et al., 2020. A High-Resolution In Vivo Atlas of the Human Brain's Benzodiazepine Binding Site of $GABA_A$ Receptors. BioRxiv April 10.
Norgaard, M., Beliveau, V., Ganz, M., Svarer, C., Pinborg, L.H., 2020. A High-Resolution In Vivo Atlas of the Human Brain's Benzodiazepine Binding Site of GABAA Receptors. BioRxiv.
Nugent, S., Potvin, O., Cunnane, S.C., Chen, T.-H., Duchesne, S., 2020. Associating type 2 diabetes risk factor genes and FDG-PET brain metabolism in normal aging and alzheimer's disease. Front. Aging Neurosci. 30 (October (12)), 580633.
Patania, A., Selvaggi, P., Veronese, M., Dipasquale, O., Expert, P., Petri, G., 2019. Topological gene expression networks recapitulate brain anatomy and function. Netw Neurosci. 3 (July (3)), 744–762.
Patel, Y., Shin, J., Drakesmith, M., Evans, J., Pausova, Z., Paus, T., 2020. Virtual histology of multi-modal magnetic resonance imaging of cerebral cortex in young men. Neuroimage. 22 (May (218)), 116968.
Pletikos, M., Sousa, A.M.M., Sedmak, G., Meyer, K.A., Zhu, Y., Cheng, F., et al., 2014. Temporal specification and bilaterality of human neocortical topographic gene expression. Neuron. 81 (January (2)), 321–332.
Richiardi, J., Altmann, A., Milazzo, A.-C., Chang, C., Chakravarty, M.M., Banaschewski, T., et al., 2015. BRAIN NETWORKS. Correlated gene expression supports synchronous activity in brain networks. Science 348 (June (6240)), 1241–1244.
Ritchie, J., Pantazatos, S.P., French, L., 2018. Transcriptomic characterization of MRI contrast with focus on the T1-w/T2-w ratio in the cerebral cortex. Neuroimage. (July (174)), 504–517.
Rizzo, G., Veronese, M., Heckemann, R.A., Selvaraj, S., Howes, O.D., Hammers, A., et al., 2014a. The predictive power of brain mRNA mappings for in vivo protein density: a positron emission tomography correlation study. J. Cereb. Blood Flow Metab. 34 (May (5)), 827–835.
Rizzo, G., Veronese, M., Tonietto, M., Zanotti-Fregonara, P., Turkheimer, F.E., Bertoldo, A., 2014b. Kinetic modeling without accounting for the vascular component impairs the quantification of [(11)C]PBR28 brain PET data. J. Cereb. Blood Flow Metab. 34 (June (6)), 1060–1069.
Rizzo, G., Veronese, M., Expert, P., Turkheimer, F.E., Bertoldo, A., 2016. MENGA: A new comprehensive tool for the integration of neuroimaging data and the allen human brain transcriptome atlas. PLoS One 11 (February (2)), e0148744.
Romero-Garcia, R., Whitaker, K.J., Váša, F., Seidlitz, J., Shinn, M., Fonagy, P., et al., 2018. Structural covariance networks are coupled to expression of genes enriched in supragranular layers of the human cortex. Neuroimage. 171 (May 1), 256–267.
Romme, I.A.C., de Reus, M.A., Ophoff, R.A., 2017. Kahn RS, van den Heuvel MP. Connectome disconnectivity and cortical gene expression in patients with schizophrenia. Biol. Psychiatry 81 (March (6)), 495–502.
Selvaggi, P., Hawkins, P.C.T., Dipasquale, O., Rizzo, G., Bertolino, A., Dukart, J., et al., 2019. Increased cerebral blood flow after single dose of antipsychotics in healthy volunteers depends on dopamine D2 receptor density profiles. Neuroimage. 188, 774–784.
Sepulcre, J., Grothe, M.J., d'Oleire Uquillas, F., Ortiz-Terán, L., Diez, I., Yang, H.-S., et al., 2018. Neurogenetic contributions to amyloid beta and tau spreading in the human cortex. Nat. Med. 24 (October (12)), 1910–1918.
Shen, E.H., Overly, C.C., Jones, A.R., 2012. The Allen Human Brain Atlas: comprehensive gene expression mapping of the human brain. Trends Neurosci. 35 (December (12)), 711–714.
Shin, J., French, L., Xu, T., Leonard, G., Perron, M., Pike, G.B., et al., 2018. Cell-specific gene-expression profiles and cortical thickness in the human brain. Cereb. Cortex 28 (September (9)), 3267–3277.
Tao-Cheng, J.H., Zhou, F.C., 1999. Differential polarization of serotonin transporters in axons versus soma-dendrites: an immunogold electron microscopy study. Neuroscience 94 (3), 821–830. https://doi.org/10.1016/s0306-4522(99)00373-5. PMID: 10579573.
Unterholzner, J., Gryglewski, G., Philippe, C., Seiger, R., Pichler, V., Godbersen, G.M., et al., 2020. Topologically guided prioritization of candidate gene transcripts coexpressed with the 5-HT1A receptor by combining in vivo PET and allen human brain atlas data. Cereb. Cortex (January), 28.
Veronese, M., Bodini, B., García-Lorenzo, D., Battaglini, M., Bongarzone, S., Comtat, C., et al., 2015. Quantification of [(11)C]PIB PET for imaging myelin in the human

brain: a test-retest reproducibility study in high-resolution research tomography. J. Cereb. Blood Flow Metab. 35 (November (11)), 1771–1782.
Veronese, M., Zanotti-Fregonara, P., Rizzo, G., Bertoldo, A., Innis, R.B., Turkheimer, F.E., 2016. Measuring specific receptor binding of a PET radioligand in human brain without pharmacological blockade: the genomic plot. Neuroimage. 15 (April (130)), 1–12.
Veronese, M., Reis Marques, T., Bloomfield, P.S., Rizzo, G., Singh, N., Jones, D., et al., 2017. Kinetic modelling of [(11)C]PBR28 for 18 kDa translocator protein PET data: a validation study of vascular modelling in the brain using XBD173 and tissue analysis. J. Cereb. Blood Flow Metab. (January), 1, 271678X17712388.
Vértes, P.E., Rittman, T., Whitaker, K.J., Romero-Garcia, R., Váša, F., Kitzbichler, M.G., et al., 2016. Gene transcription profiles associated with inter-modular hubs and connection distance in human functional magnetic resonance imaging networks. Philos. Trans. R. Soc. Lond., B, Biol. Sci. 371 (October (1705)).
Vogel, J.W., La Joie, R., Grothe, M.J., Diaz-Papkovich, A., Doyle, A., Vachon-Presseau, E., et al., 2020. A molecular gradient along the longitudinal axis of the human hippocampus informs large-scale behavioral systems. Nat. Commun. 11 (February (1)), 960.
Writing Committee for the Attention-Deficit/Hyperactivity Disorder, Autism Spectrum Disorder, Bipolar Disorder, Major Depressive Disorder, Obsessive-Compulsive Disorder, Schizophrenia ENIGMA Working Groups, et al., 2020. Virtual histology of cortical thickness and shared neurobiology in 6 psychiatric disorders. JAMA Psychiatry (August), 26.
Zanotti-Fregonara, P., Pascual, B., Veronese, M., Yu, M., Beers, D., Appel, S.H., et al., 2019. Head-to-head comparison of 11C-PBR28 and 11C-ER176 for quantification of the translocator protein in the human brain. Eur. J. Nucl. Med. Mol. Imaging 31 (May), 1–8.

Appendix C (Selvaggi et al. Psychol Med, 2022)

Psychological Medicine

cambridge.org/psm

Original Article

*Designates equal contribution as first author.

Cite this article: Selvaggi P *et al* (2022). Reduced cortical cerebral blood flow in antipsychotic-free first-episode psychosis and relationship to treatment response. *Psychological Medicine* 1–11. https://doi.org/10.1017/S0033291722002288

Received: 24 November 2021
Revised: 27 June 2022
Accepted: 4 July 2022

Key words:
Arterial spin labelling; cerebral blood flow; first-episode psychosis; schizophrenia

Author for correspondence:
Oliver D. Howes,
E-mail: oliver.howes@kcl.ac.uk

Reduced cortical cerebral blood flow in antipsychotic-free first-episode psychosis and relationship to treatment response

Pierluigi Selvaggi[1,2,*], Sameer Jauhar[3,4,*], Vasileia Kotoula[1], Fiona Pepper[3], Mattia Veronese[1], Barbara Santangelo[1], Fernando Zelaya[1], Federico E. Turkheimer[1], Mitul A. Mehta[1] and Oliver D. Howes[3,5,6]

[1]Department of Neuroimaging, Institute of Psychiatry, Psychology and Neuroscience, King's College London, London, UK; [2]Azienda Ospedaliero-Universitaria Consorziale Policlinico di Bari, Bari, Italy; [3]Department of Psychosis Studies, Institute of Psychiatry, Psychology and Neuroscience, King's College London, London, UK; [4]Early Intervention Psychosis Clinical Academic Group, South London & Maudsley NHS Foundation Trust, London, UK; [5]MRC London Institute of Medical Sciences, Hammersmith Hospital, London W12 0NN, UK and [6]Faculty of Medicine, Institute of Clinical Sciences (ICS), Imperial College London, Du Cane Road, London W12 0NN, UK

Abstract

Background. Altered cerebral blood flow (CBF) has been found in people at risk for psychosis, with first-episode psychosis (FEP) and with chronic schizophrenia (SCZ). Studies using arterial spin labelling (ASL) have shown reduction of cortical CBF and increased subcortical CBF in SCZ. Previous studies have investigated CBF using ASL in FEP, reporting increased CBF in striatum and reduced CBF in frontal cortex. However, as these people were taking antipsychotics, it is unclear whether these changes are related to the disorder or antipsychotic treatment and how they relate to treatment response.

Methods. We examined CBF in FEP free from antipsychotic medication ($N = 21$), compared to healthy controls ($N = 22$). Both absolute and relative-to-global CBF were assessed. We also investigated the association between baseline CBF and treatment response in a partially nested follow-up study ($N = 14$).

Results. There was significantly lower absolute CBF in frontal cortex (Cohen's $d = 0.84$, $p = 0.009$) and no differences in striatum or hippocampus. Whole brain voxel-wise analysis revealed widespread cortical reductions in absolute CBF in large cortical clusters that encompassed occipital, parietal and frontal cortices (Threshold-Free Cluster Enhancement (TFCE)-corrected <0.05). No differences were found in relative-to-global CBF in the selected region of interests and in voxel-wise analysis. Relative-to-global frontal CBF was correlated with percentage change in total Positive and Negative Syndrome Scale after antipsychotic treatment ($r = 0.67$, $p = 0.008$).

Conclusions. These results show lower cortical absolute perfusion in FEP prior to starting antipsychotic treatment and suggest relative-to-global frontal CBF as assessed with magnetic resonance imaging could potentially serve as a biomarker for antipsychotic response.

Introduction

Schizophrenia (SCZ) and related psychotic disorders are amongst the leading causes of global disease burden (McCutcheon, Reis Marques, & Howes, 2020b). Current treatments are ineffective for many patients (Kaar, Natesan, McCutcheon, & Howes, 2020), highlighting the need to understand the neurobiology underlying psychosis to inform development of new drug treatments (Jauhar & Howes, 2019; McCutcheon, Krystal, & Howes, 2020a). Altered brain perfusion and metabolism have been implicated in the neurobiology of SCZ (Goozée, Handley, Kempton, & Dazzan, 2014; Hill et al., 2004; Townsend et al., 2022), initially with positron emission tomography (PET). PET studies with [^{18}F]-fluorodeoxyglucose (FDG) and [^{15}O]H_2O reported hypometabolism and hypoperfusion in frontal, anterior cingulate, temporal and parietal cortices (Andreasen et al., 1997; Buchsbaum et al., 1982; Gur et al., 1995). More recently, arterial spin labelling (ASL), utilizing magnetic resonance imaging (MRI), has been used to measure cerebral blood flow (CBF). Because of the well-established phenomenon of neuro-vascular coupling, measures of regional CBF are an indirect but highly sensitive signature of regional cellular activity. ASL studies in people with chronic SCZ, treated with antipsychotics, show reduced CBF in frontal, parietal and occipital regions and increased CBF in basal ganglia (Legind et al., 2019; Liu, Qiu, Constable, & Wexler, 2012a; Oliveira et al., 2018; Pinkham et al., 2011, 2015), though the basal ganglia findings have not been consistently replicated (Ota et al., 2014; Zhu et al., 2017). Thus, there is evidence for cortical hypoperfusion in chronic SCZ, but it is unclear from these studies when this occurs in development of the

https://doi.org/10.1017/S0033291722002288 Published online by Cambridge University Press

disorder. Studies in clinical high risk for psychosis (CHR-P) individuals have reported increased CBF in basal ganglia and hippocampus (Allen et al., 2016, 2018; Modinos et al., 2018b). Increased hippocampal perfusion in CHR-P individuals has also been found with gadolinium-enhanced MRI (Schobel et al., 2013). These findings indicate that CBF alterations may occur early in development of psychosis, though, because the majority of CHR-P subjects do not go on to develop psychosis, it is unclear how specific they are to psychosis. To date, only one study has investigated cerebral perfusion using ASL in people with first-episode psychosis (FEP) (Kindler et al., 2018). This study found increased perfusion in basal ganglia and reduced CBF in frontal cortex in people with FEP, all of whom were taking antipsychotic medication.

However, antipsychotics have effects on brain metabolism and CBF (Goozée et al., 2014; Hawkins et al., 2018; Mehta et al., 2003; Miller et al., 1997; Turkheimer et al., 2020), with evidence from preclinical models (Sander et al., 2013, 2019; Sander, Hooker, Catana, Rosen, & Mandeville, 2016; Viviani, Graf, Wiegers, & Abler, 2013) and experimental medicine studies in healthy individuals (Hawkins et al., 2018; Selvaggi et al., 2019; Viviani et al., 2013) suggesting that antipsychotics increase CBF in the basal ganglia with a mechanism possibly mediated by D_2 receptors (Sander et al., 2013; Selvaggi et al., 2019). The effect of antipsychotics on cortical perfusion is even less understood. Studies using PET and single photon emission computed tomography (SPECT) found consistently reduced perfusion and metabolism in the frontal cortex in both medicated and unmedicated patients with SCZ (Makarić et al., 2017; Molina et al., 2005). Viviani et al. (2013) found decreased cortical perfusion after amisulpride administration in healthy volunteers. It is therefore unclear if previous findings in FEP were confounded by antipsychotic treatment and what is the extent of the interaction between antipsychotic effects and pathophysiology. Thus, we aimed to determine if CBF is altered in people in their first episode of psychosis who are free from antipsychotic medication (baseline study). Based on prior studies in FEP and subjects at CHR-P, we hypothesized that antipsychotic-free people with FEP would show lower absolute CBF in the frontal cortex while keeping CBF in the striatum within physiological ranges.

Moreover, while previous cross-sectional investigations have shown associations between altered CBF and severity of psychotic symptoms in SCZ (Kindler et al., 2018; Pinkham et al., 2011), it is unknown if brain perfusion before treatment is associated with subsequent symptomatic improvement with antipsychotic treatment. Thus, we aimed to explore this association in a prospective study of patients who went on to receive antipsychotic treatment (follow-up study). To summarize, we adopted a partially nested two-study design to (i) investigate differences in brain perfusion in FEP prior to start antipsychotic treatment (baseline study) and (ii) identify brain perfusion markers of treatment response possibly unbiased by antipsychotic effects on CBF.

Materials and methods

Study participants

Study participants were recruited from FEP teams within South London and Maudsley NHS Foundation Trust (Fusar-Poli et al., 2020) and Central and West London NHS Trust. All participants provided informed written consent. For both groups' exclusion criteria were history of head trauma, dependence on illicit drugs, any significant medical co-morbidity (minor illnesses such as seasonal allergies were permitted) and contra-indication to MRI scanning.

Baseline study

Inclusion criteria for the patient group were: psychotic disorder according to ICD-10 criteria (World Health Organization, 2004) in first episode of illness. Age and gender-matched healthy volunteers were recruited through local advertisement from the same geographical areas. Inclusion criteria for healthy controls (HCs) were: no personal history of psychiatric illness [assessed using the Structured Clinical Interview for the DSM (First, 2014)] and no history of psychotropic medication use. All patients were antipsychotic-naïve or antipsychotic-free for at least 6 weeks for oral antipsychotics or 6 months for depot antipsychotics (Jauhar et al., 2019; Leucht et al., 2015). The sample included nine antipsychotic-naïve and 12 antipsychotic-free patients. All but one patient included in the baseline study was not taking other psychotropic medication (i.e. antidepressants, mood stabilizers, benzodiazepines) at the time of MRI scan. Only one patient was taking antidepressant medication (sertraline) at the time of MRI scan (Viviani, Abler, Seeringer, & Stingl, 2012).

Follow-up study

Inclusion criteria for the patient group were: psychotic disorder according to ICD-10 criteria (World Health Organization, 2004); in first episode of illness; and antipsychotic-free or -naïve or minimally treated [taking antipsychotics at minimal effective dose for less than 2 weeks (Agid, Kapur, Arenovich, & Zipursky, 2003; Levine & Leucht, 2012)]. All patients were clinically assessed at baseline and reassessed after taking antipsychotic treatment, at a therapeutic dose as specified in the Maudsley Prescribing Guidelines (Taylor, Barnes, & Young, 2018), for a minimum of 4 weeks. All patients were in stable treatment at follow-up after titration. Clinical measures were rated at baseline and follow-up using the Positive and Negative Syndrome Scale (PANSS) (Kay, Fiszbein, & Opler, 1987). Patients received follow-up for at least 6 months to determine if there had been a subsequent response in patients who showed non-response at 4 weeks (duration to follow-up in months 24.73 ± 16.89). Subjects with psychosis were classified by antipsychotic exposure as antipsychotic-naïve, antipsychotic-free [prior oral antipsychotic medication but free of treatment for at least 6 week (oral) or 6 months (depot, if relevant)] or minimally treated (taking antipsychotic medication for 2 weeks or less) (Jauhar et al., 2019; Leucht et al., 2015). The sample included seven antipsychotic-naïve, four antipsychotic-free and three people minimally treated with antipsychotics.

MRI acquisition and pre-processing

MRI acquisition

Scans were acquired using a GE MR750 3-T scanner and a 12-channel head coil. A T1-weighted MPRAGE scan was also acquired (FOV = 260 mm; echo time = 2.8 ms; repetition time = 6.98 ms; 256 × 256 matrix; slice thickness = 1.2 mm, flip angle = 11) for normalization purposes. A T2-weighted image (FOV = 240 mm; echo time = 54.68 ms; repetition time = 4380 ms; 320 × 320 matrix; slice thickness = 4 mm) was also acquired and used for the pre-processing of ASL images (see below). ASL data were acquired using a pseudo-continuous arterial spin labelling sequence (PCASL). Four control-label pairs were

https://doi.org/10.1017/S0033291722002288 Published online by Cambridge University Press

used (labelling time = 1525 ms; post labelling delay = 1500 ms). Images were read with a 3D Fast-Spin echo stack of spirals scheme, consisting of eight inter-leaved spiral arms, 512 points per arm and 60 slice-locations of 3 mm thickness. The raw spatial resolution of the perfusion sensitive images was approximately 3.6 mm in plane and 3 mm through plane; and the data points were re-gridded to a rectangular matrix prior to Fourier transformation and written with a voxel size of $1 \times 1 \times 3$ mm (no gap). The sequence had background suppression for optimum reduction of the static tissue signal (for further details, see online Supplementary materials). A proton density (PD) image was also acquired over 48 s using the same acquisition parameters.

Pre-processing

PD images were used to obtain quantification of absolute CBF in standard physiological units (ml blood/100 g tissue/min) using the formula suggested in the recent ASL consensus paper (Alsop et al., 2015). The unified segmentation algorithm in SPM12 (Ashburner & Friston, 2005) was used to create grey matter, white matter and cerebrospinal fluid (CSF) images from each T1-weighted image and to create a set of flow fields to later transform each subject's T1-weighted and ASL data into standard space. The T2-weighted images were co-registered to the T1-weighted images. Each raw PD image was then co-registered to the T2 image. The parameters for this transformation were then applied to the CBF maps (as they were already in alignment with the PD image) prior to their normalization. The addition of these two co-registration steps helped us to achieve a better alignment between CBF and T1-weighted images which prevented from distortions during normalization. Images were resampled to 2 mm isotropic voxels and normalized into a standard space (Montreal Neurological Institute, MNI). Finally, the normalized CBF maps were smoothed using a 6 mm full width at half maximum (FWHM) kernel. Normalized T1-weighted images were also smoothed using a 6 mm FWHM kernel.

Statistical analysis

Demographics

Demographic characteristics (i.e. age, gender) were compared between FEP and HC using χ^2 or independent sample t tests for categorical and continuous data respectively.

Region of interest (ROI) analysis

Absolute CBF values in the whole grey matter and in each ROI were extracted using spatially normalized to individual grey matter images and the WFU-Pickatlas ROIs with the MarsBar toolbox (http://marsbar.sourceforge.net). Based on previous findings (Allen et al., 2016; Kindler et al., 2018), the following bilateral ROIs were selected as our primary ROIs: the frontal cortex (size = 61 104 mm), the hippocampus (size = 15 024 mm) and the striatum (size = 36 816 mm). For comparisons with previous investigations (Allen et al., 2016; Kindler et al., 2018), we also explored differences between FEP and HC in relative-to-global-perfusion CBF (relative CBF). For each ROI a linear regression model was performed with absolute CBF in the ROI as the dependent variable and global grey matter CBF as the independent variable. For each linear regression in each ROI unstandardized residuals were computed.

To test our primary hypothesis that FEP would show reduced absolute CBF in frontal cortex and increased CBF in striatum and hippocampus, a repeated measure analysis of variance (ANOVA) was used with 'ROI' as the within-subject factor and 'GROUP' as the between-subject factor. Tukey HSD test has been used for post-hoc pairwise comparison. An independent sample t test was used to test absolute CBF in the whole grey matter to determine if there was a global group difference in CBF. Cohen's d has been computed to obtain estimates of effect size. To test differences in relative-to-global CBF, absolute CBF unstandardized residual against global grey matter CBF were entered as dependent variables in a repeated measure ANOVA with 'ROI' as within-subject variable and 'GROUP' as between-subjects variable. Tukey HSD has been used for post-hoc pairwise comparison.

Voxel-wise analysis

Differences in absolute CBF were also tested in whole-brain voxel-wise analyses. Based on recent recommendations (Eklund, Nichols, & Knutsson, 2016), we performed non-parametric analysis as implemented in FSL *randomise* (Winkler, Ridgway, Webster, Smith, & Nichols, 2014) and threshold-free cluster enhancement (TFCE) (Smith & Nichols, 2009) with 5000 permutations to create a non-parametric null distribution and calculate a 5% significant threshold. We also tested relative-to-global-perfusion CBF differences between FEP and HC in voxel-wise analysis using FSL *randomise* by including global grey matter CBF as a nuisance covariate in the model. An independent sample t test was used to test differences in intracranial volume (ICV) between FEP and HC.

Structural analysis

In order to check whether results could be influenced by differences in grey matter volume differences between FEP and HC, standard voxel-based morphometry (VBM) analysis as implemented in SPM was performed on pre-processed T1-weighted images to determine if there were volumetric differences between groups. Voxel-wise independent sample t test as implemented in SPM were performed to assess differences in grey matter volume between FEP and controls. Grey matter, white matter and CSF images of each subject were combined to obtain estimates of total ICV. In addition, T1-weighted images were processed using FreeSurfer (version 7.1.1, http://surfer.nmr.harvard.edu) image analysis suite to produce measures of cortical thickness estimates using the FreeSurfer automated brain segmentation process (*recon-all*) (Fischl & Dale, 2000; Salat et al., 2004). An FWHM Gaussian kernel of 10 mm was applied. Vertex-wide independent sample t test was performed for both left and right hemisphere to assess differences in cortical thickness between FEP and controls. Both FEP > HC and FEP < HC contrast were analysed. Cluster-level correction for multiple comparison was implemented with $-\log 10(p)$value = 3 as cluster-defining threshold and alpha = 0.05 (Greve & Fischl, 2018).

Correlation with PANSS change

Percentage changes in PANSS was calculated, adjusting for minimum scores (% change in total PANSS = [((baseline score – 30) − (follow-up score – 30))/(baseline score − 30)] × 100) (Leucht et al., 2005).

To explore the association between baseline CBF and improvement in symptoms, linear regression analysis was performed between both baseline absolute and relative-to-global-CBF values from our primary ROIs and percentage change in total PANSS. For each linear regression model Bonferroni correction was applied for the number of ROI tested (alpha = 0.05/3 = 0.016). For all linear regression models Mahalanobis distance and

https://doi.org/10.1017/S0033291722002288 Published online by Cambridge University Press

Cook's distance were computed to examine the presence of multivariate outliers and to estimate the presence of highly influential data points. To identify multivariate outliers, Mahalanobis distance values were compared to a χ^2 distribution with degrees of freedom equal to the number of variables (two in this case) with $p = 0.001$ (Finch, 2012). Any data point with Cook's distance higher than 1 was considered a highly influential outlier and excluded from the analysis as recommended [see Cook & Weisberg, 1982]. To further test the robustness of our analysis reducing the effect of extreme observations, we used the bias-corrected accelerated bootstrap technique with 10 000 resamples (Efron & Tibshirani, 1986).

Results

Baseline study

Demographics

Twenty-one people with FEP [mean age ± standard deviation (S.D.), 24.85 ± 3.85, three female] and 22 HC (23.45 ± 3.21, eight female) were included in the baseline study. HC and FEP groups did not significantly differ in age ($t = 1.29$, $p = 0.3$) or gender ($\chi^2 = 2.8$, $p = 0.1$) (Table 1).

Absolute CBF

Absolute whole brain CBF was significantly lower in FEP (mean ± S.D., 27.642 ± 59.52) as compared to controls (mean ± S.D., 32.334 ± 43.75) ($t = -2.94$, df = 41, $p = 0.005$, Cohen's $d = 0.89$). Results did not change after removal of the subject receiving antidepressant at the time of the scan ($p < 0.001$).

Table 1. Summary of demographic and clinical characteristics of the baseline study sample

	FEP, $n = 21$	HC, $n = 22$	p value
Age (mean ± S.D.)	24.85 ± 3.85	23.45 ± 3.21	0.3
Gender (M/F)	18/3	14/8	0.1
Education (years, mean ± S.D.)	14.4 ± 2.1	15.68 ± 2.6	0.1
PANSS total baseline (mean ± S.D.)	70.7 ± 18.6	–	–
PANSS positive baseline (mean ± S.D.)	13.7 ± 4.4	–	–
PANSS negative baseline (mean ± S.D.)	13.4 ± 6.3	–	–
Antipsychotic-naïve (%)	43	–	–
Antipsychotic-free (%)	57	–	–
Minimal antipsychotic treatment (%)	0	–	
Smoking status (never/past/current)	13/2/6	12/6/4	0.3
Substance use (never/past/current)	17/3/1	15/3/4	0.4
Alcohol (never/past/current)	11/2/8	9/1/12	0.5
Ethnicity (white/black/Asian/others)	4/6/5/6	4/13/3/2	–

There was a significant main effect of 'GROUP' ($F = 4.74$, $p = 0.035$) and a significant 'ROI' × 'GROUP' interaction ($F = 3.89$, $p = 0.032$ after Greenhouse–Geisser correction) on absolute CBF. Tukey HSD *post hoc* test revealed significantly lower absolute CBF in the frontal cortex in FEP as compared to HC ($t = -2.75$, df = 41, $p = 0.009$, Cohen's $d = 0.84$) with no statistically significant differences between FEP and HC in the hippocampus ($t = -1.5$, df = 41, $p = 0.13$) or striatum ($t = -1.4$, df = 41, $p = 0.1$). Results did not change after removal of the subject receiving antidepressant at the time of the scan ($p < 0.001$). Figure 1 shows absolute CBF values in the three ROIs (i.e. frontal cortex, hippocampus and striatum).

We conducted an exploratory analysis separating the patients into antipsychotic-naïve and antipsychotic-free sub-groups. This shows that CBF levels are similar in antipsychotic-naïve and antipsychotic-free sub-groups (see online Supplementary materials).

Relative-to-global CBF

There was a trend towards a significant main effect of 'GROUP' ($F = 3.9$, $p = 0.054$), but no significant main effect of 'ROI' ($p = 0.85$) or significant 'ROI × GROUP' interaction ($p = 0.23$) on relative CBF.

CBF whole-brain voxel-wise analysis

Figure 2 shows whole-brain voxel-wise differences ($p < 0.05$, TFCE-corrected) between FEP and HC. The direct voxel-wise comparison revealed significantly lower CBF in FEP compared to HC in widespread cortical areas including frontal, parietal and occipital areas. The opposite contrast (i.e. HC < FEP) did not reveal any significant clusters.

Whole brain voxel-wise analysis of relative-to-global CBF did not reveal any TFCE-corrected cluster in either FEP > HC or FEP < HC contrasts.

Structural analysis

FEP and HC did not differ in total grey matter volume ($t = -1.8$, df = 41, $p = 0.08$) or total ICV ($t = 0.95$, df = 41, $p = 0.96$). Voxel-wise VBM analysis did not reveal any significant differences in grey matter volume between FEP and HC. FreeSurfer analysis did not reveal any significant cluster of cortical thickness differences between FEP and HC.

Follow-up study

Demographics

Fourteen FEP (23.85 ± 3.77, four female) were included in the follow-up study. Eleven patients also took part in the baseline study (Table 2).

Correlations between baseline CBF and PANSS change

There were no significant associations between absolute CBF extracted from the ROIs and percentage change in total PANSS score ($p > 0.32$). However, relative-to-global CBF in the frontal cortex correlated positively with percentage change in total PANSS (Fig. 3; $r = 0.67$, $p = 0.008$). In all linear regression models, none of the data points were identified as influential outliers (all Cook's distances < 1) or multivariate outliers (all Mahalanobis distances $p > 0.001$). Results were retained after applying bias-corrected accelerated bootstrap technique with 10 000 resamples (bootstrapped $p = 0.05$). In addition, Spearman rank correlations

https://doi.org/10.1017/S0033291722002288 Published online by Cambridge University Press

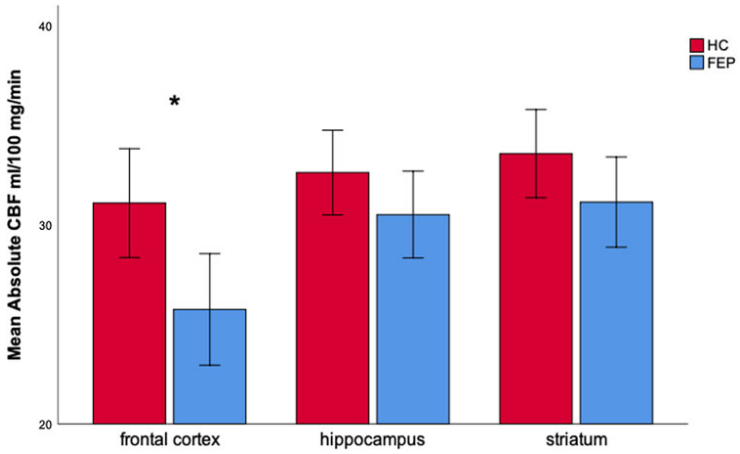

Fig. 1. Absolute CBF in the selected a priori ROIs. There were significant main effects of group and ROI, and a significant group*ROI interaction (p = 0.032, Greenhouse-Geisser correction). Post-hoc testing showed that CBF was significantly lower in the frontal cortex (Cohen's d = 0.84, p = 0.009) but not the other regions in patients with FEP relative to controls. FEP = first episode psychosis, HC = healthy controls. Asterisks (*) indicated significant tests. Bars indicate 95% confidence intervals.

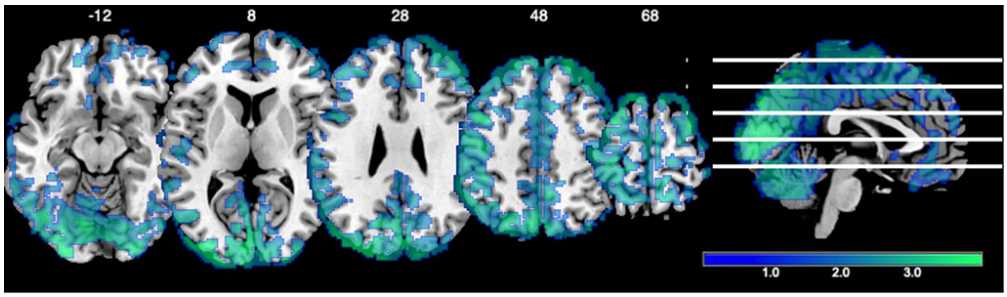

Fig. 2. Brain sections showing significantly lower absolute CBF in FEP relative to HC in frontal, parietal and occipital cortex (TFCE corrected clusters). Colorbar indicates t-statistics.

yielded similar results to linear regression analysis (Spearman rho = 0.574, p = 0.032).

Discussion

We found absolute CBF was significantly lower in frontal cortex but not striatum or hippocampus in people with FEP free of antipsychotic medication. Our whole brain analyses found significantly lower perfusion in the patients in additional cortical areas, including the parietal and occipital cortices.

Lower perfusion and metabolism of frontal cortex at rest is a replicated finding in chronic SCZ (Bullmore et al., 1999; Weinberger & Berman, 1988) demonstrated using various neuroimaging techniques including SPECT, [^{18}F]-FDG and [^{15}O]-H_2O PET, blood oxygen level dependent (BOLD) signal [i.e. functional magnetic resonance imaging (fMRI)] and recently with ASL (Hill et al., 2004; Kindler et al., 2015). Interestingly previous studies using PET and SPECT in unmedicated FEP revealed reduced cortical perfusion and metabolism (Brewer et al., 2007; Makarić et al., 2017; Molina et al., 2005). Our results corroborate and extend this evidence by showing the existence of lower frontal cortical absolute perfusion in FEP without the potential confound of antipsychotic treatment using MRI. In addition, our exploratory whole brain analyses indicate cortical hypoperfusion extends beyond the frontal cortex, including both parietal and occipital cortices. This extends evidence that the function of these regions is altered during cognitive tasks in SCZ (Calderone et al., 2013; Hahn, Robinson, Leonard, Luck, & Gold, 2018; Weiss et al., 2009) to show perfusion is also altered early in illness course. In contrast to findings in antipsychotic-treated patients and people at clinical risk of psychosis (Allen et al., 2018; Kindler et al., 2018), we found no significant difference in relative-to-global CBF in the striatum or hippocampus relative to controls. When our results are considered alongside preclinical (Mandeville et al., 2013; Sander et al., 2013, 2019) and clinical (Handley et al., 2013; Selvaggi et al., 2019; Shcherbinin et al., 2015; Viviani et al., 2013) evidence that antipsychotics increase striatal

https://doi.org/10.1017/S0033291722002288 Published online by Cambridge University Press

Table 2. Summary of demographics and clinical characteristics of the follow-up study sample

	FEP, $n = 14$	p value
Age (mean ± S.D.)	23.85 ± 3.77	–
Gender (M/F)	10/4	–
PANSS total baseline (mean ± S.D.)	75.42 ± 18.2	–
PANSS positive baseline (mean ± S.D.)	20.21 ± 6.19	–
PANSS negative baseline (mean ± S.D.)	15.57 ± 6.5	–
PANSS total follow-up (mean ± S.D.)	58.7 ± 19.22	–
PANSS positive follow-up (mean ± S.D.)	13.9 ± 5.5	–
PANSS negative follow-up (mean ± S.D.)	14.5 ± 7.1	–
PANSS total change (mean ± S.D.)	32.6 ± 33.1	0.02
PANSS positive change (mean ± S.D.)	9.4 ± 9.1	0.01
PANSS negative change (mean ± S.D.)	5.9 ± 9.3	0.29
Antipsychotic-naïve (%)	50	–
Antipsychotic-free (%)	29	–
Minimal antipsychotic treatment (%)	21	–
Smoking status (never/past/current)	6/4/4	–
Substance use (never/past/current)	7/4/3	–
Alcohol (never/past/current)	6/3/5	–
Ethnicity (white/black/Asian/others)	1/4/4/5	–

perfusion, with a mechanism possibly mediated by D_2 receptors (Selvaggi et al., 2019), this could indicate that previous evidence of higher striatal CBF in people with SCZ taking antipsychotics might be explained by D_2 receptors blockade.

Longitudinal studies are required to confirm preliminarily evidence (Goozée et al., 2014) suggesting that treatment does increase striatal perfusion in patients.

We did not find any differences in hippocampus in either absolute or relative-to-global perfusion, in contrast to findings in people at clinical risk of psychosis. Taken with our findings in frontal cortex, this could suggest that there is progression of pathophysiological alterations from the hippocampus prior to the onset of psychosis to the frontal cortex with the development of illness. However, it should be recognized that not all subjects at clinical risk develop psychosis and longitudinal studies with repeated scanning are required to test if there are changes in hypoperfusion during the development of psychosis.

Relative-to-global CBF in the frontal cortex at presentation explained approximately 40% of the variance in subsequent response to antipsychotic treatment, such that patients with higher relative-to-global CBF showed higher symptom improvement with treatment. These results extend prior evidence that response to antipsychotic treatment in FEP is associated with functional connectivity (Sarpal et al., 2016), $D_{2/3}$ availability (Wulff et al., 2015), and dopamine synthesis capacity (Jauhar et al., 2019) to suggest that relative frontal perfusion could potentially contribute to a biomarker for antipsychotic response in FEP (Veronese et al., 2021). We did not find correlations between relative-to-global CBF in the striatum and hippocampus and PANSS change. However, given the lower CBF in a number of cortical regions in patients, it might be possible that cortical regions other than the frontal cortex are also linked to treatment response but we were underpowered to detect these relationships. We did not find correlations between absolute CBF and PANSS change, suggesting that changes in local perfusion relative to whole brain perfusion are best able to capture variability in clinical response. We found that antipsychotic-free FEP show lower absolute CBF in cortical regions but no significant difference in

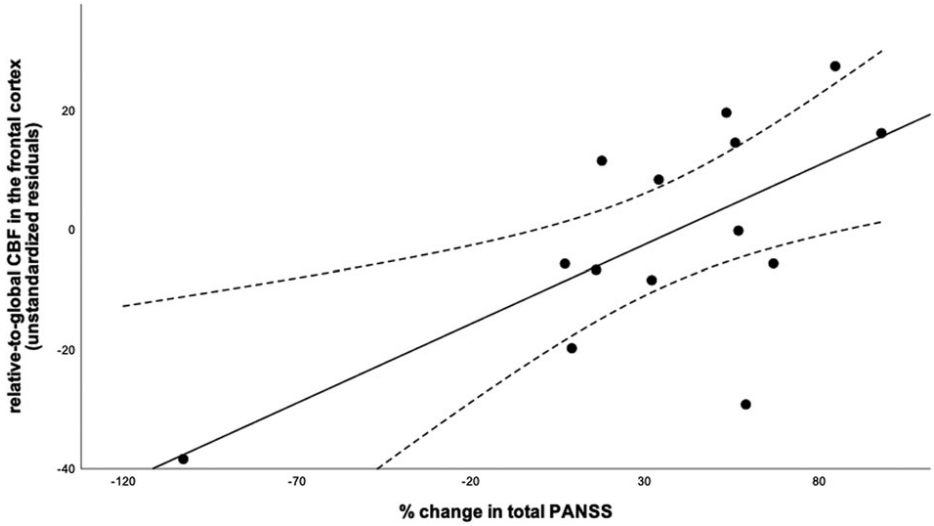

Fig. 3. Scatterplots showing significant correlations between relative-to-global frontal CBF at baseline and percentage improvement in total PANSS with subsequent treatment ($r = 0.57$, $p = 0.05$).

https://doi.org/10.1017/S0033291722002288 Published online by Cambridge University Press

relative-to-global CBF. Treatment response was associated with relative-to-global frontal CBF but not with absolute CBF. The absence of group differences in relative-to-global CBF are consistent with our whole brain findings that indicate that there is lower absolute CBF in other cortical regions, mainly driven by lower CBF in parietal and occipital cortices as compared with controls. On the other hand, subcortical CBF (i.e. striatal and hippocampal) seems to be unaltered in patients relative to controls (see Bayes factor testing in online Supplementary materials). Thus, taken together, these findings suggest an imbalance between cortical and subcortical blood flow early in SCZ. The association between relative-to-global CBF (but not absolute CBF) with treatment response might seem counterintuitive. However, this finding might be less difficult to interpret considering the direct association between the two variables. Patients with larger positive improvement in symptoms (i.e. greater symptoms reduction) were those with relatively lower alterations in frontal CBF as compared with the rest of the cortex (i.e. higher relative-to-global frontal CBF), suggesting that patients with more marked frontal hypofunction are less responsive to treatment with D_2 blockers. This extends other evidence of frontal dysfunction in patients whose illness does not respond to D_2 blockers (Mouchlianitis, McCutcheon, & Howes, 2016; Potkin et al., 2020). This interpretation is coherent with recent reports indicating neurovascular uncoupling in brain regions such the frontal cortex in SCZ (Sukumar, Sabesan, Anazodo, & Palaniyappan, 2020).

Strengths and limitations

Strengths of this study include the inclusion of people with FEP free from antipsychotic medication, and longitudinal measures in FEP patients. A methodological strength of the study is the evaluation of both absolute and relative-to-global CBF. Previous studies in CHR-P and FEP have used one metric without reporting the other (Allen et al., 2018; Kindler et al., 2018; Modinos et al., 2018b). However, our results suggest that antipsychotic-free FEP show different pattern of alteration in absolute and relative-to-global CBF. Therefore, we advise that future studies should include both metrics to facilitate comparisons. Previous works testing CBF differences in chronic SCZ as compared with HCs using ASL have shown variability in grey matter perfusion across individuals (Chen et al., 2022; Parkes, Rashid, Chard, & Tofts, 2004; Pinkham et al., 2011; Wang et al., 2004). In our study we used a 3D PCASL with background suppression which offers a non-invasive, efficient and highly reproducible tool to investigate brain perfusion as compared with other ASL methods (Alsop et al., 2015; Chen, Wang, & Detre, 2011). PCASL sequences have shown higher test–retest reliability as compared with other MRI sequences (such as BOLD task or resting state fMRI) used to identify biomarkers in psychosis (Holiga et al., 2018). In addition PCASL has shown good between- and within-subjects reliability [Intraclass coefficient (ICC) range: 0.63–0.83; (Holiga et al., 2018)], and comparable with PET [^{18}F]-DOPA [ICC range: 0.42–0.94; (Egerton, Demjaha, McGuire, Mehta, & Howes, 2010)], which has been proposed as a potential biomarker for treatment stratification in psychosis (Veronese et al., 2021). We obtained absolute CBF values on average of 40–50 ml/100 g tissue/min in grey matter in healthy volunteers which are at the lower range of previous investigations using pulsed ASL and/or other scanner manufacturers (Alsop et al., 2015). In our study we used a post-labelling approach and background suppression protocol that was slightly slower than the one recommended by the ASL white paper (Alsop et al., 2015), which could account for the slightly lower CBF values we obtained. However, we did not find artefactual hyper-perfusion regions in our analysis, suggesting that the post-labelling delay is not having a major effect on data quality. One potential issue in the imaging analysis could be the influence of partial volume effects given structural brain alterations in FEP (Brugger & Howes, 2017). However, we did not find group differences in grey matter volume, total ICV and cortical thickness, suggesting that partial volume effects are unlikely to explain our results, although we cannot completely rule out a contribution of partial volume effects to our findings. Demographic heterogeneity of the sample is thought to be an important factor contributing to variability across individuals. In particular age and gender have been strongly associated with CBF variability (Liu et al., 2012b; Viviani et al., 2009; Zhang et al., 2018). The groups were very similar in mean age and gender distribution. Nevertheless, to check for any influence of these, we conducted further analyses including these as covariates. Our findings remained essentially unchanged when gender and age were added as covariate of no interest (see online Supplementary materials), suggesting these are not influencing our findings. Body-mass index, caffeine intake or nicotine consumption immediately prior to scanning could be other sources of variability. In common with prior studies in psychosis (Davies et al., 2019; Modinos et al., 2018a; Overton, Bhagwat, Viviano, Jacobs, & Voineskos, 2020; Schneider et al., 2019), we did not control for these. However, the two groups were matched by smoking status, alcohol intake and substance use, which suggests that both caffeine intake and nicotine consumption might be similar between groups. Nevertheless, we cannot exclude group differences in use of these substances influencing our findings and further studies matching for intake on these would be useful.

In addition, it should be recognized that the frontal ROI is larger than the hippocampal and striatal ROIs. This may result in a higher signal-to-noise ratio (SNR) for the frontal region over these other regions, and consequently greater sensitivity to detect group differences. However, SNR estimates and sensitivity analyses (see online Supplementary materials) both suggest that it is unlikely that ROI size has affected our results.

Furthermore, in our follow-up study patients were treated in a naturalistic design. Thus, our findings do not provide information about the specific effects of antipsychotic treatment. Finally, although the baseline study constituted a larger cohort than that previously reported in FEP (Kindler et al., 2018), given the relatively modest sample size, further studies are needed to test the generalisability of our findings to other cohorts and settings.

Implications and future directions

Frontal dysfunction is one of the key mechanisms thought to contribute to the pathophysiology of psychosis (Howes & Murray, 2014; McCutcheon et al. 2020b; Weinberger & Berman, 1988). Our finding that frontal hypoperfusion is present early in the development of the disorder and in unmedicated patients is consistent with these models and other markers of frontal hypofunction in SCZ (Howes and McCutcheon, 2017; Onwordi et al., 2020; Osimo, Beck, Reis Marques, and Howes, 2019). In addition, given the close link between CBF and brain metabolism (Riederer et al., 2018), our results are in line with the evidence of increased lactate levels and pH (Dogan, Yuksel, Du, Chouinard, & Öngür, 2018; Du et al., 2014) and mitochondrial dysfunction in SCZ (Prince,

https://doi.org/10.1017/S0033291722002288 Published online by Cambridge University Press

Blennow, Gottfries, Karlsson, & Oreland, 1999; Rajasekaran, Venkatasubramanian, Berk, & Debnath, 2015) suggesting that altered brain oxidative capacity could be the pathophysiological substrate underlying abnormal brain function in psychosis. In addition, our results suggest alterations in brain perfusion at presentation are associated with subsequent antipsychotic response. These findings suggest that brain perfusion could be used to help predict future response.

Previous evidence suggested antipsychotics may normalize brain metabolism (Buchsbaum et al., 2009), however recently some authors have proposed that this normalization might not be sustainable in some patients (Turkheimer et al., 2020). Future longitudinal studies are therefore needed to understand the effect of antipsychotic treatment on brain metabolism in psychosis.

Conclusions

Our results provide evidence for lower frontal perfusion in FEP without the potential confound of antipsychotic treatment. In addition, relative CBF in frontal cortex at baseline is associated with subsequent antipsychotic response. These findings indicate there is cortical hypofunction early in the course of psychosis.

Supplementary material. The supplementary material for this article can be found at https://doi.org/10.1017/S0033291722002288.

Acknowledgements. We thank the patients who took part in this study, as well as the clinical teams within SLaM and CNWL who facilitated recruitment. We also thank the Guest editor and the reviewers for the critical in-depth reading of this manuscript and the very constructive comments.

Financial support. This study was funded by Medical Research Council-UK (no. MC_U120097115), Maudsley Charity (no. 666) and Wellcome Trust (no. 094849/Z/10/Z) grants to Prof. Howes. This paper represents independent research part funded by the National Institute for Health Research Biomedical Research Centre at South London and Maudsley NHS Foundation Trust and King's College London that support P. S., S. J., F. Z., M. V., M. A. M. and O. D. H. The views expressed are those of the authors and not necessarily those of the NHS, the NIHR or the Department of Health and Social Care. P. S. is supported by a Ph.D. studentship jointly funded by the NIHR-BRC at SLaM and the Department of Neuroimaging, King's College London. S. J. is funded by a JMAS Sim Fellowship from the Royal College of Physicians, Edinburgh.

Conflict of interest. S. J. has received honoraria for educational talks given for Sunovion. K. C. L. has received funding for educational talks S. J. has given. In the past 3 years M. A. M. has acted as an advisory board member for Lundbeck and Forum Pharmaceuticals. He also received research funding from Lundbeck, Takeda and Johnson & Johnson. Dr Howes is a part-time employee of Lundbeck and has received investigator-initiated research funding from and/or participated in advisory/speaker meetings organized by Angelini, Autifony, Biogen, Boehringer-Ingelheim, Eli Lilly, Heptares, Global Medical Education, Invicro, Jansenn, Lundbeck, Mylan, Neurocrine, Otsuka, Sunovion, Rand, Recordati and Roche. Dr Howes has a patent for the use of dopaminergic imaging. No other conflict of interested are disclosed.

Ethical standards. The study was approved by the East of England-Cambridge East NHS Research Ethics Committee.

References

Agid, O., Kapur, S., Arenovich, T., & Zipursky, R. B. (2003). Delayed-onset hypothesis of antipsychotic action: A hypothesis tested and rejected. *Archives of General Psychiatry*, *60*(12), 1228–1235. doi:10.1001/archpsyc.60.12.1228.

Allen, P., Azis, M., Modinos, G., Bossong, M. G., Bonoldi, I., Samson, C., … McGuire, P. (2018). Increased resting hippocampal and basal ganglia perfusion in people at ultra high risk for psychosis: Replication in a second cohort. *Schizophrenia Bulletin*, *44*(6), 1323–1331. doi:10.1093/schbul/sbx169.

Allen, P., Chaddock, C. A., Egerton, A., Howes, O. D., Bonoldi, I., Zelaya, F., … McGuire, P. (2016). Resting hyperperfusion of the hippocampus, midbrain, and basal ganglia in people at high risk for psychosis. *The American Journal of Psychiatry*, *173*(4), 392–399. doi:10.1176/appi.ajp.2015.15040485.

Alsop, D. C., Detre, J. A., Golay, X., Günther, M., Hendrikse, J., Hernandez-Garcia, L., … Zaharchuk, G. (2015). Recommended implementation of arterial spin-labeled perfusion MRI for clinical applications: A consensus of the ISMRM perfusion study group and the European consortium for ASL in dementia. *Magnetic Resonance in Medicine*, *73*(1), 102–116. doi:10.1002/mrm.25197.

Andreasen, N. C., O'Leary, D. S., Flaum, M., Nopoulos, P., Watkins, G. L., Boles Ponto, L. L., & Hichwa, R. D. (1997). Hypofrontality in schizophrenia: Distributed dysfunctional circuits in neuroleptic-naïve patients. *The Lancet*, *349*(9067), 1730–1734. doi:10.1016/s0140-6736(96)08258-x.

Ashburner, J., & Friston, K. J. (2005). Unified segmentation. *NeuroImage*, *26*(3), 839–851. doi:10.1016/j.neuroimage.2005.02.018.

Brewer, W. J., Yücel, M., Harrison, B. J., McGorry, P. D., Olver, J., Egan, G. F., … Pantelis, C. (2007). Increased prefrontal cerebral blood flow in first-episode schizophrenia following treatment: Longitudinal positron emission tomography study. *The Australian and New Zealand Journal of Psychiatry*, *41*(2), 129–135. doi:10.1080/00048670601109899.

Brugger, S. P., & Howes, O. D. (2017). Heterogeneity and homogeneity of regional brain structure in schizophrenia: A meta-analysis. *JAMA Psychiatry*, *74*(11), 1104–1111. doi:10.1001/jamapsychiatry.2017.2663.

Buchsbaum, M. S., Haznedar, M., Newmark, R. E., Chu, K.-W., Dusi, N., Entis, J. J., … Wolkin, A. (2009). FDG-PET and MRI imaging of the effects of sertindole and haloperidol in the prefrontal lobe in schizophrenia. *Schizophrenia Research*, *114*(1–3), 161–171. doi:10.1016/j.schres.2009.07.015.

Buchsbaum, M. S., Ingvar, D. H., Kessler, R., Waters, R. N., Cappelletti, J., van Kammen, D. P., … Sokoloff, L. (1982). Cerebral glucography with positron tomography. Use in normal subjects and in patients with schizophrenia. *Archives of General Psychiatry*, *39*(3), 251–259. doi:10.1001/archpsyc.1982.04290030001001.

Bullmore, E., Brammer, M., Williams, S. C., Curtis, V., McGuire, P., Morris, R., … Sharma, T. (1999). Functional MR imaging of confounded hypofrontality. *Human Brain Mapping*, *8*(2–3), 86–91. doi:10.1002/(SICI)1097-0193(1999)8:2/3<86::AID-HBM3>3.0.CO;2-S.

Calderone, D. J., Martinez, A., Zemon, V., Hoptman, M. J., Hu, G., Watkins, J. E., … Butler, P. D. (2013). Comparison of psychophysical, electrophysiological, and fMRI assessment of visual contrast responses in patients with schizophrenia. *NeuroImage*, *67*, 153–162. doi:10.1016/j.neuroimage.2012.11.019.

Chen, J., Xue, K., Yang, M., Wang, K., Xu, Y., Wen, B., ... Wei, Y. (2022). Altered coupling of cerebral blood flow and functional connectivity strength in first-episode schizophrenia patients with auditory verbal hallucinations. *Frontiers in Neuroscience*, *16*, 821078. doi:10.3389/fnins.2022.821078.

Chen, Y., Wang, D. J. J., & Detre, J. A. (2011). Test–retest reliability of arterial spin labeling with common labeling strategies. *Journal of Magnetic Resonance Imaging*, *33*(4), 940–949. doi:10.1002/jmri.22345.

Cook, R. D., & Weisberg, S. (1982). *Residuals and influence in regression*. New York: Chapman and Hall.

Davies, C., Paloyelis, Y., Rutigliano, G., Cappucciati, M., De Micheli, A., Ramella-Cravaro, V., … Fusar-Poli, P. (2019). Oxytocin modulates hippocampal perfusion in people at clinical high risk for psychosis. *Neuropsychopharmacology*, *44*(7), 1300–1309. doi:10.1038/s41386-018-0311-6.

Dogan, A. E., Yuksel, C., Du, F., Chouinard, V.-A., & Öngür, D. (2018). Brain lactate and pH in schizophrenia and bipolar disorder: A systematic review of findings from magnetic resonance studies. *Neuropsychopharmacology*, *43*(8), 1681–1690. doi:10.1038/s41386-018-0041-9.

Du, F., Cooper, A. J., Thida, T., Sehovic, S., Lukas, S. E., Cohen, B. M., … Öngür, D. (2014). In vivo evidence for cerebral bioenergetic abnormalities in schizophrenia measured using ^{31}P magnetization transfer spectroscopy. *JAMA Psychiatry*, *71*(1), 19–27. doi:10.1001/jamapsychiatry.2013.2287.

Efron, B., & Tibshirani, R. (1986). Bootstrap methods for standard errors, confidence intervals, and other measures of statistical accuracy. *Statistical Science*, *1*(1), 54–75. doi:10.1214/ss/1177013815.

Egerton, A., Demjaha, A., McGuire, P., Mehta, M. A., & Howes, O. D. (2010). The test–retest reliability of ^{18}F-DOPA PET in assessing striatal and extrastriatal presynaptic dopaminergic function. *NeuroImage*, *50*(2), 524–531. doi:10.1016/j.neuroimage.2009.12.058.

Eklund, A., Nichols, T. E., & Knutsson, H. (2016). Cluster failure: Why fMRI inferences for spatial extent have inflated false-positive rates. *Proceedings of the National Academy of Sciences of the United States of America*, *113*(28), 7900–7905. doi:10.1073/pnas.1602413113.

Finch, W. H. (2012). Distribution of variables by method of outlier detection. *Frontiers in Psychology*, *3*, 211. doi:10.3389/fpsyg.2012.00211.

First, M. B. (2014). Structured clinical interview for the DSM (SCID). In R. L. Cautin & S. O. Lilienfeld (Eds.), *The encyclopedia of clinical psychology* (pp. 1–6). Hoboken, NJ, USA: John Wiley & Sons, Inc. Retrieved from doi:10.1002/9781118625392.wbecp351.

Fischl, B., & Dale, A. M. (2000). Measuring the thickness of the human cerebral cortex from magnetic resonance images. *Proceedings of the National Academy of Sciences of the United States of America*, *97*(20), 11050–11055. doi:10.1073/pnas.200033797.

Fusar-Poli, P., Lai, S., Di Forti, M., Iacoponi, E., Thornicroft, G., McGuire, P., & Jauhar, S. (2020). Early intervention services for first episode of psychosis in South London and the Maudsley (SLAM): 20 years of care and research for young people. *Frontiers in Psychiatry*, *11*, 577110. doi:10.3389/fpsyt.2020.577110.

Goozée, R., Handley, R., Kempton, M. J., & Dazzan, P. (2014). A systematic review and meta-analysis of the effects of antipsychotic medications on regional cerebral blood flow (rCBF) in schizophrenia: Association with response to treatment. *Neuroscience and Biobehavioral Reviews*, *43*, 118–136. doi:10.1016/j.neubiorev.2014.03.014.

Greve, D. N., & Fischl, B. (2018). False positive rates in surface-based anatomical analysis. *NeuroImage*, *171*, 6–14. doi:10.1016/j.neuroimage.2017.12.072.

Gur, R. E., Mozley, P. D., Resnick, S. M., Mozley, L. H., Shtasel, D. L., Gallacher, F., … Reivich, M. (1995). Resting cerebral glucose metabolism in first-episode and previously treated patients with schizophrenia relates to clinical features. *Archives of General Psychiatry*, *52*(8), 657–667. doi:10.1001/archpsyc.1995.03950200047013.

Hahn, B., Robinson, B. M., Leonard, C. J., Luck, S. J., & Gold, J. M. (2018). Posterior parietal cortex dysfunction is central to working memory storage and broad cognitive deficits in schizophrenia. *The Journal of Neuroscience*, *38*(39), 8378–8387. doi:10.1523/JNEUROSCI.0913-18.2018.

Handley, R., Zelaya, F. O., Reinders, A. A. T. S., Marques, T. R., Mehta, M. A., O'Gorman, R., … Dazzan, P. (2013). Acute effects of single-dose aripiprazole and haloperidol on resting cerebral blood flow (rCBF) in the human brain. *Human Brain Mapping*, *34*(2), 272–282. doi:10.1002/hbm.21436.

Hawkins, P. C. T., Wood, T. C., Vernon, A. C., Bertolino, A., Sambataro, F., Dukart, J., … Mehta, M. A. (2018). An investigation of regional cerebral blood flow and tissue structure changes after acute administration of antipsychotics in healthy male volunteers. *Human Brain Mapping*, *39*(1), 319–331. doi:10.1002/hbm.23844.

Hill, K., Mann, L., Laws, K. R., Stephenson, C. M. E., Nimmo-Smith, I., & McKenna, P. J. (2004). Hypofrontality in schizophrenia: A meta-analysis of functional imaging studies. *Acta Psychiatrica Scandinavica*, *110*(4), 243–256. doi:10.1111/j.1600-0447.2004.00376.x.

Holiga, Š, Sambataro, F., Luzy, C., Greig, G., Sarkar, N., Renken, R. J., … Dukart, J. (2018). Test–retest reliability of task-based and resting-state blood oxygen level dependence and cerebral blood flow measures. *PLoS One*, *13*(11), e0206583. doi:10.1371/journal.pone.0206583.

Howes, O. D., & McCutcheon, R. (2017). Inflammation and the neural diathesis-stress hypothesis of schizophrenia: A reconceptualization. *Translational Psychiatry*, *7*(2), e1024. doi:10.1038/tp.2016.278.

Howes, O. D., & Murray, R. M. (2014). Schizophrenia: An integrated sociodevelopmental-cognitive model. *The Lancet*, *383*(9929), 1677–1687. doi:10.1016/S0140-6736(13)62036-X.

Jauhar, S., & Howes, O. D. (2019). Understanding and predicting variability in response to treatment in psychotic disorders: In vivo findings. *Clinical Pharmacology and Therapeutics*, *105*(5), 1079–1081. doi:10.1002/cpt.1357.

Jauhar, S., Veronese, M., Nour, M. M., Rogdaki, M., Hathway, P., Turkheimer, F. E., … Howes, O. D. (2019). Determinants of treatment response in first-episode psychosis: An ^{18}F-DOPA PET study. *Molecular Psychiatry*, *24*(10), 1502–1512. doi:10.1038/s41380-018-0042-4.

Kaar, S. J., Natesan, S., McCutcheon, R., & Howes, O. D. (2020). Antipsychotics: Mechanisms underlying clinical response and side-effects and novel treatment approaches based on pathophysiology. *Neuropharmacology*, *172*, 107704. doi:10.1016/j.neuropharm.2019.107704.

Kay, S. R., Fiszbein, A., & Opler, L. A. (1987). The positive and negative syndrome scale (PANSS) for schizophrenia. *Schizophrenia Bulletin*, *13*(2), 261–276. doi:10.1093/schbul/13.2.261.

Kindler, J., Jann, K., Homan, P., Hauf, M., Walther, S., Strik, W., … Hubl, D. (2015). Static and dynamic characteristics of cerebral blood flow during the resting state in schizophrenia. *Schizophrenia Bulletin*, *41*(1), 163–170. doi:10.1093/schbul/sbt180.

Kindler, J., Schultze-Lutter, F., Hauf, M., Dierks, T., Federspiel, A., Walther, S., … Hubl, D. (2018). Increased striatal and reduced prefrontal cerebral blood flow in clinical high risk for psychosis. *Schizophrenia Bulletin*, *44*(1), 182–192. doi:10.1093/schbul/sbx070.

Legind, C. S., Broberg, B. V., Brouwer, R., Mandl, R. C. W., Ebdrup, B. H., Anhøj, S. J., … Rostrup, E. (2019). Heritability of cerebral blood flow and the correlation to schizophrenia spectrum disorders: A pseudo-continuous arterial spin labeling twin study. *Schizophrenia Bulletin*, *45*(6), 1231–1241. doi:10.1093/schbul/sbz007.

Leucht, S., Kane, J. M., Kissling, W., Hamann, J., Etschel, E., & Engel, R. R. (2005). What does the PANSS mean? *Schizophrenia Research*, *79*(2–3), 231–238. doi:10.1016/j.schres.2005.04.008.

Leucht, S., Winter-van Rossum, I., Heres, S., Arango, C., Fleischhacker, W. W., Glenthøj, B., … Sommer, I. E. (2015). The optimization of treatment and management of schizophrenia in Europe (OPTiMiSE) trial: Rationale for its methodology and a review of the effectiveness of switching antipsychotics. *Schizophrenia Bulletin*, *41*(3), 549–558. doi:10.1093/schbul/sbv019.

Levine, S. Z., & Leucht, S. (2012). Early symptom response to antipsychotic medication as a marker of subsequent symptom change: An eighteen-month follow-up study of recent episode schizophrenia. *Schizophrenia Research*, *141*(2–3), 168–172. doi:10.1016/j.schres.2012.08.030.

Liu, J., Qiu, M., Constable, R. T., & Wexler, B. E. (2012a). Does baseline cerebral blood flow affect task-related blood oxygenation level dependent response in schizophrenia? *Schizophrenia Research*, *140*(1–3), 143–148. doi:10.1016/j.schres.2012.06.028.

Liu, Y., Zhu, X., Feinberg, D., Guenther, M., Gregori, J., Weiner, M. W., & Schuff, N. (2012b). Arterial spin labeling MRI study of age and gender effects on brain perfusion hemodynamics. *Magnetic Resonance in Medicine*, *68*(3), 912–922. doi:10.1002/mrm.23286.

Makarić, P., Bošnjak, D., Kekin, I., Jelacic, P., Haupert, M., Đuran, N., … Rojnić Kuzman, M. (2017). Alteration of cerebral blood flow measured with SPECT in patients with first episode psychosis. *European Psychiatry*, *41*(S1), S271–S271. doi:10.1016/j.eurpsy.2017.02.099.

Mandeville, J. B., Sander, C. Y. M., Jenkins, B. G., Hooker, J. M., Catana, C., Vanduffel, W., … Normandin, M. D. (2013). A receptor-based model for dopamine-induced fMRI signal. *NeuroImage*, *75*, 46–57. doi:10.1016/j.neuroimage.2013.02.036.

McCutcheon, R. A., Krystal, J. H., & Howes, O. D. (2020a). Dopamine and glutamate in schizophrenia: Biology, symptoms and treatment. *World Psychiatry*, *19*(1), 15–33. doi:10.1002/wps.20693.

McCutcheon, R. A., Reis Marques, T., & Howes, O. D. (2020b). Schizophrenia – An overview. *JAMA Psychiatry*, *77*(2), 201–210. doi:10.1001/jamapsychiatry.2019.3360.

Mehta, M. A., McGowan, S. W., Lawrence, A. D., Aitken, M. R. F., Montgomery, A. J., & Grasby, P. M. (2003). Systemic sulpiride modulates striatal blood flow: Relationships to spatial working memory and planning. *NeuroImage*, *20*(4), 1982–1994. doi:10.1016/j.neuroimage.2003.08.007.

Miller, D. D., Andreasen, N. C., O'Leary, D. S., Rezai, K., Watkins, G. L., Ponto, L. L., & Hichwa, R. D. (1997). Effect of antipsychotics on regional cerebral blood flow measured with positron emission tomography. *Neuropsychopharmacology*, *17*(4), 230–240. doi:10.1016/S0893-133X(97)00042-0.

Modinos, G., Egerton, A., McMullen, K., McLaughlin, A., Kumari, V., Barker, G. J., … Zelaya, F. (2018a). Increased resting perfusion of the hippocampus in high positive schizotypy: A pseudocontinuous arterial spin labeling study. *Human Brain Mapping*, *39*(10), 4055–4064. doi:10.1002/hbm.24231.

Modinos, G., Şimşek, F., Azis, M., Bossong, M., Bonoldi, I., Samson, C., … McGuire, P. (2018b). Prefrontal GABA levels, hippocampal resting

https://doi.org/10.1017/S0033291722002288 Published online by Cambridge University Press

perfusion and the risk of psychosis. *Neuropsychopharmacology*, *43*(13), 2652–2659. doi:10.1038/s41386-017-0004-6.
Molina, V., Sanz, J., Reig, S., Martínez, R., Sarramea, F., Luque, R., … Desco, M. (2005). Hypofrontality in men with first-episode psychosis. *The British Journal of Psychiatry*, *186*, 203–208. doi:10.1192/bjp.186.3.203.
Mouchlianitis, E., McCutcheon, R., & Howes, O. D. (2016). Brain-imaging studies of treatment-resistant schizophrenia: A systematic review. *The Lancet. Psychiatry*, *3*(5), 451–463. doi:10.1016/S2215-0366(15)00540-4.
Oliveira, ÍAF, Guimarães, T. M., Souza, R. M., Dos Santos, A. C., Machado-de-Sousa, J. P., Hallak, J. E. C., & Leoni, R. F. (2018). Brain functional and perfusional alterations in schizophrenia: An arterial spin labeling study. *Psychiatry Research. Neuroimaging*, *272*, 71–78. doi:10.1016/j.pscychresns.2017.12.001.
Onwordi, E. C., Halff, E. F., Whitehurst, T., Mansur, A., Cotel, M.-C., Wells, L., … Howes, O. D. (2020). Synaptic density marker SV2A is reduced in schizophrenia patients and unaffected by antipsychotics in rats. *Nature Communications*, *11*(1), 246. doi:10.1038/s41467-019-14122-0.
Osimo, E. F., Beck, K., Reis Marques, T., & Howes, O. D. (2019). Synaptic loss in schizophrenia: A meta-analysis and systematic review of synaptic protein and mRNA measures. *Molecular Psychiatry*, *24*(4), 549–561. doi:10.1038/s41380-018-0041-5.
Ota, M., Ishikawa, M., Sato, N., Okazaki, M., Maikusa, N., Hori, H., … Kunugi, H. (2014). Pseudo-continuous arterial spin labeling MRI study of schizophrenic patients. *Schizophrenia Research*, *154*(1–3), 113–118. doi:10.1016/j.schres.2014.01.035.
Overton, D. J., Bhagwat, N., Viviano, J. D., Jacobs, G. R., & Voineskos, A. N. (2020). Identifying psychosis spectrum youth using support vector machines and cerebral blood perfusion as measured by arterial spin labeled fMRI. *NeuroImage. Clinical*, *27*, 102304. doi:10.1016/j.nicl.2020.102304.
Parkes, L. M., Rashid, W., Chard, D. T., & Tofts, P. S. (2004). Normal cerebral perfusion measurements using arterial spin labeling: Reproducibility, stability, and age and gender effects. *Magnetic Resonance in Medicine*, *51*(4), 736–743. doi:10.1002/mrm.20023.
Pinkham, A., Loughead, J., Ruparel, K., Wu, W.-C., Overton, E., Gur, R., & Gur, R. (2011). Resting quantitative cerebral blood flow in schizophrenia measured by pulsed arterial spin labeling perfusion MRI. *Psychiatry Research*, *194*(1), 64–72. doi:10.1016/j.pscychresns.2011.06.013.
Pinkham, A. E., Liu, P., Lu, H., Kriegsman, M., Simpson, C., & Tamminga, C. (2015). Amygdala hyperactivity at rest in paranoid individuals with schizophrenia. *The American Journal of Psychiatry*, *172*(8), 784–792. doi:10.1176/appi.ajp.2014.14081000.
Potkin, S. G., Kane, J. M., Correll, C. U., Lindenmayer, J.-P., Agid, O., Marder, S. R., … Howes, O. D. (2020). The neurobiology of treatment-resistant schizophrenia: Paths to antipsychotic resistance and a roadmap for future research. *Focus*, *18*(4), 456–465. doi:10.1176/appi.focus.18309.
Prince, J. A., Blennow, K., Gottfries, C. G., Karlsson, I., & Oreland, L. (1999). Mitochondrial function is differentially altered in the basal ganglia of chronic schizophrenics. *Neuropsychopharmacology*, *21*(3), 372–379. doi:10.1016/S0893-133X(99)00016-0.
Rajasekaran, A., Venkatasubramanian, G., Berk, M., & Debnath, M. (2015). Mitochondrial dysfunction in schizophrenia: Pathways, mechanisms and implications. *Neuroscience and Biobehavioral Reviews*, *48*, 10–21. doi:10.1016/j.neubiorev.2014.11.005.
Riederer, I., Bohn, K. P., Preibisch, C., Wiedemann, E., Zimmer, C., Alexopoulos, P., & Förster, S. (2018). Alzheimer disease and mild cognitive impairment: Integrated pulsed arterial spin-labeling MRI and ^{18}F-FDG PET. *Radiology*, *288*(1), 198–206. doi:10.1148/radiol.2018170575.
Salat, D. H., Buckner, R. L., Snyder, A. Z., Greve, D. N., Desikan, R. S. R., Busa, E., … Fischl, B. (2004). Thinning of the cerebral cortex in aging. *Cerebral Cortex*, *14*(7), 721–730. doi:10.1093/cercor/bhh032.
Sander, C. Y., Hooker, J. M., Catana, C., Normandin, M. D., Alpert, N. M., Knudsen, G. M., … Mandeville, J. B. (2013). Neurovascular coupling to D2/D3 dopamine receptor occupancy using simultaneous PET/functional MRI. *Proceedings of the National Academy of Sciences of the United States of America*, *110*(27), 11169–11174. doi:10.1073/pnas.1220512110.
Sander, C. Y., Hooker, J. M., Catana, C., Rosen, B. R., & Mandeville, J. B. (2016). Imaging agonist-induced D2/D3 receptor desensitization and internalization in vivo with PET/fMRI. *Neuropsychopharmacology*, *41*(5), 1427–1436. doi:10.1038/npp.2015.296.
Sander, C. Y., Mandeville, J. B., Wey, H.-Y., Catana, C., Hooker, J. M., & Rosen, B. R. (2019). Effects of flow changes on radiotracer binding: Simultaneous measurement of neuroreceptor binding and cerebral blood flow modulation. *Journal of Cerebral Blood Flow and Metabolism*, *39*(1), 131–146. doi:10.1177/0271678X17725418.
Sarpal, D. K., Argyelan, M., Robinson, D. G., Szeszko, P. R., Karlsgodt, K. H., John, M., … Malhotra, A. K. (2016). Baseline striatal functional connectivity as a predictor of response to antipsychotic drug treatment. *The American Journal of Psychiatry*, *173*(1), 69–77. doi:10.1176/appi.ajp.2015.14121571.
Schneider, K., Michels, L., Hartmann-Riemer, M. N., Burrer, A., Tobler, P. N., Stämpfli, P., … Kaiser, S. (2019). Cerebral blood flow in striatal regions is associated with apathy in patients with schizophrenia. *Journal of Psychiatry & Neuroscience*, *44*(2), 102–110. doi:10.1503/jpn.170150.
Schobel, S. A., Chaudhury, N. H., Khan, U. A., Paniagua, B., Styner, M. A., Asllani, I., … Small, S. A. (2013). Imaging patients with psychosis and a mouse model establishes a spreading pattern of hippocampal dysfunction and implicates glutamate as a driver. *Neuron*, *78*(1), 81–93. doi:10.1016/j.neuron.2013.02.011.
Selvaggi, P., Hawkins, P. C. T., Dipasquale, O., Rizzo, G., Bertolino, A., Dukart, J., … Mehta, M. A. (2019). Increased cerebral blood flow after single dose of antipsychotics in healthy volunteers depends on dopamine D2 receptor density profiles. *NeuroImage*, *188*, 774–784. doi:10.1016/j.neuroimage.2018.12.028.
Shcherbinin, S., Doyle, O., Zelaya, F. O., de Simoni, S., Mehta, M. A., & Schwarz, A. J. (2015). Modulatory effects of ketamine, risperidone and lamotrigine on resting brain perfusion in healthy human subjects. *Psychopharmacology*, *232*(21–22), 4191–4204. doi:10.1007/s00213-015-4021-z.
Smith, S. M., & Nichols, T. E. (2009). Threshold-free cluster enhancement: Addressing problems of smoothing, threshold dependence and localisation in cluster inference. *NeuroImage*, *44*(1), 83–98. doi:10.1016/j.neuroimage.2008.03.061.
Sukumar, N., Sabesan, P., Anazodo, U., & Palaniyappan, L. (2020). Neurovascular uncoupling in schizophrenia: A bimodal meta-analysis of brain perfusion and glucose metabolism. *Frontiers in Psychiatry*, *11*, 754. doi:10.3389/fpsyt.2020.00754.
Taylor, D. M., Barnes, T. R. E., & Young, A. H. (2018). *The Maudsley prescribing guidelines in psychiatry* (13th ed.). Hoboken, NJ: John Wiley & Sons.
Townsend, L., Pillinger, T., Selvaggi, P., Veronese, M., Turkheimer, F., & Howes, O. (2022). Brain glucose metabolism in schizophrenia: A systematic review and meta-analysis of 18FDG-PET studies in schizophrenia. *Psychological Medicine*, *22*, 1–18. doi:0.1017/S003329172200174X.
Turkheimer, F. E., Selvaggi, P., Mehta, M. A., Veronese, M., Zelaya, F., Dazzan, P., & Vernon, A. C. (2020). Normalizing the abnormal: Do antipsychotic drugs push the cortex into an unsustainable metabolic envelope? *Schizophrenia Bulletin*, *46*(3), 484–495. doi:10.1093/schbul/sbz119.
Veronese, M., Santangelo, B., Jauhar, S., D'Ambrosio, E., Demjaha, A., Salimbeni, H., … Howes, O. (2021). A potential biomarker for treatment stratification in psychosis: Evaluation of an [18F] FDOPA PET imaging approach. *Neuropsychopharmacology*, *46*, 1122–1132. doi:10.1038/s41386-020-00866-7.
Viviani, R., Abler, B., Seeringer, A., & Stingl, J. C. (2012). Effect of paroxetine and bupropion on human resting brain perfusion: An arterial spin labeling study. *NeuroImage*, *61*(4), 773–779. doi:10.1016/j.neuroimage.2012. 03.014.
Viviani, R., Graf, H., Wiegers, M., & Abler, B. (2013). Effects of amisulpride on human resting cerebral perfusion. *Psychopharmacology*, *229*(1), 95–103. doi:10.1007/s00213-013-3091-z.
Viviani, R., Sim, E.-J., Lo, H., Richter, S., Haffer, S., Osterfeld, N., … Beschoner, P. (2009). Components of variance in brain perfusion and the design of studies of individual differences: The baseline study. *NeuroImage*, *46*(1), 12–22. doi:10.1016/j.neuroimage.2009.01.041.
Wang, J., Li, L., Roc, A. C., Alsop, D. C., Tang, K., Butler, N. S., … Detre, J. A. (2004). Reduced susceptibility effects in perfusion fMRI with single-shot spin-echo EPI acquisitions at 1.5 Tesla. *Magnetic Resonance Imaging*, *22*(1), 1–7. doi:10.1016/S0730-725X(03)00210-8.
Weinberger, D. R., & Berman, K. F. (1988). Speculation on the meaning of cerebral metabolic hypofrontality in schizophrenia. *Schizophrenia Bulletin*, *14*(2), 157–168. doi:10.1093/schbul/14.2.157.

https://doi.org/10.1017/S0033291722002288 Published online by Cambridge University Press

Weiss, A. P., Ellis, C. B., Roffman, J. L., Stufflebeam, S., Hamalainen, M. S., Duff, M., … Schacter, D. L. (2009). Aberrant frontoparietal function during recognition memory in schizophrenia: A multimodal neuroimaging investigation. *The Journal of Neuroscience*, *29*(36), 11347–11359. doi:10.1523/JNEUROSCI.0617-09.2009.

Winkler, A. M., Ridgway, G. R., Webster, M. A., Smith, S. M., & Nichols, T. E. (2014). Permutation inference for the general linear model. *NeuroImage*, *92*, 381–397. doi:10.1016/j.neuroimage.2014.01.060.

World Health Organization. (2004). *ICD-10: international statistical classification of diseases and related health problems : tenth revision* (2nd ed.). Geneve, Switzerland: World Health Organization.

Wulff, S., Pinborg, L. H., Svarer, C., Jensen, L. T., Nielsen, M. Ø., Allerup, P., … Glenthøj, B. Y. (2015). Striatal D(2/3) binding potential values in drug-naïve first-episode schizophrenia patients correlate With treatment outcome. *Schizophrenia Bulletin*, *41*(5), 1143–1152. doi:10.1093/schbul/sbu220.

Zhang, N., Gordon, M. L., Ma, Y., Chi, B., Gomar, J. J., Peng, S., … Goldberg, T. E. (2018). The age-related perfusion pattern measured with arterial spin labeling MRI in healthy subjects. *Frontiers in Aging Neuroscience*, *10*, 214. doi:10.3389/fnagi.2018.00214.

Zhu, J., Zhuo, C., Xu, L., Liu, F., Qin, W., & Yu, C. (2017). Altered coupling between resting-state cerebral blood flow and functional connectivity in schizophrenia. *Schizophrenia Bulletin*, *43*(6), 1363–1374. doi:10.1093/schbul/sbx051.

https://doi.org/10.1017/S0033291722002288 Published online by Cambridge University Press